ELECTRIC POWER RESEARCH INSTITUTE

2010-206 BWR Vessel & Internals Project (BWRVIP)

September 13, 2010

Document Control Desk
U. S. Nuclear Regulatory Commission
11555 Rockville Pike
Rockville, MD 20852

Attention: Jonathan Rowley

Subject: Project No. 704 – "BWRVIP-113NP: BWR Vessel and Internals Project, River Bend 183 Degree Surveillance Capsule Report"

Reference: BWRVIP letter 2003-173 from Carl Terry (BWRVIP Chairman) to Document Control Desk (NRC), "BWRVIP-113: BWR Vessel and Internals Project, River Bend 183 Degree Surveillance Capsule Report," dated June 10, 2003

Enclosed for your information are five (5) copies of the report "BWRVIP-113NP: BWR Vessel and Internals Project, River Bend 183 Degree Surveillance Capsule Report," EPRI Technical Report 1021555, August 2010. This report is a non-proprietary version of the proprietary report transmitted to the NRC staff by the BWRVIP letter referenced above. The technical content of the enclosed report is identical to that in the proprietary version transmitted to the NRC staff by the BWRVIP letter referenced above. The content was re-classified as non-proprietary and is being provided in response to a request from the NRC staff so that the data in the report can be used in the NRC public database of reactor pressure vessel embrittlement data.

Please note that the enclosed report is non-proprietary and is available to the public by request to EPRI.

If you have any questions on this subject please call Randy Schmidt (PSEG Nuclear, BWRVIP Assessment Committee Technical Chairman) at 856-339-3740.

Sincerely,

Dave Czufin
Exelon
Chairman, BWR Vessel and Internals Project

c: Gary Stevens, NRC
Matt Mitchell, NRC

G004
NRR

ELECTRIC POWER RESEARCH INSTITUTE

BWRVIP-113NP: BWR Vessel and Internals Project

River Bend 183 Degree Surveillance Capsule Report

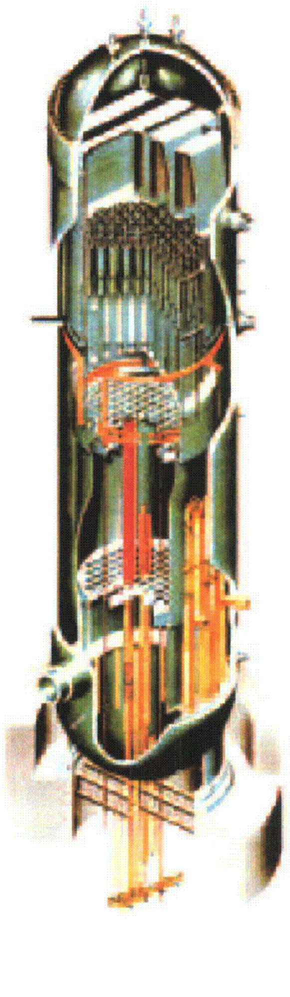

BWRVIP-113NP: BWR Vessel and Internals Project

River Bend 183 Degree Surveillance Capsule Report

1021555

Final Report, August 2010

EPRI Project Manager
R. Carter

Work to develop this product was completed under the EPRI Nuclear Quality Assurance Program in compliance with 10 CFR 50, Appendix B and 10 CFR 21,
YES NO

EPRI • 3412 Hillview Avenue, Palo Alto, California 94304 • PO Box 10412, Palo Alto, California 94303 • USA
800.313.3774 • 650.855.2121 • askepri@epri.com • www.epri.com

DISCLAIMER OF WARRANTIES AND LIMITATION OF LIABILITIES

THE FOLLOWING ORGANIZATION(S), UNDER CONTRACT TO EPRI, PREPARED THIS REPORT:

MPM Technologies, Inc.

THE TECHNICAL CONTENTS OF THIS DOCUMENT WERE PREPARED IN ACCORDANCE WITH THE EPRI QUALITY PROGRAM MANUAL THAT FULFILLS THE REQUIREMENTS OF 10 CFR 50 APPENDIX B, 10 CFR 21, ANSI N45.2-1977 AND/ OR THE INTENT OF ISO-9001 (1994).

CONTRACTUAL ARRANGEMENTS BETWEEN THE CUSTOMER AND EPRI MUST BE ESTABLISHED BEFORE QUALITY APPLICATION TO ASSURE FULFILLMENT OF QUALITY PROGRAM REQUIREMENTS.

NOTE

For further information about EPRI, call the EPRI Customer Assistance Center at 800.313.3774 or e-mail askepri@epri.com.

ACKNOWLEDGMENTS

The following organizations, under contract to the Electric Power Research Institute (EPRI), prepared this report:

MPM Technologies, Inc.
2161 Sandy Drive
State College, PA 16803

Principal Investigator
M.P. Manahan, Sr.

This report describes research sponsored by EPRI.

This publication is a corporate document that should be cited in the literature in the following manner:

BWRVIP-113NP: BWR Vessel and Internals Project, River Bend 183 Degree Surveillance Capsule Report. EPRI, Palo Alto, CA: 2010. 1021555.

PRODUCT DESCRIPTION

Each boiling water reactor (BWR) has a surveillance program for monitoring changes in reactor pressure vessel (RPV) material properties due to neutron irradiation. This report describes testing and evaluation of 183-degree surveillance capsule for River Bend. These results will be used to monitor embrittlement as part of the BWR Vessel and Internals Project (BWRVIP) Integrated Surveillance Program (ISP).

Results & Findings

The report includes specimen chemical compositions, capsule neutron exposure, specimen temperatures during irradiation, and Charpy V-notch test results. A fluence of 1.16×10^{18} n/cm^2 has been estimated for the capsule exposure at the end of Cycle 9 (10.08 EFPY). The lead factor (capsule fluence divided by vessel maximum fluence) at the vessel surface is calculated to be 0.95. Overall, the neutron transport calculation and dosimetry are in very good agreement. Revised best estimate chemistry data for the plate and surveillance weld were determined. The Charpy data trends show that the neutron-induced embrittlement of the limiting River Bend vessel plate and weld are consistent with the data trends observed for BWRs. The measured upper shelf energy (USE) of the plate was observed to increase slightly while the USE of the weld decreased as expected. Increases in the USE have been observed in other plants and may be related to low fluence improvement of the matrix material, which results in more ductile ligament response during the ductile fracture process.

Challenges & Objectives

Neutron irradiation exposure reduces the toughness of reactor vessel steel plates, welds, and forgings. The objective of this project was:

- To document results of the surveillance capsule and RPV fluence, and Charpy-V notch ductility tests for materials contained in the River Bend 183-degree capsule.

Applications, Values & Use

Results of this work will be used in the BWRVIP ISP that will integrate individual BWR surveillance programs into a single program. Data generated from the SSP specimens will provide significant additional data of high quality to monitor BWR vessel embrittlement. The ISP and the use of the SSP capsule specimen data will result in significant cost savings to the BWR fleet and provide more accurate monitoring of embrittlement in BWRs.

EPRI Perspective

The BWRVIP ISP represents a major enhancement to the process of monitoring embrittlement for the U.S. fleet of BWRs. The ISP optimizes surveillance capsule tests while at the same time maximizing the quantity and quality of data, thus resulting in a more cost-effective program. The BWRVIP ISP will provide more representative data that may be used to assess embrittlement in RPV vessel beltline materials and improve trend curves in the BWR range of irradiation conditions.

Approach

The capsule was removed from the reactor and transported to facilities for testing and evaluation. Dosimetry was used to gather information about the neutron fluence accrual of the specimens, and thermal monitors were placed in the capsule to approximate the highest temperature during irradiation. A neutron transport calculation was performed in accordance with Regulatory Guide 1.190 and compared to the results from the dosimetry. Testing of Charpy V-notch specimens were performed according to ASTM standards.

Keywords

Reactor pressure vessel integrity
Reactor vessel surveillance program
Radiation embrittlement
BWR
Charpy testing
Mechanical properties

ABSTRACT

The River Bend 183 degree surveillance capsule was irradiated from reactor start-up to the end of fuel cycle 9 (March 5, 2000) for a total exposure of 10.08 effective full power years (EFPY). Cycles 1 through 9 were operated at a full power of 2894 MWth. The capsule contained a total of 36 Charpy impact specimens and 4 dosimeter wires. The results of the capsule testing and analysis are summarized below.

Neutron Transport Results

A fast fluence of 1.16×10^{18} n/cm^2 has been calculated for the capsule. At the end of cycle 9, the lead factor (capsule fluence divided by vessel maximum fluence) at the vessel surface is calculated to be 0.95 ($1.156 \times 10^{18}/1.212 \times 10^{18}$), and the lead factor at the 1/4T location is 1.324 ($1.156 \times 10^{18}/8.73 \times 10^{17}$). Analysis of the dosimeter wires indicates good agreement between the dosimeters and the calculation. An average calculated-to-experimental (C/E) ratio of 0.86 indicates acceptable agreement between the calculation and the measurement. The experimental uncertainties for the iron and copper measurements are largely independent, and, if the small correlated component is ignored, the uncertainty in the average is 6.5%. Combining this with the 14.6% fluence uncertainty gives an uncertainty for the average C/E ratio of 16%. It is seen that the best estimate C/E value of 0.86 differs from 1.0 within this 16% uncertainty estimate. The C/E value of 0.86 is also within the Regulatory Guide 1.190 guideline of 20% for in-vessel surveillance capsules. It is concluded that the measurement provides an acceptable validation of the adequacy of the calculation. This River Bend-specific measurement provides validation of these calculations for use in vessel fluence determination. In accordance with Regulatory Guide 1.190, the calculated fluence values are recommended for use in estimating vessel embrittlement and in P-T curves.

Charpy Test Results

The Charpy data trends show that the neutron induced embrittlement of the limiting River Bend vessel plate and weld are consistent with the data trends observed for BWRs. At a fluence of 1.16×10^{18} n/cm^2, the shift in the 30 ft-lb (41 J) transition temperature for plate C-3054-2 is 44.0 F (24.4 C). The measured upper shelf energy (USE) was observed to increase by 5.3 ft-lb (7.2 J) to 100.6 ft-lb (136.4 J). Increases in the USE have been observed in other plants and may be related to low fluence improvement of the matrix material which results in more ductile ligament response during the ductile fracture process.

Similarly, the surveillance weld embrittlement data trends were observed to be consistent with BWR data trends. At a fluence of 1.16×10^{18} n/cm^2, the shift in the 30 ft-lb (41 J) transition temperature for weld heat 5P6756 is 53.7 F (29.8 C). The USE for the weld decreased by 20.0 ft-lb (27.1 J) to 84.4 ft-lb (114.4 J).

Chemical Analysis

After performing the mechanical property tests, chemical composition measurements were made on two base metal and two weld metal Charpy specimens to verify that the surveillance materials used to fabricate the specimens were actually cut from the correct vessel plate and weld. It was verified that the base metal specimens were fabricated from heat C3054 slab 2 (C3054-2) material and the weld specimens were fabricated from weld heat 5P6756. Revised best estimate chemistry data for the plate and surveillance weld were determined. The best estimate surveillance weld copper concentration is 0.059 weight percent and for nickel the best estimate concentration is 0.93 weight percent. Similarly, the best estimate vessel plate copper concentration is 0.09 weight percent and for nickel the best estimate concentration is 0.68 weight percent.

CONTENTS

1 **INTRODUCTION 1-1**
1.1 Neutron Embrittlement 1-1
1.2 Surveillance Program Description 1-2
1.3 183 Degree Capsule Opening 1-2
1.4 Chapter 1 References 1-3

2 **NEUTRON DOSIMETER MEASUREMENTS 2-1**
2.1 Dosimeter Material Description 2-1
2.2 Dosimeter Cleaning and Mass Measurement 2-1
2.3 Radiometric Analysis 2-2

3 **NEUTRON FLUENCE CALCULATION 3-1**
3.1 Introduction 3-1
3.2 Neutron Transport Model 3-2
3.3 Capsule Fluence Results 3-5
3.4 Capsule Measurement Results 3-5
3.5 Vessel Fluence Results 3-10
3.6 Uncertainty Estimation 3-11
3.6.1 Uncertainty Assumptions 3-12
3.6.2 Uncertainty Evaluation 3-15
3.7 Benchmarking 3-15
3.7.1 PCA Benchmark 3-15
3.7.2 Calculational Benchmark 3-16
3.7.3 Power Plant Benchmarks 3-17
3.7.4 Summary 3-18
3.8 Chapter 3 References 3-18

4 **TEST SPECIMEN CHEMICAL ANALYSIS 4-1**

4.1 Specimen Selection and Machining of Samples 4-1
4.2 Preparation of Samples for Analysis 4-1
4.3 ICP-MS Measurements 4-1
4.4 Best Estimate Base and Weld Metal Chemistry 4-2
4.5 Chapter 4 References 4-2

5 CHARPY TEST DATA 5-1
5.1 Charpy Test Procedure 5-1
5.2 Charpy Test Data 5-2
5.3 Chapter 5 Reference 5-3

6 CHARPY CURVE FITTING 6-1
6.1 Fitting Procedure 6-1
6.2 183 Degree Surveillance Capsule Fitting Results 6-2
6.3 Chapter 6 References 6-3

7 SUMMARY AND CONCLUSIONS 7-1

8 NOMENCLATURE 8-1

A APPENDIX – INSTRUMENTED IMPACT DATA A-1
Appendix A-1 Base Metal Data A-2
Appendix A-2 Weld Metal Data A-27
Appendix A-3 HAZ Data A-53

LIST OF FIGURES

Figure 1-1 Schematic Illustration of a Typical Charpy Curve and the Effect of Neutron Irradiation on the Curve. Ferritic Pressure Vessel Steels Exhibit a Transition in Fracture Behavior as the Notched Bar Impact Test Temperature is Increased: at Low Temperatures the Fracture is Predominantly Cleavage; at Intermediate Temperatures the Fracture is a Mixture of both Cleavage and Ductile Tearing; and Above the Transition Region the Fracture is Entirely Ductile 1-4

Figure 1-2 Photograph of the River Bend 183 Degree Surveillance Capsule Taken During Disassembly. The Cut was made Near the Bottom of the Capsule........ 1-5

Figure 3-1 River Bend R-θ Geometry Used in the DORT Calculations........ 3-36

Figure 3-2 River Bend Reactor Vessel Fluence at the End of Cycle 9 at Core Midplane........ 3-37

Figure 3-3 River Bend Reactor Vessel Fluence at the End of Cycle 9 at Azimuthal Maximum........ 3-38

Figure 5-1 Drawing Showing the Charpy Test Specimen Geometry 5-9

Figure 5-2 Typical Instrumented Striker Raw Data Signal........ 5-10

Figure 5-3 Example Plots Showing Integrations Performed to Obtain the Load-Deflection Curve........ 5-11

Figure 5-4 Typical Load-Deflection Curve Showing Critical Load Points........ 5-12

Figure 6-1 Charpy Energy Data and Curve Fits for C3054-2 Base Metal in the Unirradiated and Irradiated Conditions (TL Orientation) 6-5

Figure 6-2 Charpy Energy Data and Curve Fits for Weld Metal (5P6756) in the Irradiated and Unirradiated Conditions........ 6-6

Figure 6-3 Charpy Lateral Expansion Data and Curve Fits for C3054-2 Base Metal in the Unirradiated and Irradiated Conditions (TL Orientation) 6-7

Figure 6-4 Charpy Lateral Expansion Data and Curve Fits for Weld Metal (5P6756) in the Irradiated and Unirradiated Conditions 6-8

LIST OF TABLES

Table 1-1 River Bend Surveillance Program Mechanical Behavior/Dosimeter Wire Specimen Inventory 1-3
Table 2-1 Wire Dosimeter Masses 2-3
Table 2-2 Charpy Specimen Section Dosimeter Masses 2-3
Table 2-3 Charpy Specimen Section Dosimeter Sizes 2-4
Table 2-4 GRSS Specifications 2-4
Table 2-5 Counting Schedule for the Dosimeter Materials 2-5
Table 2-6 Neutron-Induced Reactions of Interest 2-5
Table 2-7 Results of the Radiometric Analysis 2-5
Table 3-1 Neutron Flux Spectrum at Center of Surveillance Capsule 3-21
Table 3-2 River Bend Radial Dimensions 3-22
Table 3-3 Surveillance Capsule Flux and dpa/s Results 3-24
Table 3-4 Surveillance Capsule Fluence and dpa Results 3-25
Table 3-5 River Bend Power History to End of Cycle 9 3-26
Table 3-6 Nuclear Parameters Used in the Evaluation of Neutron Sensors 3-32
Table 3-7 Tabulation of Dosimetry Results 3-32
Table 3-8 Calculated Maximum Vessel Fluence and dpa at End of Cycle 9 (10.08 EFPY) and Projected to 32 EFPY and 48 EFPY 3-33
Table 3-9 Maximum Vessel Fluence (E > 1 MeV) (n/cm^2) at End of Cycle 9 (10.08 EFPY), at 32 EFPY and 48 EFPY Using Alternate Schemes for Attenuation through the Vessel 3-34
Table 3-10 River Bend Capsule and Vessel Fluence Calculational Uncertainty 3-35
Table 4-1 Chemistry Sample Identifications and Descriptions 4-3
Table 4-2 Results of the ICP Analysis of the Base Metal Sample B-12 4-3
Table 4-3 Results of the ICP Analysis of the Surveillance Weld (5P6756) Metal Sample W-6 4-4
Table 4-4 Results of the ICP Analysis of the Base and Weld Metal Samples Taken from HAZ Specimen H-1 4-4
Table 4-5 Comparison of the Results for HAZ Specimen H-1(a) and the Base (B-12) and Weld (W-6) Samples 4-5
Table 4-6 Analysis of the NIST Traceable Sample 4-5
Table 4-7 Best Estimate Chemistry Data for Surveillance Weld Material (5P6756) 4-6
Table 4-8 Best Estimate Chemistry Data for River Bend Vessel Plate C3054-2 4-7

Table 5-1 Charpy V-Notch T-L Impact Test Results for Irradiated (Fast (E > 1MeV) Fluence of 1.16 x 10^{18} n/cm^2) C3054-2 Base Metal Specimens from the River Bend 183 Degree Surveillance Capsule 5-4

Table 5-2 Charpy V-Notch Impact Test Results for Irradiated (Fast (E > 1MeV) Fluence of 1.16 x 10^{18} n/cm^2) Weld Metal Specimens (5P6756) from the River Bend 183 Degree Surveillance Capsule 5-5

Table 5-3 Charpy V-Notch Impact Test Results for Irradiated (Fast (E > 1MeV) Fluence of 1.16 x 10^{18} n/cm^2) HAZ Metal Specimens from the River Bend 183 Degree Surveillance Capsule 5-6

Table 5-4 Charpy V-Notch T-L Impact Test Results for Unirradiated C3054-2 Base Metal Specimens from the River Bend Surveillance Program [Reference 5-2] 5-7

Table 5-5 Charpy V-Notch Impact Test Results for Unirradiated Weld Metal Specimens (5P6756) from the River Bend Surveillance Program (Reference 5-3) 5-8

Table 6-1 Base Metal (C3054-2)Charpy Energy Impact Parameters (TL Orientation) 6-3

Table 6-2 Weld Metal (5P6756) Charpy Energy Impact Parameters 6-3

Table 6-3 Base Metal (C3054-2) Charpy Test Lateral Expansion Behavior (TL Orientation) 6-4

Table 6-4 Weld Metal (5P6756) Charpy Test Lateral Expansion Behavior 6-4

1 INTRODUCTION

1.1 Neutron Embrittlement

Ferritic reactor pressure vessel (RPV) materials undergo a transition in fracture behavior from brittle to ductile as the test temperature of the material is increased. Charpy V-notch tests are conducted in the nuclear industry to monitor changes in the fracture behavior during irradiation. Neutron irradiation to fluences above about 5 x 10^{16} n/cm^2 causes an upward shift in the ductile-to-brittle transition temperature (DBTT) and a drop in the upper shelf energy (USE). The nuclear industry indexes the DBTT at 30 ft-lbs (41 J) of absorbed energy and the shift in the DBTT is referred to in the literature as the nil ductility reference temperature shift (ΔRT_{NDT}, or the ΔT_{30}). This behavior is illustrated schematically in Figure 1-1. The initial RT_{NDT} is measured in accordance with Section III of the American Society of Mechanical Engineers (ASME) Boiler & Pressure Vessel Code (the Code) and involves measurement of drop weight data and Charpy data at discrete test temperatures.

In order to ensure safe operation of a nuclear power plant during heatup, cooldown, and leakage/hydro test conditions, it is necessary to conservatively calculate allowable stress loadings for the ferritic RPV materials. These allowable loadings can be conveniently presented as a plot of measured coolant pressure versus measured coolant temperature (P-T curves). Appendix G to Title 10 of the Code of Federal Regulations (CFR) Part 50 (10CFR50) [1-1] and Appendix G to Section III of the ASME Boiler and Pressure Vessel Code [1-2] presents a procedure for obtaining the allowable loadings for ferritic pressure-retaining materials in Class 1 components using linear elastic fracture mechanics (LEFM). The latest code year approved by the Nuclear Regulatory Commission (NRC), which at present is the 1995 Edition and Addenda through 1996, must be used in P-T curve analysis.

Although the Code suggests that the lower bound toughness should be measured for the vessel materials of interest, Regulatory Guide 1.99, Revision 2 (RG 1.99(2)) [1-3] allows the use of the ASME reference stress intensity factor (K_{IR}) and requires that this curve be shifted by the Charpy shift to account for radiation effects. In particular, neutron damage within the RPV during plant operation is accounted for in the allowable pressure loading by calculating an adjusted nil-ductility reference temperature (ART_{NDT}). RG 1.99(2) defines the ART_{NDT} as the sum of the initial RT_{NDT}, plus the RT_{NDT} irradiation induced shift (ΔRT_{NDT}), plus a margin term. Within the nuclear industry, the ΔRT_{NDT} is determined from the Charpy transition curve shift indexed at 30 ft-lbs (41 J) of absorbed energy.

The requirement to conduct an RPV surveillance program is given in 10CFR50 Appendix H, and the detailed implementation is described in American Society for Testing and Materials (ASTM) standard E 185. For most boiling water reactor (BWR) plants in the US, three surveillance capsules were placed in the downcomer near the vessel inner diameter (ID) surface prior to initial startup. These capsules contain neutron dosimeters and tensile specimens in addition to Charpy specimens. Some capsules contain Charpy and tensile specimens that were machined from an ASTM reference plate (referred to as correlation monitor material) and these specimens were included so that utilities could compare data from their surveillance program with a large industry data set to confirm the validity of their program. This could be accomplished by plotting the data on a graph of ΔT_{30} versus fluence. However, because of data traceability problems, ASTM has been slow to standardize a procedure and the correlation monitor data have not been widely used. However, it is prudent to test and report these data and thereby contribute to the national data base.

1.2 Surveillance Program Description

This work was performed as part of the Boiling Water Reactor Vessel Internals Project (BWRVIP) Integrated Surveillance Program (ISP) [1-4]. The BWRVIP developed the ISP to maximize the effectiveness of BWR surveillance capsule programs. The River Bend 183 degree capsule was selected as an ISP capsule because of the importance of these capsule materials in the development of BWR trend curves.

Three surveillance capsules were installed within the River Bend downcomer region prior to initial operation. To date, one of the capsules has been removed for testing. The number and type of mechanical behavior specimens included in the original surveillance program as specified by General Electric (GE), as well as the capsule identification and location within the vessel, are summarized in Table 1-1.

1.3 183 Degree Capsule Opening

The surveillance capsule was shipped to MPM during May, 2002 and was opened on 5/21/02. The outside of the capsule had the following identification marking stamped on the stainless steel surface: GE131C8981G001 REACTOR CODE 72. As expected, a total of 36 Charpy V-notch specimens were recovered along with two Fe and two Cu dosimeter wires. One end of each Charpy specimen was stamped with the number 72. The other end of the Charpy specimen was stamped with either a B for base metal, a W for weld metal, or an H for heat-affected-zone (HAZ). Each specimen was placed in a plastic vial and MPM assigned the following numbering system to the specimens so that the identity of each specimen could be maintained in the future:

Base Metal Specimens	- B1through B12
Weld Metal Specimens	- W1 through W12
HAZ Metal Specimens	- H1through H12

As a result of uncertainty in the location of dosimeter wires in the past, MPM paid particular attention to the specimen and dosimeter wire locations during disassembly of the River Bend capsule. As shown in Figure 1-2, the dosimeter wires were recovered near the bottom of the capsule and are distributed in the radial direction along the end of the Charpy bars. In fact, the wires were placed between the ends of the Charpy bars and a flat spacer plate. As a result of the uncertainty in the radial location of the dosimeter wires, additional dosimetry analyses were performed using the Charpy bar material as the dosimeter. In particular, thin slabs of material were cut from the Charpy specimens after testing. Specimens were taken at the bottom of the capsule adjacent to the dosimetry wires (Charpy specimen H1), at mid-height (Charpy specimen W-6), and at the axial top of the capsule (Charpy specimen B-12). Further details concerning the supplemental dosimetry are given later in the report.

1.4 Chapter 1 References

[1-1] Code of Federal Regulations, Title 10, Part 50, Appendix G.

[1-2] ASME Boiler and Pressure Vessel Code, Section III, Appendix G for Nuclear Power Plant Components, Division 1, "Protection Against Nonductile Failure", 1995 Edition and Addenda through 1996.

[1-3] U.S. NRC Regulatory Guide 1.99, "Radiation Embrittlement of Reactor Vessel Materials," Revision 2, May 1988.

[1-4] BWRVIP-86-A: BWR Vessel and Internals Project, "Updated BWR Integrated Surveillance Program Implementation Plan," EPRI Technical Report 1003346, October 2002.

Table 1-1
River Bend Surveillance Program Mechanical Behavior/Dosimeter Wire Specimen Inventory

Surveillance Capsule Contents and Locations[1]							
Capsule No.	**Number of Transverse Charpy Specimens**				**Number of Flux Wires**		**Withdrawal Schedule**
	Azimuth	Base	HAZ	Weld	Fe	Cu	
3	183 degree	12	12	12	2	2	Pulled 10.08 EFPY
2	177 degree	12	12	12	2	2	2025[2]
1	3 degree	12	12	12	2	2	TBD[3]

[1] The surveillance program does not include tensile specimens.

[2] Per BWRVIP-86-A [1-4].

[3] Capsule No. 1 was removed from the vessel and remained out of the vessel during cycle 7. This capsule is designated as the "standby" capsule.

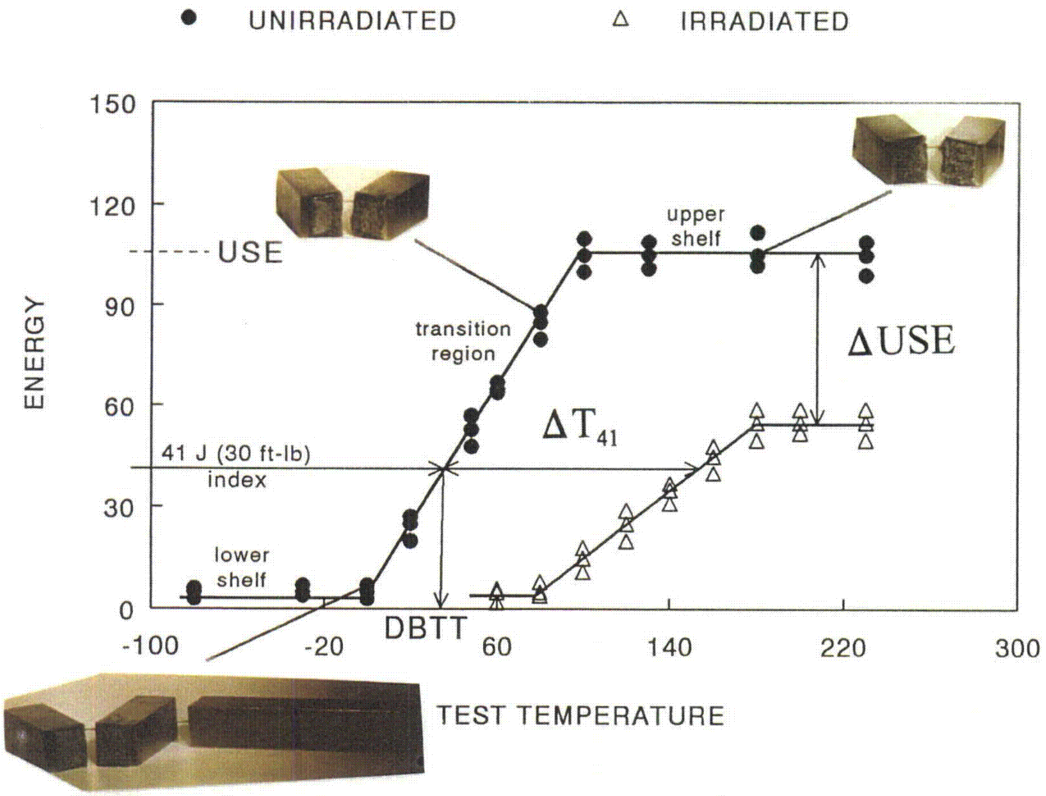

NOT ACTUAL DATA

Figure 1-1
Schematic Illustration of a Typical Charpy Curve and the Effect of Neutron Irradiation on the Curve. Ferritic Pressure Vessel Steels Exhibit a Transition in Fracture Behavior as the Notched Bar Impact Test Temperature is Increased: at Low Temperatures the Fracture is Predominantly Cleavage; at Intermediate Temperatures the Fracture is a Mixture of both Cleavage and Ductile Tearing; and Above the Transition Region the Fracture is Entirely Ductile

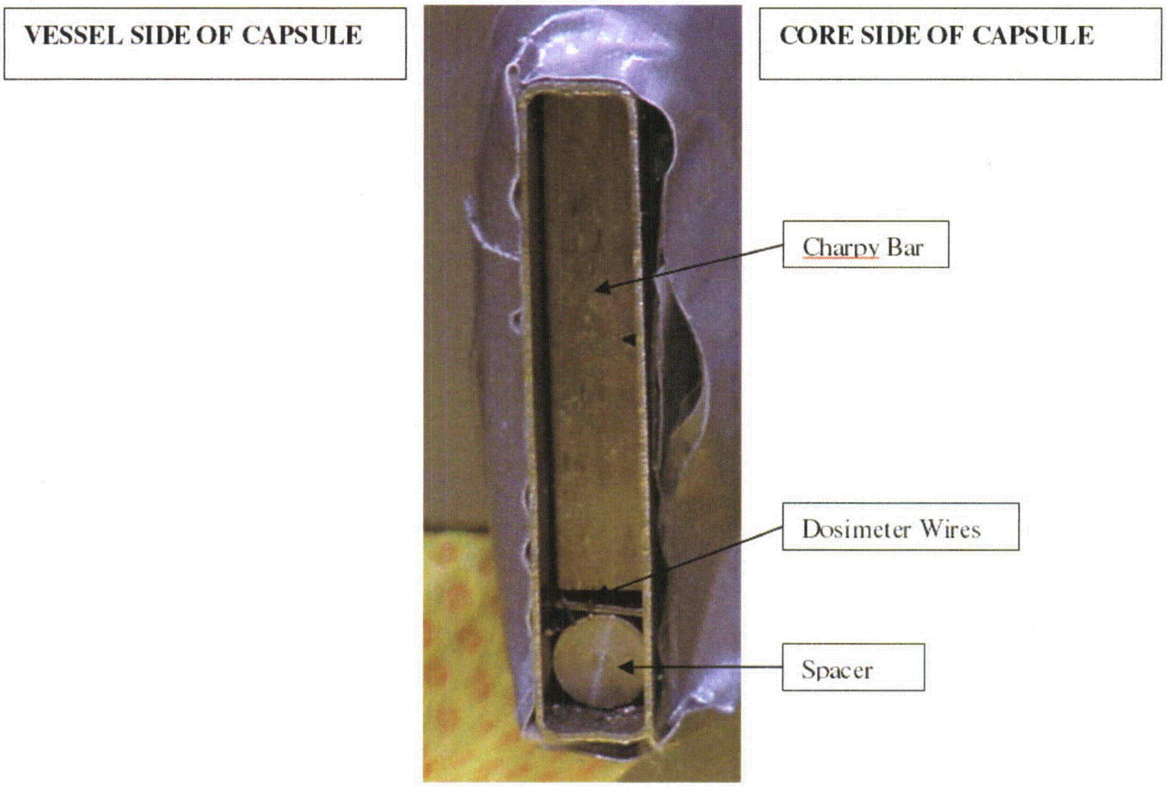

Figure 1-2
Photograph of the River Bend 183 Degree Surveillance Capsule Taken During Disassembly. The Cut was made Near the Bottom of the Capsule.

2
NEUTRON DOSIMETER MEASUREMENTS

2.1 Dosimeter Material Description

The primary dosimeter materials are pure metal wires which were located within the surveillance capsule. The wire types provided for the capsule surveillance program are copper and iron. Each wire is about 3 inches (7.62 cm) long. In addition to the pure metal wires, sections of Charpy specimens composed of base and weld metal were taken for radiometric analysis to provide additional neutron dosimetry. As discussed later in this report, the Charpy bar dosimetry material was used to resolve questions concerning the radial location of the dosimeter wires inside the capsule.

2.2 Dosimeter Cleaning and Mass Measurement

Upon receipt at the radiometric lab, the wires were visually inspected and cleaned with a lab wipe soaked in pure ethanol. The wire segments were then examined under low magnification. There appeared to be evidence of oxidation and some remaining surface contamination, indicating the need for further cleaning. This was accomplished by soaking the wire segments in a 4N solution of hydrochloric acid, followed by immersion in a 2N solution of nitric acid. The wires were then rinsed with distilled water, wiped once more with ethanol, and then allowed to dry in air at room temperature. The wires then exhibited a clean, shiny appearance. The total mass of each wire was measured using a Mettler AX-205 digital balance. Table 2-1 lists the results of these measurements, as well as the identification assigned to each dosimeter. Each wire was wrapped around a thin metal rod to form a coil of approximately 0.25 inch (6.35 mm) diameter, which yields a reasonable approximation to a point source geometry. The coiled wire segments were pressed firmly against a hard surface to flatten the coil.

The Charpy specimen dosimetry slabs were taken from the fracture surface side of one-half of a Charpy test specimen. The Charpy half was first cleaned in pure ethanol to remove any loose material. The fracture surface of the specimen had been previously machined to remove metal chips for chemical analysis. The Charpy specimen was marked to a depth of approximately 0.1 inch (2.54 mm) from the fracture surface. A hand-held rotary cutting tool equipped with a carbide cutting disk was used to section the Charpy specimen approximately, resulting in a piece of material approximately 0.1 inches (2.54 mm) thick and ~0.4 inches x 0.4 inches (10.16 mm x 10.16 mm). This sample was cleaned of loose materials and corrosion by wiping it with a clean cloth soaked in pure ethanol. The sample presented a clean, bright appearance. The specimen was then weighed using the same procedure as for the dosimeter wires. Table 2-2 lists the mass of the Charpy specimen sections and the physical size of the sections are given in Table 2-3.

2.3 Radiometric Analysis

Radiometric analysis was performed using high resolution gamma emission spectroscopy. In this method, gamma emissions from the dosimeter materials are detected and quantified using solid-state gamma ray detectors and computer-based signal processing and spectrum analysis. The specifications of the gamma ray spectrometer system (GRSS) are listed in Table 2-4. While the overall GRSS features three separate hyperpure germanium (HPGe) detectors, only one was used for this study. The detector is housed in a lead-copper shield (cave) to reduce background count rates.

System calibration was performed using a National Institute for Standards and Technology (NIST) traceable quasi-point source supplied by Amersham Corporation. The analysis software was procured from Aptec Nuclear, Inc. and provides the capability for energy resolution and efficiency calibration using specified standard source information. Calibration information is stored on magnetic disk for use by the spectrographic analysis software package.

Since detector efficiency depends on the source-detector geometry, a fixed, reproducible geometry/distance must be selected for the gamma spectrographic analysis of the dosimeter materials. For the dosimeter wires, the counting geometry was that of a quasi-point source (coiled wire) placed 5 inches (12.7 cm) vertically from the top surface of the detector shell. In this way, extended sources up to 0.5 inch (1.27 cm) can be analyzed with a good approximation to a point source. The coiled wires were well within the area needed to approximate a point source geometry. The HPGe detector was calibrated for efficiency using the NIST traceable source.

Radiometric analysis of the Charpy specimen segment was performed using the HPGe detector with a source-detector geometry that placed the source (Charpy slab specimen) 8 inches (20.32 cm) away from the surface of the detector. Since the Charpy section was only approximately 0.4 inches (10.16 mm)on a side and approximately 0.1 inches (2.54 mm) thick (or less), the small solid angle subtended by the source at the detector location allows the use of a quasi-point source efficiency calibration. As with the wire dosimeters, the HPGe detector efficiency for this geometry was calibrated using a NIST traceable quasi-point source.

The accuracy of the efficiency calibration was checked using a gamma spectrographic analysis of a NIST traceable gamma source, separate from that used to perform the efficiency calibration, and supplied by a separate vendor. The isotope contained in this check source emits gamma rays which span the energy response of the detector for the dosimeter materials. These measurements show that the efficiency calibration is providing a valid estimate of source activity. The acceptance criteria for these measurements are that the software must yield a valid isotopic identification, and that the quantified activity of each correctly identified isotope must be within the uncertainty specified in the source certification. Table 2-5 shows the counting schedule established for this work. There was no requirement for order of counting, since the dosimeter materials still contained sufficient quantities of activation products to allow accurate radioassay. As noted below, the radiometric procedure involves an overnight counting period. For this reason, checks of the system performance were done before and after the wire counts.

Neutrons interact with the constituent nuclei of the dosimeter materials, producing radionuclides in varying amounts depending on total neutron fluence and its energy spectrum, and the nuclear properties of the dosimeter materials. Table 2-6 lists the reactions of interest and their resultant radionuclide products for each element contained in the dosimeters. These are threshold reactions involving an n-p or n-α interaction.

Finally, Table 2-7 presents the primary results of interest for flux determination. The activity units are in dps/mg, which normalizes the activity to dosimeter mass. The activities are specified for both the time of the analysis, and a reference date/time, which in this case is the River Bend shutdown date and time. This was specified as March 5, 2000, at 1:16 EST.

Table 2-1
Wire Dosimeter Masses

Wire Dosimeter ID	Mass (mg)
Cu 1	217.78
Cu 2	218.64
Fe 1	63.70
Fe 2	56.91

Table 2-2
Charpy Specimen Section Dosimeter Masses

Charpy Section Dosimeter ID	Mass (mg)
W-6 (Weld Metal)	1113.78
B-12 (Base Metal)	247.28
H-1(a) (HAZ Specimen-Base Metal Half)	1525.47
H-1(b) (HAZ Specimen-Weld Metal Half)	870.63

Table 2-3
Charpy Specimen Section Dosimeter Sizes

Charpy Section Dosimeter ID	Dimensions (length x width x thickness) Inches (mm)
W-6 (Weld Metal)	0.409 x 0.421 x 0.076 (10.39 x 10.69 x 1.93)
B-12 (Base Metal)	0.401 x 0.396 x 0.022 (10.19 x 10.06 x 0.56)
H-1(a) (HAZ Specimen-Base Metal Half)	0.405 x 0.405 x 0.071 (10.29 x 10.29 x 1.80)
H-1(b) (HAZ Specimen-Weld Metal Half)	0.400 x 0.416 x 0.067 (10.16 x 10.57 x 1.70)

Table 2-4
GRSS Specifications

System Component	Description and/or Specifications
Detector	Canberra Model GC1420 HPGe
Energy Resolution	1.77 KeV @ 1332.5 KeV
Detector Efficiency (relative to a 3 inch x 3 inch (7.62 cm x 7.62 cm)NaI crystal)	14% at 1332.5 KeV
Amplifier	Aptec Nuclear Inc. Model 6300 Low-Noise Spectroscopy Amplifier
ADC	Aptec Nuclear Inc. Model S5008 PC-ISA card, 8192 Channels, 6 μsec. fixed conversion time, successive approximation conversion method
Computer System	733 MHZ Pentium III-Based PC, 256 MB Main Memory, 40 GB Hard Disk, 17-inch (43.18 cm) Monitor, Lexmark T620 Printer
Software	Aptec Nuclear Inc. OSQ/Professional Version 7.08
Bias Voltage Supply	Mechtronics Model 258

Table 2-5
Counting Schedule for the Dosimeter Materials

Dosimeter ID	Count Start Date	Count Start Time (ET)	Count Duration (Live Time Seconds)
Fe-1	7/9/02	16:15	58878
Fe-2	7/10/02	16:23	60763
Cu-1	7/11/02	16:58	55482
Cu-2	7/22/02	16:53	56939
Charpy B-12 Base Metal	11/21/02	15:27	61163
Charpy W-6 Weld Metal	11/22/02	11:18	4381
Charpy H-1(a) Base Metal	11/25/02	11:24	2680
Charpy H-1(b) Weld Metal	11/26/02	13:46	3881

Table 2-6
Neutron-Induced Reactions of Interest

Dosimeter Material	Neutron-Induced Reaction	Reaction Product Radionuclide
Iron	$Fe^{54}(n,p)Mn^{54}$	Mn^{54}
Copper	$Cu^{63}(n,\alpha)Co^{60}$	Co^{60}

Table 2-7
Results of the Radiometric Analysis

Dosimeter ID	Isotope ID	Activity At Count Date/Time (dps/mg)	Activity At Reference Date/Time[a] (dps/mg)	Activity Uncertainty (%)
Cu-1	^{60}Co	31.78	43.30	1.49
Fe-1	^{54}Mn	46.54	311.7	2.35
Cu-2	^{60}Co	30.95	42.34	1.49
Fe-2	^{54}Mn	48.33	325.2	2.35
Charpy B-12 Base Metal	^{54}Mn	36.08	326.9	1.18
Charpy W-6 Weld Metal	^{54}Mn	34.74	315.2	1.31
Charpy H-1(a) Base Metal	^{54}Mn	33.95	310.2	1.42
Charpy H-1(b) Weld Metal	^{54}Mn	34.69	317.7	1.45

[a] March 5, 2000 at 1:16 EST is the reference date and time.

3
NEUTRON FLUENCE CALCULATION

3.1 Introduction

The neutron exposure of reactor structures is determined by a neutron transport calculation, or a combination of neutron transport calculations, to represent the distribution of neutron flux in three dimensions. The calculation determines the distribution of neutrons of all energies from their source from fission in the core region to their eventual absorption or leakage from the system. The calculation uses a model of the reactor geometry that includes the significant structures and geometrical details necessary to define the neutron environment at all locations of interest.

During reactor operation, the neutron flux level at any point in the surveillance capsule or vessel will vary due to changes in fuel composition, power distributions within the core, and water void fraction. These changes occur between fuel cycles due to changes in fuel loading and fuel design, and within a fuel cycle due to fuel burnup and resultant changes in power shape, control rod position, fission contributions by nuclide, and void fraction vs. axial height in each fuel bundle. In order to evaluate the exposure, therefore, it is necessary to perform a sufficient number of calculations to provide an accurate integral over the reactor operating history. In the analysis of the River Bend surveillance capsule, which was irradiated for nine fuel cycles, a calculation was performed for the average operating condition for each fuel cycle to take into account the changes that occur between cycles. Moreover, two calculations were performed for cycle 6, which had two distinct operating periods. To provide the most accurate analysis of the iron dosimeters, which produce Mn-54 (312-day half-life), the final capsule irradiation cycle was broken into five parts. Each part was about 20% of the cycle and calculations of each part produced a detailed estimate of the time variation of the neutron leakage flux during the cycle. Thus the analysis of the reactor exposure for the first nine cycles was carried out using 14 separate calculational cases.

In March 2001, the NRC issued Regulatory Guide (RG) 1.190,"Calculational and Dosimetry Methods for Determining Pressure Vessel Neutron Fluence" [3-1]. The guide was developed to provide state-of-the-art calculational and measurement procedures that are acceptable to the NRC staff for determining pressure vessel fluence. Although specifically developed to address calculation of fluence to the vessel, the guide can be considered to apply to other reactor components such as the shroud or surveillance capsule. The calculations reported here fully satisfy the Regulatory Guide 1.190 (RG 1.190) requirements.

One of the requirements of RG 1.190 is the benchmarking of the methodology used in the fluence determination. Specifically, RG 1.190 has the following requirement:

> *Methods Qualification. The calculational methodology must be qualified by both (1) comparisons to measurement and calculational benchmarks and (2) an analytic uncertainty analysis. The methods used to calculate the benchmarks must be consistent (to the extent possible) with the methods used to calculate the vessel fluence. The overall calculational bias and uncertainty must be determined by an appropriate combination of the analytic uncertainty analysis and the uncertainty analysis based on the comparisons to the benchmarks.*

Benchmarking the methodology requires more than one analysis. Because fluence measurements cannot be made at all of the actual points of interest in an operating plant, neutron transport calculations are necessary to obtain the fluence at all important locations. Since the calculations involve many parameters, agreement of calculations with measurements at one point in space cannot guarantee the same calculational accuracy at other points. Previous analyses have been conducted to benchmark the MPM calculational methodology [3-2]. Further discussion of benchmarking is provided later in this report section.

3.2 Neutron Transport Model

The transport calculations for River Bend were carried out in R-θ and R-Z geometry using the DORT two-dimensional discrete ordinates code [3-3] and the BUGLE-96 cross-section library [3-4]. The DORT code is an update of the DOT code that has been in use for this type of problem for many years. The BUGLE-96 library is a 47-energy group ENDF/B-VI based data set produced specifically for light water reactor applications (an update of the earlier SAILOR library). The energy group boundaries for the 47 groups are given in Table 3-1. This library contains cross-sections collapsed using a BWR core spectrum which were used for the core region. Outside the core region, cross sections collapsed using pressurized water reactor (PWR) downcomer and PWR vessel spectra were used. The difference between BWR and PWR collapsing in these regions is not significant. In these analyses, anisotropic scattering was treated with a P3 expansion of the scattering cross-sections, and the angular discretization was modeled with an S8 order of angular quadrature. These procedures are in accordance with ASTM Standard E 482 [3-5].

The computer codes were obtained from the Radiation Safety Information Computational Center (RSICC) at Oak Ridge National Laboratory. Each code was then compiled on the computer used by MPM for the calculations and a series of test cases were run to verify the code performance. The test cases all agreed within allowable tolerance with established results. This verification was conducted under the MPM Nuclear Quality Assurance Program. The calculational procedures meet standards specified by the NRC and ASTM as appropriate. In particular, the analysis (including all modeling details and cross-sections) is consistent Reg. Guide 1.190.

R-θ Calculations

The R-θ layout is shown in Figure 3-1. Dimensions for the various structures are given in Table 3-2 [3-6, 3-7, 3-8, and 3-9]. In this figure, all structures outside the core were modeled with a cylindrical symmetry except for the inclusion of a surveillance capsule centered at 3 degrees and jet pump structures located in the downcomer region. The latter are not to scale in the figure. The jet pumps are approximate models of two pumps with a central pipe (riser) in between. These structures were modeled as stainless steel pipes with downcomer water inside.

The R-θ model included 170 mesh points in the radial direction covering the range from the center of the core to about 10 inches (25.4 cm) into the biological shield. This large number of mesh points was used to accurately calculate the neutron flux transport from the core edge to the outside of the vessel. In the azimuthal direction, 90 mesh points were used to model a single octant of the reactor. The 90 azimuthal points provided good definition of the variation of the core edge with angle and defined the azimuthal flux variation. The particular octant chosen was that extending from 180 to 225 degrees which is the octant containing the 183 degree surveillance capsule. Inspection of the fuel loading patterns indicated that minor deviations from an octant symmetry were present in many of the cycles, so other octants might have a fluence slightly different from the one analyzed. In addition, some other octants differ by having no surveillance capsule and by having more jet pumps. The effect of the surveillance capsule is to lower the fluence slightly to the part of the vessel directly behind the capsule. The effect of additional jet pump steel is to lower the fluence to the vessel in the vicinity of these structures.

The 90 azimuthal points provided good definition of the variation of the core edge with angle and defined the azimuthal flux variation. In the model layout, all angles are referred to in the first octant (i.e. relative to the nearest cardinal axis) and thus the 183 degree surveillance capsule is referred to as being at 3 degrees. It should be noted that the azimuthal flux shape between 45° and 90° is the mirror image of that between 0° and 45° (i.e. an angle of 50° corresponds to 40° in the first octant).

The core region used a homogenized material distribution which includes the fuel, fuel cladding, and the water. The water region in the fuel contains both liquid water and steam. The nodal water densities were supplied for each assembly at 25 axial nodes [3-7] at a number of burnup steps during each fuel cycle. These nodal values were then converted to a smeared density using a relationship that takes into account bypass and water hole flow areas that are assumed to be solid water at the saturated water density for a pressure of 1055 psia (7.27 MPa). The smeared density varies with fuel design, so the density relation is different for each type of fuel.

Inspection of the axial variation of the density values indicated that water density distributions at a burnup step near the middle of the cycle provided a good estimate of typical values for the cycle (or subcycle irradiation period). Therefore, a representative density distribution was selected for each calculation case. To model the void fraction variation in the R-θ model, midplane values of the water densities were used. To get the most accurate density distributions, each fuel bundle in the outer row was modeled as a separate region. For the next to outer row, groups of bundles with similar water density were lumped into a total of 3 regions. The remaining bundles were combined into a single density region. This resulted in a total of 14 regions in the core for the R-θ model. The fuel bundles in each of these regions are indicated by the region numbers defined in Figure 3-1.

Water density in the bypass region was taken to be an average between the core inlet density of 0.7550 g/cc and the outlet density assumed to be the saturated value of 0.7350 g/cc. The downcomer water density was calculated for a temperature of 536.3 F (280.17 C) and a pressure of 1055 psia (7.27 MPa).

The DOTSOR code (available as part of the LEPRICON code package [3-10]), was used to convert the cycle power distributions from X,Y to R,θ coordinates and to place the source in each mesh cell. The source per group was defined by an average fission spectrum calculated for a fission breakdown by isotope determined for the average burnup of the outer fuel bundles for each case. The main isotopes that contribute to the fission spectrum are U-235 and Pu-239, but contributions from U-238, Pu-240, and Pu-241 were also included. This is a good approximation to the fission spectrum because the outer assemblies were all burned assemblies with similar burnup, (except for the first cycle which had all fresh fuel), and the fission spectrum only slowly varies with burnup. Almost all of the neutrons that reach the capsule and vessel originate in the outer rows of fuel bundles.

The source calculations used the appropriate power distribution for all the fuel bundles in the octant together with cycle-specific pin power distributions for the outer three rows of bundles. The pin power distributions were used to model the spatial variation of the source within the bundles and took into account the gaps between bundles and water rods in the center. Equal pin power weighting was used for interior fuel bundles. The pin power distributions were supplied for a burnup step near the middle of each cycle (or subcycle) that was judged to be typical. The pin power distributions were supplied in three dimensions, but the approximation was made that the midplane pin powers could be used to represent the entire core height.

R-Z Calculations

A second set of transport calculations were performed for each case in R-Z geometry. For this calculation, the core was divided into 3 radial regions. Two of these regions consisted of each of the outer two rows of assemblies averaged over the octant. The third region consisted of the inner part of the core. The neutron source in each of these regions was calculated using a radial source averaged over the octant (calculated by integrating the source from the R-θ case) together with an average axial power shape for each region. The axial power distribution was supplied for each assembly in 25 nodes, each representing 6 inches (15.24 cm) of core height. Neutron source outside the equivalent core radius was eliminated.

Each radial region was also divided into 25 axial regions according to variation in water density. This resulted in a total of 75 regions in the core, each with a distinct cross section set. In addition, the GE11 fuel bundles contain 8 part length fuel pins that end at 96 inches (2.44 m) above the bottom of the active fuel (BAF). The volume of these pins was replaced with water at axial meshes above the 96 inch (2.44 m) level. The GE11 fuel bundles also have no fuel in the top 4 inches (10.16 cm) of core and the model for the fuel cycles transitioning to this fuel (cycles 7 to 9) took this into account also.

For the R-Z model, the core radius was taken to be that which gave the equivalent core volume. Regions above and below the core were approximately modeled with several upper and lower reflecting regions consisting of smeared mixtures of water and structural materials. These regions extended about 20 inches (50.80 cm) from the core with vacuum boundaries at the top and bottom of the model. The model had identical mesh points in the radial direction as in the R-θ model, and in the axial direction, the model had 148 mesh points with 95 in the core region.

Flux Synthesis

As indicated above, the calculations were carried out in 2 dimensions. In order to estimate the fluence rate in the 3 dimensional geometry, the following equation was used to evaluate the flux, N, for each cycle case:

$$N(R,\theta,Z) = N(R,\theta) * N(R,Z) / N(R)$$ **Equation 3-1**

In this equation, N (R,θ) is taken from the DORT R,θ calculation (normalized to the power at midplane in the model region), and N (R,Z) is from the R,Z calculation normalized to the power in the entire core. A third calculation determined N (R) using a one-dimensional cylindrical model normalized at core midplane. The model for the one-dimensional calculation used the same radial geometry as the R,Z calculation at midplane.

3.3 Capsule Fluence Results

The calculated fast fluxes and dpa/s for each case for the 183 degree surveillance capsule are given in Table 3-3. These values are for the radial midpoint of the capsule at the axial midplane and at the azimuthal point corresponding to the center of the Charpy specimens. The average flux spectrum at this point for the nine cycles is given in Table 3-1. The standard deviation of the flux for the nine cycles is 10%. This standard deviation is calculated using the average flux for each cycle (i.e. the two cases for cycle 6 and the five cases for cycle 9 are combined to give an average flux for each cycle to include in the calculation of the standard deviation). For the five cycle nine cases, the standard deviation is 3%. The relatively small variation in this cycle is probably due in part to the fact that this was a short cycle.

Table 3-4 gives fluence values for the capsule for each of the 9 cycles and the total fluence at the end of cycle 9. For the fluence at the end of cycle 9, the lead factor (capsule over vessel maximum) at the vessel surface is calculated to be 0.95 ($1.156 \times 10^{18}/1.212 \times 10^{18}$), and the lead factor at the 1/4T location is 1.324 ($1.156 \times 10^{18}/8.73 \times 10^{17}$) using the vessel maximum fluence results given in Section 3-5.

Uncertainty in the evaluation of the capsule fluence is evaluated in Section 3-6.

3.4 Capsule Measurement Results

The 183 degree capsule was removed at the end of cycle 9 and was irradiated from initial reactor start-up in 1985 to March 5, 2000, for a total of 10.08 effective full power years (EFPY) [3-8]. The power history was supplied as the thermal generation integrated over various intervals encompassing the time from initial criticality to the end of cycle 9, and the data are given in Table 3-5. Most of the power generation intervals fall in the range of 20 to 60 days. The use of intervals of this length for the power history data is not expected to introduce any significant error in the evaluation of the dosimetry results since the half-lives of both Mn-54 and Co-60 are significantly longer than these intervals.

The capsule dosimetry consisted of two sets of copper and iron wires. This dosimetry was counted to determine the fast neutron reactions shown in Table 3-6. This table also gives the nuclear constants used to determine the reaction rates. These data are taken from the appropriate ASTM standards [3-11, 3-12, and 3-13]. The location of the dosimetry wires in the capsule was noted upon the capsule disassembly (Figure 1-2). The wires were found to be located at the right end of the Charpy bars (as viewed from the reactor core) and at the bottom of the capsule. Although not exactly defined, the wires were taken to be located midway between the capsule radial center and the rear of the capsule. Since the wires were about 2 inches (5.08 cm) in axial length, the dosimeter location was taken to be 1 inch (2.54 cm) above the spacer bar at the bottom of the capsule.

Additional steel samples cut from selected Charpy specimens were analyzed for the iron reaction to provide confirmation of the iron reaction rate and dosimeter location. The samples were taken from near the middle of the Charpy bars and from bars located at the axial bottom, middle, and top of the capsule.

The dosimetry results that relate to fast fluence are given in Table 3-7. The dosimeter measurements are presented in units of disintegrations per second per milligram (dps/mg), adjusted to the end-of-irradiation (March 5, 2000 at 1:16 EST). Using the power history and the reaction rates for Fe and Cu determined by the DORT calculation for each cycle and the five cycle 9 cases, the activity at the end of the irradiation was calculated at the precise location of each dosimeter or steel sample. The results were obtained by multiplying the reaction rate for each reaction obtained from the synthesis procedure by the effective full power seconds (EFPS) for each time interval and then accounting for radioactive decay during the interval and to the end-of-irradiation time. The number of activation product atoms per target atom is converted to dps/mg using the parameters in Table 3-6. For the steel samples, measurements of the fraction of iron were made on each sample. These values were close to identical and the average value was 0.966. This factor was used to adjust the calculated iron activity to dps/mg for the steel samples (i.e. all values are per mg of sample, not per mg of iron).

The neutron multigroup flux spectrum at the center of the surveillance capsule averaged over the 9 cycles is given in Table 3-1. The spectrum at the dosimeter locations is close to that at the capsule center. At the wire locations, the $Fe^{54}(n,p)$ average reaction rate was calculated to be 5.74 x 10^{-16} reactions per second per atom and the average cross section above 1 MeV is equal to 157.1 mb. Similarly, the average reaction rate for $Cu^{63}(n,\alpha)$ was calculated to be 8.29 x 10^{-18} reactions per second per atom and the average cross section above 1 MeV is equal to 2.269 mb.

The calculated-to-experimental (C/E) ratios for each dosimeter measurement and the average are summarized in Table 3-7. The average C/E value for the two measurements of the $Cu^{63}(n,\alpha)$ reaction was found to be 0.80. The C/E values for the two dosimeter wire measurements and the four Charpy sample measurements of the $Fe^{54}(n,p)$ reaction were also averaged (with equal weight) to give a C/E of 0.86. As shown in Table 3-7, all of the dosimetry measurements are within 20 % of the calculation with the exception being the Cu-1 wire. Further discussion of the Cu-1 result, along with analysis of the uncertainty contributions to the C/E ratio, is provided below.

Uncertainties in the activity measurements (dps/mg of sample) fall in the range of 1.2% to 2.4% (Table 2-7). These values are regarded as precision estimates and are considered to be random.

The measurements also contain a systematic uncertainty (due primarily to calibration uncertainty) that is typically about 3% [3-11, 3-12]. Total uncertainty in each activity measurement is then between 3% and 4% (obtained by combining the random and systematic uncertainty in quadrature).

The uncertainty in the C/E ratio also contains contributions relating to dosimetry measurements due to the dosimeter position uncertainty, dosimeter spectral average cross section uncertainty, and the flux history uncertainty. These will be treated separately for iron and copper.

$Fe^{54}(n,p)Mn^{54}$ Reaction

The dosimeter position uncertainty is due mainly to radial position uncertainty. For the $Fe^{54}(n,p)$ reaction, the decrease radially across the capsule is calculated to be 20%. The radial location of the dosimetry wires is not exact, but was observed to be towards the vessel side of the capsule. If the position is assumed to be midway between the capsule center and the capsule rear, a radial position uncertainty of 25% of the distance across the capsule would be reasonable. This gives a position uncertainty for the iron wire dosimeter measurements of 5%. A similar analysis of positional uncertainty for the Charpy bar dosimeters is also warranted. The Charpy specimen dosimetry samples were cut so that the sample was taken from the entire cross section of the Charpy bar, and is therefore well approximated as being centered in the capsule. However, some error may still exist due to cutting uncertainty and due to the fact that the slice was not taken at the center of the test specimen. For conservatism, a 5 % uncertainty is assumed. All of the iron results lie closer to the mean than this assumed 5% uncertainty band.

The iron dosimeter cross section uncertainty is given in the ENDF/B cross section evaluation and is also limited by correlation with benchmark measurements. $Fe^{54}(n,p)$ integral cross section measurements in fission spectra are in very good agreement with calculated values [3-14] (differences of less than 2%). The BUGLE-96 cross sections are consistent with those recommended in ASTM standard E1018 [3-15]. This specifies the cross section uncertainty in terms of a covariance matrix that enables the integral cross section uncertainty to be calculated if the spectrum uncertainty is known. For the case here, an estimate of the cross section uncertainty is calculated using only the diagonal elements of the covariance matrix and assuming the group values are fully correlated (conservative assumption). This gives an estimate of the iron cross section uncertainty of 4%, assuming the spectrum uncertainty in the critical region is small. In the capsule spectrum, the $Fe^{54}(n,p)$ reaction has most of its response (i.e. more than 95%) above 2.5 MeV, which covers slightly over half of the fluence above 1 MeV.

The iron reaction has a high dependence on the accuracy of the flux history since the half-life of the measured activity is less than a year. As a result, 84% of the iron response is from the last two irradiation cycles and the fluence contribution from earlier cycles is almost entirely due to the calculated relative flux level. The extensive calculations used here provide a good definition of the flux at the midpoint of each cycle, but may not reflect the actual cycle average due to time effects that are not included. For the cycle 9 cases, the standard deviation of the fast flux was found to be 3%, but this cycle may not be typical. For the first 8 cycles, the standard deviation of flux was 11% (mostly taken into account since the specific values were used for each cycle). Based on these considerations, the uncertainty for the iron reaction is estimated to be twice the 3% standard deviation for the cycle 9 cases, or 6%.

Combining the above uncertainties in quadrature gives a result of 9.6% uncertainty in each individual iron measurement. For the average of the 6 measurements, the measurement precision uncertainty (P) and the location uncertainty (L) are considered to be random errors and all the remaining uncertainties [calibration (C), cross section (X), and history (H)] are systematic. The total uncertainty in the iron average reaction rate is then given by

$$\text{Uncertainty} = \{P^2/n + L^2/n + C^2 + X^2 + H^2\}^{1/2}$$

where n is the number of measurements, 6 in this case. This results in a value of 8.1%. (In the formula, the maximum value for P of 2.4% is used.)

The uncertainty in the calculated reaction rate values also contains the uncertainty in absolute fluence. This uncertainty is evaluated in Section 3-6 to be 14.6% based on estimated uncertainties in transport cross sections, model geometry, neutron source, synthesis methodology, etc. This uncertainty may be assumed to be independent of the other uncertainties in the iron reaction rate, and thus the 8.1% and 14.6% are combined in quadrature to get the total 1σ uncertainty in the C/E ratio. This gives a value of 16.7%. The 8.6% deviation of the average iron C/E ratio from unity is well within this estimated uncertainty.

$Cu^{63}(n,\alpha)Co^{60}$ Reaction

The uncertainty in the copper reaction rates is calculated similarly. For the copper, the precision is slightly better, 1.5% and the detector calibration uncertainty is 3%, the same as for the iron reaction. For the location uncertainty, the calculated change of the reaction rate from the front to the rear of the capsule averages 21% and the position uncertainty is estimated to be 25% of this value, or 5.2%.

The energy group cross section uncertainty for the copper reaction ranges from 8% to 10% over the range of the major copper response [3-15]. For the surveillance capsule spectrum, the $Cu^{63}(n,\alpha)$ reaction has about 97% of the response above 5 MeV which encompasses 21% of the neutron flux above 1 MeV, and about 85% of the response is above 6 MeV which encompasses about 12% of the neutron flux above 1 MeV. Thus the copper spectral average cross section above 1 MeV is more sensitive to spectrum uncertainty than the iron cross section since it only responds to a smaller fraction of the fast neutrons. Integral cross section measurements for $Cu^{63}(n,\alpha)$ in fission spectra are also given in [3-14]. The C/E value in the U235 fission spectrum shows excellent agreement, falling within 2%. The Cf252 fission field measurement shows a larger deviation, about 4%, but the quoted uncertainty is larger, about 13%. Thus the correlations introduced by integral measurements indicate that the cross section in the range of response to fission spectra is better known than the 8-10% from the cross section evaluation. Taking the above factors into account, the copper spectral averaged cross section uncertainty for the surveillance capsule is estimated to be 9%, calculated in the same way as described for the iron reaction above.

The time history uncertainty for the copper reaction is less important than for the iron since the product half life is much longer (about 5.3 years). Thus this reaction provides a better integration over most of the cycles (65% of the response is from cycles 7 and earlier). Therefore, the history uncertainty is estimated to be one-half of the value estimated above for the iron reaction, or 3%.

Combining the uncertainties for the copper reaction in quadrature gives a total uncertainty for each of the copper measurements of 11.3%. For the uncertainty in the average of the two copper measurements, the same formula to that used above for iron is used with n equal to 2. This gives an uncertainty estimate for the average of the two copper measurements of 10.7%. The total uncertainty in the C/E ratio is then the combination of the 10.7% with the 14.3% fluence uncertainty which gives a value of 18.1%. This value is slightly less than the deviation of the C/E ratio for the copper reaction from unity which is 19.7%. Since this is only slightly greater than the 1σ uncertainty estimate, however, the deviation is not considered statistically significant (i.e. the copper result falls within a 90% confidence interval). Although the average value of the copper C/E ratio falls within 20% of the expected value of 1.0, one of the values is slightly outside this range. Considering the uncertainty in the measurement, the deviation of the single measurement is also not considered to be significant.

Comparison of the C/E values for the iron and copper reactions shows that the copper result falls below the iron by 11%. While this is within the experimental uncertainty, it is of interest to compare to previous results to see if there is a consistent bias between these two measurements in similar reactor geometries. In previous comparisons [3-2], the copper results C/E results do not fall consistently below the iron results (see discussion in Section 3.7), but the result for a 3 degree capsule geometry in Nine Mile Point Unit 2 which is similar to River Bend does give a copper to iron comparison with a similar difference. This may indicate a bias that appears in this particular geometry, but further measurements are necessary to confirm this result.

Summary of C/E Uncertainty Analysis

Although the estimated uncertainties in the iron and copper reaction comparisons are slightly different, an average C/E value was calculated with equal weighting of these two results. The resultant average C/E ratio of 0.86 indicates acceptable agreement between the calculation and the measurement. (The weighted average is only slightly different, 0.87.) The experimental uncertainties for the iron and copper measurements are largely independent, and, if the small correlated component is ignored, the uncertainty in the average is 6.5%. Combining this with the 14.6% fluence uncertainty gives an uncertainty for the average C/E ratio of 16%. It is seen that the best estimate C/E value of 0.86 differs from 1.0 within this 16% uncertainty estimate. The C/E value of 0.86 is also within the Regulatory Guide 1.190 guideline of 20% for in-vessel surveillance capsules. It is concluded that the measurement provides an acceptable validation of the adequacy of the calculation. This River Bend-specific measurement provides validation of these calculations for use in vessel fluence determination. In accordance with Regulatory Guide 1.190, the calculated fluence values are recommended for use in estimating vessel embrittlement and in P-T curves.

Analysis of Previous Dosimetry

A measurement of iron dosimeters removed from the top of the 3 degree surveillance capsule at the end of the first fuel cycle was made by GE [3-16]. Three samples were measured and the average value was found to be 190 dps/mg of iron with an estimated uncertainty of 5%. The calculated value based on the present analysis is 176 dps/mg which results in a C/E value of 0.92. This is in excellent agreement with the iron dosimeter result from the 183 degree surveillance capsule.

3.5 Vessel Fluence Results

The fluence to the reactor vessel was also determined from the calculations for each cycle using the flux synthesis. The flux shape was found to vary somewhat from cycle to cycle due to the differences in fuel loading pattern and due to differences in axial power shape and void fraction. Inspection of the azimuthal variation of the fast flux indicated that the maximum flux in the vessel occurred at approximately 11-13 degrees for some cycles and at about 25 degrees in others. The maximum fluence at the end of cycle 9 is at about 12 degrees and the projected fluence maximum is at about 11 degrees. The difference in location of the maximum is not very significant since the fluence at 10-15 degrees and 24-25 degrees is close to the same. This is shown in Figure 3-2 which is a plot of the fluence (E > 1 MeV) at the end of cycle 9 at core midplane. The fluence is shown for the clad-base metal interface (the vessel inner radius (IR)), at 1/4 of the distance into the vessel (1/4 T), and at 3/4 of the distance through the vessel (3/4 T). The shape of these curves is influenced by the varying amount of water between the core edge and the vessel. The fluence is depressed by the jet pumps at angles between 25 degrees and 40 degrees, and a small effect around 3 degrees is noted due to the capsule.

The peak fluence point varies axially also, both during cycles and between cycles. Therefore, the maximum fluence point must be determined by integrating the flux at several axial heights to find the peak value. The maximum fluence point at the end of cycle 9 is at about 6 inches (15.24 cm) above midplane. This is shown in Figure 3-3 which plots the fluence (E > 1 MeV) at the end of cycle 9 versus axial distance from core midplane for the IR, 1/4 vessel wall thickness (T), and 3/4 T positions. The fluence in this figure is at the maximum azimuth.

Values for the calculated maximum vessel fluence E > 1 MeV, fluence E > 0.1 MeV, and dpa are given in Table 3-8 for the inner radius of the vessel clad (wetted surface), the vessel base metal IR, the 1/4 T position, and the 3/4 T position calculated at the end of cycle 9 (10.08 EFPY). Exposure values extrapolated to 32 EFPY and 48 EFPY are also given in Table 3-8. The data in Table 3-8 have been extrapolated using cycle 7 average flux and dpa/s values since future cycles are projected to be most similar to cycle 7. The values in Table 3-8 are the calculated maxima and thus the axial and azimuthal position of the fluence values in this table for 10.08 and 32 or 48 EFPY are not the same. It should also noted that extrapolation using cycle 7 is conservative since the fluence rate and dpa rate values for this cycle are the highest for the maximum exposure position. The extrapolated fluence values also assume reactor upratings as noted in the footnote to the table. The EFPY values are all referenced to maximum power at the time of operation and thus the upratings increase the fluence per EFPY.

It should be noted that the result calculated for the peak fast fluence (E > 1 MeV) at the vessel base metal surface at 32 EFPY (4.38E18 n/cm2) is considerably below the GE previously estimated value of 7.95E18 n/cm2 [3-17] (GE did not include the clad in the conservative estimate). This is most likely due to several causes. The present calculations were carried out with the more recent cross section set and used the synthesis method to produce the determination of the maximum fluence point. The present calculations also utilized River Bend specific fuel cycle analyses that covered the span of the first nine cycles. In contrast, the earlier fluence estimates are based on calculations using generic plant power distributions. These calculations produced a lead factor estimate of 0.67 as contrasted with the value of 0.95 in the present calculations. Part of this difference may be due to the inclusion of the jet pumps in the model of the reactor midplane geometry. Values of fluence based on the dosimetry measurements reported in [3-16] are also much higher than would be derived using the current methodology. Using the BUGLE-96 dosimetry cross section for the Fe(n,p) reaction, and the calculated capsule spectrum for cycle 1, the ratio of flux (E > 1 MeV) to the iron reaction rate is 17% lower than the GE value from 1988. Using the present calculated lead factor and dosimetry result, the maximum cycle 1 vessel fluence based on the cycle 1 dosimetry would be 1.2E17 in contrast to the value of 2.8E17 in [3-16].

Radiation embrittlement effects are usually correlated with fluence E > 1 MeV. However, it is generally thought that dpa might be a better correlation parameter and, if this is correct, the use of the fluence E > 1 MeV values within the vessel are non-conservative. Accordingly, a dpa attenuation factor is used for fluence through the vessel. This can be done using calculated dpa attenuation from Table 3-8 or using a formulation specified in the RG 1.99(2). The fluence values using both these attenuation methods are given in Table 3-9 for 10.08, 32, and 48 EFPY.

The dpa values in this report are calculated from the ASTM E693-94 Standard dpa cross-section [3-18]. This evaluation of the dpa cross section is based on the ENDF-IV cross-section file. A new dpa cross-section evaluation based on ENDF-VI (consistent with the cross-sections in BUGLE-96) is expected to be used as the standard in the future. The new standard was not used here in order to be consistent with past practice. Change to the new cross section would result in at most a few percent change in the dpa results.

3.6 Uncertainty Estimation

A detailed uncertainty analysis was performed to estimate each source of uncertainty in the calculated fluence values. This analysis made use of defined uncertainties and tolerances where possible, but some of the uncertainty estimates had to be based on estimates derived from data variation, such as the detailed power distribution and void fraction variations within a single cycle. The geometry uncertainty assignments are from Reference [3-6]. Discussion of each uncertainty assumption is given below. Based on these uncertainty values, detailed uncertainty evaluations were performed for the surveillance capsule and reactor vessel. The uncertainty evaluations for reactor beltline locations are summarized in Table 3-10.

In the uncertainty evaluations, uncertainties were treated as normally distributed and all uncertainties were valued in terms of 1 standard deviation (1σ). The individual uncertainties were assumed to be randomly distributed and independent (except where correlations occur such as increases in steel thickness, which results in a decreased water thickness). The total uncertainty is then determined by quadrature (square root of the sum of the squares of the contributing uncertainty components given as 1σ values).

3.6.1 Uncertainty Assumptions

Nuclear Data

Nuclear data input to the transport calculations includes the multigroup cross sections and neutron spectrum. Uncertainties in the cross sections are complicated because of the large number of cross section values and the correlations between these values. Although the uncertainties in individual cross section values may be relatively large, the total effect of cross section uncertainties is limited by adjustments made by cross section evaluators to agree with benchmark data. The approach taken here is to limit the cross section uncertainty effects to just the total cross-section and to evaluate this by varying the material densities (see below).

Uncertainty in the multigroup fission source arises from uncertainty in the fission spectra for each fissioning isotope, the distribution of fission among the fissioning isotopes, the energy release per fission (υ), and the number of neutrons produced per fission (κ). Uncertainty in the fission spectrum is mainly at the higher energies, which has little effect on the fluence above 1 MeV (but does affect the copper reaction rate). The uncertainty was represented as an uncertainty in burnup, which was conservatively taken to be 10,000 MWd/MTU (megawatt days per metric ton of uranium). The uncertainty is assumed to be fairly large to encompass the use of average burnup of the outer fuel bundles rather than including explicitly the detailed radial and axial burnup variation. A 1-D calculation was performed to determine the spectral effect and it was found to vary between 0.2% in the core to less than 2% in the vessel.

The parameters υ and κ both increase slowly with burnup, but the source normalization is proportional to the ratio υ/κ. Thus, the variation with burnup is small. For an uncertainty of 10,000 MWd/MTU, the normalization uncertainty is 1.1%. Since this is in the same direction as the spectrum uncertainty, it is added to the spectrum contribution to give the values in Table 3-10.

Normalization

In addition to the normalization uncertainty due to υ/κ, there is an overall normalization uncertainty in reactor power as measured by the heat balance. This uncertainty is normally assumed to be 2%. For River Bend, the 2% value is appropriate at the current power level, but after the Appendix K uprate this uncertainty will be reduced to 0.3% [3-6].

Geometry

Geometric uncertainties are taken from Reference [3-6]. The vessel inner radius uncertainty was taken to be 0.375 inches (9.53 mm) based on as-built drawings VPF3535-625, VPF3614-704, and VPF3614-450. The uncertainties in the shroud inner radius and thickness were based on as-built measurements given in drawing 50978D70. The 1σ uncertainty was taken as one-half the range of measured values.

Jet Pumps

The jet pumps could not be exactly modeled in the calculations due to the complex geometry of the jet pumps. The steel from the jet pumps was approximately included as cylindrical pipes placed appropriately in the downcomer region in the R,θ calculation. The jet pumps were not included in the R,Z calculation. Modeling of the pipes can only be carried out approximately in the R,θ mesh, but the volume of steel is preserved. Error in the exact location of the steel has only a small effect due to the distance to the vessel. To estimate the uncertainty introduced by the jet pump model, a separate R,θ calculation was made with the jet pumps omitted. This had no effect on the surveillance capsule fluence, but the maximum fluence at the vessel inner radius increased up to 30%. For fluence at the maximum fluence points, a reasonable estimate of uncertainty from the imperfect modeling of the jet pumps is 10% of this value, or 3.0%. Note that in the axial regions where the jet pump structures change geometry or are not present, the calculated fluence derived from the 2-D synthesis should be increased by up to this 30% amount.

Material Densities

The material density uncertainty was treated differently for the water density and the steel density. The water density in the core decreases dramatically with height as the void fraction increases. This change is taken into account by supplying the varying water density in 25 axial nodes. However, the water density also changes during the cycle as the fuel burns and control rods are moved. For the longer cycles, this variation will be larger. In the calculations here, except for cycle 9, the mid-cycle water density pattern was used to represent an average of the density during the whole cycle. Inspection of the changes in water density for cycle 7 (one of the longest cycles to date) indicated that the nodal water density at midplane varied in the edge fuel bundles by ± 15-25% from the average. Shorter cycles had smaller variations. A conservative assumption is that the 1σ deviation in nodal density is one-half the average of these values, or 10%. This results in a total water density variation at axial midplane of 7%.

The bypass water is not thought to have any void volume, but the temperature may vary from the value that was assumed. The uncertainty was estimated by taking one half of the difference between the estimated bypass water density at the bottom and top. This indicates an uncertainty of 1.3%. The uncertainty in the downcomer water density was calculated from an assumed temperature uncertainty of 5 F (2.8 C).

The effect of each of the water density uncertainties on the fluence was calculated separately. Because of the relatively large azimuthal variation in vessel fluence, the effect of the core water density uncertainty and the bypass water density uncertainty were calculated using 2-dimensional R,θ calculations. The uncertainty due to the downcomer water density was determined by a 1-dimensional calculation.

The uncertainty in steel density is less than about 1%. However, as noted above, the cross section uncertainty was included as an addition to the steel density uncertainty. An estimate for this uncertainty was derived by considering vessel mockup benchmark results [3-19], comparisons of reactor cavity and surveillance capsule measurements [3-20, 3-21, 3-22, 3-23], and comparisons of cross section evaluations [3-24]. It was concluded that uncertainties due to the iron cross section contribute a 10% effect on fluence through a PWR reactor vessel. This translates into a cross section uncertainty of 3.5%. This value was adopted as the density variation and uncertainties were calculated based on this uncertainty estimate. In addition, the core cross sections for the fuel and cladding were also assumed to have this uncertainty. This estimate includes effects due to the core homogenization.

Source Uncertainty

Source uncertainties were estimated based on the variation of the calculated power distributions at points within a single cycle, similar to the evaluation of the water density uncertainty. During cycle 7, the midplane relative power for the outer fuel bundles had a standard deviation in the range of 8% to 16%. In the calculations, the exact average was used for the midplane power based on the calculated fuel burnup at each node. However, due to the large variation in relative power during the cycle, the uncertainty was taken to be one-half the average standard deviation, or 6%. To this value, an additional uncertainty of 4% was added to take into account the axial variation of the pin power distributions within the outer fuel bundles. This variation in pin power was not included in the model. Combining these two uncertainties results in a total source uncertainty of 7.7%.

Methods Uncertainty

The neutron transport was calculated using 2-dimensional models of the reactor and the discrete ordinates code. This is only an approximation to the solution of the Boltzmann transport equation and thus also contributes uncertainty. Three components of this uncertainty were included. First, the uncertainty of the fuel model was considered. From the VENUS benchmark measurements, it was found that a typical range of C/E results was about 10% [3-25]. Thus, the standard deviation was about 5% and this value was used here. The second component was the adequacy of the S8 calculation. To test this, S16 calculations were performed for a typical BWR calculation to indicate the accuracy. Differences of 1.4% were observed in the shroud and as high as 3% at the outside of the vessel.

Additional uncertainty is introduced by the 3-D synthesis procedure due to asymmetries in power shapes and geometries. A recent paper [3-26] suggests that differences between DORT results and 3-dimensional calculations using TORT are in the range of 2% to 15% in a BWR shroud, depending on axial height. Of course the 3-dimensional calculation has its own limitations in accurate representation of the geometry. Based on these differences, an additional 5% uncertainty is assigned to the synthesis procedure in the beltline region. In regions near the top or bottom edge of the core where the synthesis is less precise, the uncertainty is larger. As mentioned, effects due to the fact that the capsule and jet pumps do not extend through the entire core height are also not taken into account. Uncertainty contributions due to these effects only are significant for vessel fluences well below the maxima. Significant deviations in the accuracy of the synthesis would be expected above the top of the jet pumps (about four feet above core centerline) at angles behind the pump locations.

The total modeling uncertainty was obtained by summing the above effects in quadrature to give 7.7%.

Flux History

The time integration of reactor power has inaccuracies in addition to the power normalization. These come about because of operation at powers less than maximum, round-off error, etc. These uncertainties are estimated to be about 2%.

3.6.2 Uncertainty Evaluation

The results for the uncertainty evaluation are summarized in Table 3-10, which is applicable to the vessel in the beltline region and the surveillance capsule. In this table, some of the uncertainty results are given as ranges that are derived from the 2-dimensional calculations.

A total uncertainty was derived by combining the independent individual contributors in quadrature. This gave an uncertainty for the maximum vessel fluence of 17.4%, with the largest contributor being the vessel radius uncertainty. The vessel fluence uncertainty is evaluated at the maximum fluence point, but the variation in vessel uncertainty with position is relatively small.

The uncertainty for the capsule fluence was found to be 14.6%. The uncertainty in the surveillance capsule fluence is similar to that for the reactor vessel inner radius with only minor differences. The uncertainty in the capsule radial location is smaller than the vessel IR uncertainty because it is located at a single point and the as-built vessel radius varies somewhat with location. The uncertainty in axial and azimuthal capsule location contributes no significant uncertainty to the fluence. The jet pumps are not near the capsule so no error is contributed from the jet pump model.

3.7 Benchmarking

Previous analyses have been conducted to benchmark the MPM calculational methodology against the Pool Critical Assembly (PCA) simulated reactor vessel benchmark, a BWR geometry calculational benchmark, and a number of Nine Mile Point Unit 1 and 2 (NMP-1, NMP-2) operating plant measurements [3-2]. Complete details are given in [3-2] and the results will be summarized here.

3.7.1 PCA Benchmark

The PCA pressure vessel simulator was constructed to provide a well-characterized geometry that is a mockup of typical reactor geometries. Measurements were made with this simulator arranged in a variety of geometries, including in some cases simulated surveillance capsules, but the recommended benchmark described in Reference [3-27] consists of a single geometry with a 4.724 inch (12 cm) water gap between the reactor core and a thermal shield plate, and a 5.118 inch (13 cm) gap between the thermal shield and the vessel simulator. This geometry, while more typical of PWRs than BWRs, can be used to evaluate the adequacy of the calculational methodology to accurately determine fluence from the core to the rear of the pressure vessel. In particular, measurements within the pressure vessel mockup provide validation of the calculations in this region where dosimetry measurements cannot normally be made.

Average C/E ratios were calculated at each of the PCA measurement locations which include the front and rear of the simulated thermal shield, and positions through the vessel (0T, 1/4T, 1/2T, 3/4T, and cavity). The calculated values were found to be consistently low by 3 to 8%. There was no obvious trend to the bias in going from the location nearest the core to the one at the back of the vessel. The bias results were almost identical to the C/E ratios calculated by Remec [3-27]. Results calculated using BUGLE-96 transport cross sections are also reported in Reference [3-28]. Results in this reference using the synthesis approach show a slight increase in bias going through the pressure vessel, and a three-dimensional calculation was made which largely eliminated this bias. The latter reference did not use the BUGLE-96 dosimetry cross sections and also made comparisons with a slightly different set of measured data. The fact that the three-dimensional calculation eliminated some of the bias illustrates that the synthesis method may contribute a small amount of bias. However, this would be a small effect in evaluating the fluence within the beltline region of a power reactor where streaming is very small except possibly in the reactor cavity.

The conclusion is that the MPM methodology obtains results consistent with calculations performed by qualified NRC contractors and with measurements reported for the PCA. The results show some consistent bias (possibly due to errors in dimensions or source distributions) but this bias is within acceptable tolerance. The results indicate that the calculation produces consistent results in flux variation from the thermal shield through the outside of the vessel.

3.7.2 Calculational Benchmark

In addition to benchmarking against measurements, RG 1.190 has a requirement to benchmark the methodology against a calculational benchmark. The calculational benchmarks to satisfy this requirement are documented in Reference [3-29]. The benchmark problems include 3 different PWR geometries and a single BWR problem. It is intended that the analyst select the benchmark problem or problems appropriate to the plant being analyzed. Accordingly, the BWR problem has been calculated since this problem is the one particularly appropriate for BWR applications. The benchmark problems are designed to ensure that two major difficulties encountered in neutron transport analysis are addressed. First is the strong attenuation of the neutron flux between the edge of the core and the vessel and through the vessel. This large attenuation makes the vessel fluence dependent on the cross section sets used as well as the numerical procedures to approximate the Boltzmann transport equation. The second calculational difficulty is the evaluation of the neutron source which includes taking into account the irregular (in cylindrical coordinates) core boundary, conversion of the source geometry from X,Y to R, θ coordinates, and the burnup dependence of the source data. In addition, in the case of the BWR problem, the changing amount of water in the axial direction due to steam formation must be taken into account.

The BWR vessel fluence benchmark problem is for a typical BWR geometry. Since this is a calculational benchmark, no measurement results are available and comparisons are made with the reference calculated results at selected locations in the geometry. The model contains a surveillance capsule which is centered at 3 degrees as at River Bend. Comparisons at the center of the surveillance capsule were made for 6 fast neutron dosimetry reactions and very good agreement was obtained for all the reactions. The non-fission reaction rates agree to within 3%. The fission reactions (U238 and Np237) show a slightly bigger difference (4% to 7%) which is likely due to differences between the BUGLE-96 and BUGLE-93 dosimetry cross sections for these reactions as observed in Reference [3-27]. The average ratio (MPM calculation/reference benchmark) for all six reactions is 0.968 with a standard deviation of 0.016.

Comparisons were also made for a variety of positions at the vessel inner surface and at locations within the vessel. The MPM calculated results are very consistent with the benchmark, but do show some scatter. This is presumably due to differences in the source calculation, which can affect the relative flux at different angles. The average deviation is about +2%. Variation through the vessel also shows some scatter, but no trends are evident. The scatter in this case is probably due to differences in the model mesh.

The results for the capsule and vessel comparisons with the benchmark calculation indicate agreement at most points within ±5%, with differences slightly larger at some angles. All results agree with the benchmark within ±10%. It is concluded that the comparisons between the present calculations and the benchmark calculation are within acceptable tolerances and that the present calculational method applied to BWR geometries is therefore validated.

3.7.3 Power Plant Benchmarks

The remaining element of neutron transport method benchmarking is to compare calculations with dosimetry measurements from the actual plant of interest, or with one that has similar geometry and fuel power distributions. It is, of course, preferred that this element of benchmarking be performed using data from the plant itself, and C/E comparisons for the River Bend surveillance capsule described in Section 3.4 satisfy this requirement. Comparisons with measurements from NMP-1 and NMP-2 [3-2] provide additional verification of the accuracy of MPM fluence evaluations for BWR plants. These measurements enable possible errors not detected by the other benchmarking efforts to be identified and properly addressed. Such errors may arise from uncertainties in plant dimensions, fuel power distributions, time variations in flux level, or void fractions in outer fuel bundles.

Measurements at NMP-1 consisted of samples taken from two shroud weld locations (located at angles symmetric with 20degrees), each at 3 depths into the shroud, and a surveillance capsule with iron, nickel, and copper monitor wires. The shroud samples were analyzed for nickel and iron reactions. The shroud results were very consistent, within uncertainty, and showed an average C/E bias of 15.7% with a standard deviation of 3.1%. This is considered to be excellent consistency and the bias falls within expected bounds of calculational accuracy for the flux at a given point in the shroud. The analytic uncertainty analysis indicated the uncertainty in the calculated shroud fluence to be 16%. The most important contributors to this uncertainty are uncertainties in the shroud inner radius value, the fuel power distribution, and the uncertainty in power history. However, the most likely cause of the C/E bias is uncertainty in the azimuthal location of the welds. Since the 20 degree position was assumed to represent the weld azimuthal location, and the 20 degree position is very close to the azimuthal peak of 19.38 degrees, the calculated flux can only increase upward by about 1%. However, if the welds were located at the assumed 5 degree limit of uncertainty, then the calculated fluence could be lower by as much as 30%.

The NMP-1capsule dosimetry results gave an average C/E ratio of 0.84. When the average reaction rate uncertainty of 8% and the estimated capsule fluence calculation uncertainty of 14% are considered, it is concluded that the results are consistent within uncertainty. In the NMP-1 case, the power history must be considered to be less accurate than for other cases, due to larger time variation in power shapes. The copper result in this case fell 13% above the iron result.

In the NMP-2 case, measurement results were available for a surveillance capsule located at 3 degrees from the cardinal axis as in River Bend. The C/E values for copper averaged 0.95 and for iron the average was 1.09. This gave an average C/E for the capsule of 1.02, which is excellent agreement. The bias between the copper and iron results is very similar to that found for the River Bend capsule. Uncertainties in the NMP-2 capsule evaluation were similar to those for River Bend, except that there was a greater uncertainty in position of the wires within the capsule. As in River Bend, a measurement was made of the iron reaction from a Charpy specimen to confirm the dosimetry position.

3.7.4 Summary

Taken together, these analyses successfully provide a validation of the MPM calculational method for accurate determination of the fluence at all regions between the core and the outside of the reactor vessel for BWR geometries. The methods applied for the River Bend work and the benchmark analyses are similar in source handling (where required), mesh spacing, cross sections, and uncertainty treatment. All the benchmark results are considered to lie within acceptable tolerances of measured or reference results. Therefore, the benchmarking, together with the detailed uncertainty analysis of the River Bend fluence calculations, completely satisfies the requirements of Reg. Guide 1.190 for applications to River Bend.

3.8 Chapter 3 References

[3-1] Regulatory Guide 1.190, Calculational and Dosimetry Methods for Determining Pressure Vessel Neutron Fluence, U. S. Nuclear Regulatory Commission, March 2001.

[3-2] "Benchmarking of Nine Mile Point Unit 1 and Unit 2 Neutron Transport Calculations", Report Number MPM-402781, January, 2003, submitted to the US NRC under transmittal letter NMP1L 1708, Nine Mile Point Unit 1 Docket No. 50-220, "Transmittal of Neutron Transport Calculations Benchmarking Report, TAC Nos. MB6687 and MB6703, January 15, 2003.

[3-3] RSICC Computer Code Collection, CCC-543, TORT-DORT-PC, Two- and Three-Dimensional Discrete Ordinates Transport Version 2.7.3, available from the Radiation Safety Information Computational Center, Oak Ridge National Laboratory, Oak Ridge, TN, June 1996.

[3-4] RSICC Data Library Collection, DLC-185, BUGLE-96, Coupled 47 Neutron, 20 Gamma Ray Group Cross Section Library Derived from ENDF/B-VI for LWR Shielding and Pressure Vessel Dosimetry Applications, available from the Radiation Safety Information Computational Center, Oak Ridge National Laboratory, Oak Ridge, TN, March 1996.

[3-5] ASTM Designation E 482-89, Standard Guide for Application of Neutron Transport Methods for Reactor Vessel Surveillance, in ASTM Standards, Section 12, American Society for Testing and Materials, Philadelphia, PA, 2000.

[3-6] Entergy Operations, Inc. Letter to MPM Technologies, Inc., CEXO-2002/00328, "Transmittal of Materials and Dimensional Inputs to the Neutron Transport and Fluence Analysis in Regards to the Surveillance Capsule Work Under the BWRVIP ISP for the River Bend Station (RBS)," September 12, 2002.

[3-7] Entergy Operations, Inc. Letter to MPM Technologies, Inc., "RBS Vessel Fluence Source Terms Data," September 19, 2002.

[3-8] Entergy Operations, Inc. Letter to MPM Technologies, Inc., CEXO-2002/00375, "Supplemental and Corrected Data for Previously Transmitted Information under Letter CEXO-2002/00328, dated September 12, 2002," September 30, 2002.

[3-9] Entergy Operations, Inc. Letter to MPM Technologies, Inc., CEXO-2002/00415, "Supplemental Data for Previously Transmitted Information under Letter CEXO-2002/00328, dated September 12, 2002 and Transmittal Letter CEXO-2002/00375, dated September 30, 2002," October 23, 2002.

[3-10] RSICC Peripheral Shielding Routine Code Collection, PSR-277, LEPRICON, PWR Pressure Vessel Surveillance Dosimetry Analysis System, available from the Radiation Safety Information Computational Center, Oak Ridge National Laboratory, Oak Ridge, TN, June 1995.

[3-11] ASTM Designation E 263-00, Standard Test Method for Measuring Fast-Neutron Reaction Rates by Radioactivation of Iron, in ASTM Standards, Section 12, American Society for Testing and Materials, Philadelphia, PA, 2000.

[3-12] ASTM Designation E 523-92, Standard Test Method for Measuring Fast-Neutron Reaction Rates by Radioactivation of Copper, in ASTM Standards, Section 12, American Society for Testing and Materials, Philadelphia, PA, 2000.

[3-13] ASTM Designation E 1005-97, Standard Test Method for Application and Analysis of Radiometric Monitors for Reactor Vessel Surveillance, E706(IIIA), in ASTM Standards, Section 12, American Society for Testing and Materials, Philadelphia, PA, 2000.

[3-14] ASTM Designation E 261-94, Standard Practice for Determining Neutron Fluence, Fluence Rate, and Spectra by Radioactivation Techniques, in ASTM Standards, Section 12, American Society for Testing and Materials, Philadelphia, PA, 2000.

[3-15] ASTM Designation E 1018-01, Standard Guide for Application of ASTM Evaluated Cross Section Data File, Matrix E706(IIB), in ASTM Standards, Section 12, American Society for Testing and Materials, Philadelphia, PA, 2001.

[3-16] Caine, T. A., "Flux Wire Dosimeter Evaluation for River Bend Station," SASR 88-49, General Electric Company, June, 1988.

[3-17] River Bend Updated Safety Analysis Report, Revision 14, September, 2001.

[3-18] ASTM Designation E 693-94, Standard Practice for Characterizing Neutron Exposures in Iron and Low Alloy Steels in Terms of Displacements Per Atom (DPA), E706(ID), in ASTM Standards, Section 12, American Society for Testing and Materials, Philadelphia, PA, 2000.

[3-19] McElroy, W.N., Ed., "LWR-PV-SDIP: PCA Experiments and Blind Test", NUREG/CR-1861, 1981.

[3-20] Lippincott, E.P., "Consumers Power Company Palisades Nuclear Plant Reactor Vessel Fluence Analysis", WCAP-13348, Westinghouse Electric Corporation, May 1992.

[3-21] Maerker, R.E., et. al., "Application of LEPRICON Methodology to LWR Pressure Vessel Dosimetry", Reactor Dosimetry: Methods, Applications, and Standardization, ASTM STP 1001, 1989, pp 405-414.

[3-22] Anderson, S.L., "Westinghouse Fast Neutron Exposure Methodology for Pressure Vessel Fluence Determination and Dosimetry Evaluation", WCAP-13362, Westinghouse Electric Corporation, May 1992.

[3-23] Lippincott, E.P., et. al., "Evaluation of Surveillance Capsule and Reactor Cavity Dosimetry from H. B. Robinson Unit 2, Cycle 9", WCAP-11104, NUREG/CR-4576, February 1987.

[3-24] Haghighat, A. and Veerasingam, R., "Comparison of the Different Cross Section Libraries used for Reactor Pressure Vessel Fluence Calculations", Trans. Amer. Nuclear Society, 64, p. 357, 1991.

[3-25] Fero, A.H., "Neutron and Gamma Ray Flux Calculations for the Venus PWR Engineering Mockup," NUREG/CR-4827 (WCAP-11173), January, 1987.

[3-26] Tsukiyama, T., et. al., "Benchmark Validation of TORT Code Using KKM Measurement and its Application to 800 MWe BWR," Proceedings of the 11th International Symposium on Reactor Dosimetry, Brussels, Belgium, August 18-23, 2002, World Scientific, to be published.

[3-27] Remec, I. and Kam, F.B.K., *Pool Critical Assembly Pressure Vessel Facility Benchmark*, NUREG/CR-6454, (ORNL/TM-13205), USNRC, July 1997.

[3-28] Fero, A.H., Anderson, S.L. and Roberts, G.K., "Analysis of the ORNL PCA Benchmark Using TORT and BUGLE-96," Reactor Dosimetry: Radiation Metrology and Assessment, ASTM STP 1398, John G. Williams, David W. Vehar, Frank H. Ruddy, and

David Gilliam, Eds., American Society for Testing and Materials, West Conshohocken, PA, 2001.

[3-29] Carew, J. F., Hu, K., Aronson, A., Prince, A., and Zamonsky, G., "PWR and BWR Pressure Vessel Fluence Calculational Benchmark Problems and Solutions," NUREG/CR-6115 (BNL-NUREG-52395), Draft completed May 20, 1997.

Table 3-1
Neutron Flux Spectrum at Center of Surveillance Capsule

Energy Group	Upper Energy (MeV)	Average Capsule Flux n/cm^2-s	Energy Group	Upper Energy (MeV)	Average Capsule Flux n/cm^2-s
1	1.733E+01	3.43E+06	25	2.972E-01	4.71E+08
2	1.419E+01	9.80E+06	26	1.832E-01	4.10E+08
3	1.221E+01	3.51E+07	27	1.111E-01	3.19E+08
4	1.000E+01	6.27E+07	28	6.738E-02	2.55E+08
5	8.607E+00	9.76E+07	29	4.087E-02	1.07E+08
6	7.408E+00	2.44E+08	30	3.183E-02	7.56E+07
7	6.065E+00	3.14E+08	31	2.606E-02	6.78E+07
8	4.966E+00	4.69E+08	32	2.418E-02	4.81E+07
9	3.679E+00	2.89E+08	33	2.188E-02	1.58E+08
10	3.012E+00	1.91E+08	34	1.503E-02	2.77E+08
11	2.725E+00	2.03E+08	35	7.102E-03	3.06E+08
12	2.466E+00	9.64E+07	36	3.355E-03	2.83E+08
13	2.365E+00	2.36E+07	37	1.585E-03	4.49E+08
14	2.346E+00	1.17E+08	38	4.540E-04	2.68E+08
15	2.231E+00	2.92E+08	39	2.145E-04	2.66E+08
16	1.920E+00	2.90E+08	40	1.013E-04	3.51E+08
17	1.653E+00	3.80E+08	41	3.727E-05	4.31E+08
18	1.353E+00	5.32E+08	42	1.068E-05	2.53E+08
19	1.003E+00	3.29E+08	43	5.044E-06	3.37E+08
20	8.208E-01	1.74E+08	44	1.855E-06	2.51E+08
21	7.427E-01	4.11E+08	45	8.764E-07	2.27E+08
22	6.081E-01	3.18E+08	46	4.140E-07	3.64E+08
23	4.979E-01	3.70E+08	47	1.000E-07	6.48E+09
24	3.688E-01	3.17E+08		1.000E-11	

Table 3-2
River Bend Radial Dimensions

Component	Dimension (in)	Dimension (cm)	Reference
Fuel Bundle Size	6.000	15.240	[3-7]
Core edge at 0 degrees	89.759	227.988	[3-7] (Note 1)
Shroud IR	90.827	230.701	50978D70 (Note 2)
Shroud OR	92.875	235.903	50978D70 (Note 2)
Vessel Clad IR	109.5625	278.289	VPF3535-625, VPF3614-704, VPF3614-450 (Note 3)
Vessel Base Metal IR	109.750	278.765	VPF3614-450 (Note 3)
Vessel OR	115.156	292.496	VPF3614-450, GE-NE-B13-0294-00-01 (Rev 0)
Bio Shield Iron IR	155.0	393.700	ES-59A, GE768E384
Bio Shield Concrete IR	156.5	397.510	ES-59A, EC-40C, GE768E384
Capsule IR	108.764	276.261	VPF-3614-704, VPF-3614-714, VPF-3614-450, VPF-3535-625, GE-767E956, GE-105D5036
Capsule OR	109.304	277.632	
Capsule Width	2.86	7.276	GE-112D1065
Jet Pump Exit Pipe ID	6.000	15.240	GE-768E312
Jet Pump Exit Pipe OD	6.730	17.094	GE-768E312
Jet Pump Exit Pipe centerline radius	99.870	253.670	GE-768E312
Jet Pump Riser ID	9.560	24.282	GE-768E312
Jet Pump Riser OD	10.750	27.305	GE-768E312
Jet Pump Riser centerline radius	100.910	256.311	GE-768E312

See notes on following page.

Table 3-2 (continued)
River Bend Radial Dimensions

Notes to Table 3-2:

1. The core edge at 0 degrees is calculated by taking 14 bundles with 6 inch (15.24 cm) pitch minus a gap of 0.2725 inch (6.92 mm). This gap is appropriate for GE 6/7/8 fuel which is loaded on the periphery of the River Bend core for the first nine cycles.
2. The shroud dimensions are taken from as-built measurements made near 180o and not nominal values. Based on drawing 50978D71, the shroud thickness is reduced from 2.048 inches (5.20 cm) to 1.861 inches (4.73 cm) (reducing the OR by 0.187 inches (4.75 mm)) in the region from 81.51 to 91.51 inches (2.07 to 2.32 m) above the bottom of the core.
3. The vessel clad IR is taken to be the value at 180o measured at elevation 358 which is near the top of the active fuel (identified as dimension R3 on the reference drawings). This is the minimum value and was used in the model to give a conservative result. It is also most appropriate for the capsule elevation. As-built measurements were apparently not made elsewhere in the beltline region. The clad thickness is taken as the nominal value (0.1875 inches (4.76 mm)). The difference between this and the minimum clad thickness is included in the uncertainty estimate.

Surveillance capsules are located at 3o, 177o, and 183o. The 183o capsule is analyzed in this report. Jet pumps are centered at angles of 30, 60, 90, 120, 150, 210, 240, 270, 300, and 330 degrees. Thus the River Bend plant has three types of octants: (1) surveillance capsule at 3 degrees plus jet pump exit pipes at 22 degrees and 38 degrees and jet pump riser at 30 degrees; (2) same as (1) without the surveillance capsule; and (3) same as (2) with an additional jet pump exit pipe at 8 degrees and ½ riser pipe at 0 degrees. There are three octants of the first type, one of the second, and four of the third. Only the first type of octant geometry was analyzed in the present calculations.

Table 3-3
Surveillance Capsule Flux and dpa/s Results

Case	Flux (E > 1 MeV) $n/cm^2/s$	Flux (E > 0.1 MeV) $n/cm^2/s$	dpa/s
Cycle 1	3.37E+09	6.02E+09	5.15E-12
Cycle 2	3.75E+09	6.67E+09	5.71E-12
Cycle 3	4.09E+09	7.30E+09	6.24E-12
Cycle 4	3.52E+09	6.30E+09	5.38E-12
Cycle 5	3.88E+09	6.92E+09	5.91E-12
Cycle 6a	3.40E+09	6.08E+09	5.20E-12
Cycle 6b	2.91E+09	5.21E+09	4.45E-12
Cycle 7	4.22E+09	7.52E+09	6.43E-12
Cycle 8	3.48E+09	6.20E+09	5.31E-12
Cycle 9a	3.53E+09	6.27E+09	5.38E-12
Cycle 9b	3.54E+09	6.30E+09	5.41E-12
Cycle 9c	3.42E+09	6.08E+09	5.21E-12
Cycle 9d	3.39E+09	6.02E+09	5.16E-12
Cycle 9e	3.26E+09	5.79E+09	4.97E-12
Average (all cycles)	3.65E+09	6.52E+09	5.57E-12
Percent std. dev.	10.0	10.0	10.0

Note: All the values in the above table are normalized to a full power of 2894 MWth. Cycles 1 through 9 operated at this maximum power. The average flux and dpa/s values are calculated by integrating the flux over the 9 cycles of operation. The percent standard deviation is calculated using the flux value or average flux value for each fuel cycle.

Table 3-4
Surveillance Capsule Fluence and dpa Results

Cycle	Effective Full-Power Seconds	Fluence (E > 1 MeV) n/cm²	Fluence (E > 0.1 MeV) n/cm²	dpa
1	3.10E+07	1.04E+17	1.86E+17	1.59E-04
2	3.23E+07	1.21E+17	2.15E+17	1.84E-04
3	3.45E+07	1.41E+17	2.52E+17	2.15E-04
4	3.14E+07	1.11E+17	1.98E+17	1.69E-04
5	3.71E+07	1.44E+17	2.57E+17	2.19E-04
6	4.11E+07	1.22E+17	2.19E+17	1.87E-04
7	4.60E+07	1.94E+17	3.46E+17	2.96E-04
8	4.29E+07	1.49E+17	2.66E+17	2.28E-04
9	2.01E+07	6.89E+16	1.22E+17	1.05E-04
Total	3.16E+08	1.16E+18	2.06E+18	1.76E-03

Table 3-5
River Bend Power History to End of Cycle 9

Days in Period	Date	Cycle Cumulative MWD/MT	Period Effective Full Power Days	Period Average Fraction of Full Power
Cycle 1				
Begin	31-Oct-85	0		
235	23-Jun-86	1356	53.4	0.2272
45	07-Aug-86	1912	21.9	0.4866
44	20-Sep-86	2692	30.7	0.6981
97	26-Dec-86	3503	31.9	0.3293
37	01-Feb-87	4233	28.7	0.7770
40	13-Mar-87	5226	39.1	0.9777
28	10-Apr-87	5924	27.5	0.9817
34	14-May-87	6769	33.3	0.9788
55	08-Jul-87	7619	33.5	0.6086
33	10-Aug-87	8416	31.4	0.9511
35	14-Sep-87	9103	27.1	0.7730
Cycle 2				
100	23-Dec-87	0	0	0
43	04-Feb-88	785	30.9	0.7189
40	15-Mar-88	1610	32.5	0.8122
28	12-Apr-88	2307	27.4	0.9802
36	18-May-88	3193	34.9	0.9691
28	15-Jun-88	3857	26.1	0.9338
31	16-Jul-88	4626	30.3	0.9768
33	18-Aug-88	5430	31.7	0.9594
41	28-Sep-88	6186	29.8	0.7261
40	07-Nov-88	6858	26.5	0.6616
24	01-Dec-88	7456	23.5	0.9812
25	26-Dec-88	8053	23.5	0.9404
31	26-Jan-89	8698	25.4	0.8193
47	14-Mar-89	9492	31.3	0.6652

Table 3-5 (continued)
River Bend Power History to End of Cycle 9

Days in Period	Date	Cycle Cumulative MWD/MT	Period Effective Full Power Days	Period Average Fraction of Full Power
		Cycle 3		
97	19-Jun-89	0	0	0.0000
50	08-Aug-89	974	38.0	0.7603
36	13-Sep-89	1738	29.8	0.8282
27	10-Oct-89	2375	24.9	0.9208
31	10-Nov-89	3150	30.2	0.9757
40	20-Dec-89	3996	33.0	0.8254
37	26-Jan-90	4927	36.3	0.9820
32	27-Feb-90	5736	31.6	0.9867
38	06-Apr-90	6346	23.8	0.6265
33	09-May-90	7062	27.9	0.8468
31	09-Jun-90	7839	30.3	0.9782
32	11-Jul-90	8625	30.7	0.9586
33	13-Aug-90	9446	32.0	0.9710
46	28-Sep-90	10238	30.9	0.6719
		Cycle 4		
63	30-Nov-90	0	0	0.0000
38	07-Jan-91	735	28.5	0.7491
31	07-Feb-91	1505	29.8	0.9620
42	21-Mar-91	2316	31.4	0.7478
26	16-Apr-91	2977	25.6	0.9846
30	16-May-91	3702	28.1	0.9359
34	19-Jun-91	4554	33.0	0.9705
94	21-Sep-91	6947	92.7	0.9859
52	12-Nov-91	7754	31.3	0.6010
76	27-Jan-92	8526	29.9	0.3934
38	05-Mar-92	9394	33.6	0.8846

Table 3-5 (continued)
River Bend Power History to End of Cycle 9

Days in Period	Date	Cycle Cumulative MWD/MT	Period Effective Full Power Days	Period Average Fraction of Full Power
Cycle 5				
197	18-Sep-92	0		0.0000
79	06-Dec-92	1824	70.0	0.8858
30	05-Jan-93	2373	21.1	0.7021
27	01-Feb-93	3073	26.9	0.9946
32	05-Mar-93	3894	31.5	0.9843
27	01-Apr-93	4545	25.0	0.9250
85	25-Jun-93	5079	20.5	0.2410
77	10-Sep-93	5787	27.2	0.3527
32	12-Oct-93	6616	31.8	0.9939
24	05-Nov-93	7094	18.3	0.7641
35	10-Dec-93	7937	32.3	0.9240
33	12-Jan-94	8789	32.7	0.9905
30	11-Feb-94	9566	29.8	0.9936
63	15-Apr-94	11198	62.6	0.9938

Table 3-5 (continued)
River Bend Power History to End of Cycle 9

Days in Period	Date	Cycle Cumulative MWD/MT	Period Effective Full Power Days	Period Average Fraction of Full Power
Cycle 6				
77	01-Jul-94	0	0	0.0000
21	22-Jul-94	374.9	14.3	0.6833
48	08-Sep-94	1616	47.5	0.9897
41	19-Oct-94	1616	0.0	0.0000
30	18-Nov-94	2173	21.3	0.7107
32	20-Dec-94	2800	24.0	0.7500
38	27-Jan-95	3793	38.0	1.0002
35	03-Mar-95	4706	34.9	0.9985
35	07-Apr-95	5613	34.7	0.9919
45	22-May-95	6782	44.7	0.9943
81	11-Aug-95	8891	80.7	0.9966
40	20-Sep-95	9903	38.7	0.9684
47	06-Nov-95	11120	46.6	0.9911
35	11-Dec-95	11955	32.0	0.9131
24	04-Jan-96	12427	18.1	0.7528

Table 3-5 (continued)
River Bend Power History to End of Cycle 9

Days in Period	Date	Cycle Cumulative MWD/MT	Period Effective Full Power Days	Period Average Fraction of Full Power
Cycle 7				
40	13-Feb-96	0	0	0.0000
31	15-Mar-96	773	29.2	0.9404
36	20-Apr-96	1726	35.9	0.9984
47	06-Jun-96	2968	46.8	0.9966
15	21-Jun-96	3118	5.7	0.3771
20	11-Jul-96	3642	19.8	0.9881
17	28-Jul-96	3819	6.7	0.3927
47	13-Sep-96	5065	47.0	0.9998
42	25-Oct-96	6168	41.6	0.9904
42	06-Dec-96	7255	41.0	0.9761
42	17-Jan-97	8368	42.0	0.9994
35	21-Feb-97	9272	34.1	0.9741
42	04-Apr-97	10377	41.7	0.9922
32	06-May-97	11223	31.9	0.9971
17	23-May-97	11376	5.8	0.3394
32	24-Jun-97	12220	31.8	0.9947
39	02-Aug-97	13122	34.0	0.8722
41	12-Sep-97	14122	37.7	0.9198

Table 3-5 (continued)
River Bend Power History to End of Cycle 9

Days in Period	Date	Cycle Cumulative MWD/MT	Period Effective Full Power Days	Period Average Fraction of Full Power
		Cycle 8		
36	18-Oct-97	0	0	0.0000
34	21-Nov-97	785	29.2	0.8586
42	02-Jan-98	1892	41.2	0.9801
42	13-Feb-98	3021	42.0	0.9996
29	14-Mar-98	3800	29.0	0.9989
30	13-Apr-98	4600	29.7	0.9916
25	08-May-98	4854	9.4	0.3778
35	12-Jun-98	5795	35.0	0.9998
39	21-Jul-98	6843	39.0	0.9993
34	24-Aug-98	7741	33.4	0.9822
39	02-Oct-98	8762	38.0	0.9735
56	27-Nov-98	10251	55.4	0.9888
39	05-Jan-99	11287	38.5	0.9878
36	10-Feb-99	12183	33.3	0.9255
51	02-Apr-99	13341	43.1	0.8443
		Cycle 9		
74	15-Jun-99	0	0	0.0000
30	15-Jul-99	256	9.5	0.3163
29	13-Aug-99	1025	28.5	0.9830
29	11-Sep-99	1779	28.0	0.9638
27	08-Oct-99	2507	27.0	0.9995
21	29-Oct-99	3063	20.6	0.9815
21	19-Nov-99	3496	16.1	0.7643
30	19-Dec-99	4305	30.0	0.9996
27	15-Jan-00	5026	26.7	0.9899
27	11-Feb-00	5680	24.2	0.8979
22	04-Mar-00	6271	21.9	0.9958

Table 3-6
Nuclear Parameters Used in the Evaluation of Neutron Sensors

Monitor Material	Reaction of Interest	Isotopic Fraction	Approximate Response Threshold	Product Half-Life
Copper	$Cu^{63}(n,\alpha)Co^{60}$	0.6917	5 MeV	1925.5 days
Iron	$Fe^{54}(n,p)Mn^{54}$	0.05845	2 MeV	312.3 days

Table 3-7
Tabulation of Dosimetry Results

Dosimeter	Measured (E) Activity (dps/mg)	Calculated (C) Activity (dps/mg) [a]	Ratio(C/E)
Copper Wires			
Cu-1	43.30	34.40	0.794
Cu-2	42.34	34.40	0.812
Average Copper Result			0.803
Iron Wires			
Fe-1	311.7	284.8	0.914
Fe-2	325.2	284.8	0.876
Charpy Iron Samples			
H-1a	310.2	286.2	0.922
H-1b	317.7	286.2	0.901
W-6	315.2	298.9	0.948
B-12	326.9	301.0	0.921
Average Iron Result			0.914
Capsule Average			0.858

Calculated values are per mg of sample; the Charpy sample calculated values have been corrected by a factor of 0.966 to account for the fraction of iron in the sample.

Table 3-8
Calculated Maximum Vessel Fluence and dpa at End of Cycle 9 (10.08 EFPY) and Projected to 32 EFPY and 48 EFPY

Position	Fluence (E > 1 MeV) n/cm²	Fluence (E > 0.1 MeV) n/cm²	dpa
End of Cycle 9 (10.08 EFPY)			
Clad IR	1.23E+18	2.27E+18	1.89E-03
Vessel IR	1.21E+18	2.32E+18	1.85E-03
Vessel 1/4 T	8.73E+17	2.09E+18	1.38E-03
Vessel 3/4 T	4.13E+17	1.32E+18	7.16E-04
32 EFPY[a]			
Clad IR	4.45E+18	8.14E+18	6.84E-03
Vessel IR	4.38E+18	8.30E+18	6.71E-03
Vessel 1/4 T	3.15E+18	7.46E+18	4.96E-03
Vessel 3/4 T	1.31E+18	4.39E+18	2.31E-03
48 EFPY[a]			
Clad IR	6.82E+18	1.24E+19	1.05E-02
Vessel IR	6.70E+18	1.27E+19	1.03E-02
Vessel 1/4 T	4.82E+18	1.14E+19	7.59E-03
Vessel 3/4 T	1.97E+18	6.65E+18	3.49E-03

Note: a. The fluence and dpa values projected to 32 and 48 EFPY assume that the maximum reactor power is increased to 3039 MWth in the middle of cycle 10 and to 3091 MWth starting in cycle 12. Future cycles are assumed to be identical in fluence rate and duration to cycle 7. Use of the cycle 7 values is conservative since this cycle produced the highest exposure rate at the maximum position in the vessel.

Table 3-9
Maximum Vessel Fluence (E > 1 MeV) (n/cm^2) at End of Cycle 9 (10.08 EFPY), at 32 EFPY and 48 EFPY Using Alternate Schemes for Attenuation through the Vessel

Position	Calculated Fluence (E > 1 MeV) n/cm^2	Attenuation using Calculated dpa [a] n/cm^2	Attenuation using RG1.99(Rev 2) [b] n/cm^2
End of Cycle 9 (10.08 EFPY)			
Vessel IR	1.21E+18	1.21E+18	1.18E+18
1/4 T	8.73E+17	8.96E+17	8.51E+17
3/4 T	4.13E+17	4.66E+17	4.45E+17
32 EFPY			
Vessel IR	4.38E+18	4.37E+18	4.26E+18
1/4 T	3.15E+18	3.23E+18	3.08E+18
3/4 T	1.31E+18	1.51E+18	1.61E+18
48 EFPY			
Vessel IR	6.70E+18	6.69E+18	6.52E+18
1/4 T	4.82E+18	4.95E+18	4.71E+18
3/4 T	1.97E+18	2.27E+18	2.46E+18

Note: a. Calculated fluence at the vessel inner wetted surface (clad IR) times the ratio of dpa at the vessel interior points to the dpa at the inner wetted surface.

b. Calculated fluence at the vessel inner wetted surface (clad IR) times exp(-0.24*x) where x is the distance into the vessel in inches.

Table 3-10
River Bend Capsule and Vessel Fluence Calculational Uncertainty

Uncertainty Contributor	Assigned Uncertainty	Vessel IR Fluence Uncertainty % (1σ)	Capsule Fluence Uncertainty % (1σ)
Fission Spectrum and nu/kappa	10000 MWd/MTU	2.9	2.9
Heat Balance	2%	2.0	2.0
Shroud IR	0.075 inches (1.91 mm)	0.0	0.0
Shroud Thickness	0.0125 inches (0.318 mm)	0.3	0.3
Vessel Clad Thickness	0.0625 inches (1.59 mm)	0.6	0.0
Vessel IR	0.375 inches (9.53 mm)	10.2	0.0
Core Midplane Water Density	7%	4.4	4.4
Bypass Water Density	1.3%	2.6	2.3
Downcomer Water Temperature	5 F (2.8 C)	3.0	3.0
Steel Density (total cross section)	3.5%	3.5	3.5
Core Fuel Density	3.5%	2.5	2.4
Radial Source Dist.	7.7%	7.7	7.7
Methods Uncertainty	7.7%	7.7	7.7
Flux History	2%	2.0	2.0
Jet Pump Model	10% of effect	0.0 – 3.0	0.0
Capsule Radial Location	0.1875 inches (4.763 mm)	0.0	5.1
Total		17.4	14.6

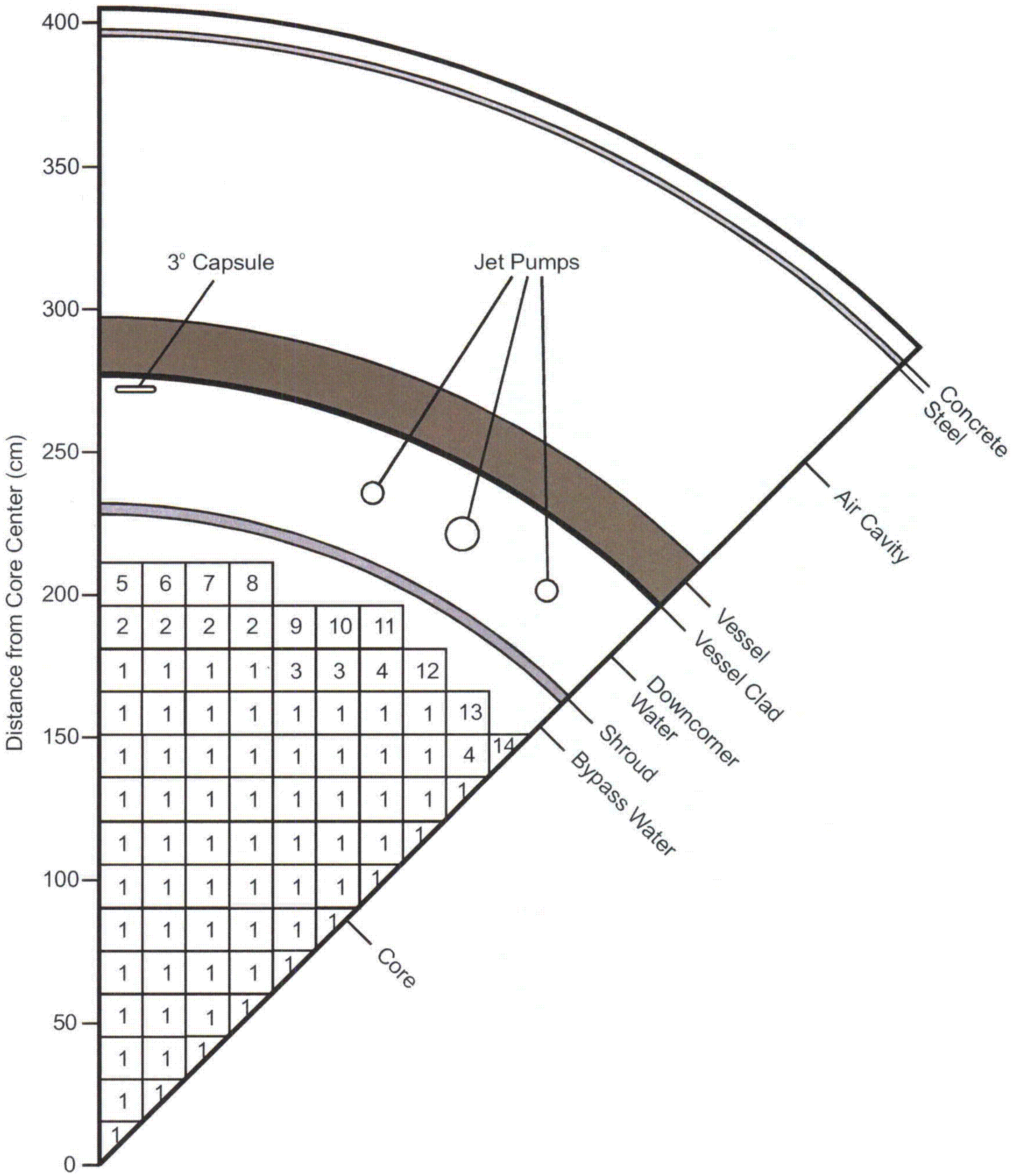

Note: Jet pumps and capsule are not drawn to scale; other components are approximately to scale.

A total of 14 regions of varying density were used to model the core.

Figure 3-1
River Bend R-θ Geometry Used in the DORT Calculations

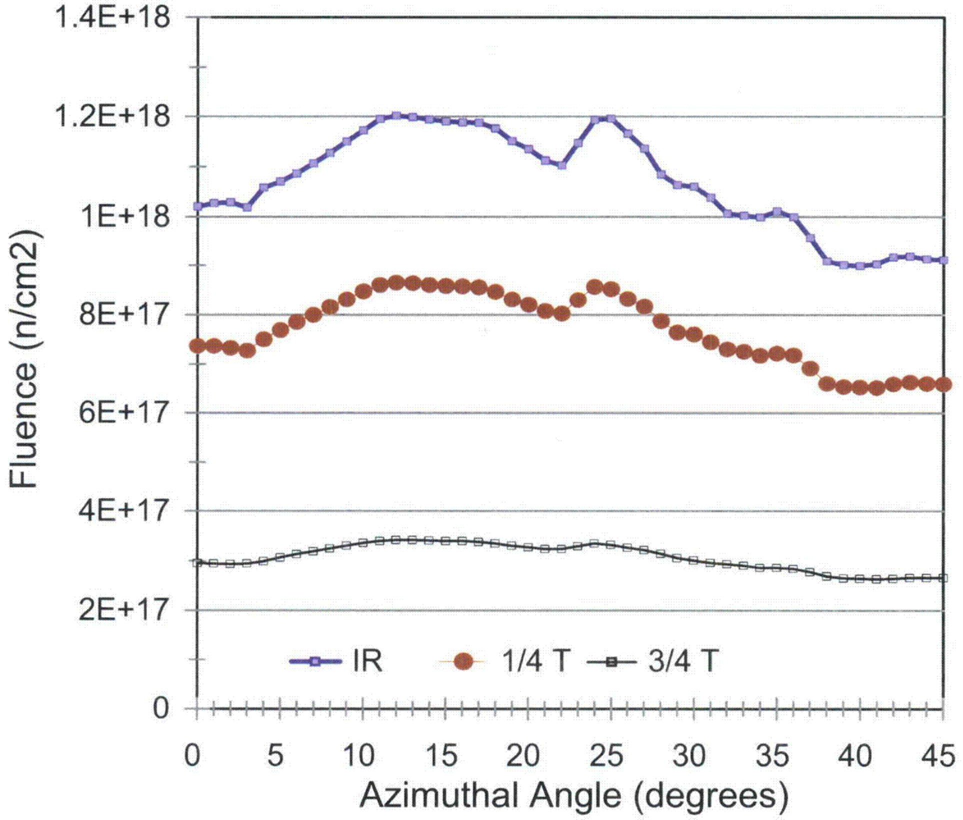

Figure 3-2
River Bend Reactor Vessel Fluence at the End of Cycle 9 at Core Midplane

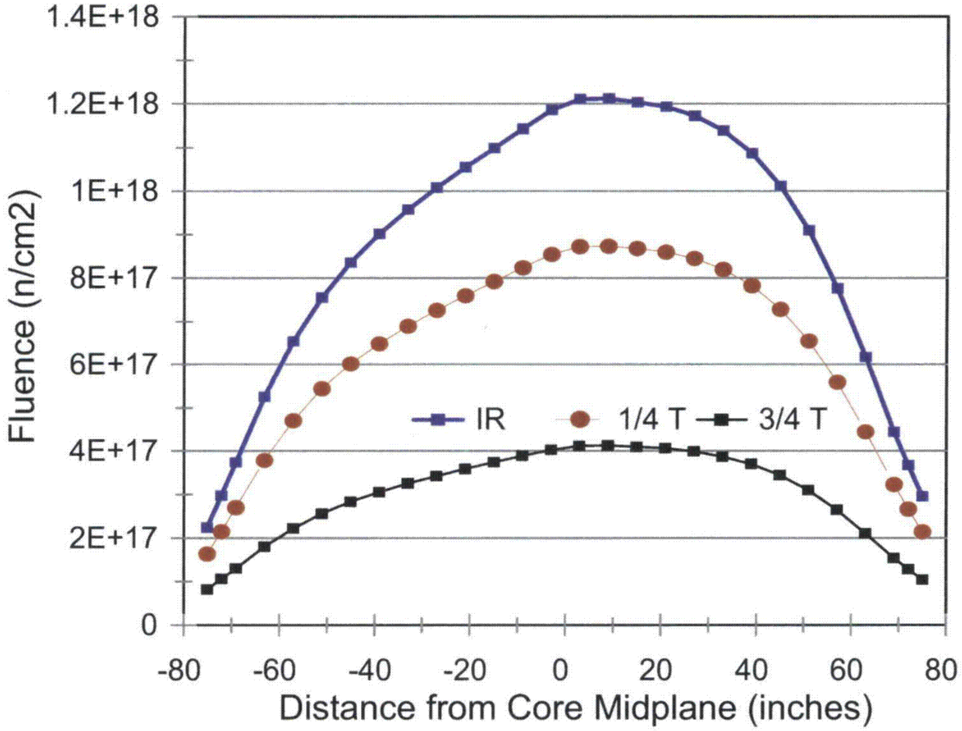

Figure 3-3
River Bend Reactor Vessel Fluence at the End of Cycle 9 at Azimuthal Maximum

4 TEST SPECIMEN CHEMICAL ANALYSIS

4.1 Specimen Selection and Machining of Samples

Charpy specimens were used for chemical analysis after Charpy testing was completed. Three test specimens were selected for analysis and included one base metal specimen, one weld metal specimen, and one HAZ specimen. The HAZ specimen (H-1) was selected because it was adjacent to the dosimeter wires in the capsule near the axial bottom of the capsule. The weld metal specimen (W-6) was located near the axial center of the capsule. The base metal specimen (B12) was located at the axial bottom of the capsule.

The samples were machined using a clean end mill to ensure that no contamination of the sample occurred. The chemical analysis samples were machined from the fracture surface ends of the base and weld metal. For the two HAZ sample halves, a thickness of approximately 0.1 inch (2.54 mm) was machined from the fracture surface, and then the chemical analysis samples were taken. In this way, the HAZ metal was avoided.

4.2 Preparation of Samples for Analysis

The chemistry samples were placed in marked plastic vials. Table 4-1 lists the sample identifications and their corresponding descriptions. Prior to analysis via Inductively Coupled Plasma-Mass Spectrometry (ICP-MS), the samples were cleaned by immersion in a bath of 100% ethyl alcohol to remove any surface contaminants.

4.3 ICP-MS Measurements

The ICP-MS system used in this work is a quadrupole mass spectrometer manufactured by Perkin-Elmer and is designated as the Sciex ELAN 6000 system. It was calibrated using NIST traceable ICP standard solutions. The specimens taken for analysis were dissolved in an acid solution in preparation for introduction to the ICP-MS system. ICP-MS data were accumulated to show well-defined peaks for the elements of interest. Tables 4-2 and 4-3 list the elements of interest and the results obtained from the ICP-MS analysis. It should be noted that iron is quantified by direct measurement and by difference assuming it is the matrix element.

Review of the base metal results in Table 4-2 confirms that the capsule base metal specimen results are in agreement with previously reported data for the manufactured base metal. The baseline data is from the Reference [4-1] Lukens test certificate for the beltline plate. Similarly, Table 4-3 shows that the weld metal specimen results agree with earlier measurements for the surveillance weld 5P6756. The surveillance weld chemistry data is available from Reference

[4-2]. It is important to note that although the surveillance weld and the vessel weld are the same heat (5P6756), the welds were produced at different times and therefore the chemistries for the surveillance weld are averaged separately. Further discussion is provided later in this section of the report.

Table 4-4 lists the results for the base and weld composition determinations made using the HAZ specimen samples. In order to avoid the need for a metallographic examination, it was necessary to compare the element compositions of each HAZ Charpy specimen half with either base or weld metal composition. Table 4-5 compares the measured results for sample H-1(a) to the measured results for samples B-12 and W-6. The composition difference between H-1(a) and the base metal is much less than the difference with the weld measurements. The differences are especially noteworthy for Ni and Si. Therefore, it was concluded that sample H-1(a) is the base metal half, and sample H-1(b) is the weld metal half. This can also be seen by comparison of the H-1(b) data with the known weld metal composition.

In addition to the Charpy samples, the chemical analysis included a comparison with a NIST traceable steel sample, denoted as SRM 1262A (AISI 94B17). Table 4-6 shows the results of this study and comparison with accepted values. In general, there is good agreement. The measured values appear to be consistently on the low side, with phosphorus showing a somewhat larger deviation than the other analytes.

4.4 Best Estimate Base and Weld Metal Chemistry

As mentioned previously, the vessel welds and the surveillance capsule welds are the same heat (5P6756), but the welds were done at different times. Therefore, for the purpose of defining the best estimate weld chemistry, it is necessary to define two chemistries for River Bend. In the case of the surveillance weld, the best estimate is the average of all unique measurements on the River Bend surveillance weld 5P6756. These data are summarized in Table 4-7. When considering the vessel weld for the purpose of P-T curve analysis, it will be necessary to calculate the best estimate chemistry as a weighted average of all available data for heat 5P6756, which will include the Table 4-7 data, weld qualification, and other data.

Similarly, Table 4-8 provides the revised best estimate chemistry for the plate. In the case of the plate, the only available data is for the vessel plate material. It is important to note that the data obtained from the HAZ Charpy specimen have not been included in the best estimate averages. This is because it is preferable to use weld or base metal specimens for chemistry determination to avoid any possible sampling problems. Also, the primary purpose in measuring the HAZ specimen chemistry was for use in the dosimetry analysis.

4.5 Chapter 4 References

[4-1] Lukens Steel Company Test Certificates, File 1540-06-13, Melt C3054, Slab 2, October, 15, 1973.

[4-2] "Progress Report on Phase 2 of the BWR Owner's Group Supplemental Surveillance Program", GE-NE-523-101-1290, DRF B11-00392-1, January, 1992.

Table 4-1
Chemistry Sample Identifications and Descriptions

Sample ID	Material Description
B-12	Charpy Base Metal
W-6	Charpy Weld Metal
H-1(a)	Charpy HAZ Specimen-Base Metal (Half a)
H-1(b)	Charpy HAZ Specimen-Weld Metal (Half b)
STD	NIST SRM 1262A (AISI 94B17)

Table 4-2
Results of the ICP Analysis of the Base Metal Sample B-12

Element ID	Measured Concentration (wt %)	Baseline Concentration(3) (wt %)
Cu	0.075	0.09
Fe(1)	97.4	Not Reported
Fe(2)	97	Not Reported
Mn	1.31	1.29
Mo	0.55	0.56
Ni	0.66	0.69
P	0.0069	0.007
Si	0.30	0.26

(1) Concentration by direct measurement.

(2) Concentration by difference (matrix element).

(3) Plate No. C3054-2. All elements are two sample averages rounded up since they are from the same single specimen. Source: RBS material certification data [4-1].

Table 4-3
Results of the ICP Analysis of the Surveillance Weld (5P6756) Metal Sample W-6

Element ID	Measured Concentration (wt %)	Baseline Concentration[(3)] (wt %)
Cu	0.067	0.05
Fe[(1)]	96.3	Not Reported
Fe[(2)]	97	Not Reported
Mn	1.35	1.28
Mo	0.48	0.39
Ni	0.93	0.93
P	0.00659	0.022
Si	0.42	0.37

(1) Concentration by direct measurement.

(2) Concentration by difference (matrix element).

(3) Surveillance heat 5P6756. P, Ni, and Cu are two sample averages rounded up since they are from the same single specimen. Source: GE-NE-523-101-1290, Supplemental Surveillance Program Report, January, 1992 [4-2].

Table 4-4
Results of the ICP Analysis of the Base and Weld Metal Samples Taken from HAZ Specimen H-1

Element ID	Measured Concentration (wt %) for Sample H-1(a) Base Metal Half	Measured Concentration (wt %) for Sample H-1(b) Weld Metal Half
Cu	0.075	0.067
Fe[(1)]	97.1	95.6
Fe[(2)]	97	97
Mn	1.29	1.32
Mo	0.52	0.48
Ni	0.64	0.85
P	0.0069	0.0063
Si	0.28	0.42

(1) Concentration by direct measurement.

(2) Concentration by difference (matrix element).

Table 4-5
Comparison of the Results for HAZ Specimen H-1(a) and the Base (B-12) and Weld (W-6) Samples

Element ID	Measured Concentration (wt %) for Sample H-1(a) Base Metal	Measured Concentration (wt %) for Sample B-12	Percent Difference Between Samples H-1(a) and B-12	Measured Concentration (wt %) for Sample W-6	Percent Difference Between Samples H-1(a) and W-6
Cu	0.075	0.075	0.0	0.067	-10.7
Fe(1)	97.1	97.4	0.3	96.3	-1.1
Fe(2)	97	97	0.0	97	0.0
Mn	1.29	1.31	1.6	1.35	4.7
Mo	0.52	0.55	5.8	0.48	-7.7
Ni	0.64	0.66	3.1	0.93	45.3
P	0.0069	0.0069	0.0	0.0065	4.5
Si	0.28	0.30	7.1	0.42	50.0

(1) Concentration by direct measurement.

(2) Concentration by difference (matrix element).

Table 4-6
Analysis of the NIST Traceable Sample

Element ID	Measured Concentration (wt %) for Sample STD	NIST Reported Concentration (wt %) for Sample STD	Percent Difference Between Reported and Measured Concentrations
Cu	0.48	0.51	-5.9
Fe(1)	96.6	Not Reported	Not Calculated
Fe(2)	97	97	0
Mn	1.02	1.05	-2.9
Mo	0.64	0.70	-8.6
Ni	0.58	0.60	-3.3
P	0.036	0.044	-18.9
Si	0.42	0.40	5.0

(1) Concentration by direct measurement.

(2) Concentration by difference (matrix element).

Table 4-7
Best Estimate Chemistry Data for Surveillance Weld Material (5P6756)

Element ID	Baseline Concentration(3) (wt %)	183 Degree Capsule Measured Concentration (wt %)	Best Estimate Concentration (wt %)
Cu	0.05	0.067	0.059
Fe(1)	Not Reported	96.3	96.3
Fe(2)	Not Reported	97	97
Mn	1.28	1.35	1.32
Mo	0.39	0.48	0.44
Ni	0.93	0.93	0.93
P	0.022	0.00659	0.01430
Si	0.37	0.42	0.40
S	0.015	Not Measured	0.015
C	0.09	Not Measured	0.09

(1) Concentration by direct measurement.

(2) Concentration by difference (matrix element).

(3) Surveillance heat 5P6756. P, Ni, and Cu are two sample averages rounded up since they are from the same single specimen. Source: GE-NE-523-101-1290, Supplemental Surveillance Program Report, January, 1992 [4-2].

Table 4-8
Best Estimate Chemistry Data for River Bend Vessel Plate C3054-2

Element ID	Baseline Concentration[3] (wt %)	183 Degree Capsule Measured Concentration (wt %)	Best Estimate Concentration (wt %)
Cu	0.09	0.075	0.09
Fe[1]	Not Reported	97.4	97.4
Fe[2]	Not Reported	97	97
Mn	1.29	1.31	1.30
Mo	0.56	0.55	0.56
Ni	0.69	0.66	0.68
P	0.007	0.0069	0.007
Si	0.26	0.30	0.28
S	0.02	Not Measured	0.02
C	0.18	Not Measured	0.18
V	0.00	Not Measured	0.00
Al	0.028	Not Measured	0.028

(1) Concentration by direct measurement.

(2) Concentration by difference (matrix element).

(3) Plate No. C3054-2. All elements are two sample averages rounded up since they are from the same single specimen. Source: RBS material certification data [4-1]).

5 CHARPY TEST DATA

5.1 Charpy Test Procedure

Charpy impact tests were conducted in accordance with ASTM Standards E 185-82 and E 23-02. A drawing showing the Charpy test specimen geometry is given in Figure 5-1. The 1982 version of E 185 has been reviewed and approved by NRC for surveillance capsule testing applications. This standard references ASTM E 23. The tests were conducted using a Tinius Olsen Testing Machine Company, Inc. Model 84 impact test machine with a 300 ft-lb (406.75 J) range. The Model 84 is equipped with a dial gage as well as the MPM optical encoder system for accurate absorbed energy measurement. In all cases, the optical encoder measured energy was reported as the impact energy because it is much more accurate than the dial. The optical encoder can resolve the energy to within 0.04 ft-lbs (0.054 J), whereas, for the dial, the resolution is around 0.25 ft-lbs (0.34 J). The impact energy was corrected for windage and friction for each test performed. The velocity of the striker at impact was nominally 18 ft/s (5.49 m/s). The MPM encoder system measures the exact impact velocity for every test. Calibration of the machine was verified as specified in E 23 and verification specimens were provided by NIST.

Impact tests were conducted using an instrumented striker system fabricated by MPM. A standard is currently being developed by ASTM for instrumented testing but is not yet available for use in testing. The guidance provided in the draft standard was followed in the testing, however, the instrumented data provided should not be considered as nuclear quality assurance data at the present time. Figure 5-2 illustrates the raw data recorded by the instrumented system software. The voltage-time signal is converted to a force-time (Figure 5-3) signal through calibration of the striker. The force-time curve is integrated to produce the velocity-time curve, which in turn is integrated to yield the striker displacement-time curve. Figure 5-4 shows a typical force-displacement curve along with the critical load points. This curve is the key result from instrumented testing. The instrumented data, as shown in Figure 5-4, can be used in materials embrittlement research and for development of fracture toughness correlations.

The E 23 procedure for specimen temperature control using an in-situ heating and cooling system was followed. The advantage of using the MPM in-situ heating/cooling technology is that each specimen is thermally conditioned right up to the instant of impact. Thermal losses, such as those associated with liquid bath systems, are completely eliminated. Each specimen was held at the desired test temperature for at least 5 minutes prior to testing and the fracture process zone temperature was held to within ± 1.8 F (± 1 C) up to the instant of strike. Precision calibrated tongs were used for specimen centering on the test machine.

Lateral expansion was determined from measurements made with a lateral expansion gage. The lateral expansion gage was calibrated using precision gage blocks which are traceable to NIST.

The percentage of shear fracture area was determined by integrating the ductile and brittle fracture areas using the MPM image analysis system.

The number of Charpy specimens for measurement of the transition region and upper shelf was limited. Therefore, the choice of test temperatures was very important. Prior to testing, the Charpy energy-temperature curve was predicted using embrittlement models and previous data. The first test was then conducted near the middle of the transition region and test temperature decisions were then made based on the test results. Overall, the goal was to perform four tests on the upper shelf and to use the remaining eight specimens to characterize the 30 ft-lb (41 J) index. This approach was successful as illustrated in the next report section.

5.2 Charpy Test Data

Twelve irradiated base metal, twelve weld metal, and twelve HAZ specimens were tested over the transition region temperature range and on the upper shelf. The data are summarized in Tables 5-1 through 5-3. The heat C3054 slab 2 (C3054-2) base metal surveillance specimens have a T-L orientation. In addition to the energy absorbed by the specimen during impact, the measured lateral expansion values and the percentage shear fracture area for each test specimen are listed in the tables. The Charpy energy was read from the optical encoder and has been corrected for windage and friction in accordance with ASTM E 23. The impact energy is the energy required to initiate and propagate a crack. The optical encoder and the dial cannot correct for tossing energy and therefore this small amount of additional energy, if present, may be included in the data for some tests. The instrumented striker data is provided in Appendix A. As discussed earlier, these data were not obtained under the nuclear quality assurance program because there is not yet an ASTM test procedure available. However, since research is currently being conducted to extract fracture toughness from instrumented Charpy data, it was considered prudent to perform the tests with an instrumented striker. The instrumented integrated energy is typically different from the dial measured energy for several reasons. Many of the causes for differences between the dial and instrumented striker energies are discussed in Reference [5-1]. Since the dial/optical encoder is the energy measurement method used to establish the US reactor pressure vessel embrittlement database, the instrumented striker data has been normalized to agree with the encoder energy. This approach has the advantage that the characteristic load data is consistent with the energy measurement method.

The lateral expansion is a measure of the transverse plastic deformation produced by the striking edge of the striker during the impact event. Lateral expansion is determined by measuring the maximum change of specimen thickness along the sides of the specimen. Lateral expansion is a measure of the ductility of the specimen. The nuclear industry tracks the embrittlement shift using the 35 mil (0.89 mm) lateral expansion index.

The percentage of shear fracture area is a direct quantification of the transition in the fracture modes as the temperature increases. All metals with a body centered cubic lattice structure, such as ferritic pressure vessel materials, undergo a transition in fracture modes. At low test temperatures, a crack propagates in a brittle manner and cleaves across the grains. As the temperature increases, the percentage of shear (or ductile) fracture increases. This temperature range is referred to as the transition region and the fracture process is mixed mode. As the temperature increases further, the fracture process is eventually completely ductile (ie., no brittle component) and this temperature range is referred to as the upper shelf region.

Preparation of P-T operating curves requires the determination of the Charpy 30 ft-lb (41 J) transition temperature shift. This index is determined by fitting the energy-temperature data to find the mean curve. It is also necessary to estimate the upper shelf energy to ensure that the shelf has not dropped below the 10CFR50, Appendix G, 50 ft-lb (67.8 J) screening criterion. The Charpy data analysis results are provided in the next section of this report. 10CFR50, Appendix H requires that the unirradiated data be included in the surveillance report. Therefore, the base and weld unirradiated data are given in Tables 5-4 and 5-5, respectively. Charpy energies, lateral expansions, and fracture appearances for the C3054-2 base metal were obtained from the Lukens Steel Company test certificates [5-2]. Charpy energies, lateral expansions, and fracture appearances for the surveillance welds were obtained from the Phase 2 report of the BWR Owner's Group Supplemental Surveillance Program [5-3]. Unirradiated HAZ data was not developed for this plant.

5.3 Chapter 5 Reference

[5-1] Manahan, M. P., Sr., and Stonesifer, R. B., "The Difference Between Total Absorbed Energy Measured Using An Instrumented Striker and That Obtained Using and Optical Encoder", Pendulum Impact Testing: A Century of Progress, ASTM STP 1380, T. A. Siewert and M. P. Manahan, Sr., Eds., American Society for Testing and Materials, West Conshohocken, PA, 1999.

[5-2] Lukens Steel Company Test Certificates, File 1540-06-13, Melt C3054, Slab 2, October, 15, 1973.

[5-3] "Progress Report on Phase 2 of the BWR Owner's Group Supplemental Surveillance Program", GE-NE-523-101-1290, DRF B11-00392-1, January, 1992.

Table 5-1
Charpy V-Notch T-L Impact Test Results for Irradiated (Fast (E > 1MeV) Fluence of 1.16 x 10^{18} n/cm^2) C3054-2 Base Metal Specimens from the River Bend 183 Degree Surveillance Capsule

Specimen Identification	Test Temperature F (C)	Impact Energy ft-lb (J)	Fracture Appearance (% Shear Area)	Lateral Expansion mils (mm)
B1	-45.40 (-43.00)	6.47 (8.77)	7.1	6.5 (0.2)
B12	-43.60 (-42.00)	8.89 (12.05)	8.4	10.5 (0.3)
B3	20.30 (-6.50)	39.38 (53.39)	25.1	34.5 (0.9)
B7	22.80 (-5.11)	33.93 (46.00)	22.5	30.5 (0.8)
B2	70.16 (21.20)	43.25 (58.64)	30.6	42.0 (1.1)
B11	70.88 (21.60)	44.93 (60.92)	29.7	44.0 (1.1)
B8	100.22 (37.90)	60.75 (82.37)	39.1	48.0 (1.2)
B9	128.66 (53.70)	79.24 (107.44)	52.8	67.0 (1.7)
B10	129.00 (53.89)	80.94 (109.74)	60.9	66.5 (1.7
B6	176.54 (80.30)	99.59 (135.03)	100.0	75.0 (1.9)
B5	212.90 (100.50)	103.42 (140.22)	100.0	79.0 (2.0)
B4	217.04 (102.80)	98.64 (133.74)	100.0	74.0 (1.9)

Table 5-2
Charpy V-Notch Impact Test Results for Irradiated (Fast (E > 1MeV) Fluence of 1.16 x 10^{18} n/cm^2) Weld Metal Specimens (5P6756) from the River Bend 183 Degree Surveillance Capsule

Specimen Identification	Test Temperature F (C)	Impact Energy ft-lb (J)	Fracture Appearance (% Shear Area)	Lateral Expansion mils (mm)
W2	-42.52 (-41.40)	21.43 (29.06)	21.5	20.0 (0.5)
W5	-41.98 (-41.10)	36.74 (49.81)	28.7	33.0 (0.8)
W8	11.30 (-11.50)	25.95 (35.18)	31.6	24.0 (0.6)
W6	11.48 (-11.40)	27.43 (37.19)	31.8	23.0 (0.6)
W1	37.04 (2.80)	68.18 (92.44)	66.1	52.5 (1.3)
W10	37.22 (2.90)	48.05 (65.15)	55.6	41.0 (1.0)
W4	69.62 (20.90)	63.52 (86.12)	62.7	53.5 (1.4)
W9	69.98 (21.10)	66.41 (90.04)	79.3	58.0 (1.5)
W11	127.76 (53.20)	79.78 (108.17)	100.0	72.0 (1.8)
W3	131.18 (55.10)	80.22 (108.76)	93.3	71.0 (1.8)
W12	159.26 (70.70)	77.20 (104.67)	97.1	65.5 (1.7)
W7	199.76 (93.20)	96.33 (130.61)	100.0	78.0 (2.0)

Table 5-3
Charpy V-Notch Impact Test Results for Irradiated (Fast (E > 1MeV) Fluence of 1.16 x 10^{18} n/cm^2) HAZ Metal Specimens from the River Bend 183 Degree Surveillance Capsule

Specimen Identification	Test Temperature F (C)	Impact Energy ft-lb (J)	Fracture Appearance (% Shear Area)	Lateral Expansion mils (mm)
H12	-102.64 (-74.80)	11.53 (15.63)	13.0	7.0 (0.2)
H4	-102.46 (-74.70)	17.38 (23.56)	13.0	11.0 (0.3)
H8	-63.22 (-52.90)	18.66 (25.30)	17.0	12.0 (0.3)
H1	-61.42 (-51.90)	27.67 (37.52)	20.4	19.0 (0.5)
H2	-36.58 (-38.10)	35.16 (47.67)	38.2	28.0 (0.7)
H11	-28.48 (-33.60)	36.24 (49.13)	35.6	30.0 (0.8)
H9	7.52 (-13.60)	74.04 (100.38)	64.4	50.0 (1.3)
H5	7.88 (-13.40)	46.20 (62.64)	53.2	35.5 (0.9)
H3	67.82 (19.9)	87.29 (118.35)	100.0	63.0 (1.6)
H7	68.18 (20.10)	76.16 (103.26)	73.5	47.5 (1.2)
H10	126.32 (52.40)	86.69 (117.54)	100.0	75.5 (1.9)
H6	128.84 (53.80)	101.50 (137.62)	100.0	63.0 (1.6)

Table 5-4
Charpy V-Notch T-L Impact Test Results for Unirradiated C3054-2 Base Metal Specimens from the River Bend Surveillance Program [Reference 5-2]

Test Temperature F (C)	Impact Energy ft-lb (J)	Fracture Appearance (% Shear Area)	Lateral Expansion mils (mm)	Test Temperature F (C)	Impact Energy ft-lb (J)	Fracture Appearance (% Shear Area)	Lateral Expansion mils (mm)
-100 (-73.33)	6 (8.13)	1	1 (0.0)	30 (-1.11)	65 (88.13)	50	54 (1.4)
-100 (-73.33)	6 (8.13)	1	1 (0.0)	50 (10.00)	45 (61.01)	60	46 (1.2)
-100 (-73.33)	7 (9.49)	1	2 (0.1)	50 (10.00)	64 (86.77)	60	58 (1.5)
-40 (-40.00)	18 (24.40)	20	18 (0.5)	50 (10.00)	64 (86.77)	60	59 (1.5)
-40 (-40.00)	22 (29.83)	20	14 (0.4)	70 (21.11)	51 (69.15)	50	44 (1.1)
-40 (-40.00)	26 (35.25)	20	14 (0.4)	70 (21.11)	64 (86.77)	50	54 (1.4)
0 (-17.78)	32 (43.39)	30	31 (0.8)	70 (21.11)	62 (84.06)	50	54 (1.4)
0 (-17.78)	34 (46.10)	30	28 (0.7)	100 (37.78)	72 (97.62)	80	64 (1.6)
0 (-17.78)	42 (56.94)	30	30 (0.8)	100 (37.78)	75 (101.69)	80	62 (1.6)
20 (-6.67)	34 (46.10)	30	32 (0.8)	100 (37.78)	79 (107.11)	80	64 (1.6)
20 (-6.67)	34 (46.10)	30	31 (0.8)	212 (100.00)	92 (124.74)	99	74 (1.9)
20 (-6.67)	36 (48.81)	30	32 (0.8)	212 (100.00)	92 (124.74)	99	74 (1.9)
20 (-6.67)	49 (66.44)	40	46 (1.2)	212 (100.00)	102 (138.29)	99	76 (1.9)
20 (-6.67)	53 (71.86)	40	41 (1.0)				
20 (-6.67)	48 (65.08)	40	39 (1.0)				
30 (-1.11)	59 (79.99)	50	54 (1.4)				
30 (-1.11)	63 (85.42)	50	44 (1.1)				

Table 5-5
Charpy V-Notch Impact Test Results for Unirradiated Weld Metal Specimens (5P6756) from the River Bend Surveillance Program
(Reference 5-3)

Test Temperature F (C)	Impact Energy ft-lb (J)	Fracture Appearance (% Shear Area)	Lateral Expansion mils (mm)
-100 (-73.33)	7.5 (10.17)	14	0.0 (0.0)
-80 (-62.22)	22.0 (29.83)	16	13.5 (0.3)
-60 (-51.11)	43.0 (58.30)	26	27.5 (0.7)
-60 (-51.11)	32.5 (44.06)	29	23.0 (0.6)
-40 (-40.00)	47.0 (63.72)	34	30.5 (0.8)
-20 (-28.89)	54.5 (73.89)	28	40.5 (1.0)
0 (-17.78)	53.5 (72.54)	51	35.5 (0.9)
20 (-6.67)	72.5 (98.30)	69	52.0 (1.3)
40 (4.44)	75.5 (102.36)	72	56.0 (1.4)
60 (15.56)	70.0 (94.91)	66	55.0 (1.4)
60 (15.56)	88.0 (119.31)	90	66.0 (1.7)
100 (37.78)	102.0 (138.29)	100	78.0 (2.0)
180 (82.22)	102.0 (138.29)	100	77.0 (2.0)
300 (148.89)	106.0 (143.72)	100	78.5 (2.0)
400 (204.44)	107.5 (145.75)	100	78.0 (2.0)

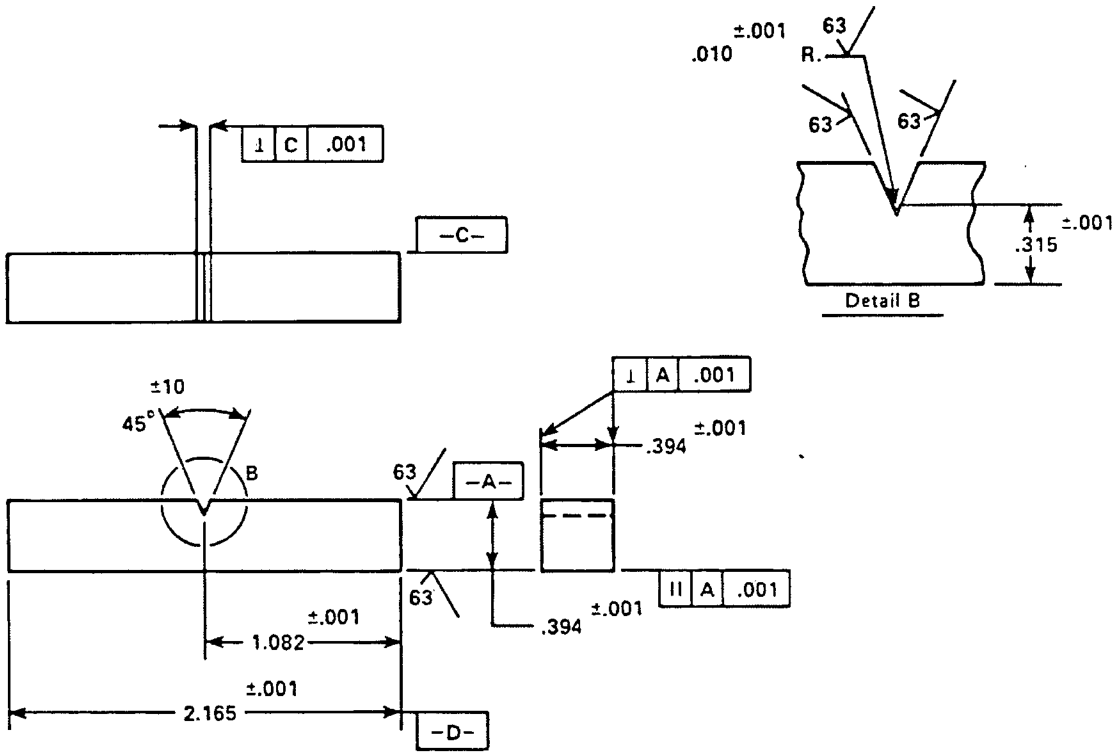

Figure 5-1
Drawing Showing the Charpy Test Specimen Geometry

Sample ID

W4METRIC

Comments

Impact™ V3.0

Summary Report

Test Parameters	Value
Group ID	RiverBend-Weld
Date	11/11/2002 09:50
Operator	Dr. Michael P. Manahan, Sr.
Temperature	20.9 °C
Oscilloscope	MPM Internal Oscilloscope
Striker	8mm Metals
Interpolation	Point-Point Linear
Encoder Controller	MPM Encoder System
Velocity Determination	Encoder
Material	Metal
Size	Type A
Orientation	Isotropic
Notch Type	V Notch, no Side-Groove
Units Normalization	None
Energy Adjustment	1.0437
Length	55.0000 mm
Width	10.0000 mm
Thickness	10.0000 mm
Span	40.0000 mm
Uncracked Ligament	8.0000 mm
Notch Rafius	0.2500 mm
Failure Type	complete fracture
Post Test Comments	good test
Impact Velocity	5.479 m/s
Striker Energy	86.112 J
Dial Gage Energy	85.412 J
Encoder Energy	86.112 J
Latch Angle	134.15°
Final Angle	109.69°
Potential Energy	415.902 J
Windage & Friction	0.888 J
Percent Shear	62.72 %
Lateral Expansion	1.3589 mm

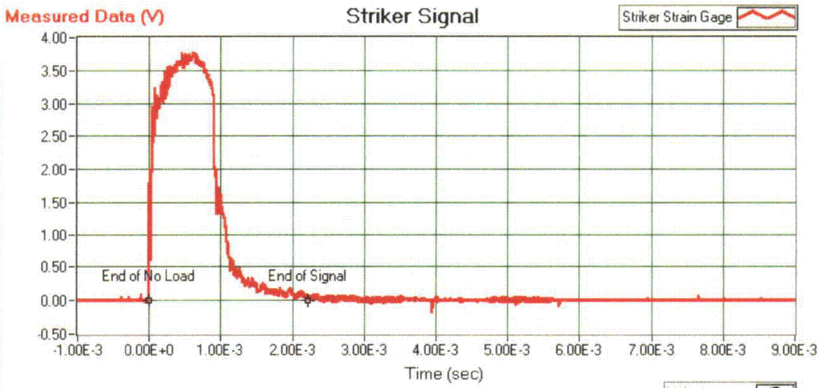

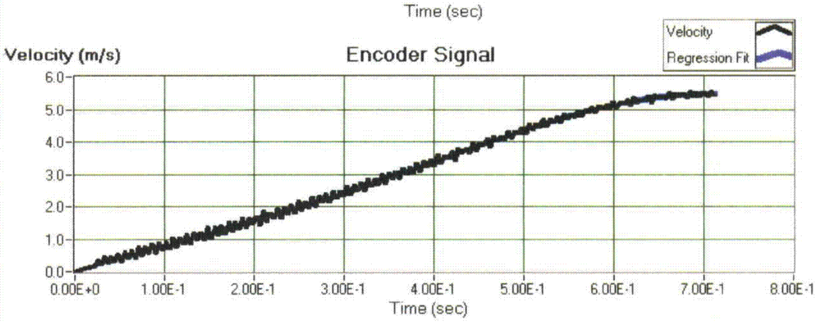

	Load (N)	Displacement (mm)	Velocity (m/s)	Time (s)	Energy (J)
General Yield	1.3034E+4	3.158E-1	5.465E+0	5.087E-5	2.22415E+0
Peak Load	1.7178E+4	3.140E+0	5.178E+0	5.810E-4	4.65558E+1
Brittle Fracture	1.5373E+4	4.642E+0	5.010E+0	8.760E-4	7.13967E+1
Arrest Load	7.5586E+3	4.967E+0	4.983E+0	9.410E-4	7.52964E+1
End of Signal	9.0164E+1	1.119E+1	4.907E+0	2.205E-3	8.61117E+1

Figure 5-2
Typical Instrumented Striker Raw Data Signal

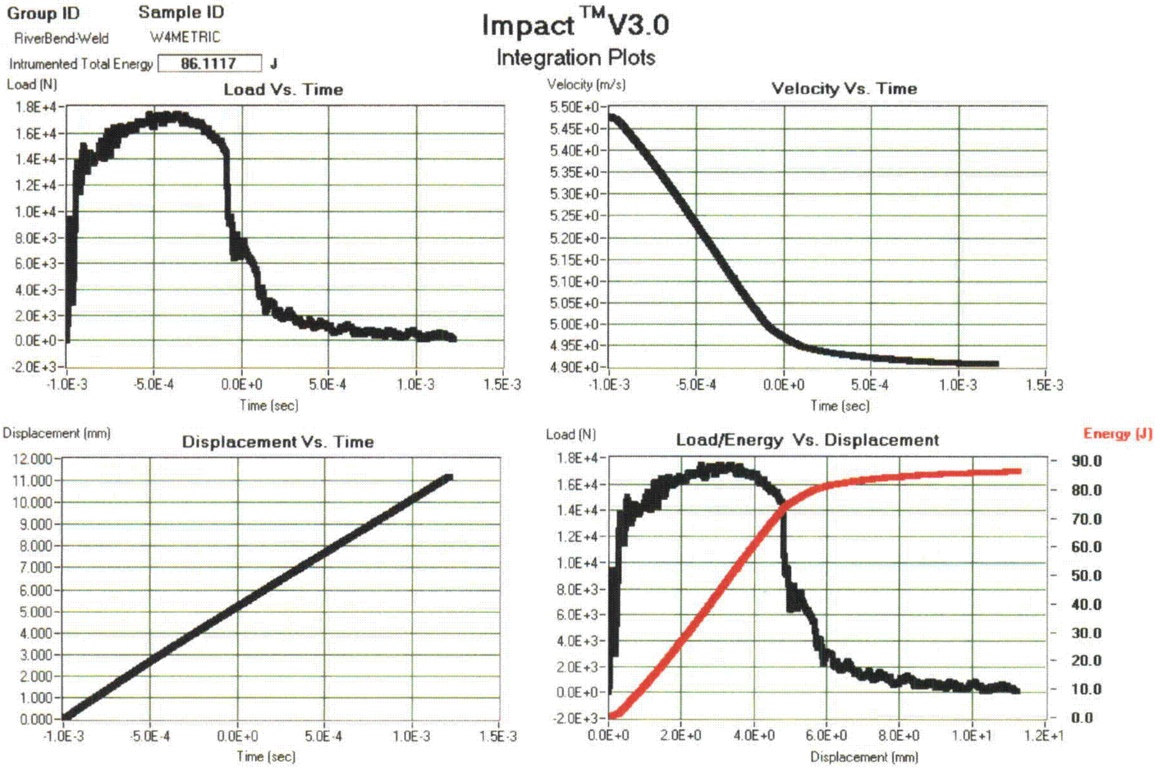

Figure 5-3
Example Plots Showing Integrations Performed to Obtain the Load-Deflection Curve

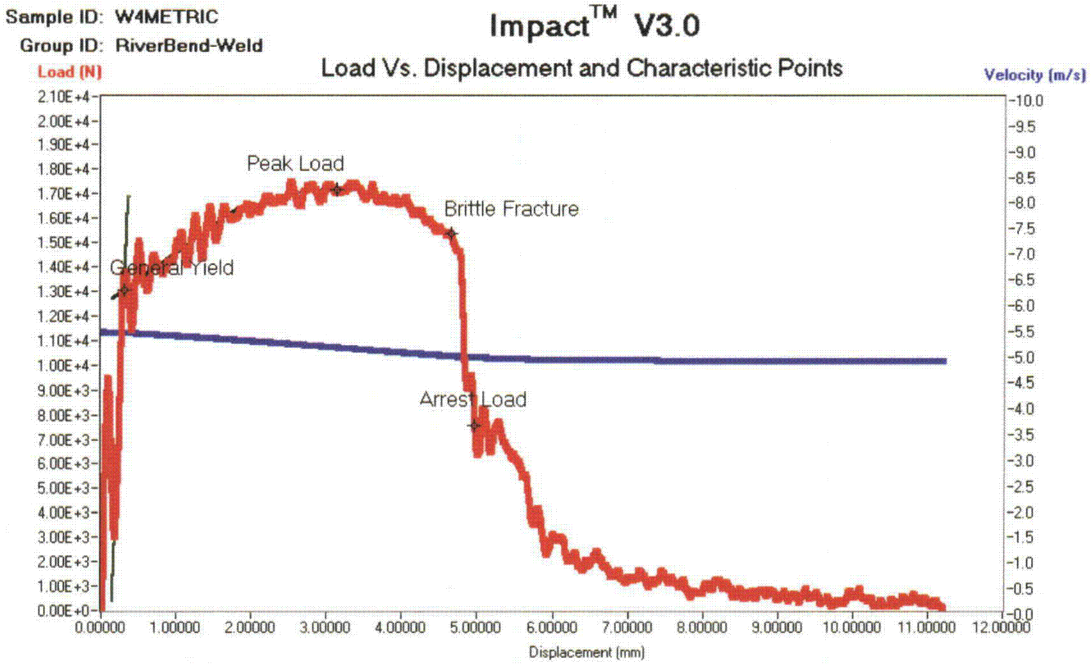

	Load (N)	Displacement (mm)	Velocity (m/s)	Time (s)	Energy (J)
General Yield	1.3034E+4	3.158E-1	5.465E+0	5.087E-5	2.22415E+0
Peak Load	1.7178E+4	3.140E+0	5.178E+0	5.810E-4	4.65558E+1
Brittle Fracture	1.5373E+4	4.642E+0	5.010E+0	8.760E-4	7.13967E+1
Arrest Load	7.5586E+3	4.967E+0	4.983E+0	9.410E-4	7.52964E+1
End of Signal	9.0164E+1	1.119E+1	4.907E+0	2.205E-3	8.61117E+1

Figure 5-4
Typical Load-Deflection Curve Showing Critical Load Points

6 CHARPY CURVE FITTING

Charpy curve fitting for pressure vessel surveillance applications is a challenging task because, for most capsules, there are relatively few data points. For each of the base, weld, and HAZ metals of the current 183 degree capsule analysis, there are twelve data points available to characterize the entire transition region and upper shelf. Several organizations have developed curve fitting software to address this issue. However, differences in model assumptions and fitting techniques result in differences in the fitted parameters. In an effort to standardize the Charpy data fitting results, the BWRVIP ISP has selected the CVGRAPH program [6-1] to fit the baseline ISP data. This program fits the Charpy data to a symmetric hyperbolic tangent function. In order to maintain consistency with the unirradiated fits, EPRI requested that ATI consulting use CVGRAPH Version 5.0.2 to fit the River Bend irradiated data.

The curve fitting results are given in terms of plots of Charpy energy and lateral expansion as functions of temperature. These plots show the data points as well as the best fit trends. In addition, three definitions of transition temperature are applied to the fitted data and the results are summarized in tabular form. The three transition temperature definitions, referred to as the Charpy indices, are:

- 30 ft-lb (41 J) Charpy energy
- 50 ft-lb (67.8 J) Charpy energy
- 35 mil (0.89 mm) lateral expansion

Upper shelf Charpy energy and lateral expansion (LE) are also tabulated. The fitting results are discussed later in this report section.

6.1 Fitting Procedure

The BWRVIP ISP has established rules for analyzing Charpy test data. The upper shelf energy for a given data set is established as the average of all test points which exhibit 95% and greater shear fracture area. If an outlier point skews the USE when calculated by the rule, engineering judgment may be exercised to exclude the outlier if a better overall fit is achieved. Exclusion of outliers is rarely imposed in practice. The lower shelf energy is fixed at 2.5 ft-lbs (3.4 J). With regard to LE, the upper shelf LE (USLE) is set at the average of all test points exhibiting 95% and greater shear. As with energy, a rare engineering judgment may be exercised to obtain a better fit. The lower shelf LE is fixed at 1.0 mils (0.0254 mm). Fracture appearance data are not fit under the ISP, but these data are used to distinguish the upper shelf data points.

CVGRAPH uses a symmetric hyperbolic tangent function to fit the data. The functional form for energy fitting is given below:

$$E = A + B\left[Tanh\left(\frac{(T - T_0)}{(C + DT)}\right)\right] \qquad \textbf{Equation 6-1}$$

where,

E	=	Charpy energy
A, B, C	=	regression coefficients
D	=	0.0 (the asymmetry term is not used in the fit)

The minimization function used by ATI assumes constant variance over the entire temperature range.

6.2 183 Degree Surveillance Capsule Fitting Results

The reason for testing irradiated material is to determine the extent to which the irradiation has embrittled the material. It is therefore necessary to compare the irradiated material test results to the test results of the same material in the unirradiated condition. Unirradiated Charpy energies, lateral expansions, and fracture appearances for the C3054-2 base metal were obtained from the Lukens Steel Company test certificates [6-2]. Similar data for the surveillance weld were obtained from Reference [6-3]. No test data was available for unirradiated HAZ material. The surveillance capsule base metal specimens are in the transverse-longitudinal (TL) orientation.

The above fitting procedures were applied to the irradiated base and weld metal data from the 183 degree capsule specimens as well as the unirradiated data. The data and the resulting best fit trends are shown in Figures 6-1 through 6-4. The key Charpy test parameters are summarized in Tables 6-1 through 6-4.

As expected, the base metal energy data (Figure 6-1) show a temperature shift of the Charpy energy transition region to higher temperatures due to the irradiation. The average of the three irradiated upper shelf energy data points is slightly higher than the average of the unirradiated USE data points. The 30 ft-lb (41 J) and 50 ft-lb (67.8 J) transition temperatures and the USE are summarized in Table 6-1. At the 30 ft-lb (41 J) level, the temperature shift is +44.0 F (+24.4 C). At the 50 ft-lb (67.8 J) level, the temperature shift is +36.7 F (20.4 C). The irradiated USE increased by 5.3 ft-lbs (+7.2 J). Increases in the USE have been observed in other plants. This material behavior may be related to low fluence improvement of the matrix material which results in more ductile ligament response during the ductile fracture process. At higher fluences, the USE is expected to decrease below the unirradiated average.

Similarly, the weld metal energy data (Figure 6-2) show a temperature shift of the Charpy energy transition region to higher temperatures due to the irradiation. The 30 ft-lb (41 J) and 50 ft-lb (67.8 J) transition temperatures and the USE are summarized in Table 6-2. At the 30 ft-lb (41 J) level, the temperature shift is +53.7 F (29.8 C). At the 50 ft-lb (67.8 J) level, the temperature shift is +54.4 F (30.2 C). These shifts are 9.7 F (5.4 C) and 17.7 F (9.8 C) larger than found for the base metal 30 ft-lb (41 J) and 50 ft-lb (67.8 J) transition temperature shifts, respectively. The irradiated USE decreased by 20 ft-lbs (-27.1 J).

The lateral expansion data trends are consistent with the energy data trends for both weld and base metal. The 35 mil (0.89 mm) lateral expansion change for weld metal was larger than that for the base metal. The USLE for the base metal increased as was observed for the energy based parameter (USE). Similarly, the USLE for weld metal decreased, and a decrease was also observed for the weld metal USE. The LE parameters are summarized in Tables 6-3 and 6-4.

6.3 Chapter 6 References

[6-1] CVGRAPH, Hyperbolic Tangent Curve Fitting Program, Developed by ATI Consulting, Version 5.0.2, Revision 1, 3/26/02.

[6-2] Lukens Steel Company Test Certificates, File 1540-06-13, Melt C3054, Slab 2, October, 15, 1973.

[6-3] "Progress Report on Phase 2 of the BWR Owner's Group Supplemental Surveillance Program", GE-NE-523-101-1290, DRF B11-00392-1, January, 1992.

Table 6-1
Base Metal (C3054-2)Charpy Energy Impact Parameters (TL Orientation)

Fluence (n/cm2)	30 ft-lb (41 J) Transition Temperature F (C)	50 ft-lb (67.8 J) Transition Temperature F (C)	Upper Shelf Energy ft-lb (J)
0	-16.6 (-27.0)	31.7 (-0.2)	95.3[1] (129.2)
1.16×10^{18}	27.4 (-2.6)	68.4 (20.2)	100.6[1] (136.4)
Change	44.0 (24.4)	36.7 (20.4)	+5.3 (+7.2)

[1]Based on the average of three upper shelf data points.

Table 6-2
Weld Metal (5P6756) Charpy Energy Impact Parameters

Fluence (n/cm2)	30 ft-lb (41 J) Transition Temperature F (C)	50 ft-lb (67.8 J) Transition Temperature F (C)	Upper Shelf Energy ft-lb (J)
0	-67.1 (-55.1)	-21.3 (-29.6)	104.4[1] (141.6)
1.16×10^{18}	-13.4 (-25.2)	33.1 (0.6)	84.4[2] (114.4)
Change	53.7 (29.8)	54.4 (30.2)	-20.0 (-27.1)

[1]Based on the average of four upper shelf data points.

[2]Based on the average of three upper shelf data points.

Table 6-3
Base Metal (C3054-2) Charpy Test Lateral Expansion Behavior (TL Orientation)

Fluence (n/cm^2)	35 mil (0.89 mm) Lateral Expansion Transition Temperature F (C)	Upper Shelf Lateral Expansion mils (mm)
0	11.9 (-11.2)	74.7[(1)] (1.90)
1.16 x 10^{18}	41.2 (5.1)	76.0[(1)] (1.93)
Change	29.3 (16.3)	+1.3 (+0.03)

[(1)]Based on the average of three upper shelf data points.

Table 6-4
Weld Metal (5P6756) Charpy Test Lateral Expansion Behavior

Fluence (n/cm^2)	35 mil (0.89 mm) Lateral Expansion Transition Temperature F (C)	Upper Shelf Lateral Expansion mils (mm)
0	-20.3 (-29.1)	77.9[(1)] (1.98)
1.16 x 10^{18}	11.4 (-11.4)	71.8[(2)] (1.82)
Change	31.7 (17.6)	-6.1 (-0.15)

[(1)]Based on the average of four upper shelf data points.

[(2)]Based on the average of three upper shelf data points.

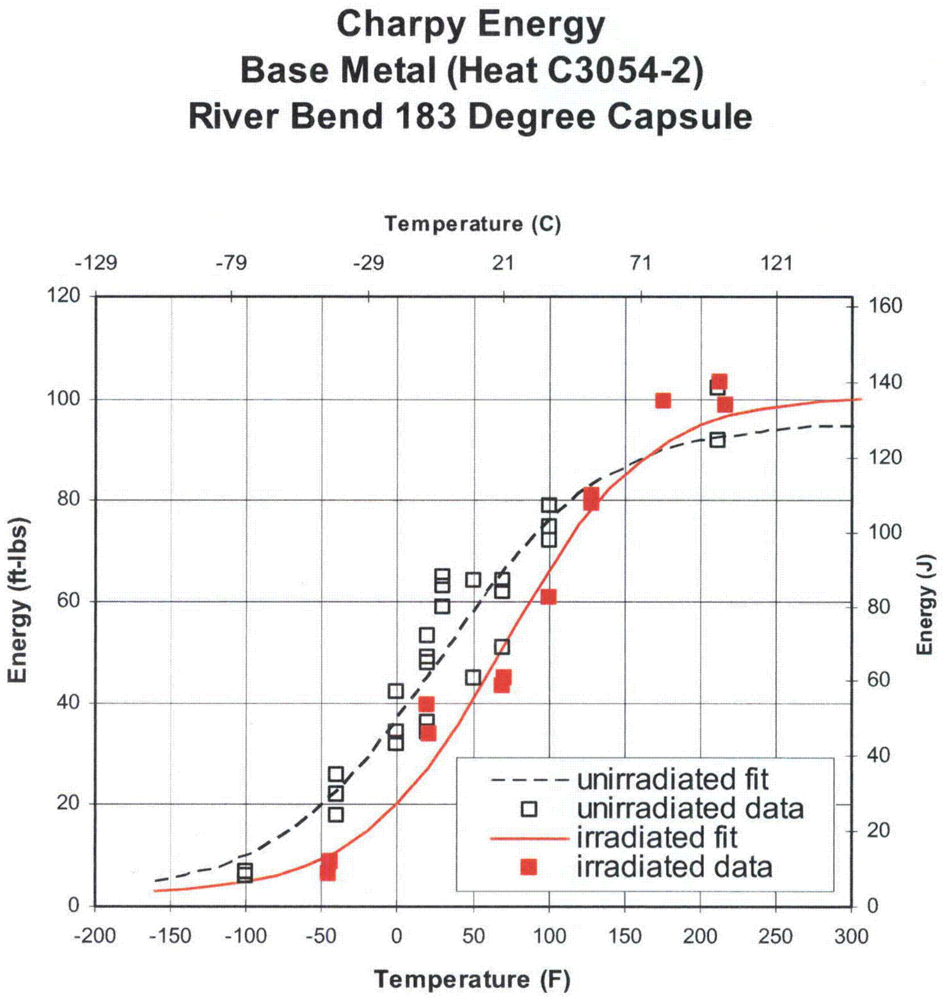

Figure 6-1
Charpy Energy Data and Curve Fits for C3054-2 Base Metal in the Unirradiated and Irradiated Conditions (TL Orientation)

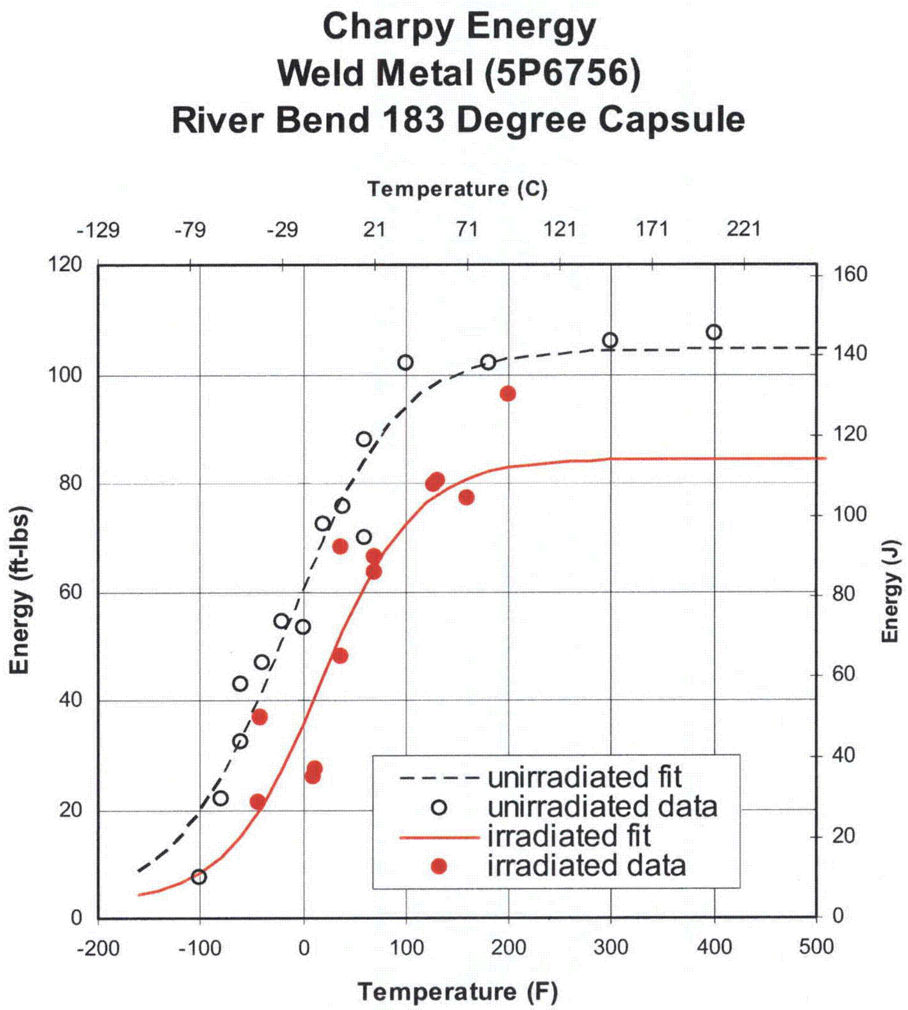

Figure 6-2
Charpy Energy Data and Curve Fits for Weld Metal (5P6756) in the Irradiated and Unirradiated Conditions

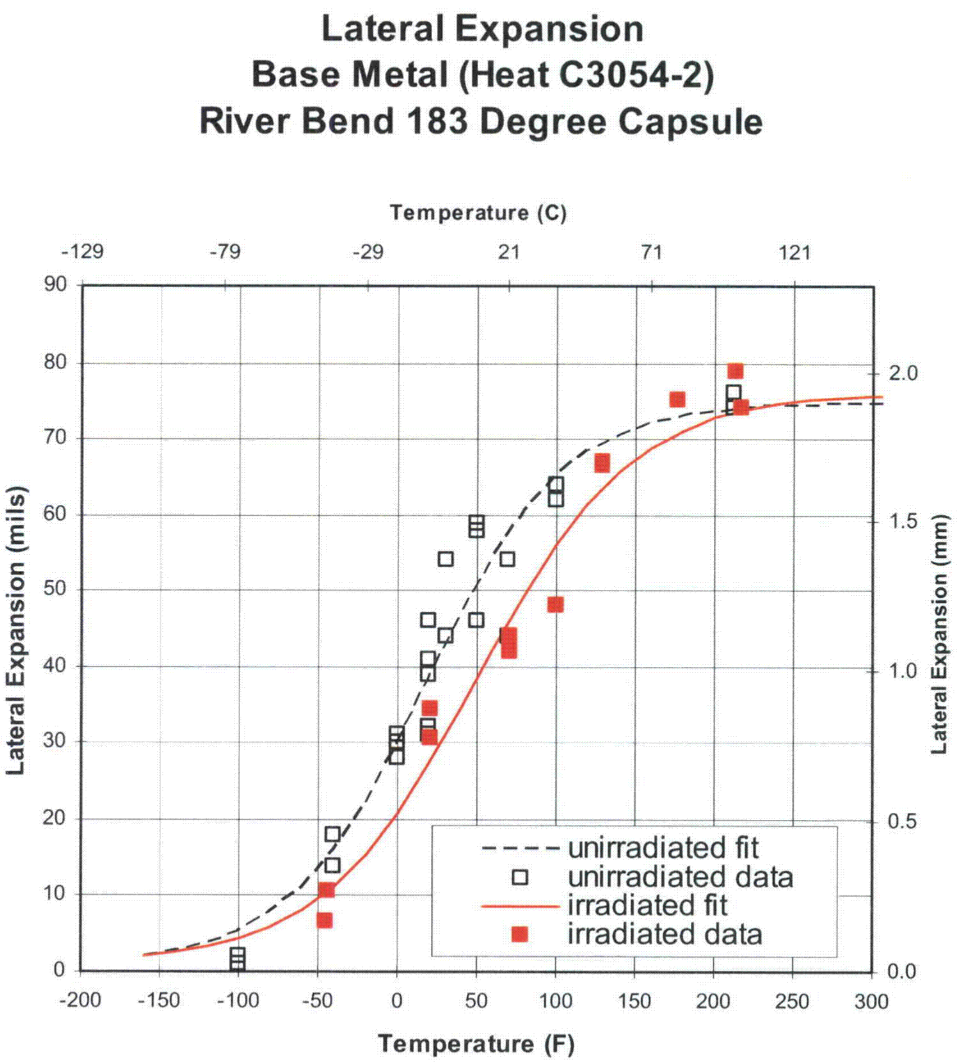

Figure 6-3
Charpy Lateral Expansion Data and Curve Fits for C3054-2 Base Metal in the Unirradiated and Irradiated Conditions (TL Orientation)

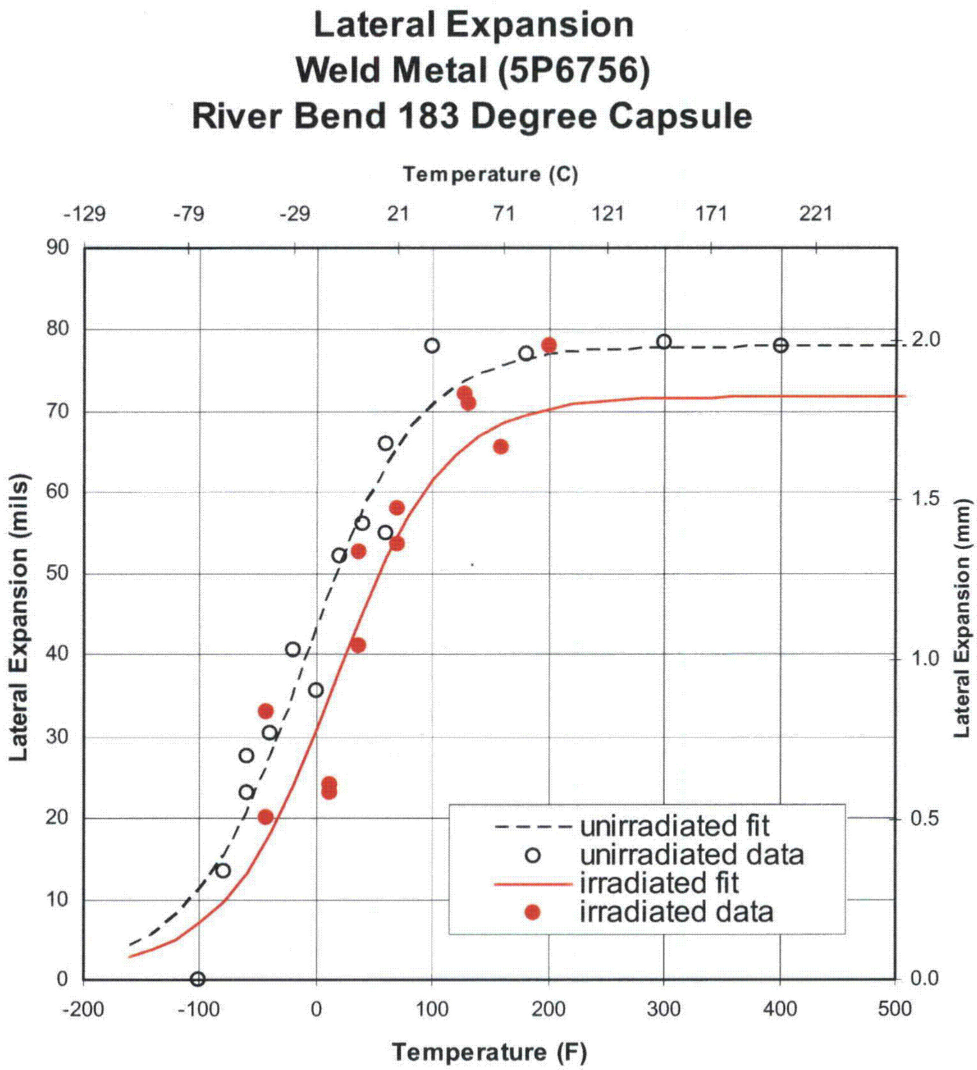

Figure 6-4
Charpy Lateral Expansion Data and Curve Fits for Weld Metal (5P6756) in the Irradiated and Unirradiated Conditions

7 SUMMARY AND CONCLUSIONS

Testing of the River Bend 183 degree surveillance capsule and evaluation of the data has led to the following conclusions:

- A fluence of 1.16 x 10^{18} n/cm^2 has been estimated for the 183 degree capsule exposure at 10.08 EFPY. Analysis of the dosimetry data has resulted in an average C/E ratio of 0.803 for the Cu dosimeter and 0.914 for the Fe dosimeter. The capsule average C/E ratio is 0.86. Overall, the transport calculation and dosimetry are in very good agreement.
- At the end of cycle 9, the lead factor (capsule fluence divided by vessel maximum fluence) at the vessel surface is calculated to be 0.95 (1.156 x 10^{18}/1.212 x 10^{18}). This value is significantly higher than that based on pre-operational estimates. The lead factor at the 1/4T location is 1.324 (1.156 x 10^{18}/8.73 x 10^{17}).
- The peak vessel surface fluence at 32 EFPY used by GE in the current P-T curve calculations is 6.6 x 10^{18} n/cm^2 before uprate, and 7.95 x 10^{18} n/cm^2 after uprate (after cycle 9). The peak surface fluence calculated by MPM at 32 EFPY, including the power uprate after cycle 9, is 4.45 x 10^{18} n/cm^2. Although a P-T curve revision is not required, the fluence reported here is significantly lower than the fluence used to calculate the current P-T limits and there would be significant reduction in the leak/hydro test temperature if the P-T limits were to be recalculated.
- The neutron induced plate C3054-2 embristtlement is consistent with BWR data trends. At a fluence of 1.16 x 10^{18} n/cm^2, the 183 degree capsule measured shift in the 30 ft-lb (41 J) transition temperature is 44.0 F (24.4 C).
- Similarly, the measured weld (heat 5P6756) embrittlement results are consistent with BWR data trends. The measured weld metal shift in the 30 ft-lb (41 J) transition temperature at a fluence of 1.16 x 10^{18} n/cm^2 is 53.7 F (29.8 C). Since there are no unirradiated HAZ data available, it is not possible to report the shift or shelf drop for the HAZ material.
- The River Bend base metal USE after irradiation is slightly higher (+5.3 ft-lbs (+7.2 J)) than the unirradiated value. This phenomenon has been observed in other plants and may be related to low fluence improvement of the matrix material which results in more ductile ligament response during the ductile fracture process. The weld metal USE after irradiation is lower (-20.0 ft-lbs (-27.1 J)) than the unirradiated value.
- Chemical measurements made on the capsule Charpy specimens have verified that the base metal specimens were fabricated from plate C3054-2 material. Similarly, the chemical measurements made on the capsule weld specimens confirmed that these specimens were prepared from the surveillance weld (heat 5P6756).
- Revised best estimate chemistry data for the plate and surveillance weld were determined. The best estimate surveillance weld copper concentration is 0.059 weight percent and for

nickel the best estimate concentration is 0.93 weight percent. Similarly, the best estimate vessel plate copper concentration is 0.09 weight percent and for nickel the best estimate concentration is 0.68 weight percent.

8
NOMENCLATURE

ASME	-	American Society of Mechanical Engineers
ASTM	-	American Society for Testing and Materials
ART_{NDT}	-	Adjusted Nil-Ductility Reference Temperature
ATI	-	Applying Technical Innovations Consulting
BAF	-	Bottom of Active Fuel
BWR	-	Boiling Water Reactor
BWRVIP	-	Boiling Water Reactor Vessel Internals Project
DBTT	-	Ductile-Brittle Transition Temperature
C	-	Degrees Celsius
CF	-	Chemistry Factor Specified in RG 1.99(2)
C/E	-	Calculated-to-Experimental
CFR	-	Code of Federal Regulations
DPA	-	Displacements Per Atom
EFPY	-	Effective Full Power Years
EFPS	-	Effective Full Power Seconds
EPRI	-	Electric Power Research Institute
F	-	Degrees Fahrenheit
GE	-	General Electric
GRSS	-	Gamma Ray Spectrometer System

HPGe	-	HyperPure Germanium Gamma Ray Detector
HAZ	-	Heat Affected Zone
ICP-MS	-	Inductively-Coupled Plasma - Mass Spectrometry
ID	-	Inner Diameter
IR	-	Inner Radius
ISP	-	Integrated Surveillance Program
LE	-	Lateral Expansion
LEFM	-	Linear-Elastic Fracture Mechanics
LWR	-	Light Water Reactor
MPM	-	MPM Technologies, Inc.
NRC	-	Nuclear Regulatory Commission
NIST	-	National Institute for Standards and Technology
NMP-1	-	Nine Mile Point Unit 1
NMP-2	-	Nine Mile Point Unit 2
OSQ	-	On-Screen Quantification Software Package
P-T	-	Pressure-Temperature
PCA	-	Pool Critical Assembly
PWR	-	Pressurized Water Reactor
RG 1.99(2)	-	Regulatory Guide 1.99 (Revision 2)
RG 1.190	-	Regulatory Guide 1.190
RBS	-	River Bend Station
RPV	-	Reactor Pressure Vessel
RSICC	-	Radiation Safety Information Computational Center

RT_{NDT} - Nil-Ductility Reference Temperature

ΔRT_{NDT},ΔT_{30} - Neutron Induced Shift in Nil-Ductility Reference Temperature Indexed at 30 ft-lbs (41 J) of absorbed energy

T - Vessel Wall Thickness

TL - Transverse-Longitudinal

USE - Upper Shelf Energy

USLE - Upper Shelf Lateral Expansion

A
APPENDIX – INSTRUMENTED IMPACT DATA

Appendix A-1 Base Metal Data

Impact™ V3.0
Summary Report

Sample ID
b1
Comments
River Bend 183 Degree Surveillance Capsule

Test Parameters	Value
Group ID	RiverBend-Base
Date	11/08/2002 16:04
Operator	Dr. Michael P. Manahan, Sr.
Temperature	-45.4 °F
Oscilloscope	MPM Internal Oscilloscope
Striker	8mm Metals
Interpolation	Point-Point Linear
Encoder Controller	MPM Encoder System
Velocity Determination	Encoder
Material	Metal
Size	Type A
Orientation	TL
Notch Type	V Notch, no Side-Groove
Units Normalization	None
Energy Adjustment	1.2643
Length	2.1654 in
Width	0.3937 in
Thickness	0.3937 in
Span	1.5748 in
Uncracked Ligament	0.3150 in
Notch Rafius	0.0098 in
Failure Type	incomplete fracture
Post Test Comments	good test
Impact Velocity	17.938 ft/s
Striker Energy	6.471 ft lbf
Dial Gage Energy	6.500 ft lbf
Encoder Energy	6.471 ft lbf
Latch Angle	134.14°
Final Angle	130.77°
Potential Energy	306.728 ft lbf
Windage & Friction	0.635 ft lbf
Percent Shear	7.08 %
Lateral Expansion	0.0065 in

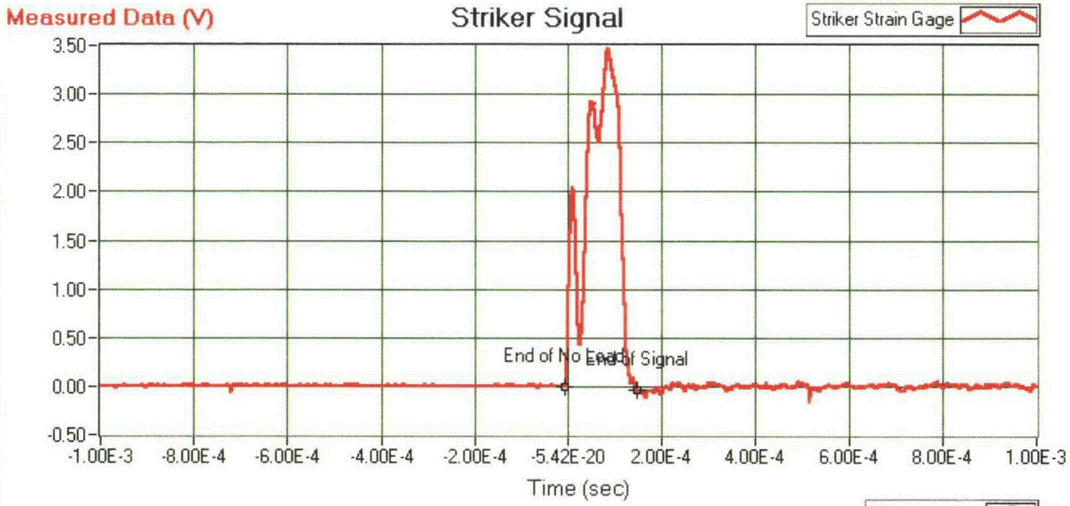

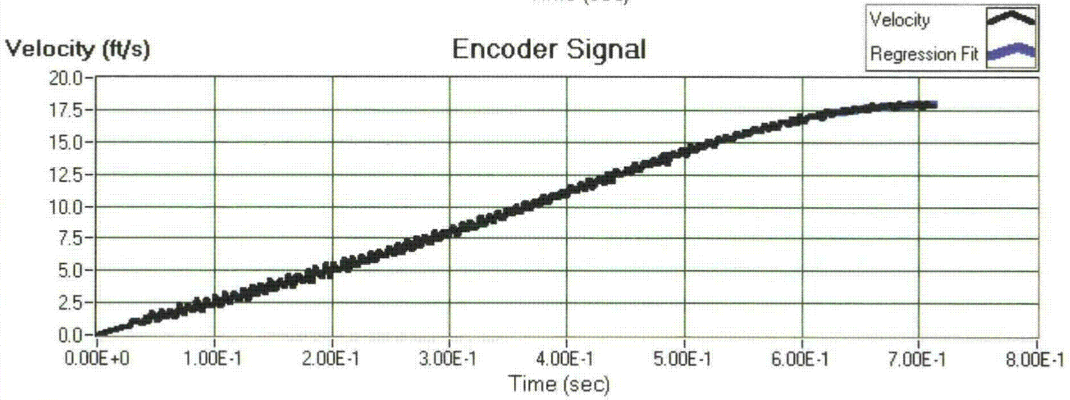

	Load (lbf)	Displacement (in)	Velocity (ft/s)	Time (s)	Energy (ft lbf)
Peak Load	4.3793E+3	2.035E-2	1.784E+1	8.700E-5	4.28699E+0
Brittle Fracture	3.7911E+3	2.465E-2	1.781E+1	1.070E-4	5.73292E+0
End of Signal	-4.6384E+1	3.295E-2	1.779E+1	1.460E-4	6.47120E+0

Sample ID: b1
Group ID: RiverBend-Base

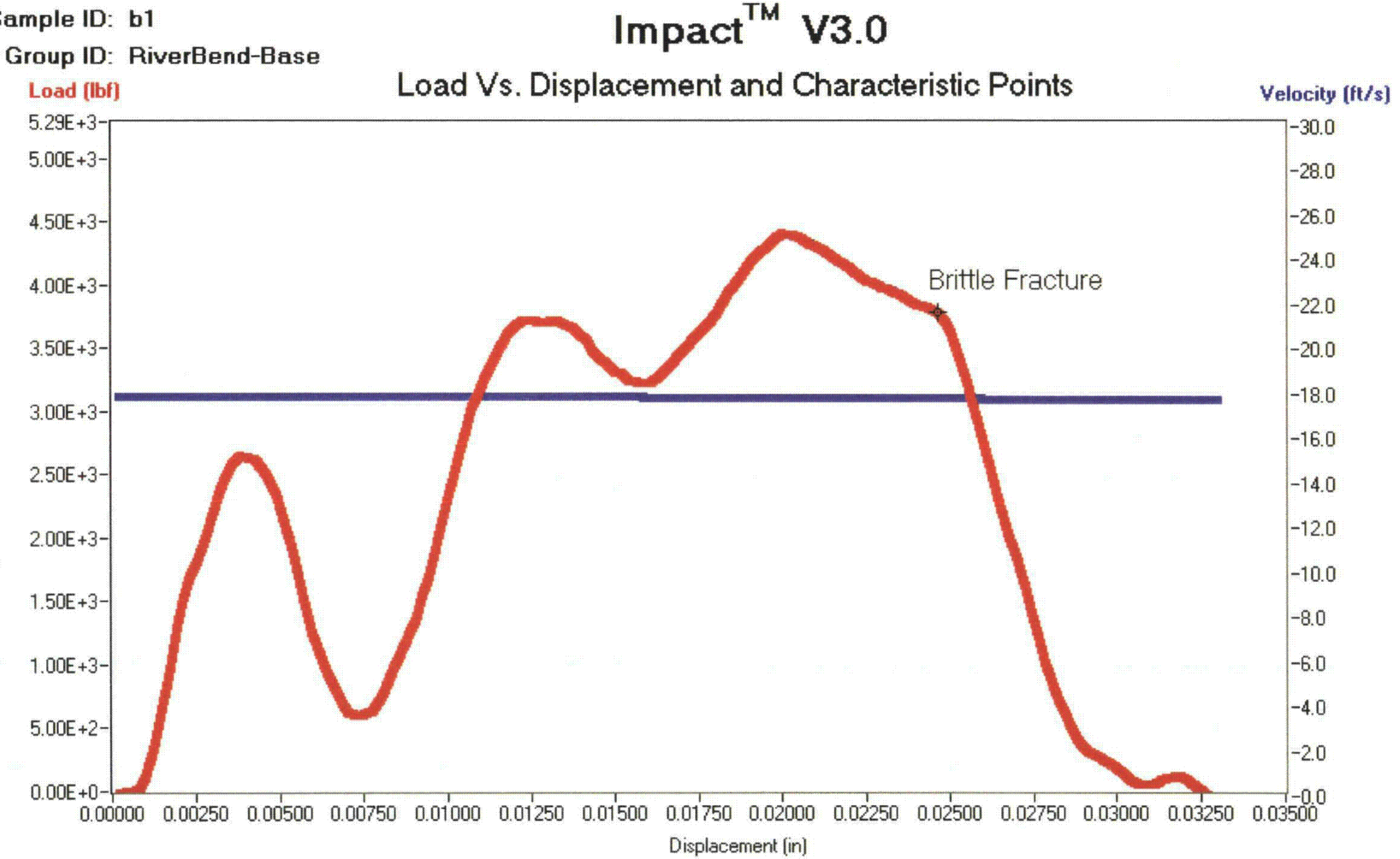

	Load (lbf)	Displacement (in)	Velocity (ft/s)	Time (s)	Energy (ft lbf)
Peak Load	4.3793E+3	2.035E-2	1.784E+1	8.700E-5	4.28699E+0
Brittle Fracture	3.7911E+3	2.465E-2	1.781E+1	1.070E-4	5.73292E+0
End of Signal	-4.6384E+1	3.295E-2	1.779E+1	1.460E-4	6.47120E+0

Sample ID

b12

Comments

River Bend 183 Degree Surveillance Capsule

Impact™ V3.0

Summary Report

Test Parameters	Value
Group ID	RiverBend-Base
Date	11/08/2002 15:29
Operator	Dr. Michael P. Manahan, Sr.
Temperature	-43.6 °F
Oscilloscope	MPM Internal Oscilloscope
Striker	8mm Metals
Interpolation	Point-Point Linear
Encoder Controller	MPM Encoder System
Velocity Determination	Encoder
Material	Metal
Size	Type A
Orientation	TL
Notch Type	V Notch, no Side-Groove
Units Normalization	None
Energy Adjustment	1.2157
Length	2.1654 in
Width	0.3937 in
Thickness	0.3937 in
Span	1.5748 in
Uncracked Ligament	0.3150 in
Notch Rafius	0.0098 in
Failure Type	complete fracture
Post Test Comments	good test
Impact Velocity	17.937 ft/s
Striker Energy	8.894 ft lbf
Dial Gage Energy	8.700 ft lbf
Encoder Energy	8.894 ft lbf
Latch Angle	134.14°
Final Angle	129.76°
Potential Energy	306.728 ft lbf
Windage & Friction	0.635 ft lbf
Percent Shear	8.42 %
Lateral Expansion	0.0105 in

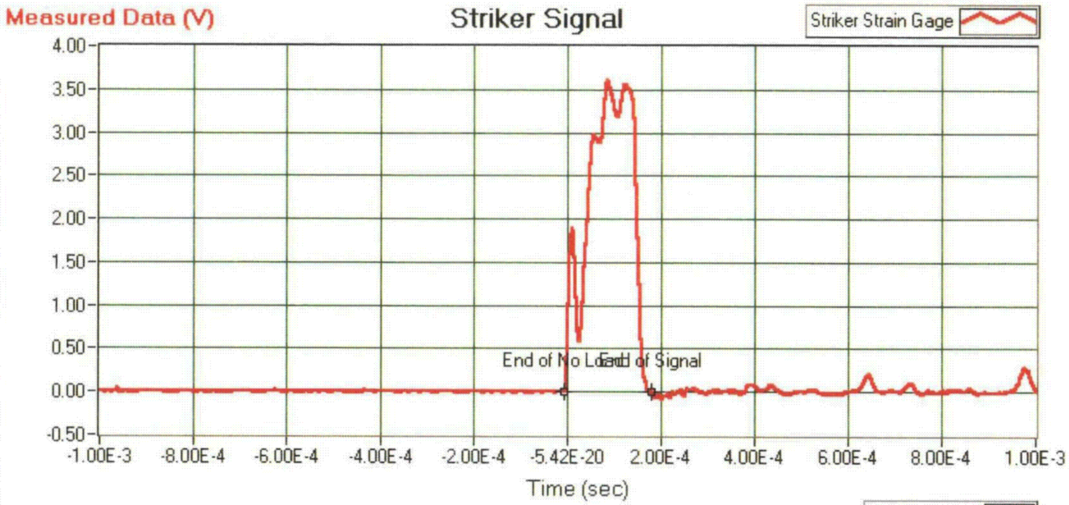

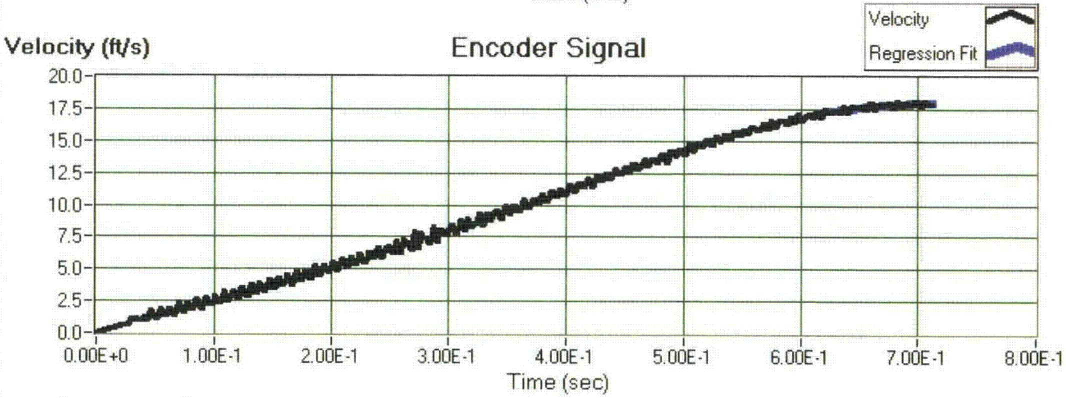

	Load (lbf)	Displacement (in)	Velocity (ft/s)	Time (s)	Energy (ft lbf)
Peak Load	4.3236E+3	2.846E-2	1.777E+1	1.260E-4	7.05717E+0
Brittle Fracture	7.7257E+2	7.047E-3	1.792E+1	2.600E-5	8.21299E-1
End of Signal	1.1051E+1	3.953E-2	1.772E+1	1.780E-4	8.89367E+0

Sample ID: b12
Group ID: RiverBend-Base

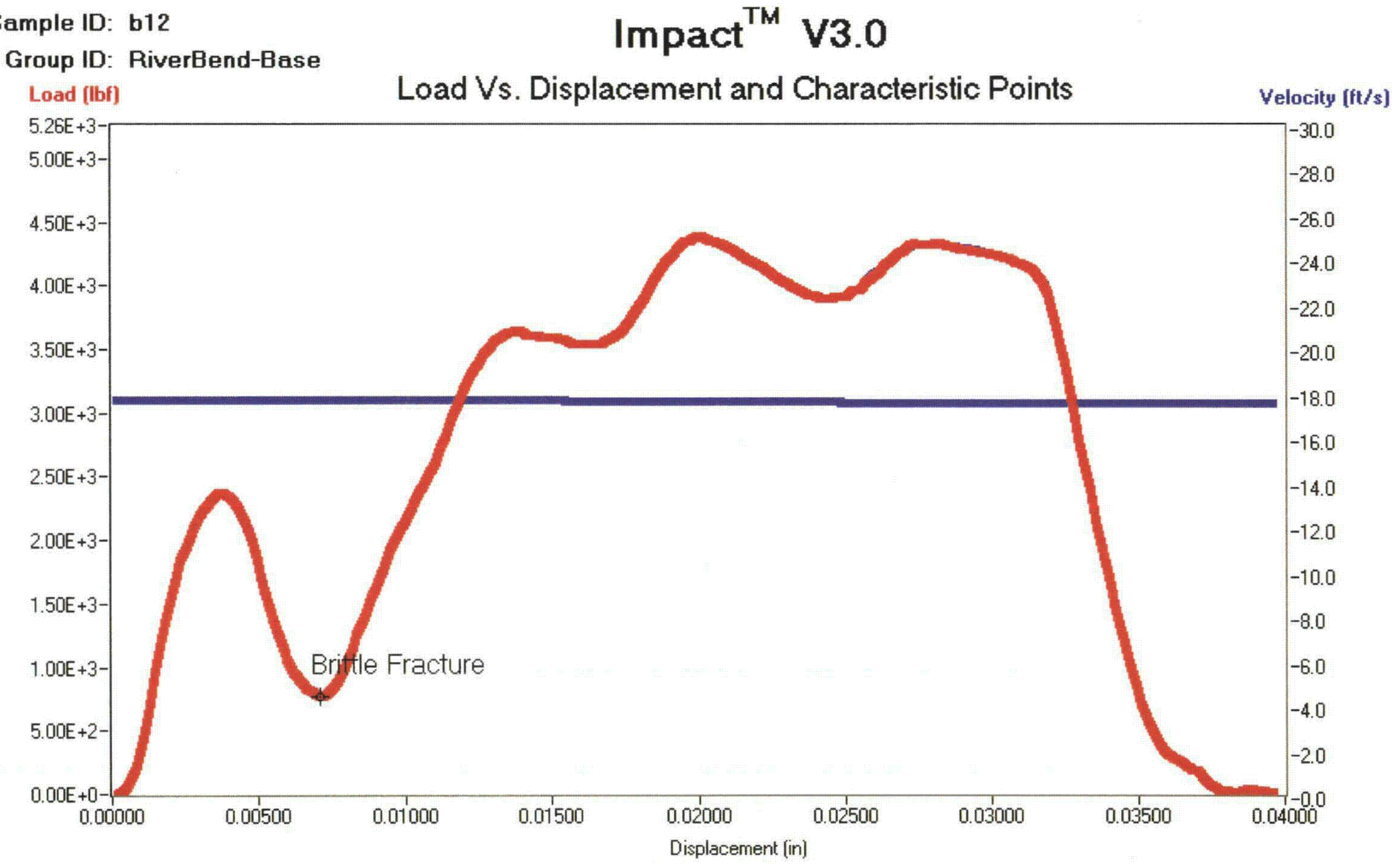

	Load (lbf)	Displacement (in)	Velocity (ft/s)	Time (s)	Energy (ft lbf)
Peak Load	4.3236E+3	2.846E-2	1.777E+1	1.260E-4	7.05717E+0
Brittle Fracture	7.7257E+2	7.047E-3	1.792E+1	2.600E-5	8.21299E-1
End of Signal	1.1051E+1	3.953E-2	1.772E+1	1.780E-4	8.89367E+0

Sample ID

b3

Comments

River Bend 183 Degree Surveillance Capsule

Impact™ V3.0

Summary Report

Test Parameters	Value
Group ID	RiverBend-Base
Date	11/08/2002 15:00
Operator	Dr. Michael P. Manahan, Sr.
Temperature	20.3 °F
Oscilloscope	MPM Internal Oscilloscope
Striker	8mm Metals
Interpolation	Point-Point Linear
Encoder Controller	MPM Encoder System
Velocity Determination	Encoder
Material	Metal
Size	Type A
Orientation	TL
Notch Type	V Notch, no Side-Groove
Units Normalization	None
Energy Adjustment	1.1363
Length	2.1654 in
Width	0.3937 in
Thickness	0.3937 in
Span	1.5748 in
Uncracked Ligament	0.3150 in
Notch Rafius	0.0098 in
Failure Type	incomplete fracture
Post Test Comments	good test
Impact Velocity	17.935 ft/s
Striker Energy	39.377 ft lbf
Dial Gage Energy	39.100 ft lbf
Encoder Energy	39.377 ft lbf
Latch Angle	134.14°
Final Angle	118.08°
Potential Energy	306.728 ft lbf
Windage & Friction	0.635 ft lbf
Percent Shear	25.06 %
Lateral Expansion	0.0345 in

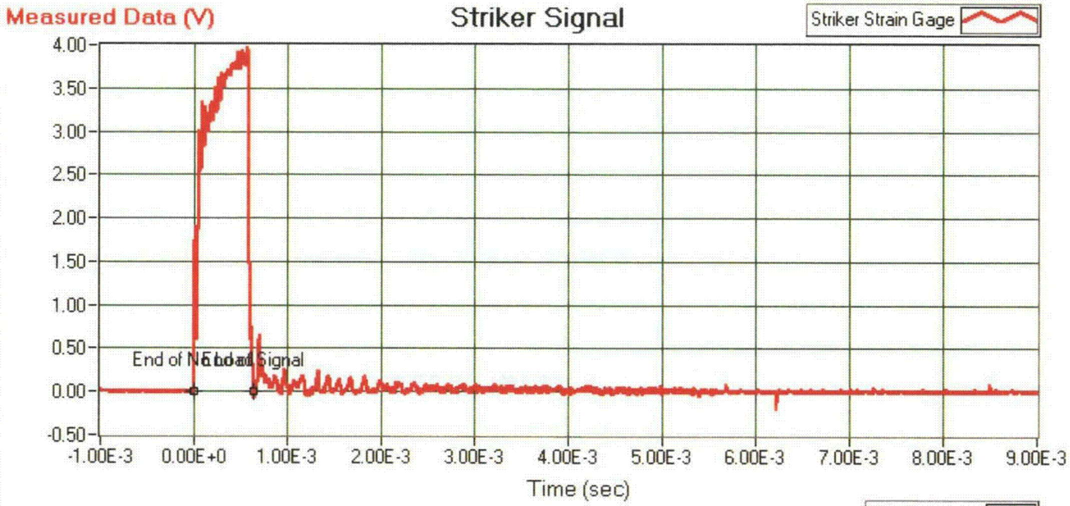

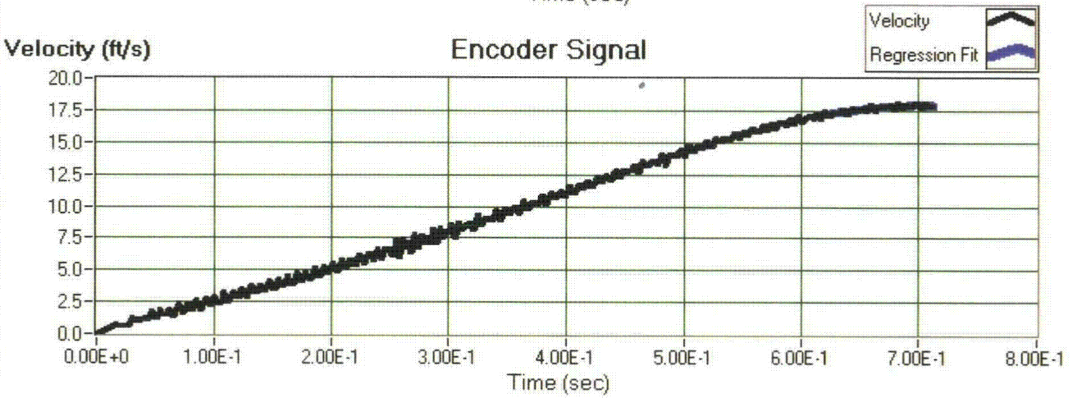

	Load (lbf)	Displacement (in)	Velocity (ft/s)	Time (s)	Energy (ft lbf)
General Yield	3.3441E+3	1.390E-2	1.789E+1	5.380E-5	1.90065E+0
Peak Load	4.4760E+3	1.207E-1	1.695E+1	5.640E-4	3.72237E+1
Brittle Fracture	4.3869E+3	1.231E-1	1.692E+1	5.760E-4	3.81253E+1
Arrest Load	1.6689E+2	1.343E-1	1.689E+1	6.310E-4	3.93745E+1
End of Signal	5.3761E+1	1.346E-1	1.689E+1	6.330E-4	3.93772E+1

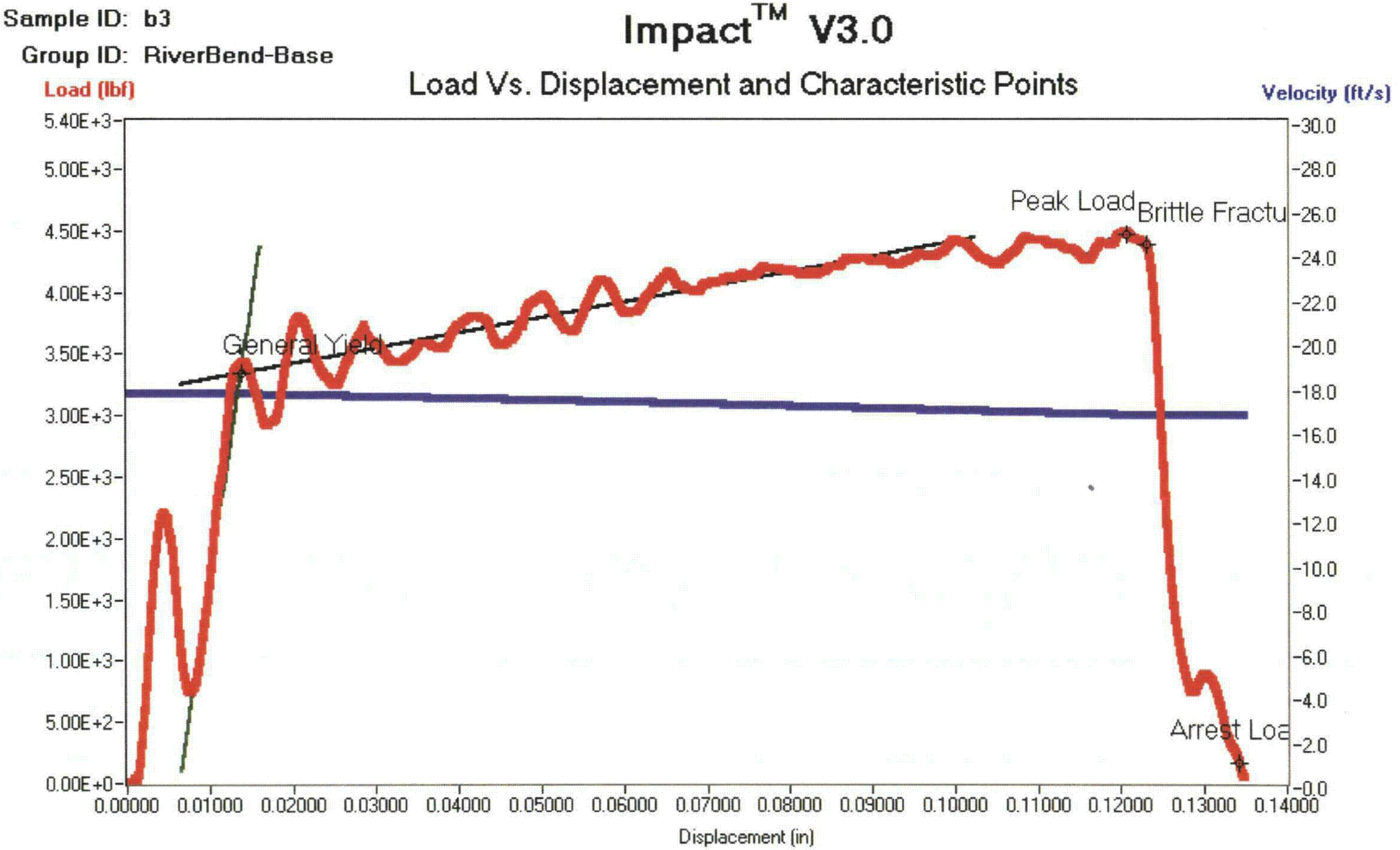

	Load (lbf)	Displacement (in)	Velocity (ft/s)	Time (s)	Energy (ft lbf)
General Yield	3.3441E+3	1.390E-2	1.789E+1	5.380E-5	1.90065E+0
Peak Load	4.4760E+3	1.207E-1	1.695E+1	5.640E-4	3.72237E+1
Brittle Fracture	4.3869E+3	1.231E-1	1.692E+1	5.760E-4	3.81253E+1
Arrest Load	1.6689E+2	1.343E-1	1.689E+1	6.310E-4	3.93745E+1
End of Signal	5.3761E+1	1.346E-1	1.689E+1	6.330E-4	3.93772E+1

Sample ID

b7

Comments

River Bend 183 Degree Surveillance Capsule

Impact™ V3.0

Summary Report

Test Parameters	Value
Group ID	RiverBend-Base
Date	11/08/2002 14:26
Operator	Dr. Michael P. Manahan, Sr.
Temperature	22.8 °F
Oscilloscope	MPM Internal Oscilloscope
Striker	8mm Metals
Interpolation	Point-Point Linear
Encoder Controller	MPM Encoder System
Velocity Determination	Encoder
Material	Metal
Size	Type A
Orientation	TL
Notch Type	V Notch, no Side-Groove
Units Normalization	None
Energy Adjustment	1.1339
Length	2.1654 in
Width	0.3937 in
Thickness	0.3937 in
Span	1.5748 in
Uncracked Ligament	0.3150 in
Notch Rafius	0.0098 in
Failure Type	incomplete fracture
Post Test Comments	good test
Impact Velocity	17.935 ft/s
Striker Energy	33.925 ft lbf
Dial Gage Energy	33.700 ft lbf
Encoder Energy	33.925 ft lbf
Latch Angle	134.14°
Final Angle	120.06°
Potential Energy	306.728 ft lbf
Windage & Friction	0.635 ft lbf
Percent Shear	22.54 %
Lateral Expansion	0.0305 in

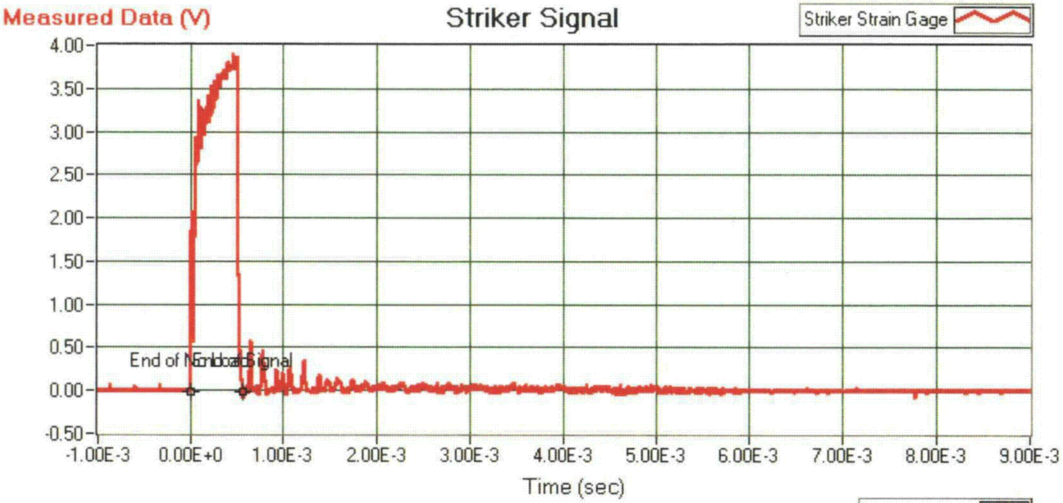

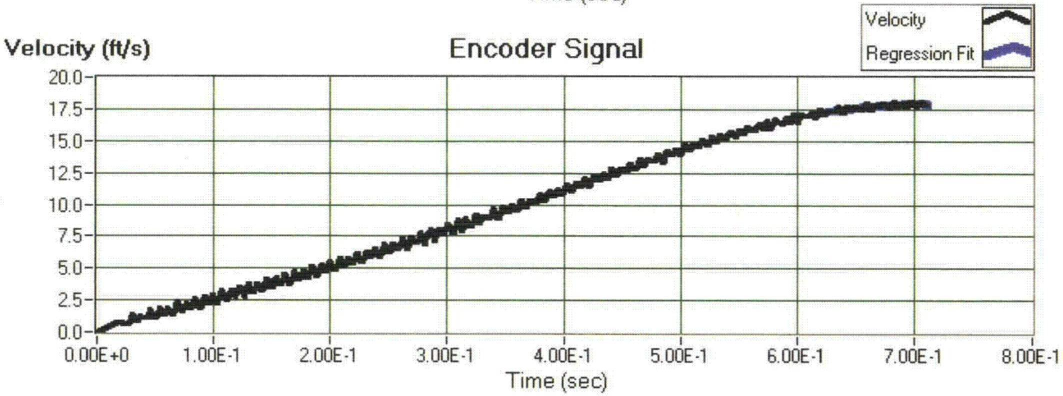

	Load (lbf)	Displacement (in)	Velocity (ft/s)	Time (s)	Energy (ft lbf)
General Yield	3.3081E+3	1.283E-2	1.789E+1	5.483E-5	1.95107E+0
Peak Load	4.3778E+3	1.073E-1	1.707E+1	5.050E-4	3.27172E+1
Brittle Fracture	4.3719E+3	1.076E-1	1.707E+1	5.060E-4	3.27918E+1
Arrest Load	9.2069E+1	1.180E-1	1.704E+1	5.570E-4	3.39184E+1
End of Signal	2.4334E+1	1.192E-1	1.704E+1	5.630E-4	3.39254E+1

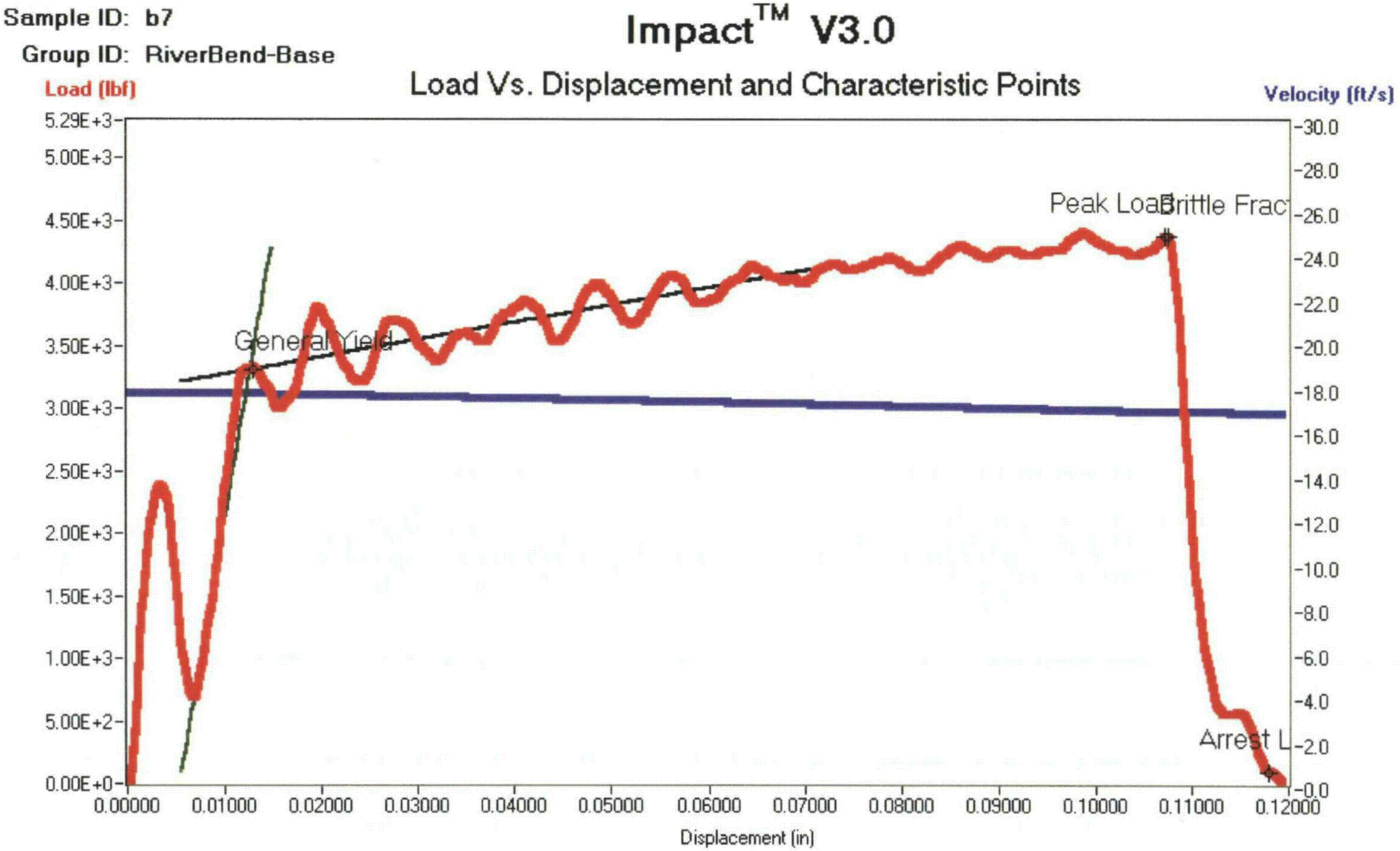

	Load (lbf)	Displacement (in)	Velocity (ft/s)	Time (s)	Energy (ft lbf)
General Yield	3.3081E+3	1.283E-2	1.789E+1	5.483E-5	1.95107E+0
Peak Load	4.3778E+3	1.073E-1	1.707E+1	5.050E-4	3.27172E+1
Brittle Fracture	4.3719E+3	1.076E-1	1.707E+1	5.060E-4	3.27918E+1
Arrest Load	9.2069E+1	1.180E-1	1.704E+1	5.570E-4	3.39184E+1
End of Signal	2.4334E+1	1.192E-1	1.704E+1	5.630E-4	3.39254E+1

Sample ID

b2

Comments

River Bend 183 Degree Surveillance Capsule

Impact™ V3.0

Summary Report

Test Parameters	Value
Group ID	RiverBend-Base
Date	11/08/2002 12:20
Operator	Dr. Michael P. Manahan, Sr.
Temperature	70.2 °F
Oscilloscope	MPM Internal Oscilloscope
Striker	8mm Metals
Interpolation	Point-Point Linear
Encoder Controller	MPM Encoder System
Velocity Determination	Encoder
Material	Metal
Size	Type A
Orientation	TL
Notch Type	V Notch, no Side-Groove
Units Normalization	None
Energy Adjustment	1.1070
Length	2.1654 in
Width	0.3937 in
Thickness	0.3937 in
Span	1.5748 in
Uncracked Ligament	0.3150 in
Notch Rafius	0.0098 in
Failure Type	incomplete fracture
Post Test Comments	good test
Impact Velocity	17.939 ft/s
Striker Energy	43.254 ft lbf
Dial Gage Energy	43.000 ft lbf
Encoder Energy	43.254 ft lbf
Latch Angle	134.14°
Final Angle	116.69°
Potential Energy	306.728 ft lbf
Windage & Friction	0.635 ft lbf
Percent Shear	30.57 %
Lateral Expansion	0.0420 in

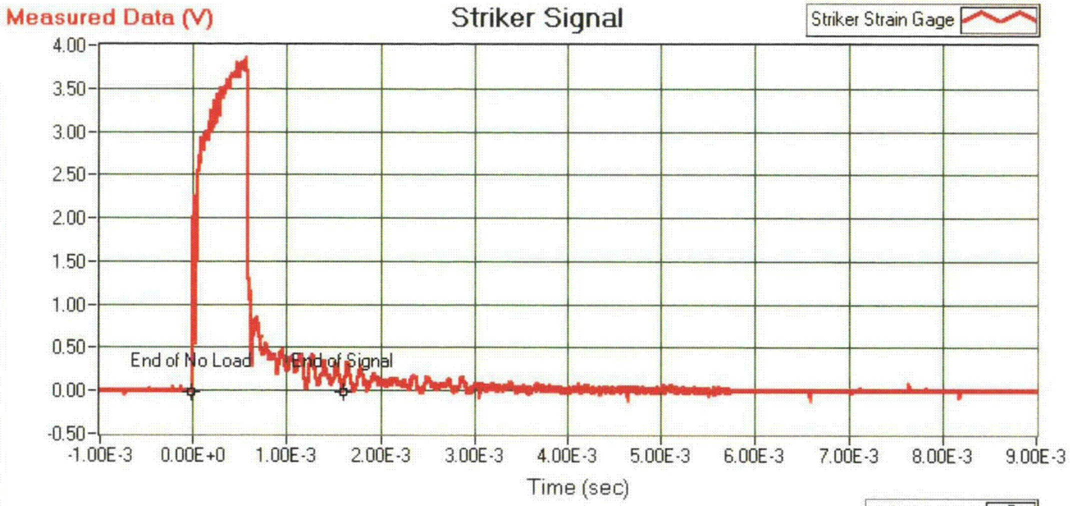

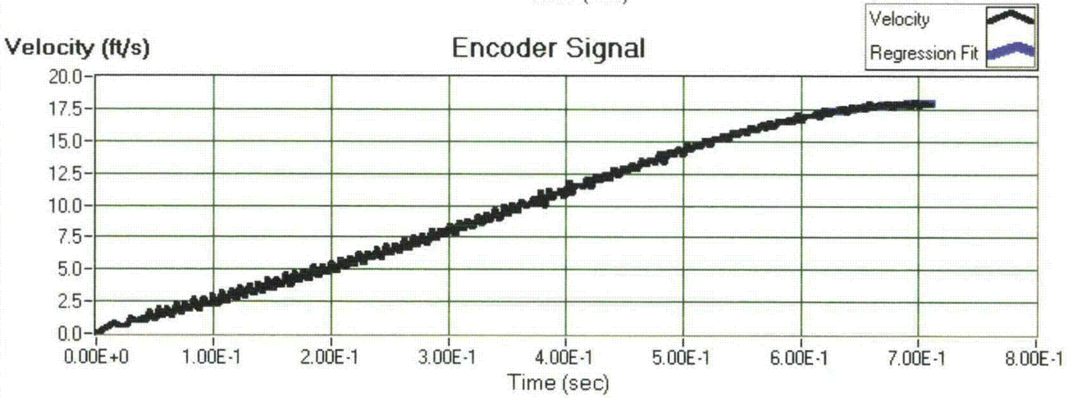

	Load (lbf)	Displacement (in)	Velocity (ft/s)	Time (s)	Energy (ft lbf)
General Yield	2.9874E+3	1.630E-2	1.789E+1	5.600E-5	1.86397E+0
Peak Load	4.2635E+3	1.226E-1	1.699E+1	5.630E-4	3.48470E+1
Brittle Fracture	2.2938E+3	5.787E-3	1.793E+1	7.000E-6	2.73117E-1
Arrest Load	8.1776E+2	1.333E-1	1.694E+1	6.160E-4	3.68594E+1
End of Signal	1.2247E+0	3.289E-1	1.676E+1	1.585E-3	4.32542E+1

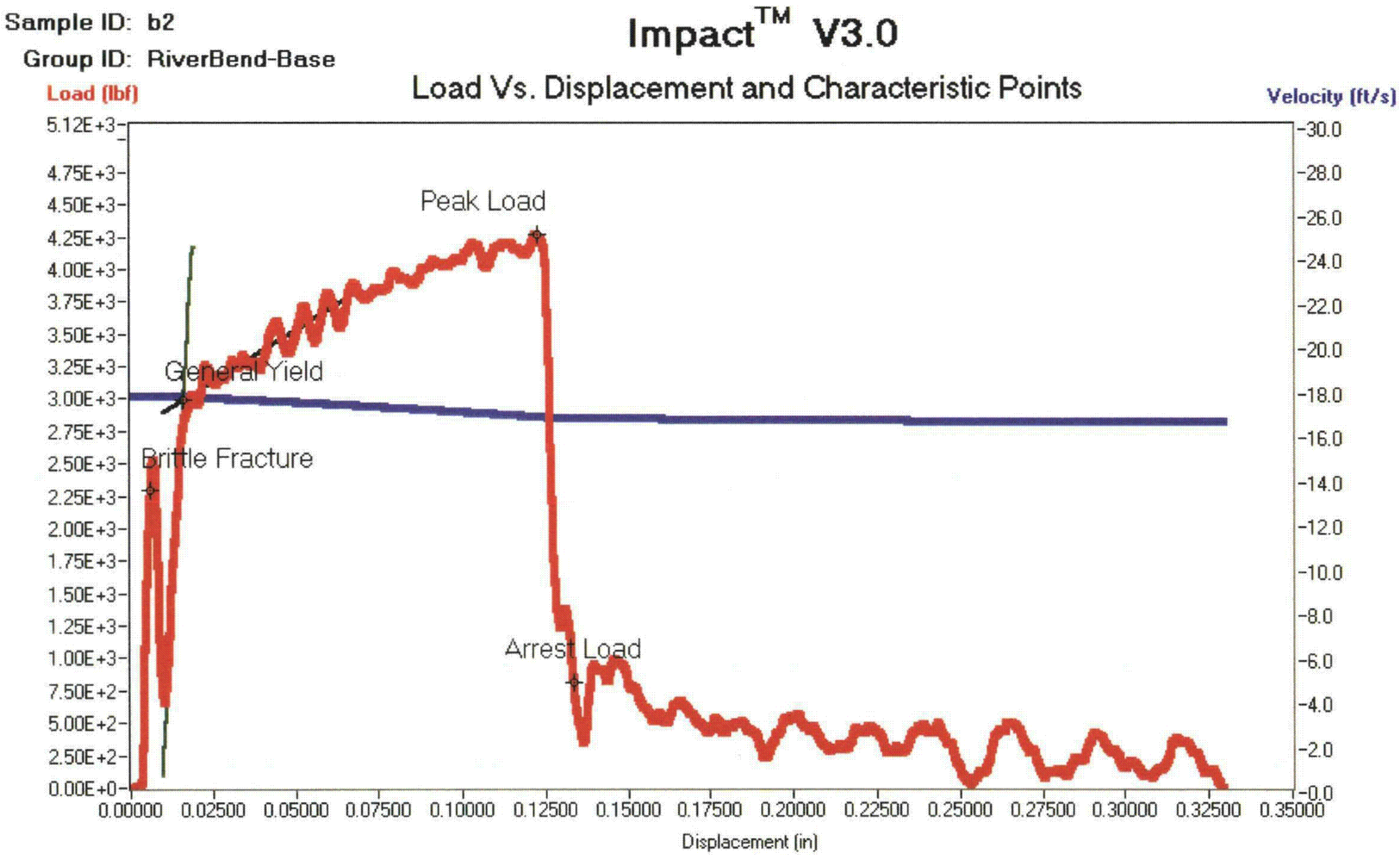

	Load (lbf)	Displacement (in)	Velocity (ft/s)	Time (s)	Energy (ft lbf)
General Yield	2.9874E+3	1.630E-2	1.789E+1	5.600E-5	1.86397E+0
Peak Load	4.2635E+3	1.226E-1	1.699E+1	5.630E-4	3.48470E+1
Brittle Fracture	2.2938E+3	5.787E-3	1.793E+1	7.000E-6	2.73117E-1
Arrest Load	8.1776E+2	1.333E-1	1.694E+1	6.160E-4	3.68594E+1
End of Signal	1.2247E+0	3.289E-1	1.676E+1	1.585E-3	4.32542E+1

Sample ID

b11

Comments

River Bend 183 Degree Surveillance Capsule

Impact™ V3.0

Summary Report

Test Parameters	Value
Group ID	RiverBend-Base
Date	11/08/2002 12:44
Operator	Dr. Michael P. Manahan, Sr.
Temperature	70.9 °F
Oscilloscope	MPM Internal Oscilloscope
Striker	8mm Metals
Interpolation	Point-Point Linear
Encoder Controller	MPM Encoder System
Velocity Determination	Encoder
Material	Metal
Size	Type A
Orientation	TL
Notch Type	V Notch, no Side-Groove
Units Normalization	None
Energy Adjustment	1.0627
Length	2.1654 in
Width	0.3937 in
Thickness	0.3937 in
Span	1.5748 in
Uncracked Ligament	0.3150 in
Notch Rafius	0.0098 in
Failure Type	incomplete fracture
Post Test Comments	good test
Impact Velocity	17.939 ft/s
Striker Energy	44.930 ft lbf
Dial Gage Energy	44.500 ft lbf
Encoder Energy	44.930 ft lbf
Latch Angle	134.14°
Final Angle	116.10°
Potential Energy	306.728 ft lbf
Windage & Friction	0.635 ft lbf
Percent Shear	29.67 %
Lateral Expansion	0.0440 in

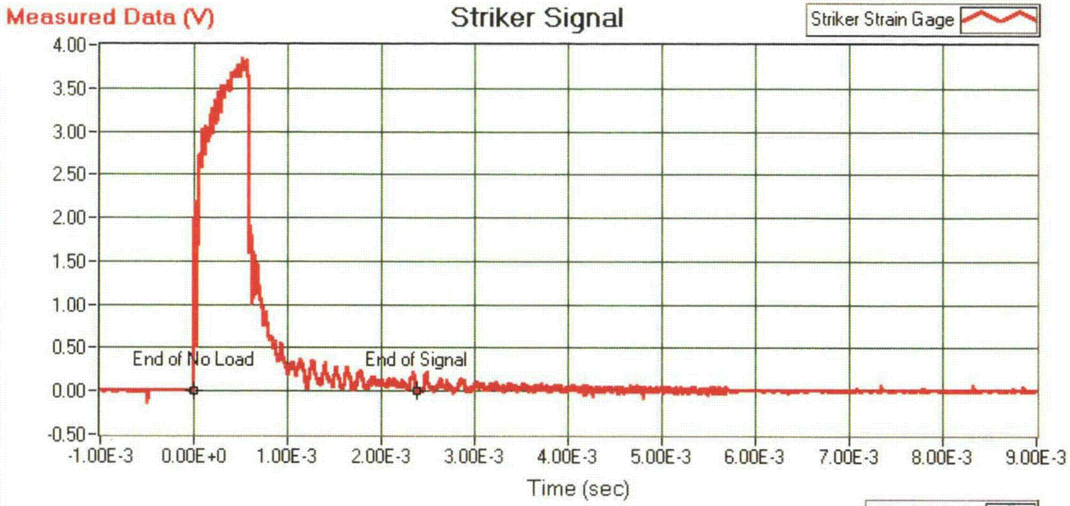

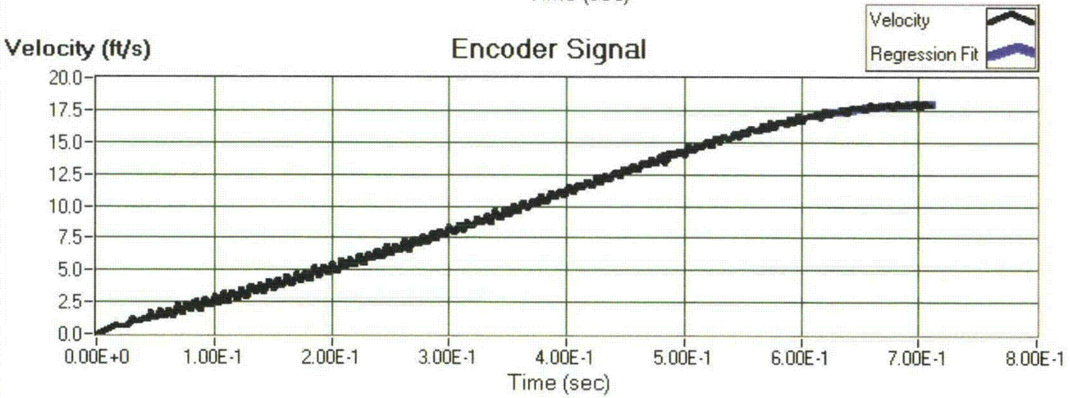

	Load (lbf)	Displacement (in)	Velocity (ft/s)	Time (s)	Energy (ft lbf)
General Yield	2.8922E+3	1.283E-2	1.789E+1	5.283E-5	1.70802E+0
Peak Load	4.0536E+3	1.200E-1	1.699E+1	5.640E-4	3.36729E+1
Brittle Fracture	4.0443E+3	1.206E-1	1.698E+1	5.670E-4	3.38791E+1
Arrest Load	1.4583E+3	1.295E-1	1.693E+1	6.110E-4	3.56541E+1
End of Signal	5.0482E+0	4.865E-1	1.666E+1	2.390E-3	4.49305E+1

Sample ID: b11

Group ID: RiverBend-Base

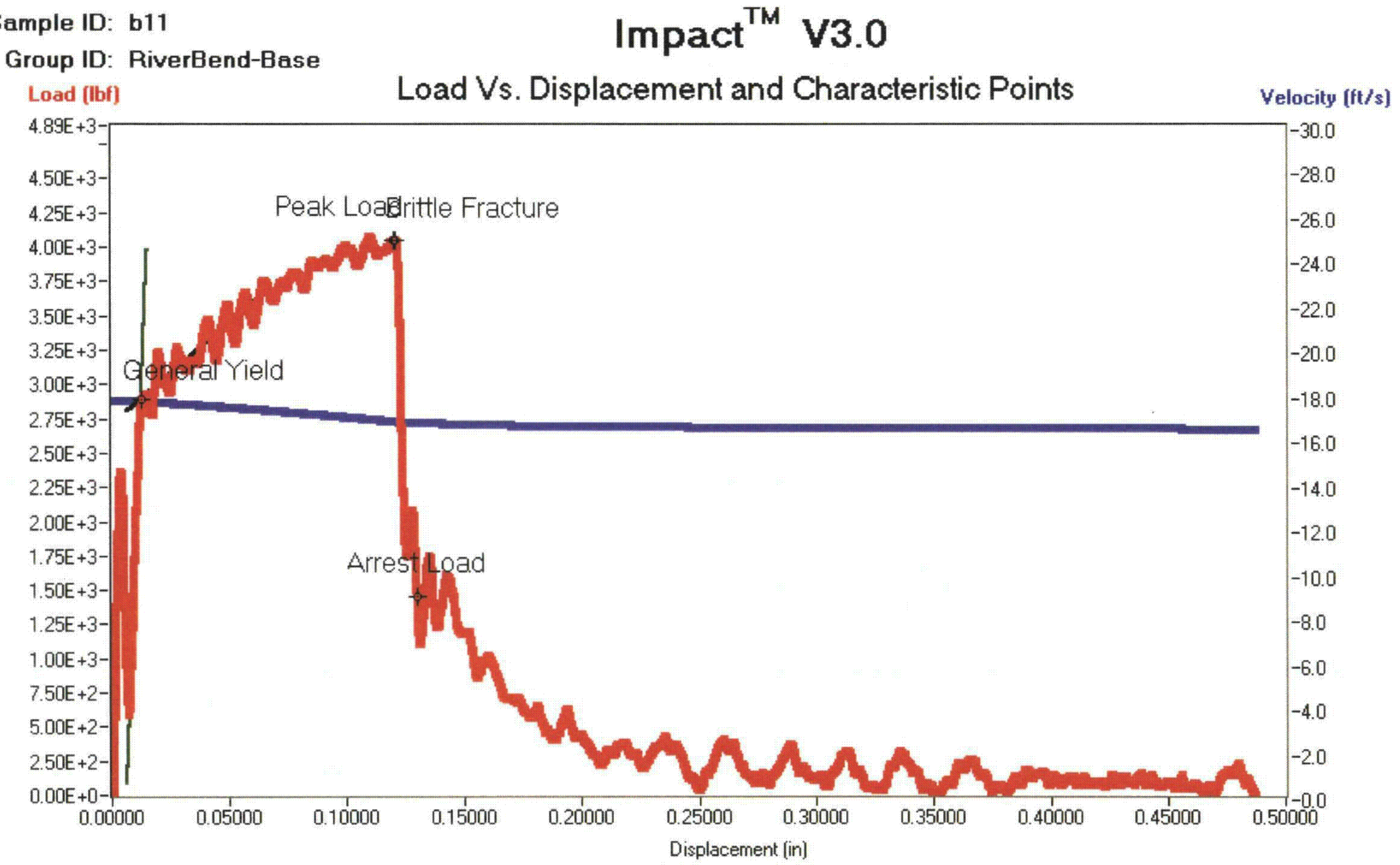

	Load (lbf)	Displacement (in)	Velocity (ft/s)	Time (s)	Energy (ft lbf)
General Yield	2.8922E+3	1.283E-2	1.789E+1	5.283E-5	1.70802E+0
Peak Load	4.0536E+3	1.200E-1	1.699E+1	5.640E-4	3.36729E+1
Brittle Fracture	4.0443E+3	1.206E-1	1.698E+1	5.670E-4	3.38791E+1
Arrest Load	1.4583E+3	1.295E-1	1.693E+1	6.110E-4	3.56541E+1
End of Signal	5.0482E+0	4.865E-1	1.666E+1	2.390E-3	4.49305E+1

Sample ID

b8

Comments

River Bend 183 Degree Surveillance Capsule

Impact™ V3.0

Summary Report

Test Parameters	Value
Group ID	RiverBend-Base
Date	11/08/2002 18:21
Operator	Dr. Michael P. Manahan, Sr.
Temperature	100.2 °F
Oscilloscope	MPM Internal Oscilloscope
Striker	8mm Metals
Interpolation	Point-Point Linear
Encoder Controller	MPM Encoder System
Velocity Determination	Encoder
Material	Metal
Size	Type A
Orientation	TL
Notch Type	V Notch, no Side-Groove
Units Normalization	None
Energy Adjustment	1.0765
Length	2.1654 in
Width	0.3937 in
Thickness	0.3937 in
Span	1.5748 in
Uncracked Ligament	0.3150 in
Notch Rafius	0.0098 in
Failure Type	incomplete fracture
Post Test Comments	good test
Impact Velocity	17.943 ft/s
Striker Energy	60.751 ft lbf
Dial Gage Energy	60.100 ft lbf
Encoder Energy	60.751 ft lbf
Latch Angle	134.14°
Final Angle	110.63°
Potential Energy	306.728 ft lbf
Windage & Friction	0.635 ft lbf
Percent Shear	39.09 %
Lateral Expansion	0.0480 in

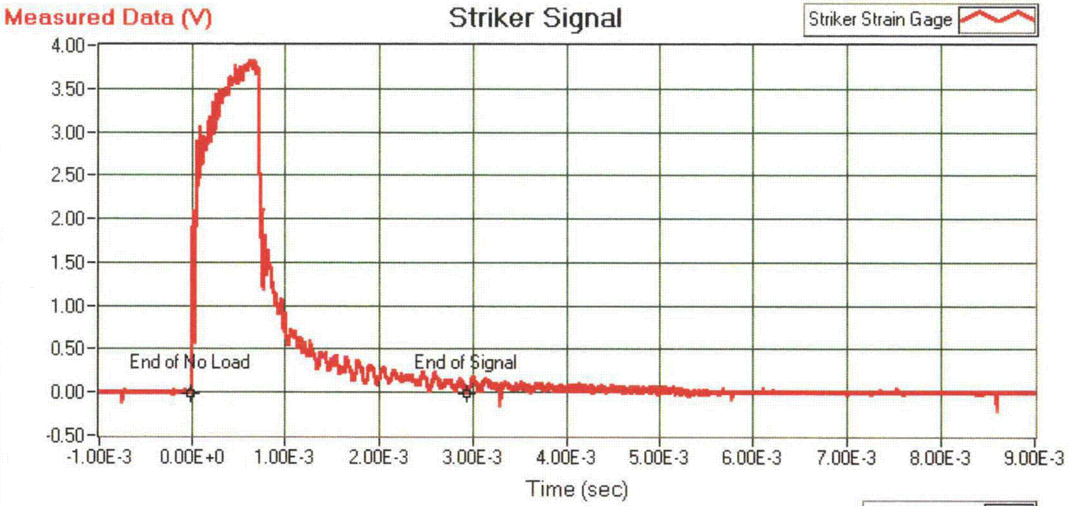

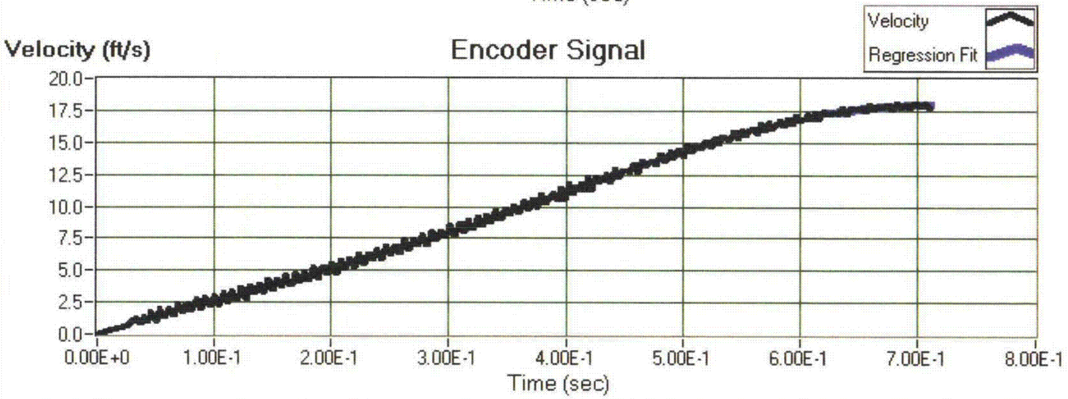

	Load (lbf)	Displacement (in)	Velocity (ft/s)	Time (s)	Energy (ft lbf)
General Yield	2.8665E+3	1.543E-2	1.790E+1	4.983E-5	1.63436E+0
Peak Load	4.0735E+3	1.379E-1	1.686E+1	6.360E-4	3.84947E+1
Brittle Fracture	4.0084E+3	1.536E-1	1.671E+1	7.140E-4	4.37724E+1
Arrest Load	1.9741E+3	1.580E-1	1.668E+1	7.360E-4	4.48550E+1
End of Signal	8.0058E-1	5.898E-1	1.621E+1	2.939E-3	6.07511E+1

Sample ID: **b8**

Group ID: **RiverBend-Base**

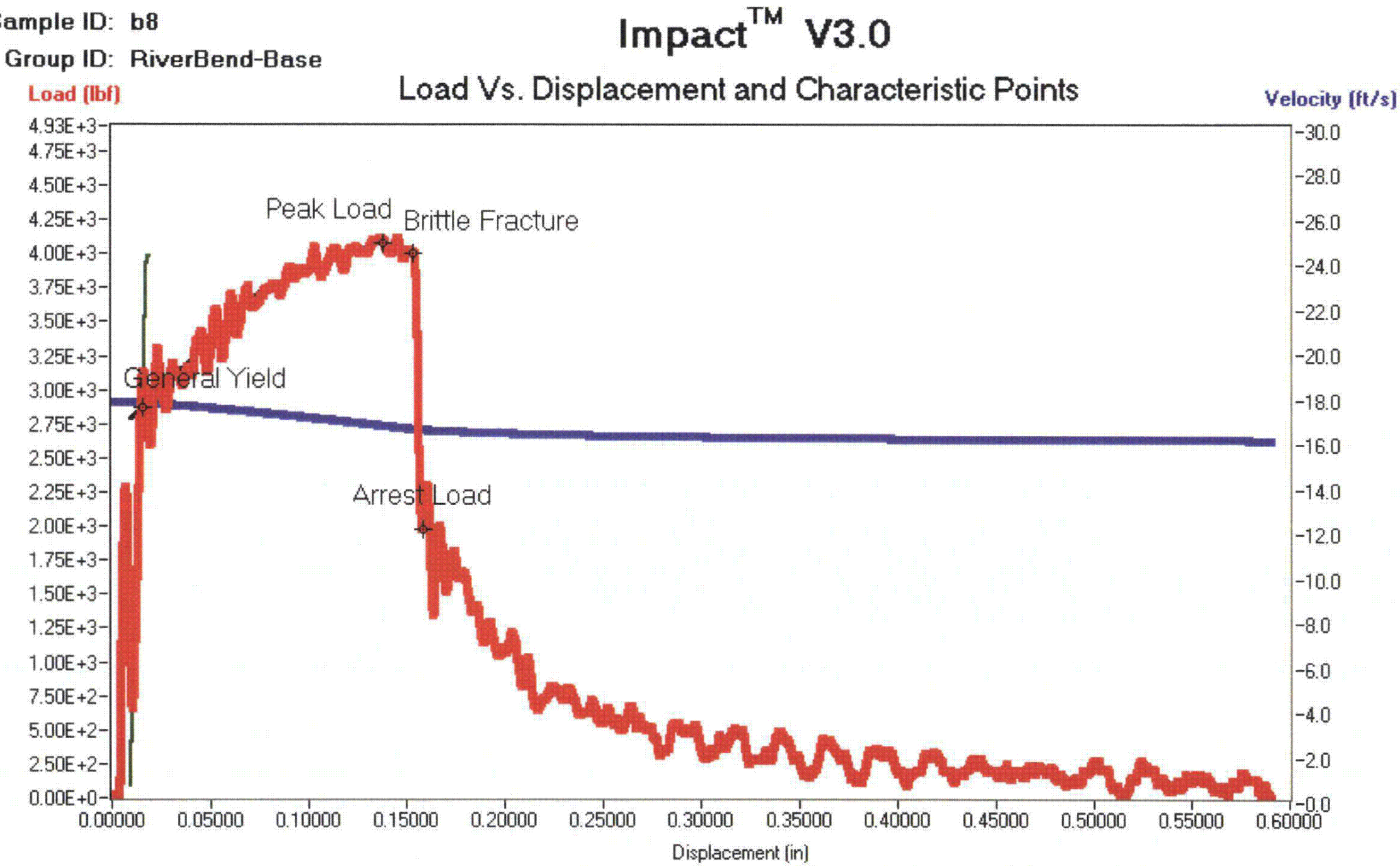

	Load (lbf)	Displacement (in)	Velocity (ft/s)	Time (s)	Energy (ft lbf)
General Yield	2.8665E+3	1.543E-2	1.790E+1	4.983E-5	1.63436E+0
Peak Load	4.0735E+3	1.379E-1	1.686E+1	6.360E-4	3.84947E+1
Brittle Fracture	4.0084E+3	1.536E-1	1.671E+1	7.140E-4	4.37724E+1
Arrest Load	1.9741E+3	1.580E-1	1.668E+1	7.360E-4	4.48550E+1
End of Signal	8.0058E-1	5.898E-1	1.621E+1	2.939E-3	6.07511E+1

Sample ID

b9

Comments

River Bend 183 Degree Surveillance Capsule

Impact™ V3.0

Summary Report

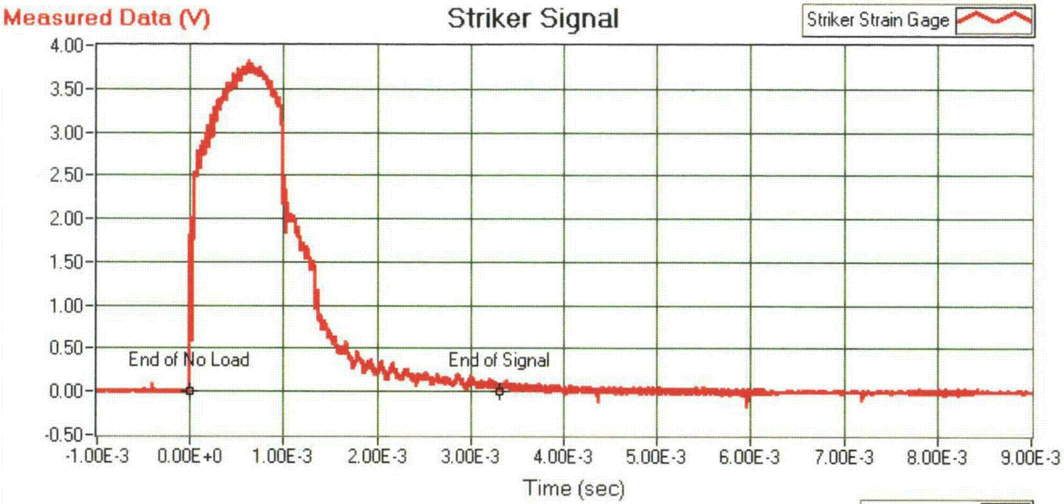

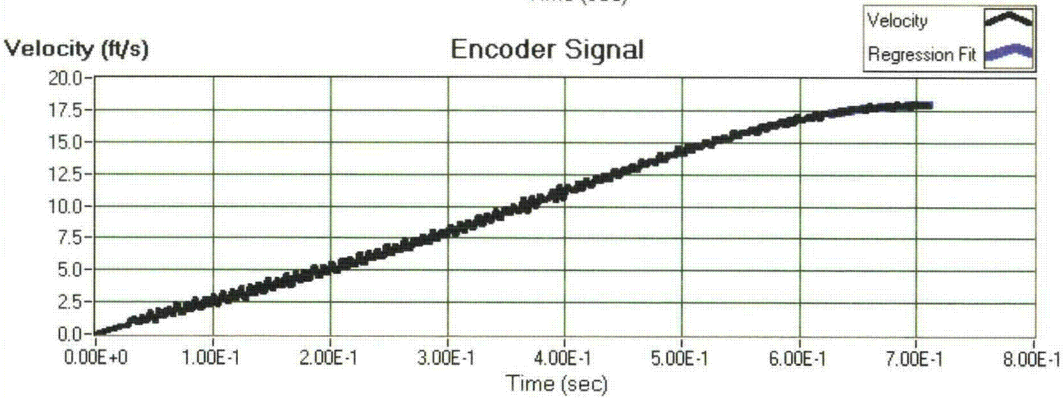

Test Parameters	Value
Group ID	RiverBend-Base
Date	11/08/2002 16:32
Operator	Dr. Michael P. Manahan, Sr.
Temperature	128.7 °F
Oscilloscope	MPM Internal Oscilloscope
Striker	8mm Metals
Interpolation	Point-Point Linear
Encoder Controller	MPM Encoder System
Velocity Determination	Encoder
Material	Metal
Size	Type A
Orientation	TL
Notch Type	V Notch, no Side-Groove
Units Normalization	None
Energy Adjustment	1.0558
Length	2.1654 in
Width	0.3937 in
Thickness	0.3937 in
Span	1.5748 in
Uncracked Ligament	0.3150 in
Notch Rafius	0.0098 in
Failure Type	incomplete fracture
Post Test Comments	good test
Impact Velocity	17.949 ft/s
Striker Energy	79.236 ft lbf
Dial Gage Energy	78.300 ft lbf
Encoder Energy	79.236 ft lbf
Latch Angle	134.14°
Final Angle	104.47°
Potential Energy	306.728 ft lbf
Windage & Friction	0.635 ft lbf
Percent Shear	52.79 %
Lateral Expansion	0.0670 in

	Load (lbf)	Displacement (in)	Velocity (ft/s)	Time (s)	Energy (ft lbf)
General Yield	2.6861E+3	1.198E-2	1.791E+1	4.986E-5	1.48185E+0
Peak Load	3.9409E+3	1.376E-1	1.687E+1	6.510E-4	3.79098E+1
Brittle Fracture	3.5787E+3	1.985E-1	1.629E+1	9.570E-4	5.71323E+1
Arrest Load	2.1768E+3	2.111E-1	1.619E+1	1.022E-3	6.02343E+1
End of Signal	9.5552E+0	6.448E-1	1.560E+1	3.319E-3	7.92358E+1

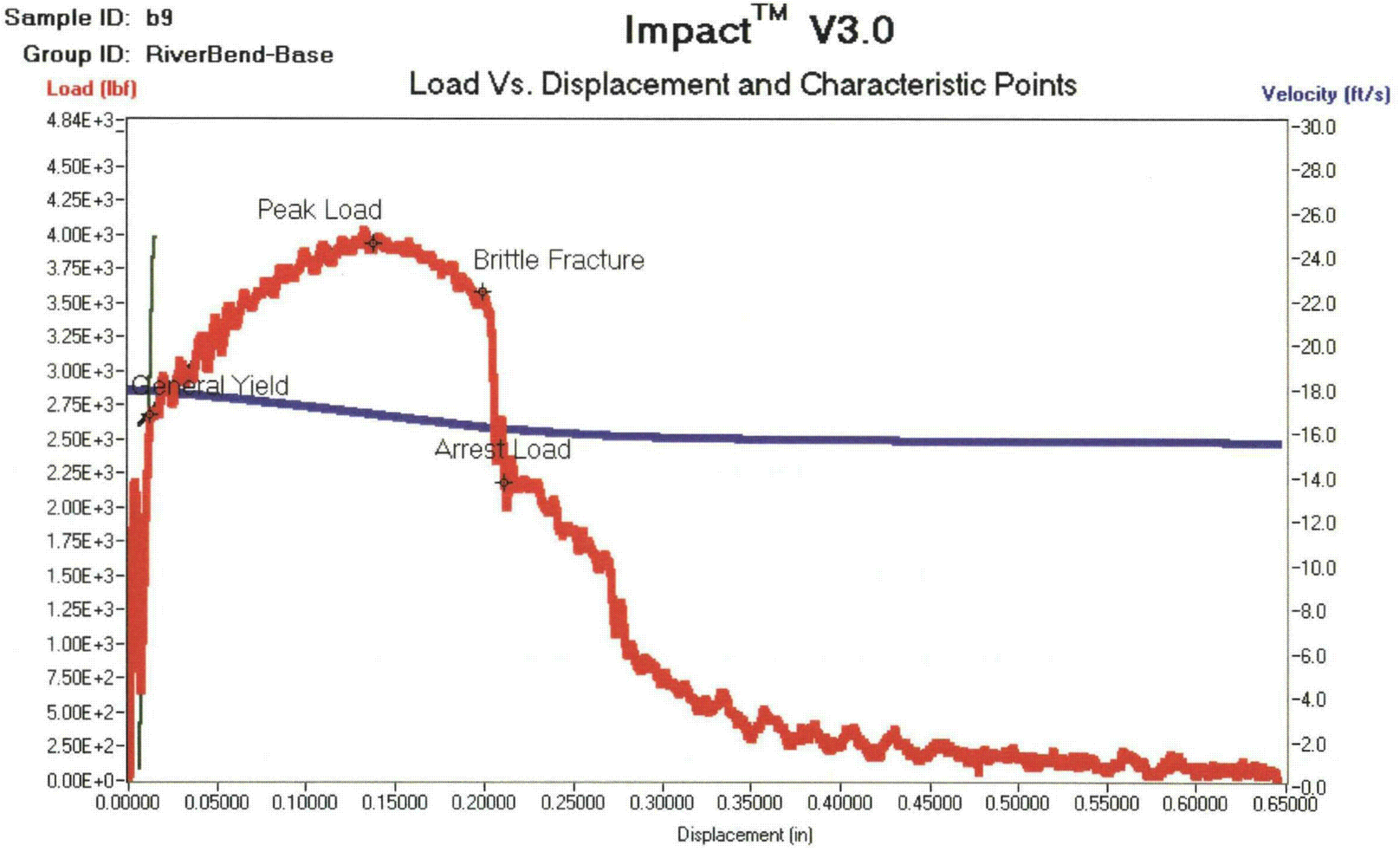

	Load (lbf)	Displacement (in)	Velocity (ft/s)	Time (s)	Energy (ft lbf)
General Yield	2.6858E+3	1.197E-2	1.791E+1	4.980E-5	1.48185E+0
Peak Load	3.9409E+3	1.376E-1	1.687E+1	6.510E-4	3.79098E+1
Brittle Fracture	3.5787E+3	1.985E-1	1.629E+1	9.570E-4	5.71323E+1
Arrest Load	2.1768E+3	2.111E-1	1.619E+1	1.022E-3	6.02343E+1
End of Signal	9.5552E+0	6.448E-1	1.560E+1	3.319E-3	7.92358E+1

Sample ID

b10

Comments

River Bend 183 Degree Surveillance Capsule

Impact™ V3.0

Summary Report

Test Parameters	Value
Group ID	RiverBend-Base
Date	11/08/2002 16:30
Operator	Dr. Michael P. Manahan, Sr.
Temperature	129.0 °F
Oscilloscope	MPM Internal Oscilloscope
Striker	8mm Metals
Interpolation	Point-Point Linear
Encoder Controller	MPM Encoder System
Velocity Determination	Encoder
Material	Metal
Size	Type A
Orientation	TL
Notch Type	V Notch, no Side-Groove
Units Normalization	None
Energy Adjustment	1.0460
Length	2.1654 in
Width	0.3937 in
Thickness	0.3937 in
Span	1.5748 in
Uncracked Ligament	0.3150 in
Notch Rafius	0.0098 in
Failure Type	incomplete fracture
Post Test Comments	good test
Impact Velocity	17.945 ft/s
Striker Energy	80.940 ft lbf
Dial Gage Energy	80.000 ft lbf
Encoder Energy	80.940 ft lbf
Latch Angle	134.14°
Final Angle	103.91°
Potential Energy	306.728 ft lbf
Windage & Friction	0.635 ft lbf
Percent Shear	60.91 %
Lateral Expansion	0.0665 in

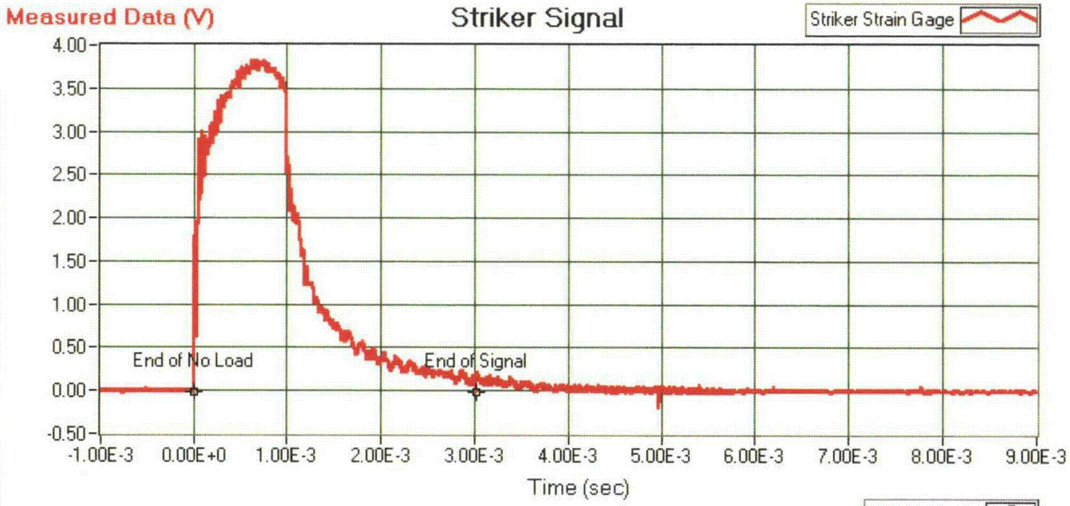

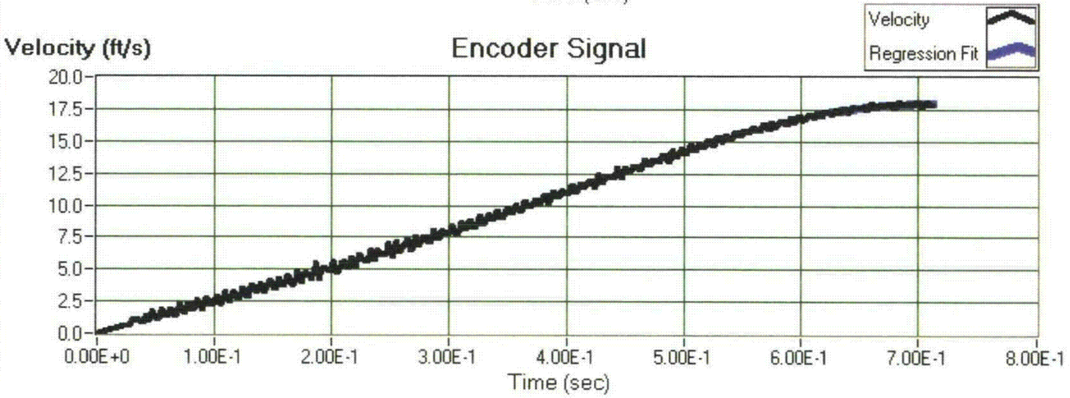

	Load (lbf)	Displacement (in)	Velocity (ft/s)	Time (s)	Energy (ft lbf)
General Yield	2.6875E+3	1.307E-2	1.790E+1	4.800E-5	1.45531E+0
Peak Load	3.9513E+3	1.489E-1	1.675E+1	7.000E-4	4.11625E+1
Brittle Fracture	3.6964E+3	2.043E-1	1.621E+1	9.800E-4	5.89668E+1
Arrest Load	2.3513E+3	2.130E-1	1.614E+1	1.025E-3	6.11040E+1
End of Signal	1.9176E+2	5.882E-1	1.552E+1	3.017E-3	8.09404E+1

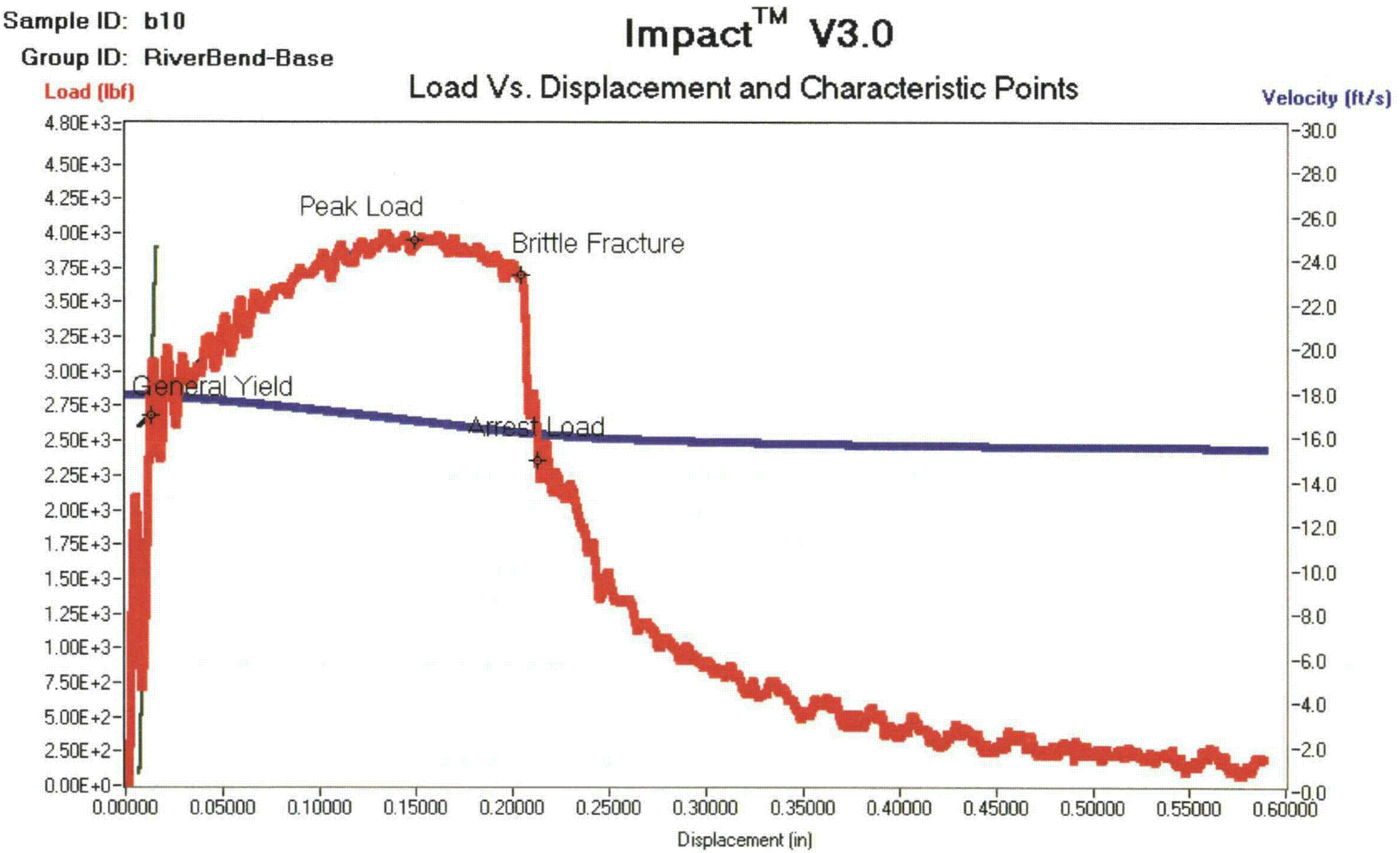

	Load (lbf)	Displacement (in)	Velocity (ft/s)	Time (s)	Energy (ft lbf)
General Yield	2.6875E+3	1.307E-2	1.790E+1	4.800E-5	1.45531E+0
Peak Load	3.9513E+3	1.489E-1	1.675E+1	7.000E-4	4.11625E+1
Brittle Fracture	3.6964E+3	2.043E-1	1.621E+1	9.800E-4	5.89668E+1
Arrest Load	2.3513E+3	2.130E-1	1.614E+1	1.025E-3	6.11040E+1
End of Signal	1.9176E+2	5.882E-1	1.552E+1	3.017E-3	8.09404E+1

Sample ID

b6

Comments

River Bend 183 Degree Surveillance Capsule

Impact[TM] V3.0

Summary Report

Test Parameters	Value
Group ID	RiverBend-Base
Date	11/08/2002 17:45
Operator	Dr. Michael P. Manahan, Sr.
Temperature	176.5 °F
Oscilloscope	MPM Internal Oscilloscope
Striker	8mm Metals
Interpolation	Point-Point Linear
Encoder Controller	MPM Encoder System
Velocity Determination	Encoder
Material	Metal
Size	Type A
Orientation	TL
Notch Type	V Notch, no Side-Groove
Units Normalization	None
Energy Adjustment	1.0665
Length	2.1654 in
Width	0.3937 in
Thickness	0.3937 in
Span	1.5748 in
Uncracked Ligament	0.3150 in
Notch Rafius	0.0098 in
Failure Type	incomplete fracture
Post Test Comments	good test
Impact Velocity	17.942 ft/s
Striker Energy	99.589 ft lbf
Dial Gage Energy	98.600 ft lbf
Encoder Energy	99.589 ft lbf
Latch Angle	134.14°
Final Angle	97.88°
Potential Energy	306.728 ft lbf
Windage & Friction	0.635 ft lbf
Percent Shear	100.00 %
Lateral Expansion	0.0750 in

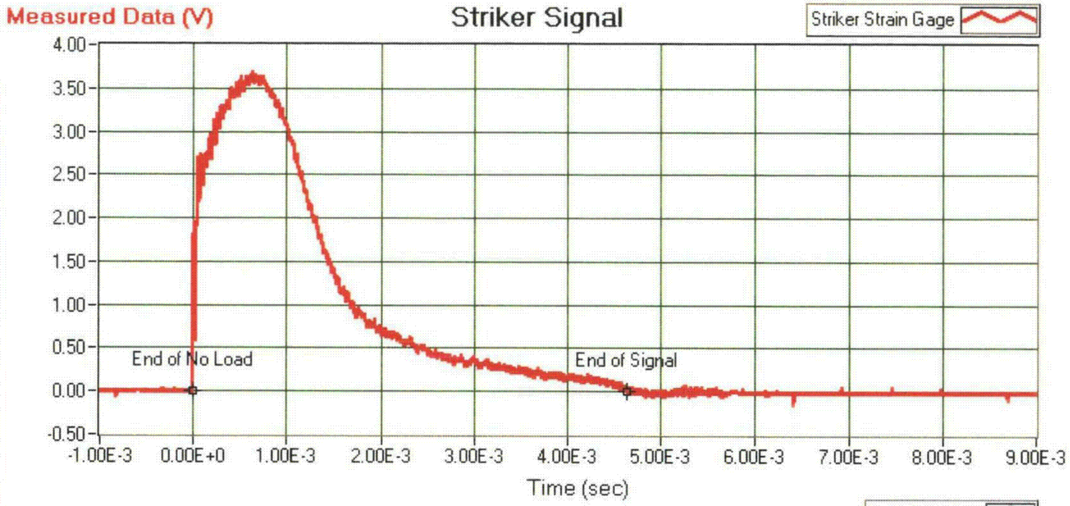

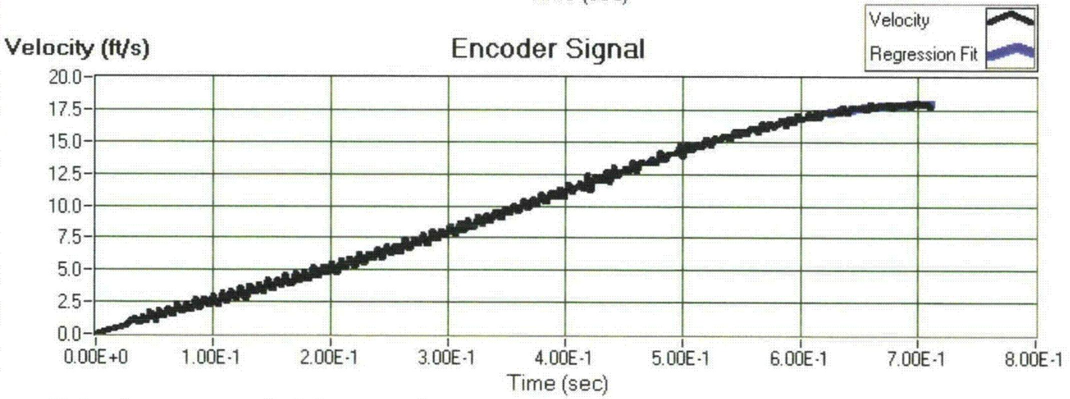

	Load (lbf)	Displacement (in)	Velocity (ft/s)	Time (s)	Energy (ft lbf)
General Yield	2.5824E+3	1.134E-2	1.790E+1	4.683E-5	1.40066E+0
Peak Load	3.8540E+3	1.367E-1	1.690E+1	6.460E-4	3.68922E+1
End of Signal	1.0662E+1	8.726E-1	1.496E+1	4.628E-3	9.95891E+1

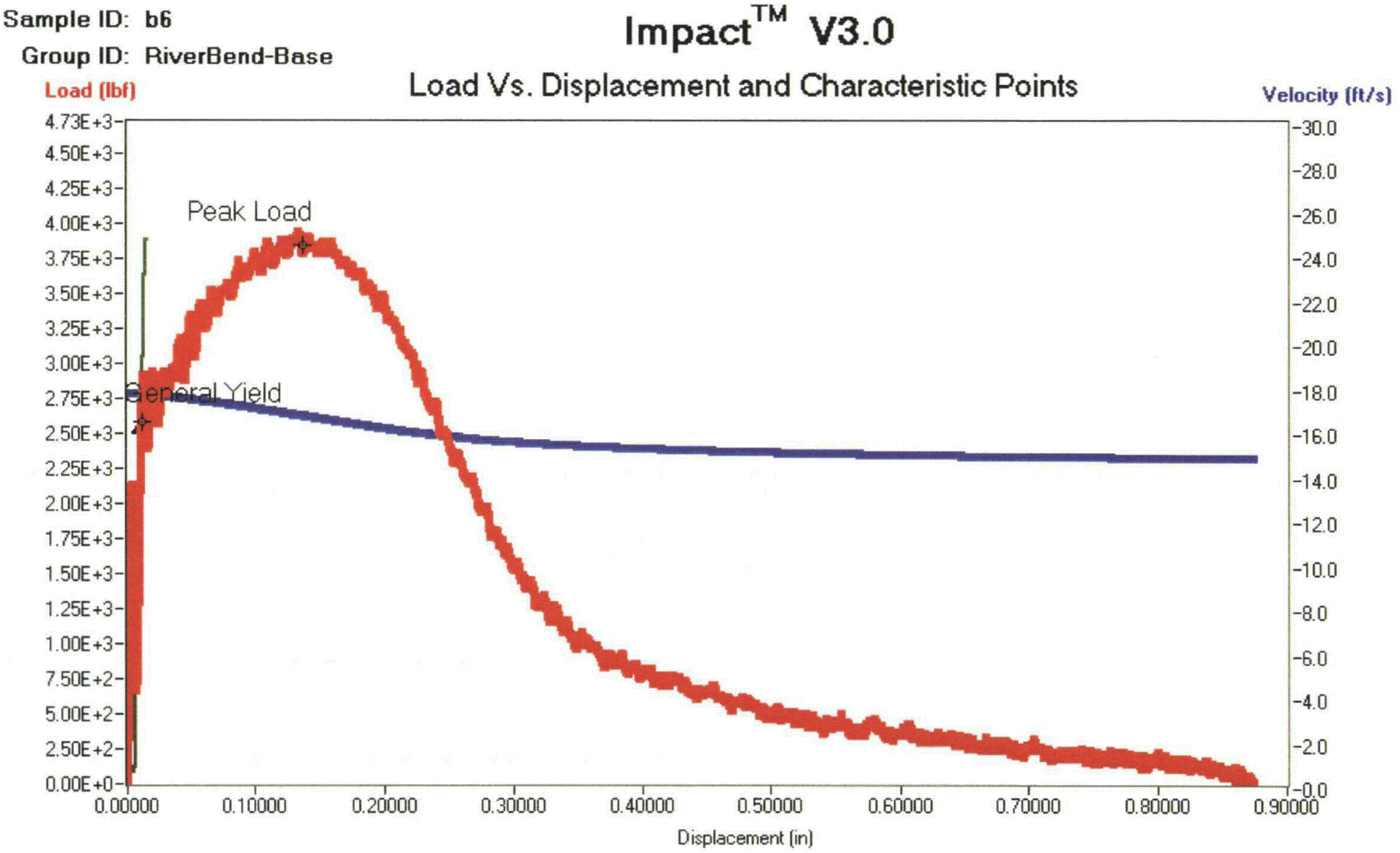

	Load (lbf)	Displacement (in)	Velocity (ft/s)	Time (s)	Energy (ft lbf)
General Yield	2.5824E+3	1.134E-2	1.790E+1	4.683E-5	1.40066E+0
Peak Load	3.8540E+3	1.367E-1	1.690E+1	6.460E-4	3.68922E+1
End of Signal	1.0662E+1	8.726E-1	1.496E+1	4.628E-3	9.95891E+1

Sample ID

b5

Comments

River Bend 183 Degree Surveillance Capsule

Impact™ V3.0

Summary Report

Test Parameters	Value
Group ID	RiverBend-Base
Date	11/08/2002 17:18
Operator	Dr. Michael P. Manahan, Sr.
Temperature	212.9 °F
Oscilloscope	MPM Internal Oscilloscope
Striker	8mm Metals
Interpolation	Point-Point Linear
Encoder Controller	MPM Encoder System
Velocity Determination	Encoder
Material	Metal
Size	Type A
Orientation	TL
Notch Type	V Notch, no Side-Groove
Units Normalization	None
Energy Adjustment	1.0639
Length	2.1654 in
Width	0.3937 in
Thickness	0.3937 in
Span	1.5748 in
Uncracked Ligament	0.3150 in
Notch Rafius	0.0098 in
Failure Type	incomplete fracture
Post Test Comments	good test
Impact Velocity	17.950 ft/s
Striker Energy	103.415 ft lbf
Dial Gage Energy	102.200 ft lbf
Encoder Energy	103.415 ft lbf
Latch Angle	134.14°
Final Angle	96.66°
Potential Energy	306.728 ft lbf
Windage & Friction	0.635 ft lbf
Percent Shear	100.00 %
Lateral Expansion	0.0790 in

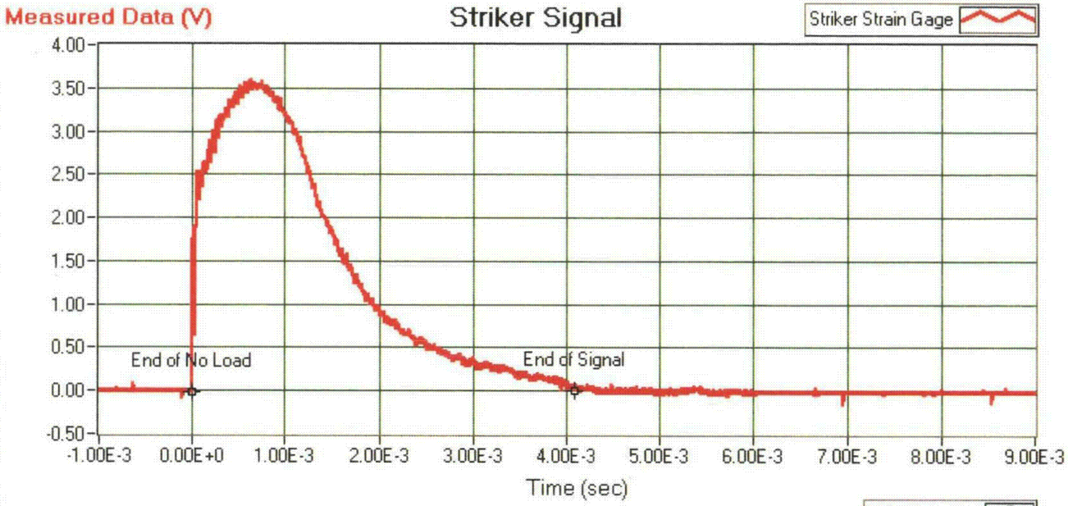

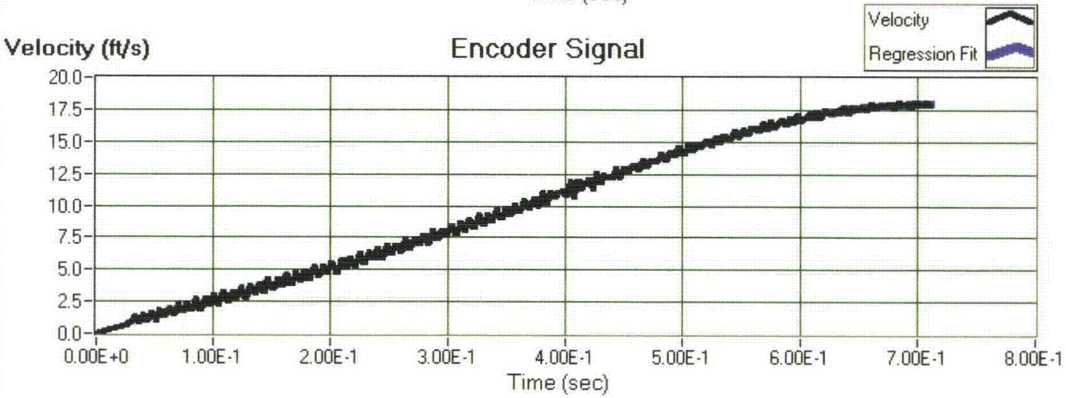

	Load (lbf)	Displacement (in)	Velocity (ft/s)	Time (s)	Energy (ft lbf)
General Yield	2.4860E+3	1.134E-2	1.791E+1	4.583E-5	1.32507E+0
Peak Load	3.7602E+3	1.403E-1	1.691E+1	6.620E-4	3.68219E+1
End of Signal	1.0126E+1	7.708E-1	1.484E+1	4.087E-3	1.03415E+2

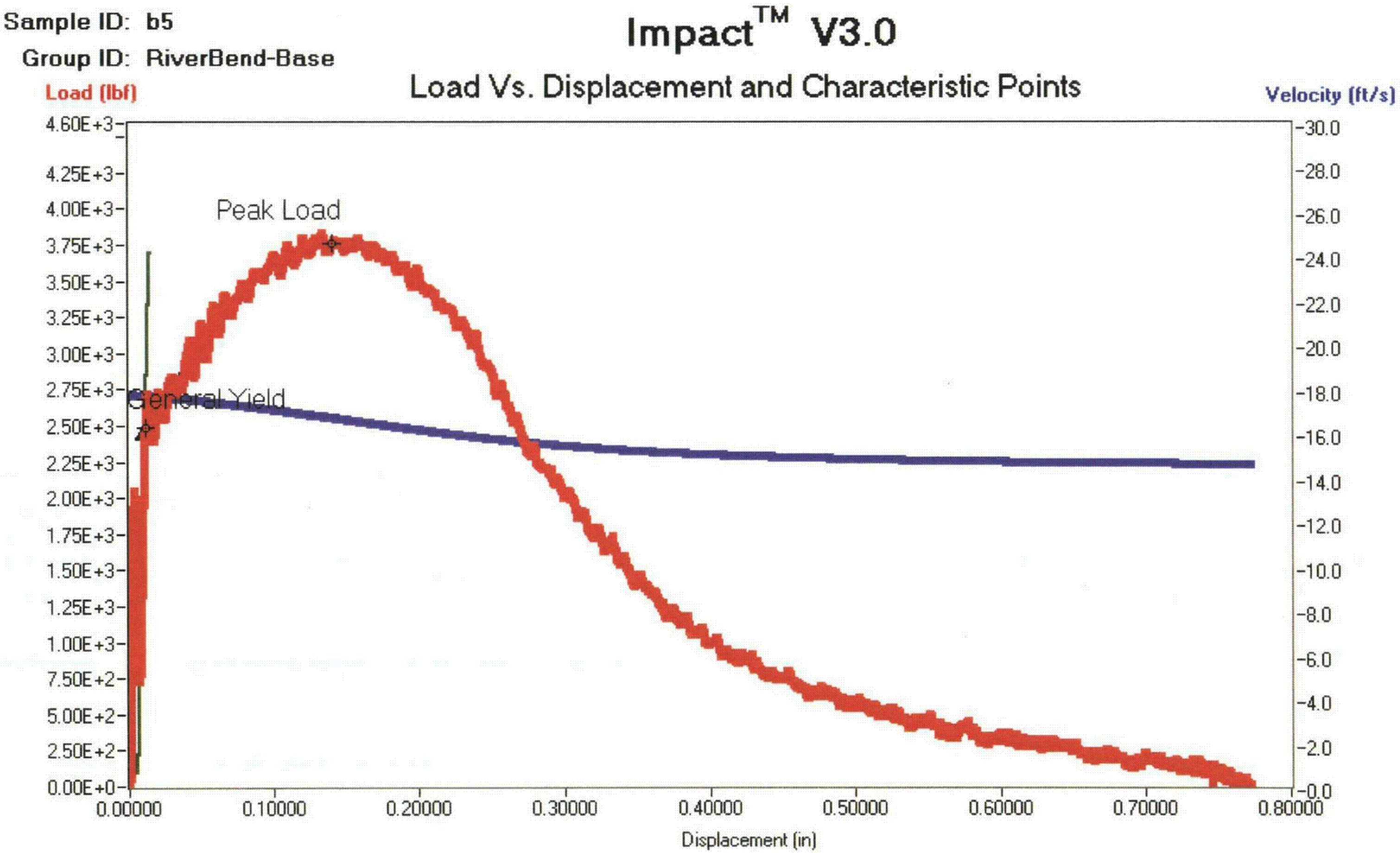

	Load (lbf)	Displacement (in)	Velocity (ft/s)	Time (s)	Energy (ft lbf)
General Yield	2.4860E+3	1.134E-2	1.791E+1	4.583E-5	1.32507E+0
Peak Load	3.7602E+3	1.403E-1	1.691E+1	6.620E-4	3.68219E+1
End of Signal	1.0126E+1	7.708E-1	1.484E+1	4.087E-3	1.03415E+2

Sample ID

b4

Comments

River Bend 183 Degree Surveillance Capsule

Impact™ V3.0

Summary Report

Test Parameters	Value
Group ID	RiverBend-Base
Date	11/08/2002 17:14
Operator	Dr. Michael P. Manahan, Sr.
Temperature	217.0 °F
Oscilloscope	MPM Internal Oscilloscope
Striker	8mm Metals
Interpolation	Point-Point Linear
Encoder Controller	MPM Encoder System
Velocity Determination	Encoder
Material	Metal
Size	Type A
Orientation	TL
Notch Type	V Notch, no Side-Groove
Units Normalization	None
Energy Adjustment	1.0580
Length	2.1654 in
Width	0.3937 in
Thickness	0.3937 in
Span	1.5748 in
Uncracked Ligament	0.3150 in
Notch Rafius	0.0098 in
Failure Type	incomplete fracture
Post Test Comments	good test
Impact Velocity	17.942 ft/s
Striker Energy	98.635 ft lbf
Dial Gage Energy	97.500 ft lbf
Encoder Energy	98.635 ft lbf
Latch Angle	134.14°
Final Angle	98.19°
Potential Energy	306.728 ft lbf
Windage & Friction	0.635 ft lbf
Percent Shear	100.00 %
Lateral Expansion	0.0740 in

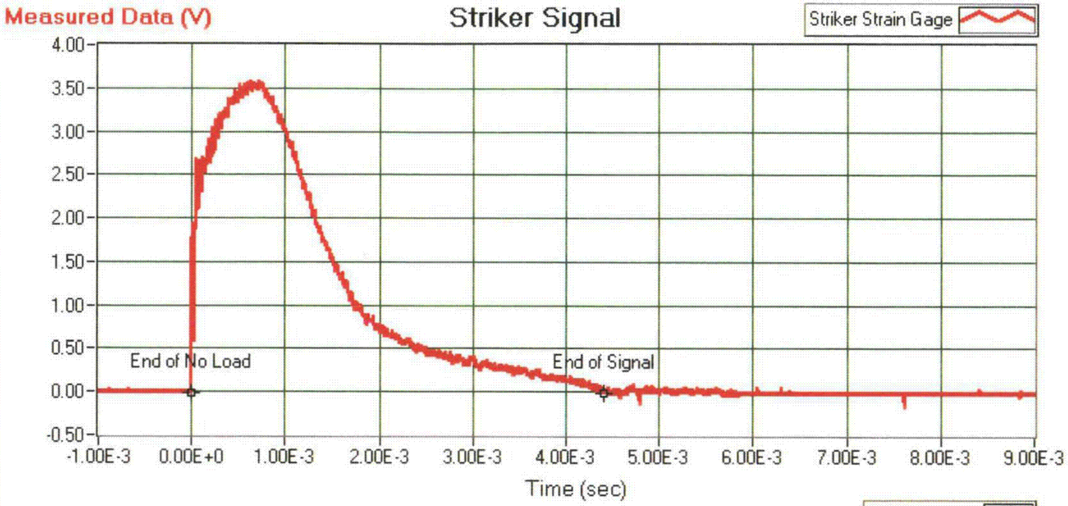

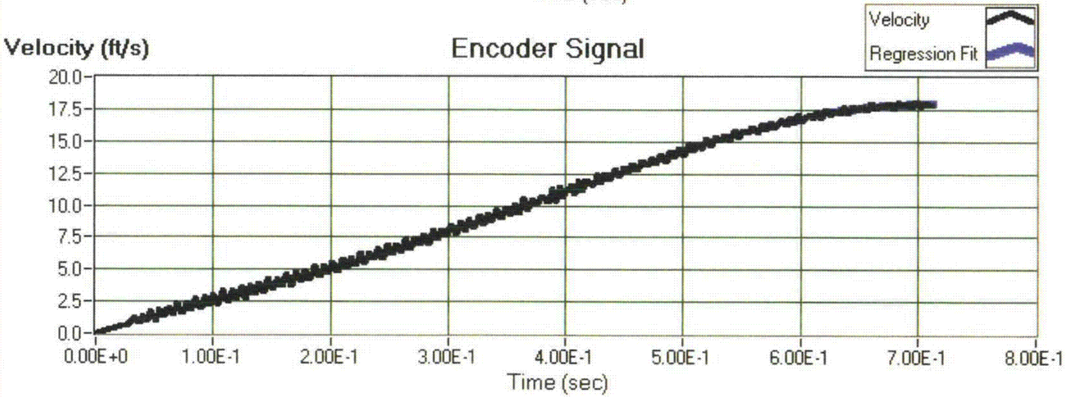

	Load (lbf)	Displacement (in)	Velocity (ft/s)	Time (s)	Energy (ft lbf)
General Yield	2.4485E+3	1.177E-2	1.790E+1	4.683E-5	1.36687E+0
Peak Load	3.7415E+3	1.396E-1	1.690E+1	6.580E-4	3.65178E+1
End of Signal	3.7313E-1	8.346E-1	1.497E+1	4.414E-3	9.86347E+1

Sample ID: b4

Group ID: RiverBend-Base

Impact™ V3.0

Load Vs. Displacement and Characteristic Points

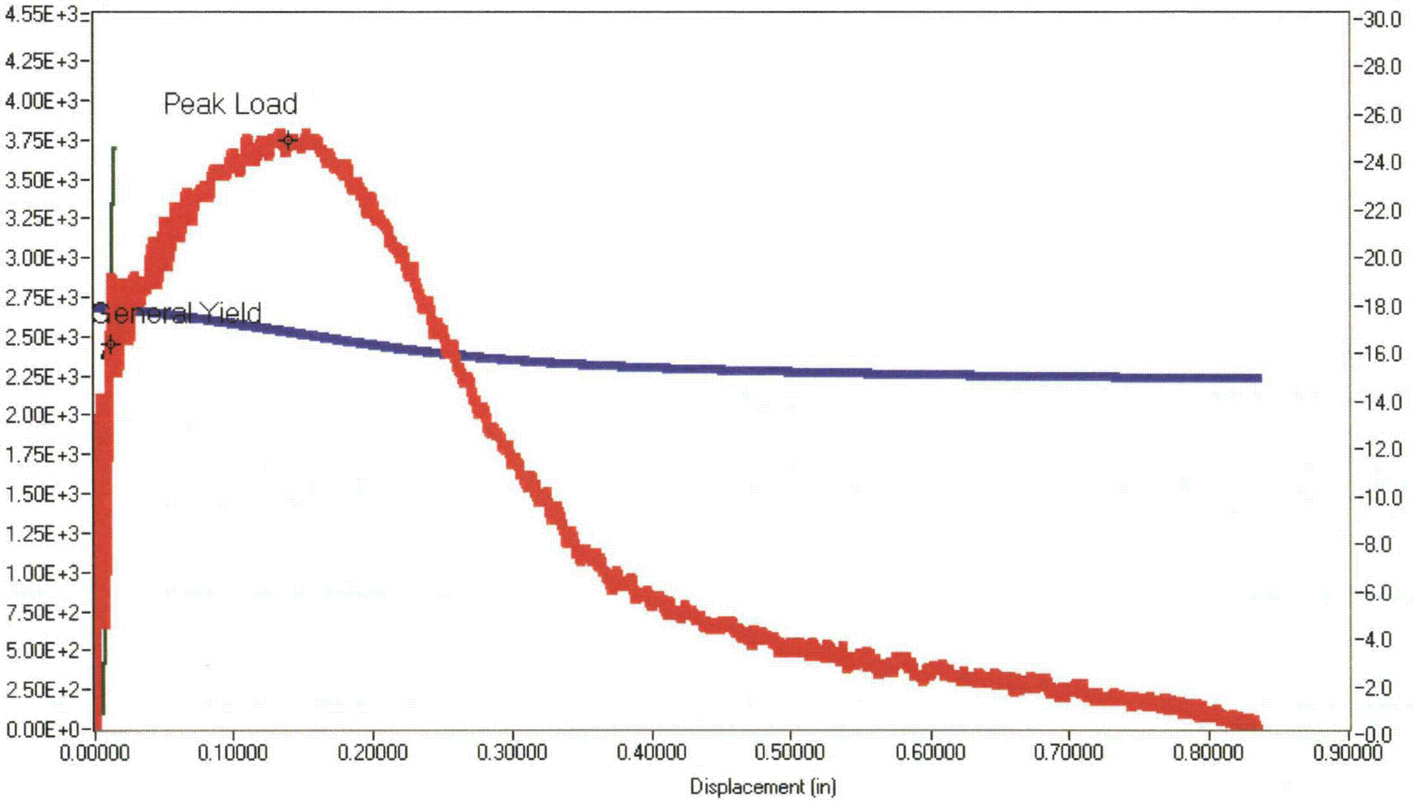

	Load (lbf)	Displacement (in)	Velocity (ft/s)	Time (s)	Energy (ft lbf)
General Yield	2.4485E+3	1.177E-2	1.790E+1	4.683E-5	1.36687E+0
Peak Load	3.7415E+3	1.396E-1	1.690E+1	6.580E-4	3.65178E+1
End of Signal	3.7313E-1	8.346E-1	1.497E+1	4.414E-3	9.86347E+1

Appendix A-2 Weld Metal Data

Sample ID

W2

Comments

River Bend 183 Degree Surveillance Capsule

Impact™ V3.0

Summary Report

Test Parameters	Value
Group ID	RiverBend-Weld
Date	11/11/2002 11:42
Operator	Dr. Michael P. Manahan, Sr.
Temperature	-42.5 °F
Oscilloscope	MPM Internal Oscilloscope
Striker	8mm Metals
Interpolation	Point-Point Linear
Encoder Controller	MPM Encoder System
Velocity Determination	Encoder
Material	Metal
Size	Type A
Orientation	Isotropic
Notch Type	V Notch, no Side-Groove
Units Normalization	None
Energy Adjustment	1.1030
Length	2.1654 in
Width	0.3937 in
Thickness	0.3937 in
Span	1.5748 in
Uncracked Ligament	0.3150 in
Notch Rafius	0.0098 in
Failure Type	complete fracture
Post Test Comments	good test
Impact Velocity	17.948 ft/s
Striker Energy	21.433 ft lbf
Dial Gage Energy	21.000 ft lbf
Encoder Energy	21.433 ft lbf
Latch Angle	134.15°
Final Angle	124.76°
Potential Energy	306.769 ft lbf
Windage & Friction	0.655 ft lbf
Percent Shear	21.50 %
Lateral Expansion	0.0200 in

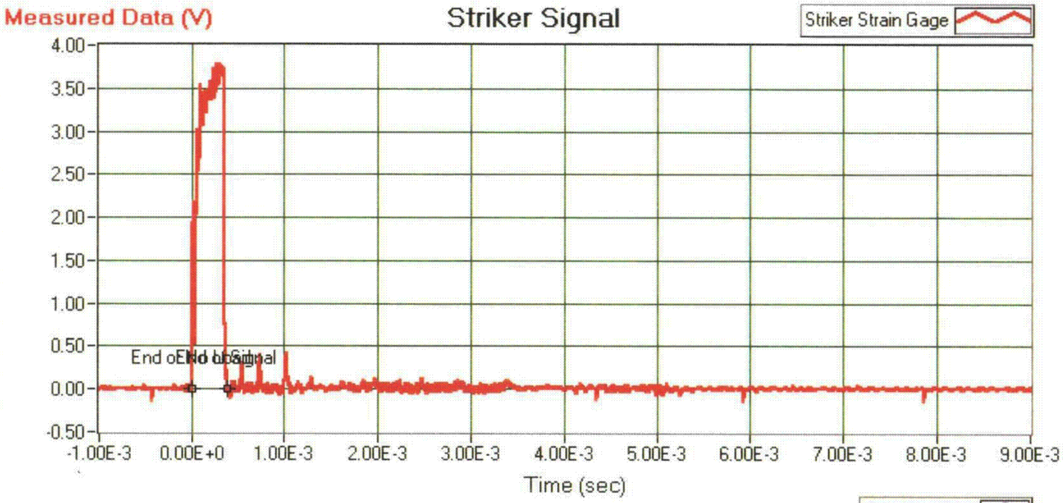

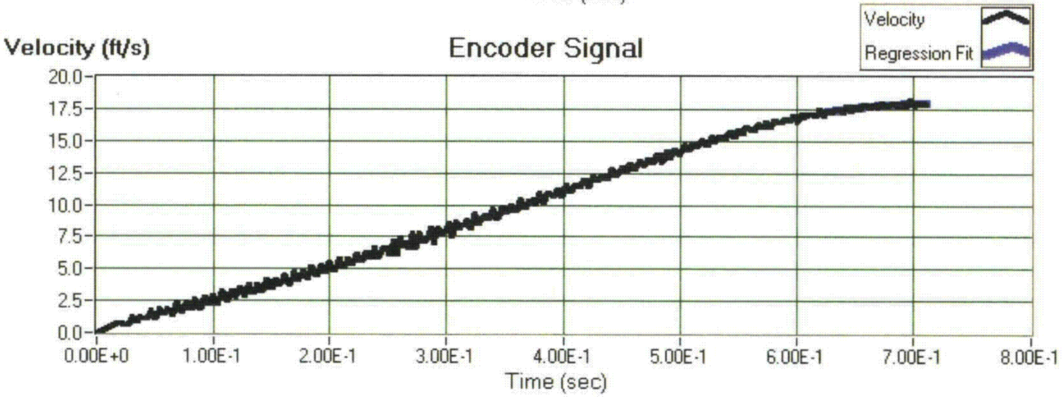

	Load (lbf)	Displacement (in)	Velocity (ft/s)	Time (s)	Energy (ft lbf)
General Yield	3.2347E+3	1.307E-2	1.790E+1	5.400E-5	1.95280E+0
Peak Load	4.1025E+3	6.843E-2	1.743E+1	3.150E-4	1.93912E+1
Brittle Fracture	4.1218E+3	7.177E-2	1.739E+1	3.310E-4	2.05243E+1
Arrest Load	1.3864E+2	7.803E-2	1.737E+1	3.610E-4	2.13764E+1
End of Signal	6.8710E+0	8.217E-2	1.737E+1	3.810E-4	2.14332E+1

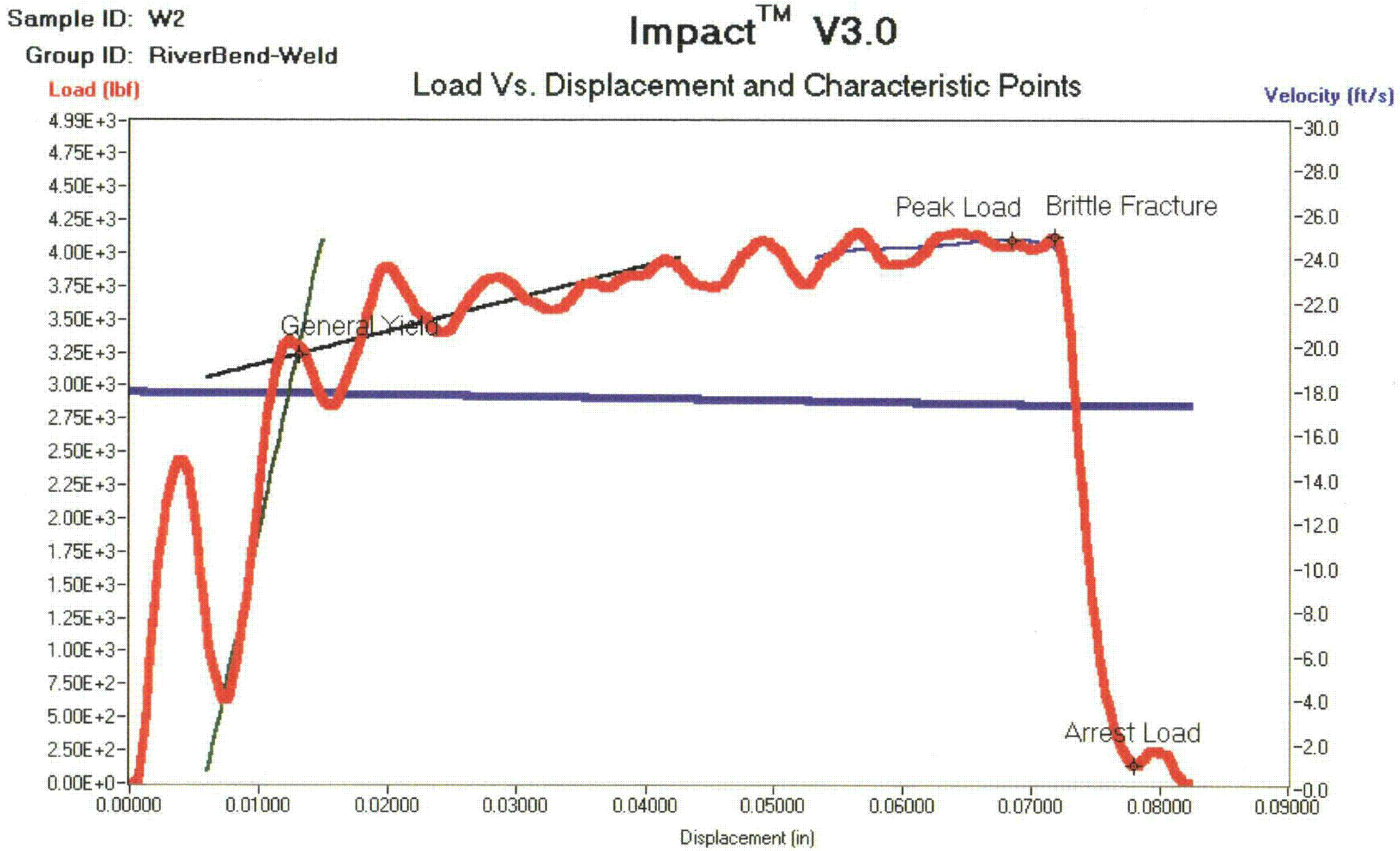

	Load (lbf)	Displacement (in)	Velocity (ft/s)	Time (s)	Energy (ft lbf)
General Yield	3.2347E+3	1.307E-2	1.790E+1	5.400E-5	1.95280E+0
Peak Load	4.1025E+3	6.843E-2	1.743E+1	3.150E-4	1.93912E+1
Brittle Fracture	4.1218E+3	7.177E-2	1.739E+1	3.310E-4	2.05243E+1
Arrest Load	1.3864E+2	7.803E-2	1.737E+1	3.610E-4	2.13764E+1
End of Signal	6.8710E+0	8.217E-2	1.737E+1	3.810E-4	2.14332E+1

Sample ID

W5

Comments

River Bend 183 Degree Surveillance Capsule

Impact™ V3.0

Summary Report

Test Parameters	Value
Group ID	RiverBend-Weld
Date	11/11/2002 11:21
Operator	Dr. Michael P. Manahan, Sr.
Temperature	-42.0 °F
Oscilloscope	MPM Internal Oscilloscope
Striker	8mm Metals
Interpolation	Point-Point Linear
Encoder Controller	MPM Encoder System
Velocity Determination	Encoder
Material	Metal
Size	Type A
Orientation	Isotropic
Notch Type	V Notch, no Side-Groove
Units Normalization	None
Energy Adjustment	1.0815
Length	2.1654 in
Width	0.3937 in
Thickness	0.3937 in
Span	1.5748 in
Uncracked Ligament	0.3150 in
Notch Rafius	0.0098 in
Failure Type	complete fracture
Post Test Comments	good test
Impact Velocity	17.945 ft/s
Striker Energy	36.735 ft lbf
Dial Gage Energy	36.200 ft lbf
Encoder Energy	36.735 ft lbf
Latch Angle	134.15°
Final Angle	119.03°
Potential Energy	306.769 ft lbf
Windage & Friction	0.655 ft lbf
Percent Shear	28.68 %
Lateral Expansion	0.0330 in

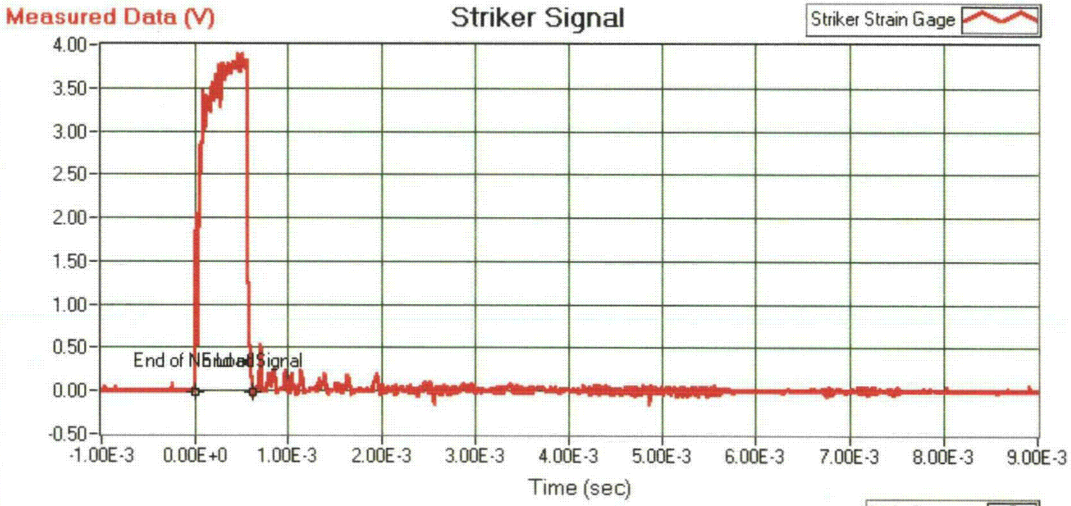

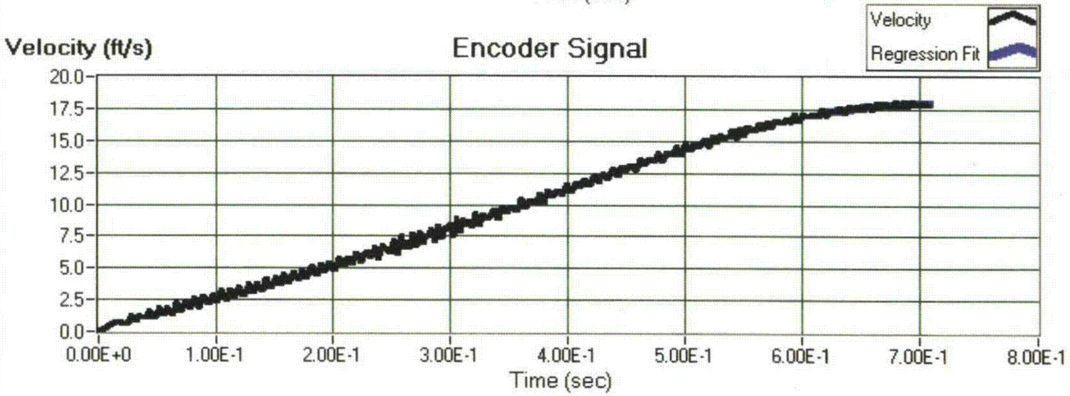

	Load (lbf)	Displacement (in)	Velocity (ft/s)	Time (s)	Energy (ft lbf)
General Yield	3.2767E+3	1.394E-2	1.789E+1	5.500E-5	1.87763E+0
Peak Load	4.1212E+3	1.053E-1	1.709E+1	4.900E-4	3.09752E+1
Brittle Fracture	4.1317E+3	1.186E-1	1.696E+1	5.550E-4	3.55281E+1
Arrest Load	1.0933E+2	1.296E-1	1.692E+1	6.090E-4	3.67315E+1
End of Signal	1.2426E+1	1.306E-1	1.692E+1	6.140E-4	3.67351E+1

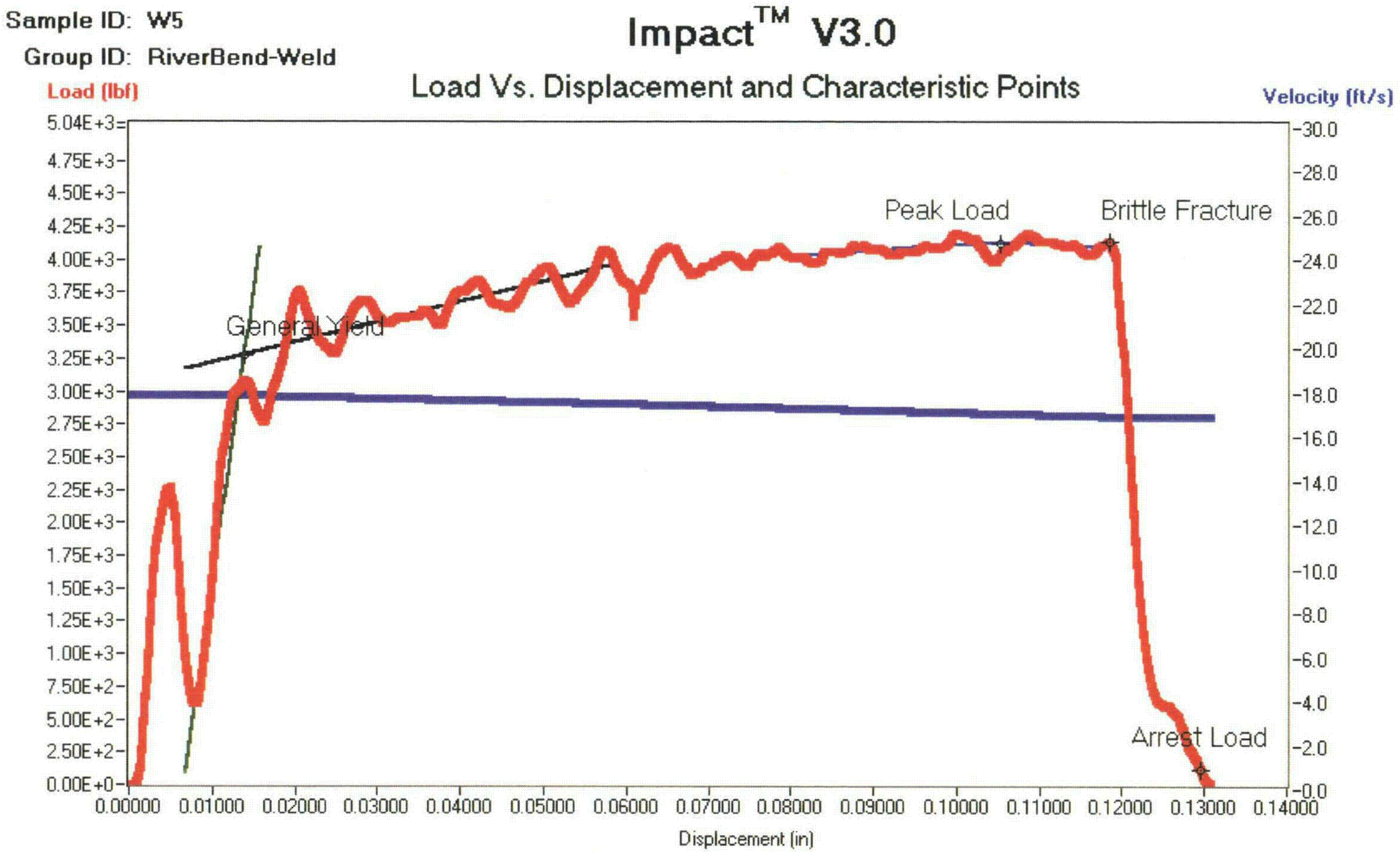

	Load (lbf)	Displacement (in)	Velocity (ft/s)	Time (s)	Energy (ft lbf)
General Yield	3.2767E+3	1.394E-2	1.789E+1	5.500E-5	1.87763E+0
Peak Load	4.1212E+3	1.053E-1	1.709E+1	4.900E-4	3.09752E+1
Brittle Fracture	4.1317E+3	1.186E-1	1.696E+1	5.550E-4	3.55281E+1
Arrest Load	1.0933E+2	1.296E-1	1.692E+1	6.090E-4	3.67315E+1
End of Signal	1.2426E+1	1.306E-1	1.692E+1	6.140E-4	3.67351E+1

Sample ID

W8

Comments

Impact™ V3.0

Summary Report

Test Parameters	Value
Group ID	RiverBend-Weld
Date	11/11/2002 10:38
Operator	Dr. Michael P. Manahan, Sr.
Temperature	11.3 °F
Oscilloscope	MPM Internal Oscilloscope
Striker	8mm Metals
Interpolation	Point-Point Linear
Encoder Controller	MPM Encoder System
Velocity Determination	Encoder
Material	Metal
Size	Type A
Orientation	Isotropic
Notch Type	V Notch, no Side-Groove
Units Normalization	None
Energy Adjustment	1.1701
Length	2.1654 in
Width	0.3937 in
Thickness	0.3937 in
Span	1.5748 in
Uncracked Ligament	0.3150 in
Notch Rafius	0.0098 in
Failure Type	complete fracture
Post Test Comments	good test
Impact Velocity	17.964 ft/s
Striker Energy	25.951 ft lbf
Dial Gage Energy	25.600 ft lbf
Encoder Energy	25.951 ft lbf
Latch Angle	134.15°
Final Angle	123.03°
Potential Energy	306.769 ft lbf
Windage & Friction	0.655 ft lbf
Percent Shear	31.64 %
Lateral Expansion	0.0240 in

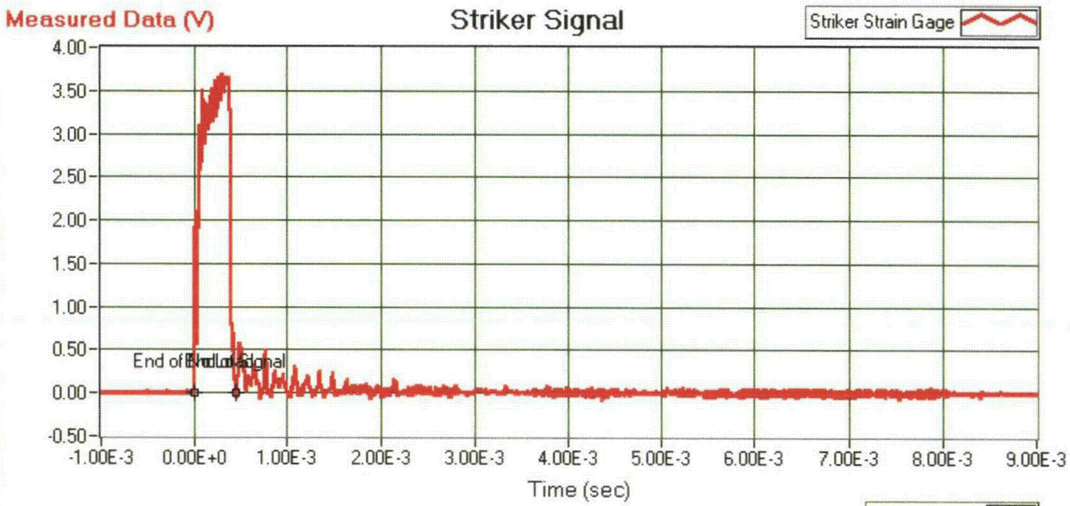

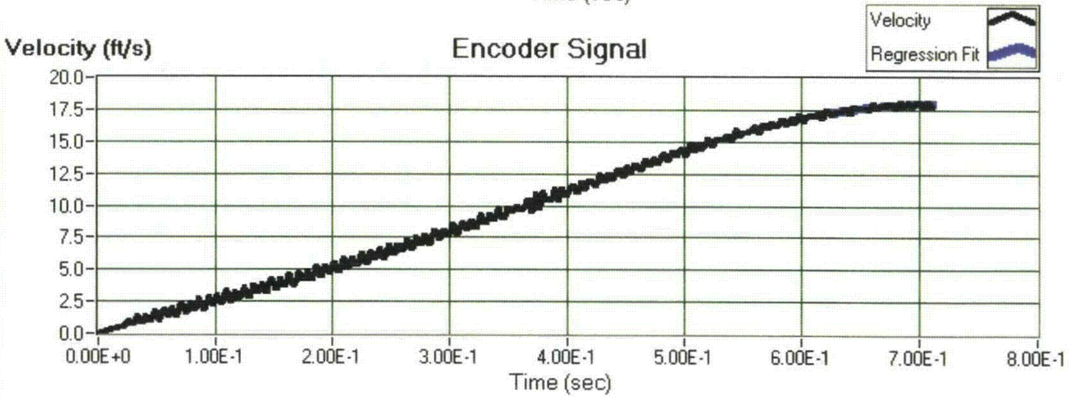

	Load (lbf)	Displacement (in)	Velocity (ft/s)	Time (s)	Energy (ft lbf)
General Yield	3.4807E+3	1.307E-2	1.791E+1	5.483E-5	2.12706E+0
Peak Load	4.2725E+3	7.831E-2	1.737E+1	3.630E-4	2.34513E+1
Brittle Fracture	3.8233E+3	2.126E-2	1.785E+1	9.300E-5	4.54500E+0
Arrest Load	8.0878E+1	9.390E-2	1.730E+1	4.380E-4	2.59500E+1
End of Signal	2.2632E+1	9.429E-2	1.730E+1	4.400E-4	2.59511E+1

Sample ID: W8

Group ID: RiverBend-Weld

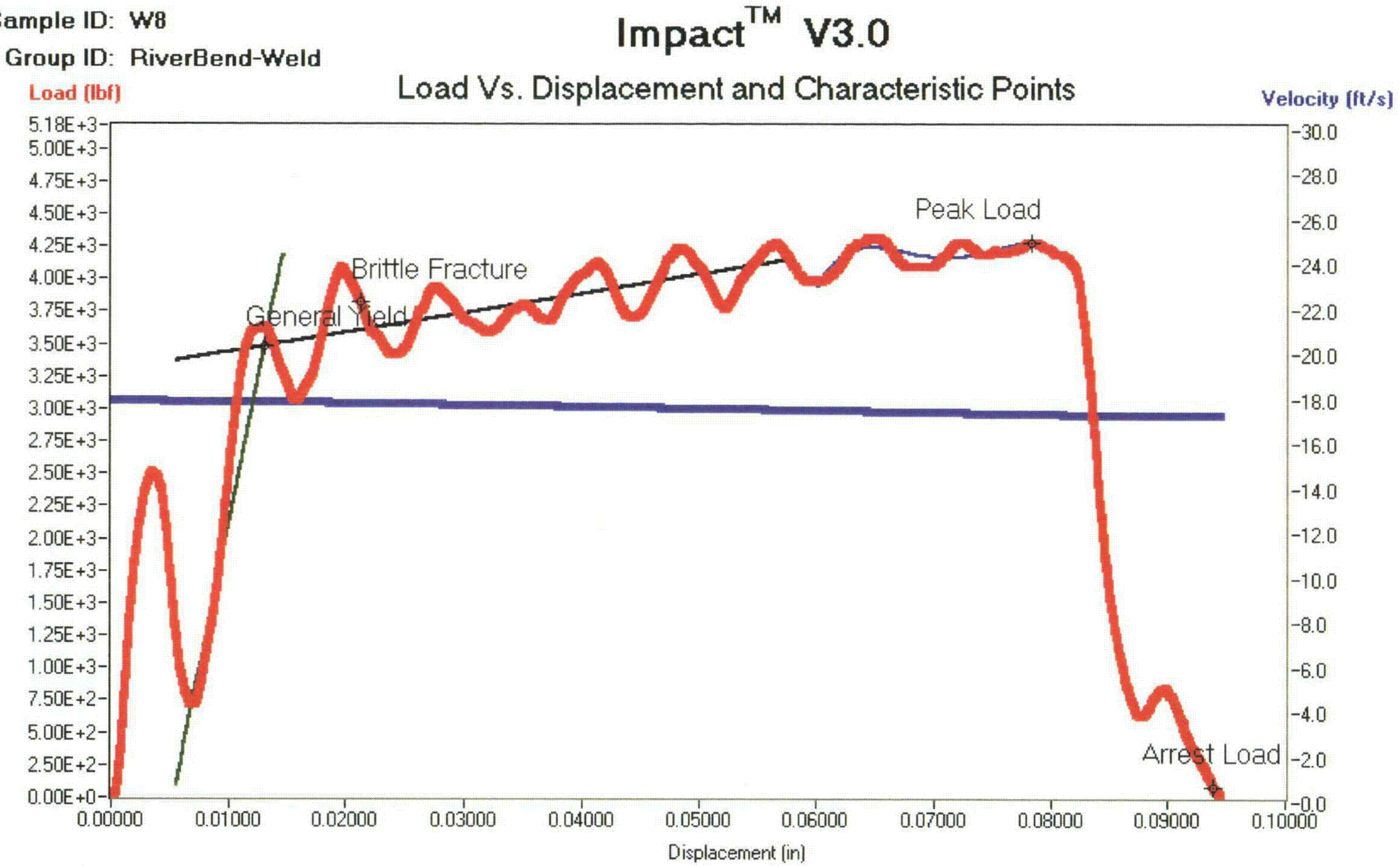

	Load (lbf)	Displacement (in)	Velocity (ft/s)	Time (s)	Energy (ft lbf)
General Yield	3.4807E+3	1.307E-2	1.791E+1	5.483E-5	2.12706E+0
Peak Load	4.2725E+3	7.831E-2	1.737E+1	3.630E-4	2.34513E+1
Brittle Fracture	3.8233E+3	2.126E-2	1.785E+1	9.300E-5	4.54500E+0
Arrest Load	8.0878E+1	9.390E-2	1.730E+1	4.380E-4	2.59500E+1
End of Signal	2.2632E+1	9.429E-2	1.730E+1	4.400E-4	2.59511E+1

Sample ID
W6
Comments

Impact™ V3.0
Summary Report

Test Parameters	Value
Group ID	RiverBend-Weld
Date	11/11/2002 10:55
Operator	Dr. Michael P. Manahan, Sr.
Temperature	11.5 °F
Oscilloscope	MPM Internal Oscilloscope
Striker	8mm Metals
Interpolation	Point-Point Linear
Encoder Controller	MPM Encoder System
Velocity Determination	Encoder
Material	Metal
Size	Type A
Orientation	Isotropic
Notch Type	V Notch, no Side-Groove
Units Normalization	None
Energy Adjustment	1.0986
Length	2.1654 in
Width	0.3937 in
Thickness	0.3937 in
Span	1.5748 in
Uncracked Ligament	0.3150 in
Notch Rafius	0.0098 in
Failure Type	complete fracture
Post Test Comments	good test
Impact Velocity	17.945 ft/s
Striker Energy	27.429 ft lbf
Dial Gage Energy	27.100 ft lbf
Encoder Energy	27.429 ft lbf
Latch Angle	134.15°
Final Angle	122.47°
Potential Energy	306.769 ft lbf
Windage & Friction	0.655 ft lbf
Percent Shear	31.77 %
Lateral Expansion	0.0230 in

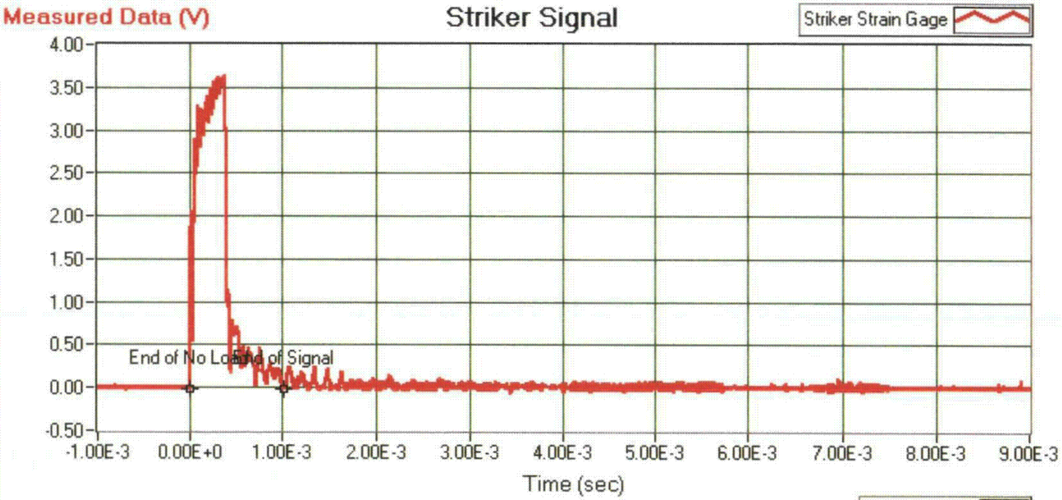

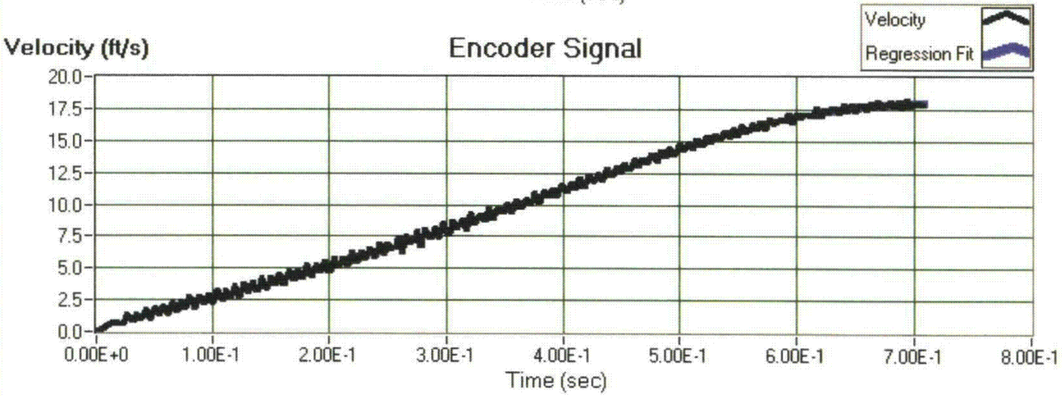

	Load (lbf)	Displacement (in)	Velocity (ft/s)	Time (s)	Energy (ft lbf)
General Yield	3.1253E+3	1.260E-2	1.790E+1	5.280E-5	1.81585E+0
Peak Load	3.9736E+3	7.890E-2	1.736E+1	3.660E-4	2.16635E+1
Brittle Fracture	3.9484E+3	8.035E-2	1.734E+1	3.730E-4	2.21467E+1
Arrest Load	6.0061E+2	9.177E-2	1.730E+1	4.280E-4	2.39058E+1
End of Signal	3.1746E+0	2.109E-1	1.720E+1	1.004E-3	2.74294E+1

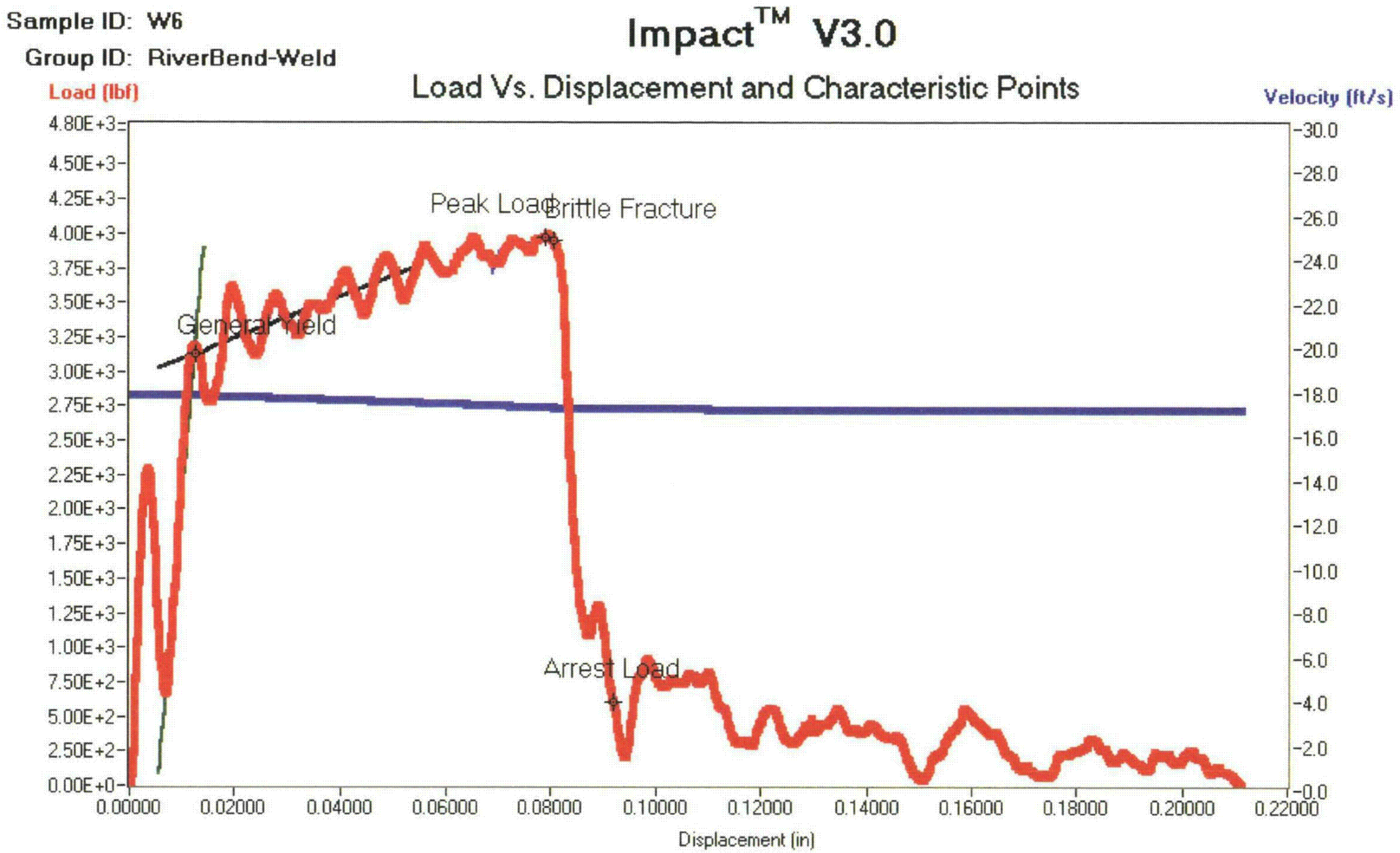

	Load (lbf)	Displacement (in)	Velocity (ft/s)	Time (s)	Energy (ft lbf)
General Yield	3.1253E+3	1.260E-2	1.790E+1	5.280E-5	1.81585E+0
Peak Load	3.9736E+3	7.890E-2	1.736E+1	3.660E-4	2.16635E+1
Brittle Fracture	3.9484E+3	8.035E-2	1.734E+1	3.730E-4	2.21467E+1
Arrest Load	6.0061E+2	9.177E-2	1.730E+1	4.280E-4	2.39058E+1
End of Signal	3.1746E+0	2.109E-1	1.720E+1	1.004E-3	2.74294E+1

Sample ID

W1

Comments

River Bend 183 Degree Surveillance Capsule

Impact™ V3.0

Summary Report

Test Parameters	Value
Group ID	RiverBend-Weld
Date	11/11/2002 16:28
Operator	Dr. Michael P. Manahan, Sr.
Temperature	37.0 °F
Oscilloscope	MPM Internal Oscilloscope
Striker	8mm Metals
Interpolation	Point-Point Linear
Encoder Controller	MPM Encoder System
Velocity Determination	Encoder
Material	Metal
Size	Type A
Orientation	Isotropic
Notch Type	V Notch, no Side-Groove
Units Normalization	None
Energy Adjustment	1.0566
Length	2.1654 in
Width	0.3937 in
Thickness	0.3937 in
Span	1.5748 in
Uncracked Ligament	0.3150 in
Notch Rafius	0.0098 in
Failure Type	complete fracture
Post Test Comments	good test
Impact Velocity	17.937 ft/s
Striker Energy	68.183 ft lbf
Dial Gage Energy	67.200 ft lbf
Encoder Energy	68.183 ft lbf
Latch Angle	134.15°
Final Angle	108.13°
Potential Energy	306.769 ft lbf
Windage & Friction	0.655 ft lbf
Percent Shear	66.11 %
Lateral Expansion	0.0525 in

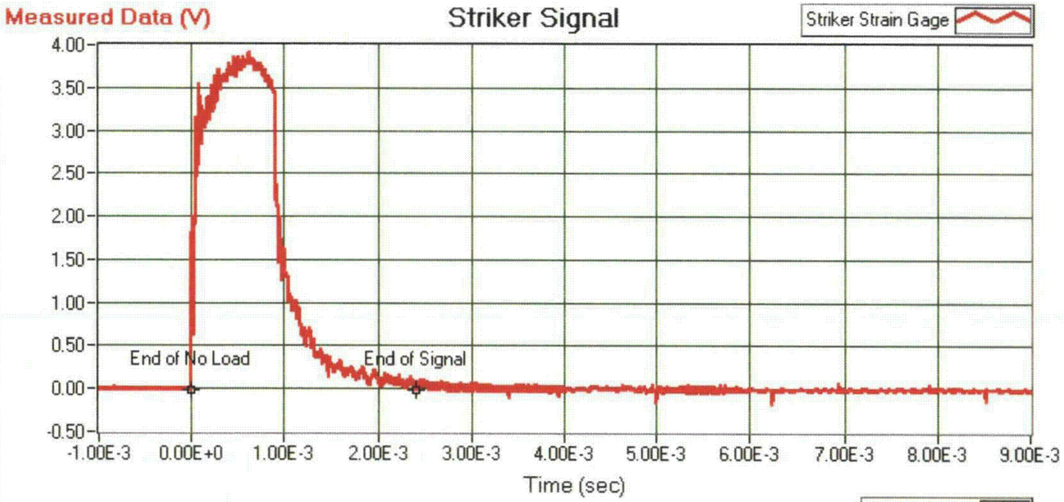

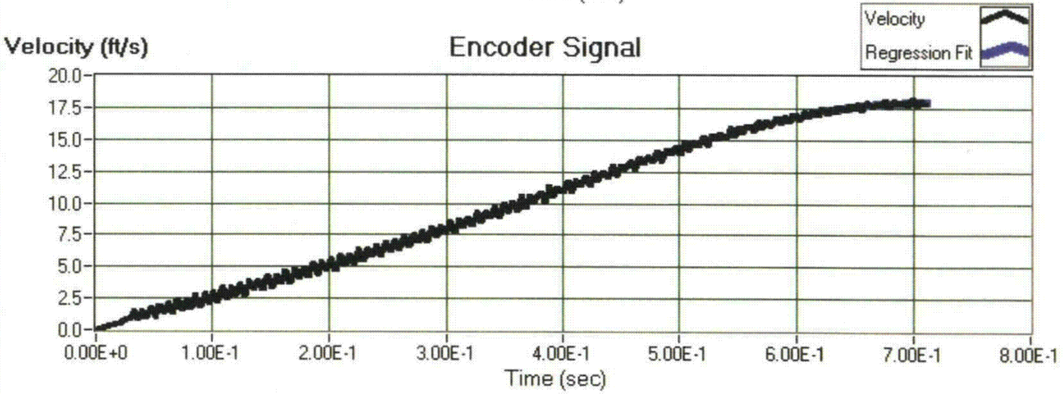

	Load (lbf)	Displacement (in)	Velocity (ft/s)	Time (s)	Energy (ft lbf)
General Yield	3.1150E+3	1.390E-2	1.789E+1	5.180E-5	1.74090E+0
Peak Load	4.0192E+3	1.298E-1	1.687E+1	6.070E-4	3.74809E+1
Brittle Fracture	3.6699E+3	1.873E-1	1.630E+1	8.960E-4	5.62185E+1
Arrest Load	1.8287E+3	1.955E-1	1.625E+1	9.380E-4	5.80021E+1
End of Signal	5.1458E+0	4.751E-1	1.594E+1	2.393E-3	6.81833E+1

Sample ID: W1

Group ID: RiverBend-Weld

Impact™ V3.0

Load Vs. Displacement and Characteristic Points

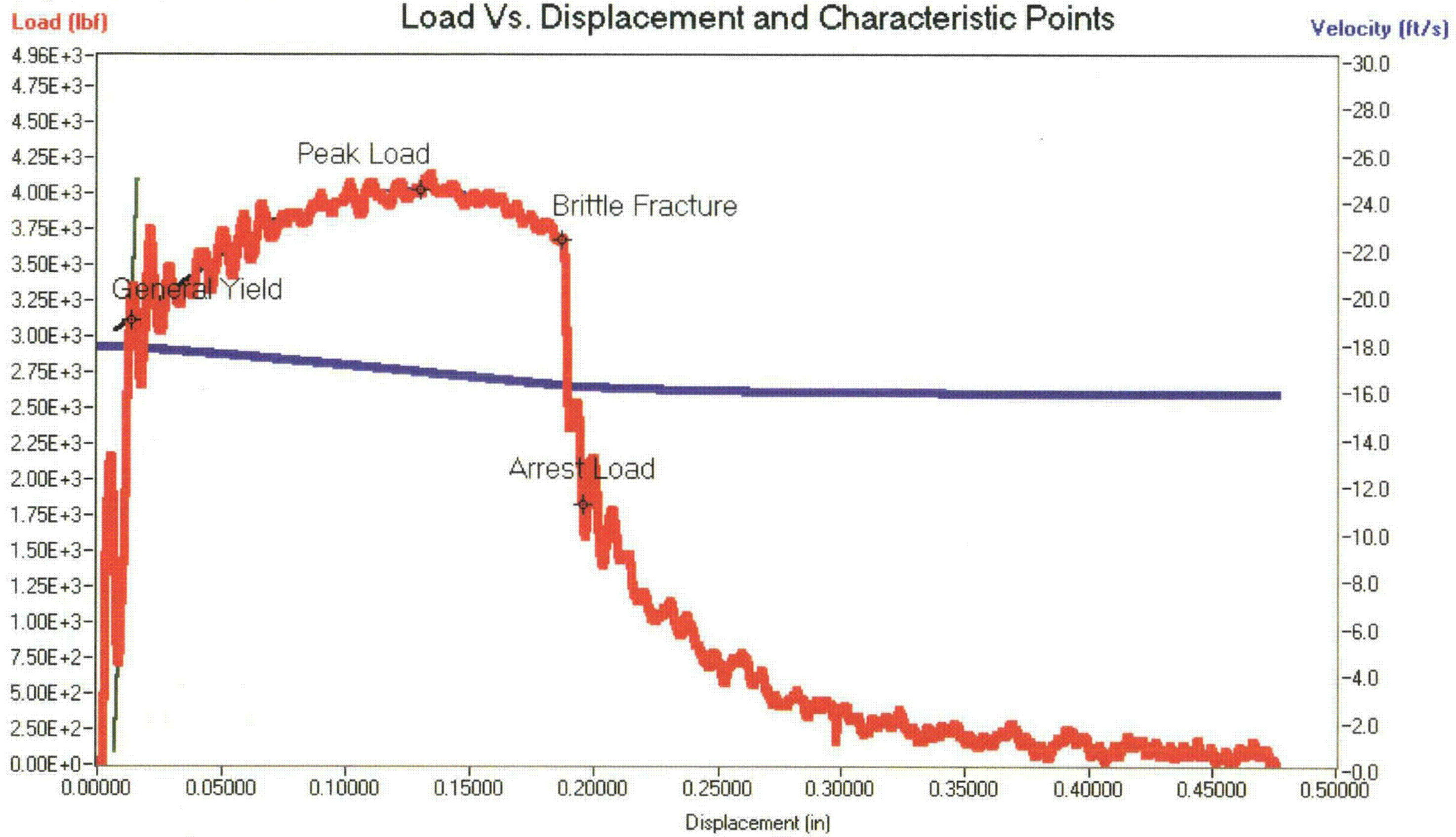

	Load (lbf)	Displacement (in)	Velocity (ft/s)	Time (s)	Energy (ft lbf)
General Yield	3.1150E+3	1.390E-2	1.789E+1	5.180E-5	1.74090E+0
Peak Load	4.0192E+3	1.298E-1	1.687E+1	6.070E-4	3.74809E+1
Brittle Fracture	3.6699E+3	1.873E-1	1.630E+1	8.960E-4	5.62185E+1
Arrest Load	1.8287E+3	1.955E-1	1.625E+1	9.380E-4	5.80021E+1
End of Signal	5.1458E+0	4.751E-1	1.594E+1	2.393E-3	6.81833E+1

Sample ID

W10

Comments

River Bend 183 Degree Surveillance Capsule

Impact™ V3.0

Summary Report

Test Parameters	Value
Group ID	RiverBend-Weld
Date	11/11/2002 16:42
Operator	Dr. Michael P. Manahan, Sr.
Temperature	37.2 °F
Oscilloscope	MPM Internal Oscilloscope
Striker	8mm Metals
Interpolation	Point-Point Linear
Encoder Controller	MPM Encoder System
Velocity Determination	Encoder
Material	Metal
Size	Type A
Orientation	Isotropic
Notch Type	V Notch, no Side-Groove
Units Normalization	None
Energy Adjustment	1.0622
Length	2.1654 in
Width	0.3937 in
Thickness	0.3937 in
Span	1.5748 in
Uncracked Ligament	0.3150 in
Notch Rafius	0.0098 in
Failure Type	complete fracture
Post Test Comments	good test
Impact Velocity	17.940 ft/s
Striker Energy	48.049 ft lbf
Dial Gage Energy	47.400 ft lbf
Encoder Energy	48.049 ft lbf
Latch Angle	134.15°
Final Angle	115.00°
Potential Energy	306.769 ft lbf
Windage & Friction	0.655 ft lbf
Percent Shear	55.62 %
Lateral Expansion	0.0410 in

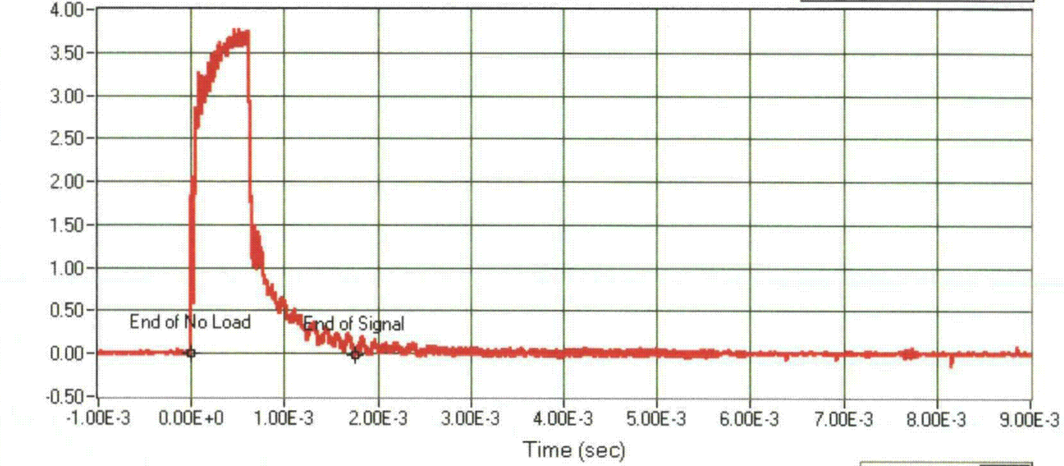

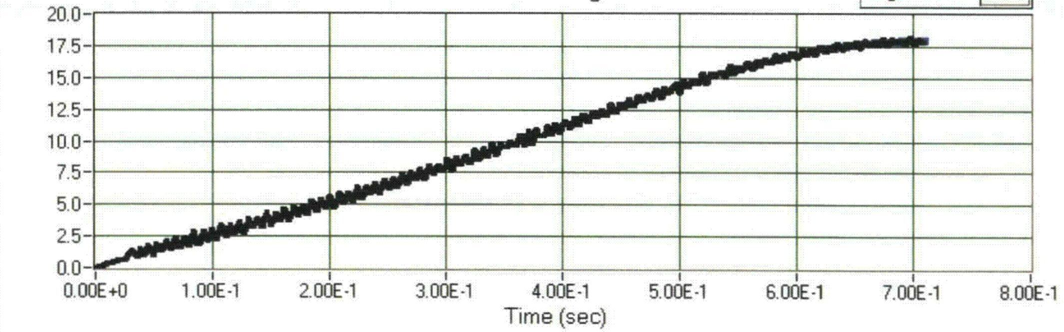

	Load (lbf)	Displacement (in)	Velocity (ft/s)	Time (s)	Energy (ft lbf)
General Yield	3.0347E+3	1.264E-2	1.789E+1	5.300E-5	1.72167E+0
Peak Load	3.8988E+3	1.258E-1	1.692E+1	5.940E-4	3.58754E+1
Brittle Fracture	3.9046E+3	1.304E-1	1.688E+1	6.170E-4	3.73955E+1
Arrest Load	1.3628E+3	1.387E-1	1.683E+1	6.580E-4	3.89659E+1
End of Signal	6.5779E+0	3.562E-1	1.656E+1	1.747E-3	4.80486E+1

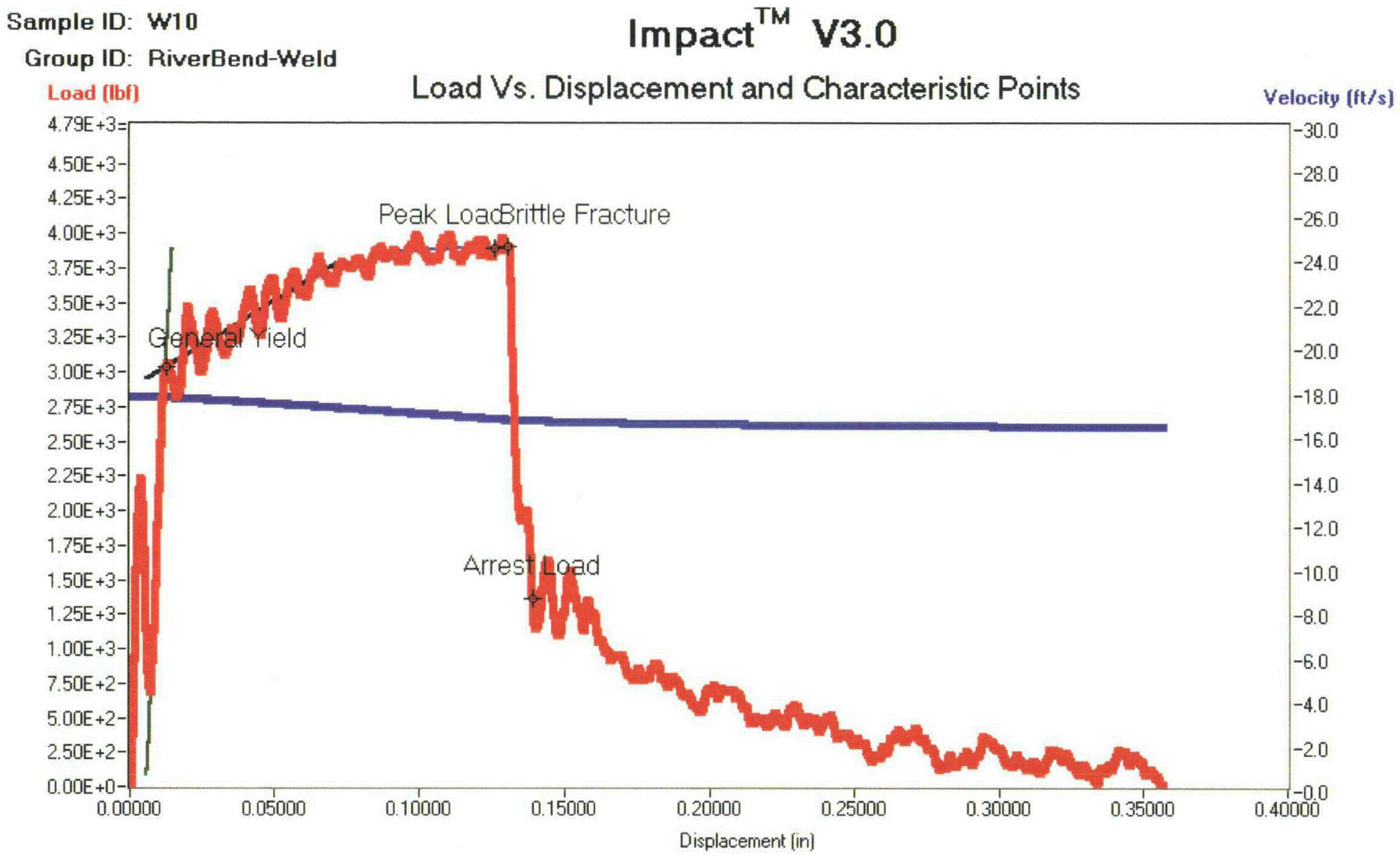

	Load (lbf)	Displacement (in)	Velocity (ft/s)	Time (s)	Energy (ft lbf)
General Yield	3.0347E+3	1.264E-2	1.789E+1	5.300E-5	1.72167E+0
Peak Load	3.8988E+3	1.258E-1	1.692E+1	5.940E-4	3.58754E+1
Brittle Fracture	3.9046E+3	1.304E-1	1.688E+1	6.170E-4	3.73955E+1
Arrest Load	1.3628E+3	1.387E-1	1.683E+1	6.580E-4	3.89659E+1
End of Signal	6.5779E+0	3.562E-1	1.656E+1	1.747E-3	4.80486E+1

Sample ID

W4

Comments

Impact™ V3.0

Summary Report

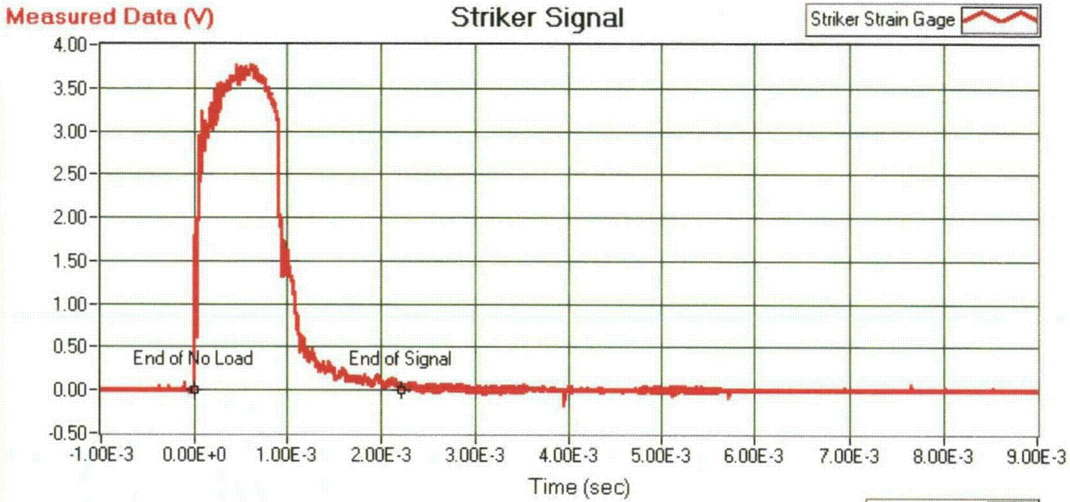

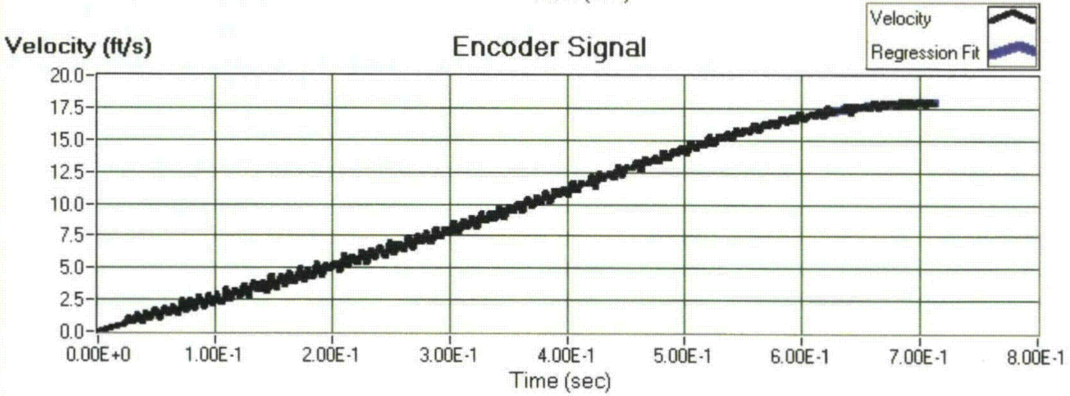

Test Parameters	Value
Group ID	RiverBend-Weld
Date	11/11/2002 09:50
Operator	Dr. Michael P. Manahan, Sr.
Temperature	69.6 °F
Oscilloscope	MPM Internal Oscilloscope
Striker	8mm Metals
Interpolation	Point-Point Linear
Encoder Controller	MPM Encoder System
Velocity Determination	Encoder
Material	Metal
Size	Type A
Orientation	Isotropic
Notch Type	V Notch, no Side-Groove
Units Normalization	None
Energy Adjustment	1.0437
Length	2.1654 in
Width	0.3937 in
Thickness	0.3937 in
Span	1.5748 in
Uncracked Ligament	0.3150 in
Notch Rafius	0.0098 in
Failure Type	complete fracture
Post Test Comments	good test
Impact Velocity	17.976 ft/s
Striker Energy	63.516 ft lbf
Dial Gage Energy	63.000 ft lbf
Encoder Energy	63.516 ft lbf
Latch Angle	134.15°
Final Angle	109.69°
Potential Energy	306.769 ft lbf
Windage & Friction	0.655 ft lbf
Percent Shear	62.72 %
Lateral Expansion	0.0535 in

	Load (lbf)	Displacement (in)	Velocity (ft/s)	Time (s)	Energy (ft lbf)
General Yield	2.9304E+3	1.244E-2	1.793E+1	5.083E-5	1.64053E+0
Peak Load	3.8619E+3	1.236E-1	1.699E+1	5.810E-4	3.43395E+1
Brittle Fracture	3.4562E+3	1.828E-1	1.644E+1	8.760E-4	5.26621E+1
Arrest Load	1.6993E+3	1.956E-1	1.635E+1	9.410E-4	5.55385E+1
End of Signal	2.0271E+1	4.406E-1	1.610E+1	2.205E-3	6.35159E+1

Sample ID: W4

Group ID: RiverBend-Weld

Impact™ V3.0

Load Vs. Displacement and Characteristic Points

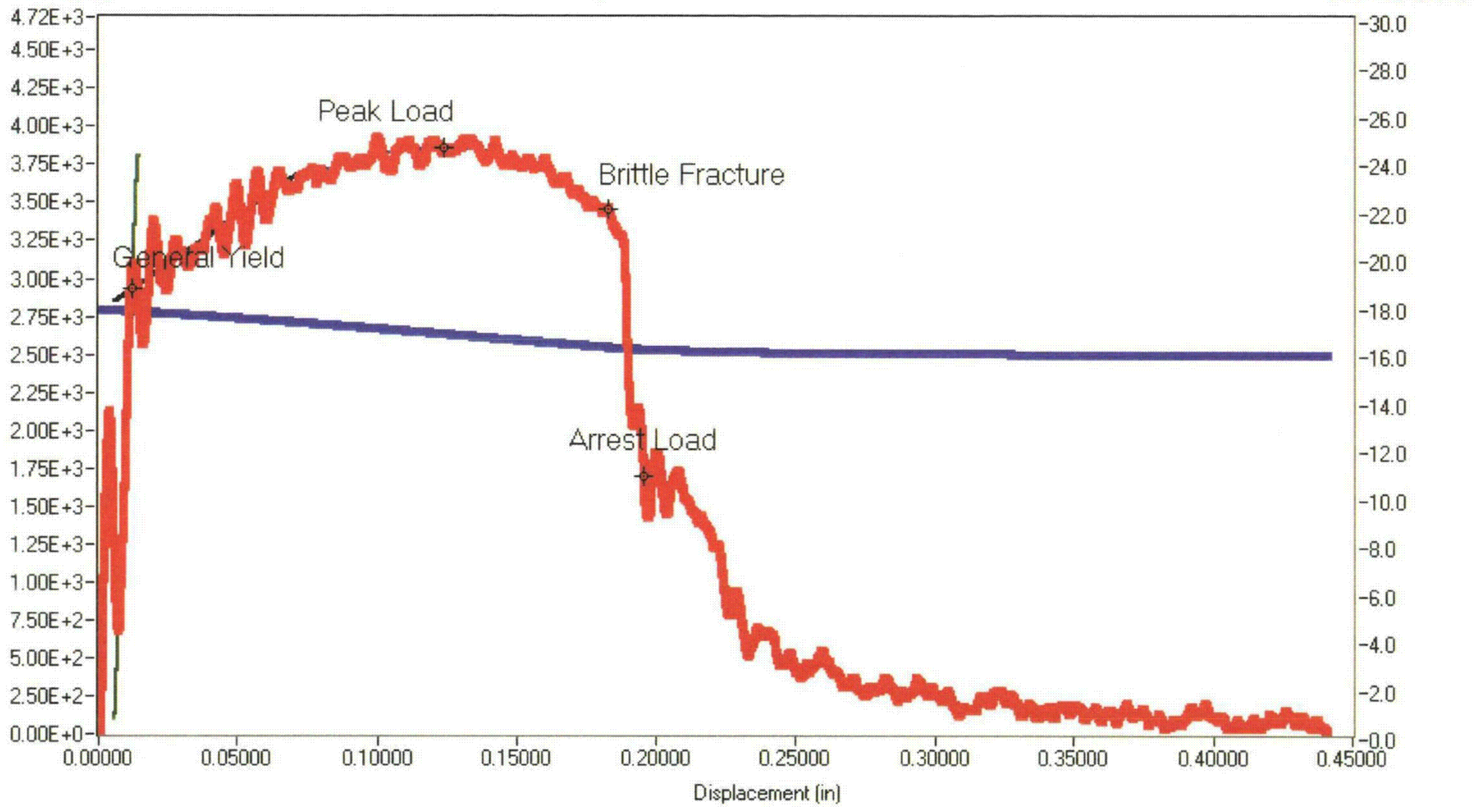

	Load (lbf)	Displacement (in)	Velocity (ft/s)	Time (s)	Energy (ft lbf)
General Yield	2.9304E+3	1.244E-2	1.793E+1	5.083E-5	1.64053E+0
Peak Load	3.8619E+3	1.236E-1	1.699E+1	5.810E-4	3.43395E+1
Brittle Fracture	3.4562E+3	1.828E-1	1.644E+1	8.760E-4	5.26621E+1
Arrest Load	1.6993E+3	1.956E-1	1.635E+1	9.410E-4	5.55385E+1
End of Signal	2.0271E+1	4.406E-1	1.610E+1	2.205E-3	6.35159E+1

Sample ID
W9
Comments

Impact™ V3.0
Summary Report

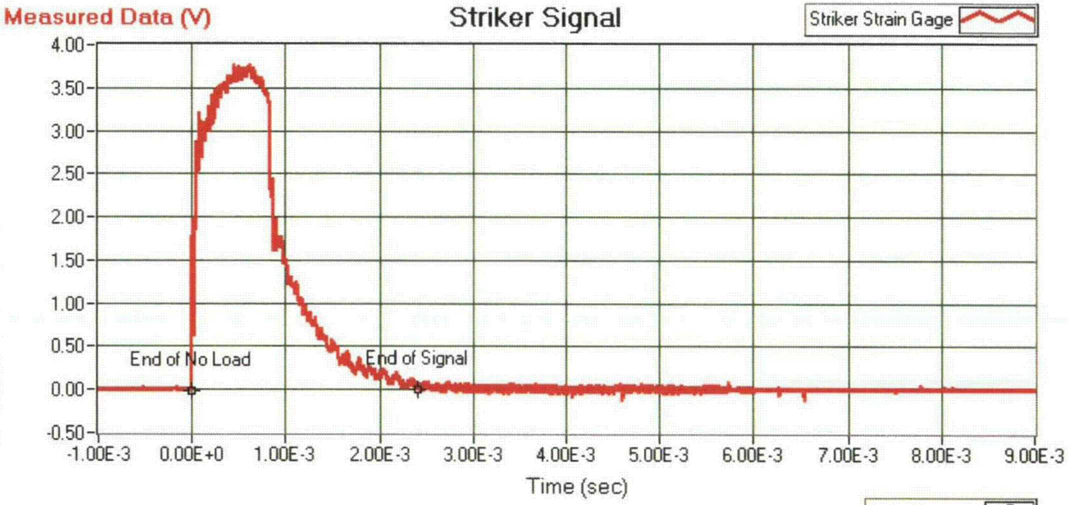

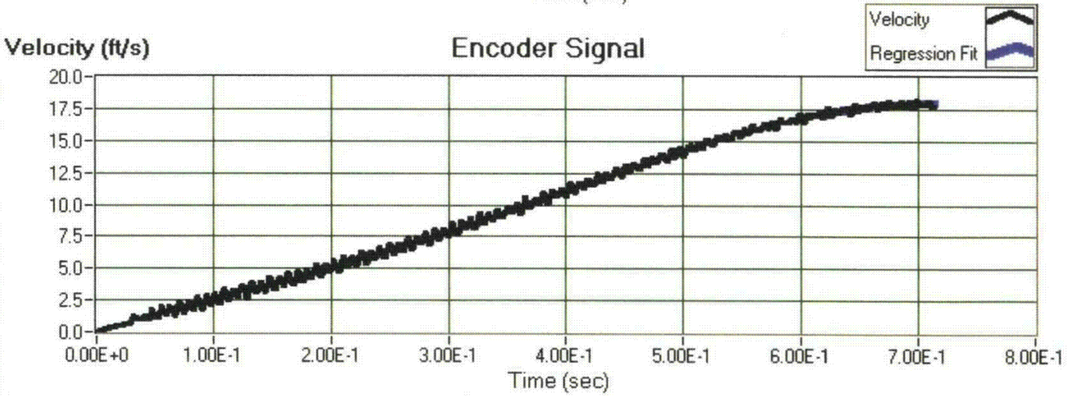

Test Parameters	Value
Group ID	RiverBend-Weld
Date	11/11/2002 10:16
Operator	Dr. Michael P. Manahan, Sr.
Temperature	70.0 °F
Oscilloscope	MPM Internal Oscilloscope
Striker	8mm Metals
Interpolation	Point-Point Linear
Encoder Controller	MPM Encoder System
Velocity Determination	Encoder
Material	Metal
Size	Type A
Orientation	Isotropic
Notch Type	V Notch, no Side-Groove
Units Normalization	None
Energy Adjustment	1.0391
Length	2.1654 in
Width	0.3937 in
Thickness	0.3937 in
Span	1.5748 in
Uncracked Ligament	0.3150 in
Notch Rafius	0.0098 in
Failure Type	complete fracture
Post Test Comments	good test
Impact Velocity	17.949 ft/s
Striker Energy	66.408 ft lbf
Dial Gage Energy	65.500 ft lbf
Encoder Energy	66.408 ft lbf
Latch Angle	134.15°
Final Angle	108.72°
Potential Energy	306.769 ft lbf
Windage & Friction	0.655 ft lbf
Percent Shear	79.31 %
Lateral Expansion	0.0580 in

	Load (lbf)	Displacement (in)	Velocity (ft/s)	Time (s)	Energy (ft lbf)
General Yield	2.8875E+3	1.220E-2	1.790E+1	5.083E-5	1.56675E+0
Peak Load	3.8418E+3	1.218E-1	1.698E+1	5.740E-4	3.35064E+1
Brittle Fracture	3.4761E+3	1.732E-1	1.650E+1	8.300E-4	4.95040E+1
Arrest Load	1.8941E+3	1.827E-1	1.643E+1	8.780E-4	5.16137E+1
End of Signal	8.9658E+0	4.773E-1	1.597E+1	2.404E-3	6.64078E+1

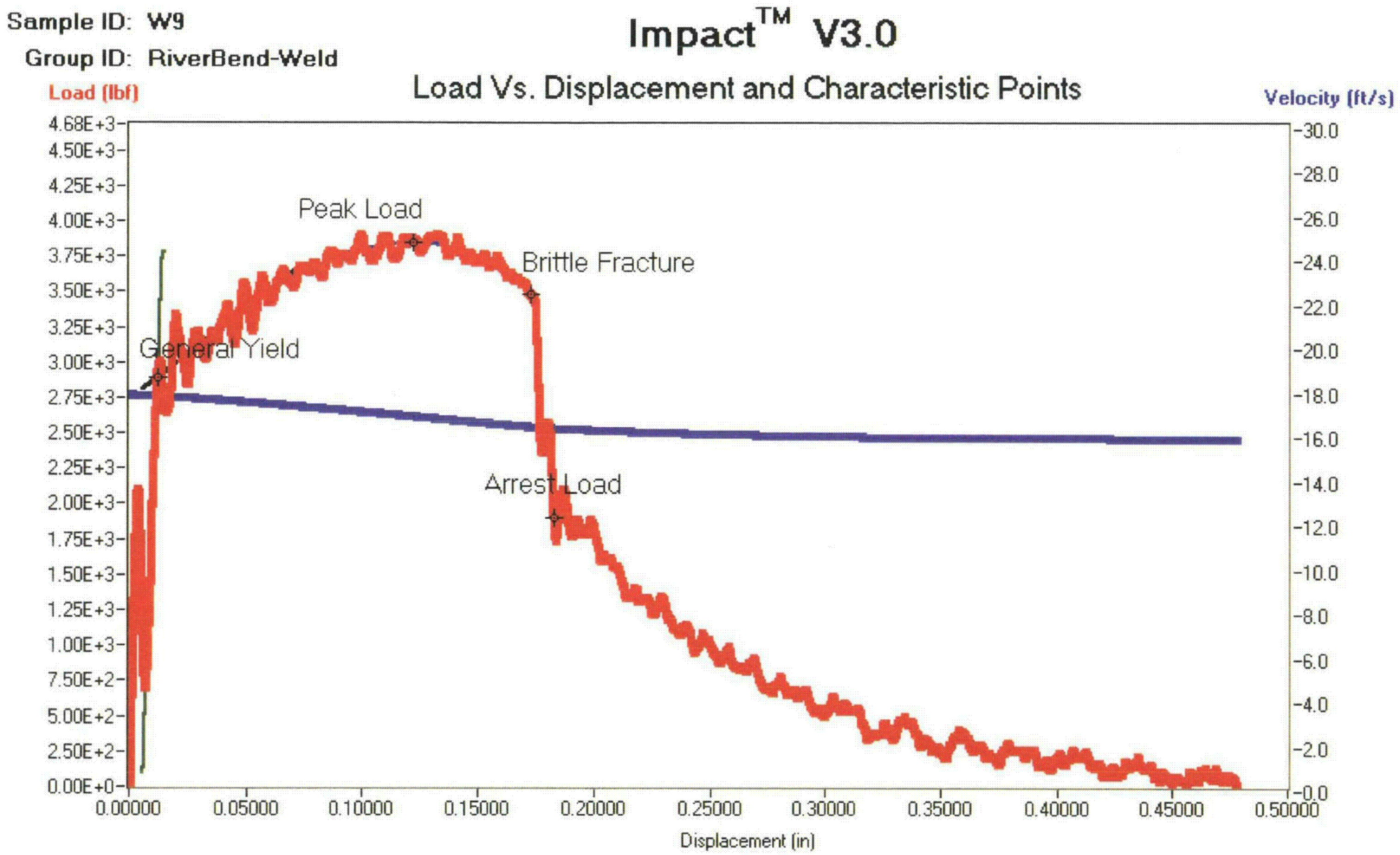

	Load (lbf)	Displacement (in)	Velocity (ft/s)	Time (s)	Energy (ft lbf)
General Yield	2.8875E+3	1.220E-2	1.790E+1	5.083E-5	1.56675E+0
Peak Load	3.8418E+3	1.218E-1	1.698E+1	5.740E-4	3.35064E+1
Brittle Fracture	3.4761E+3	1.732E-1	1.650E+1	8.300E-4	4.95040E+1
Arrest Load	1.8941E+3	1.827E-1	1.643E+1	8.780E-4	5.16137E+1
End of Signal	8.9658E+0	4.773E-1	1.597E+1	2.404E-3	6.64078E+1

Sample ID
W11
Comments
River Bend 183 Degree Surveillance Capsule

Impact™ V3.0
Summary Report

Test Parameters	Value
Group ID	RiverBend-Weld
Date	11/11/2002 11:54
Operator	Dr. Michael P. Manahan, Sr.
Temperature	127.8 °F
Oscilloscope	MPM Internal Oscilloscope
Striker	8mm Metals
Interpolation	Point-Point Linear
Encoder Controller	MPM Encoder System
Velocity Determination	Encoder
Material	Metal
Size	Type A
Orientation	Isotropic
Notch Type	V Notch, no Side-Groove
Units Normalization	None
Energy Adjustment	1.0547
Length	2.1654 in
Width	0.3937 in
Thickness	0.3937 in
Span	1.5748 in
Uncracked Ligament	0.3150 in
Notch Rafius	0.0098 in
Failure Type	complete fracture
Post Test Comments	good test
Impact Velocity	17.952 ft/s
Striker Energy	79.781 ft lbf
Dial Gage Energy	78.800 ft lbf
Encoder Energy	79.781 ft lbf
Latch Angle	134.15°
Final Angle	104.29°
Potential Energy	306.769 ft lbf
Windage & Friction	0.655 ft lbf
Percent Shear	100.00 %
Lateral Expansion	0.0720 in

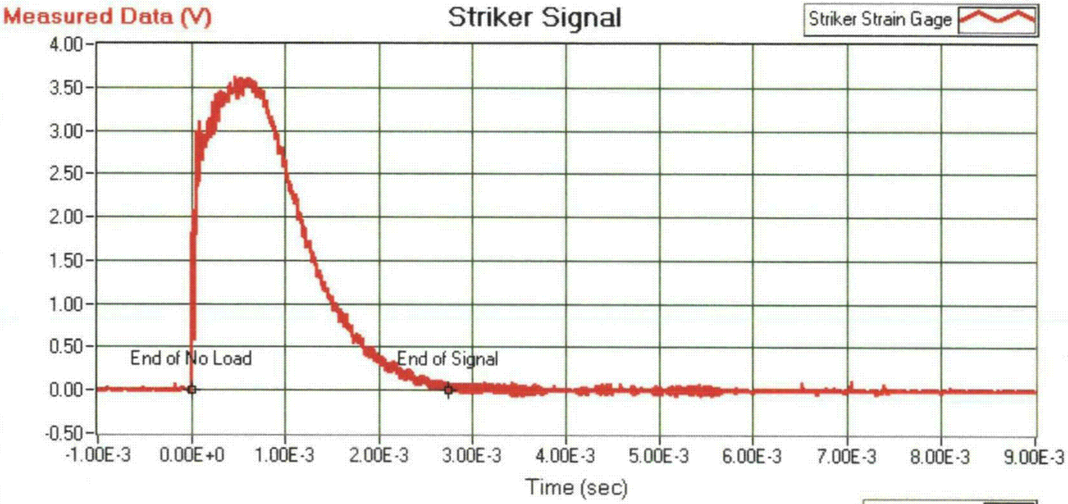

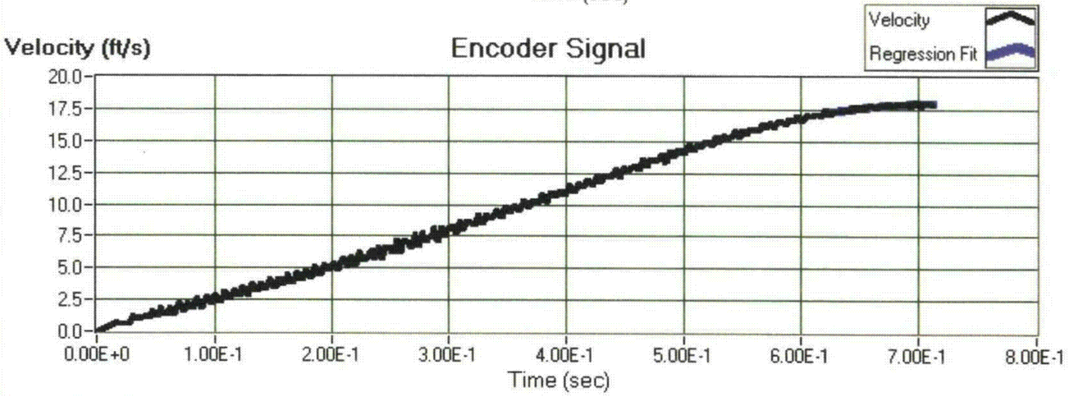

	Load (lbf)	Displacement (in)	Velocity (ft/s)	Time (s)	Energy (ft lbf)
General Yield	2.8396E+3	1.220E-2	1.791E+1	5.083E-5	1.61360E+0
Peak Load	3.7355E+3	1.246E-1	1.699E+1	5.870E-4	3.37092E+1
End of Signal	7.4351E+0	5.356E-1	1.558E+1	2.738E-3	7.97809E+1

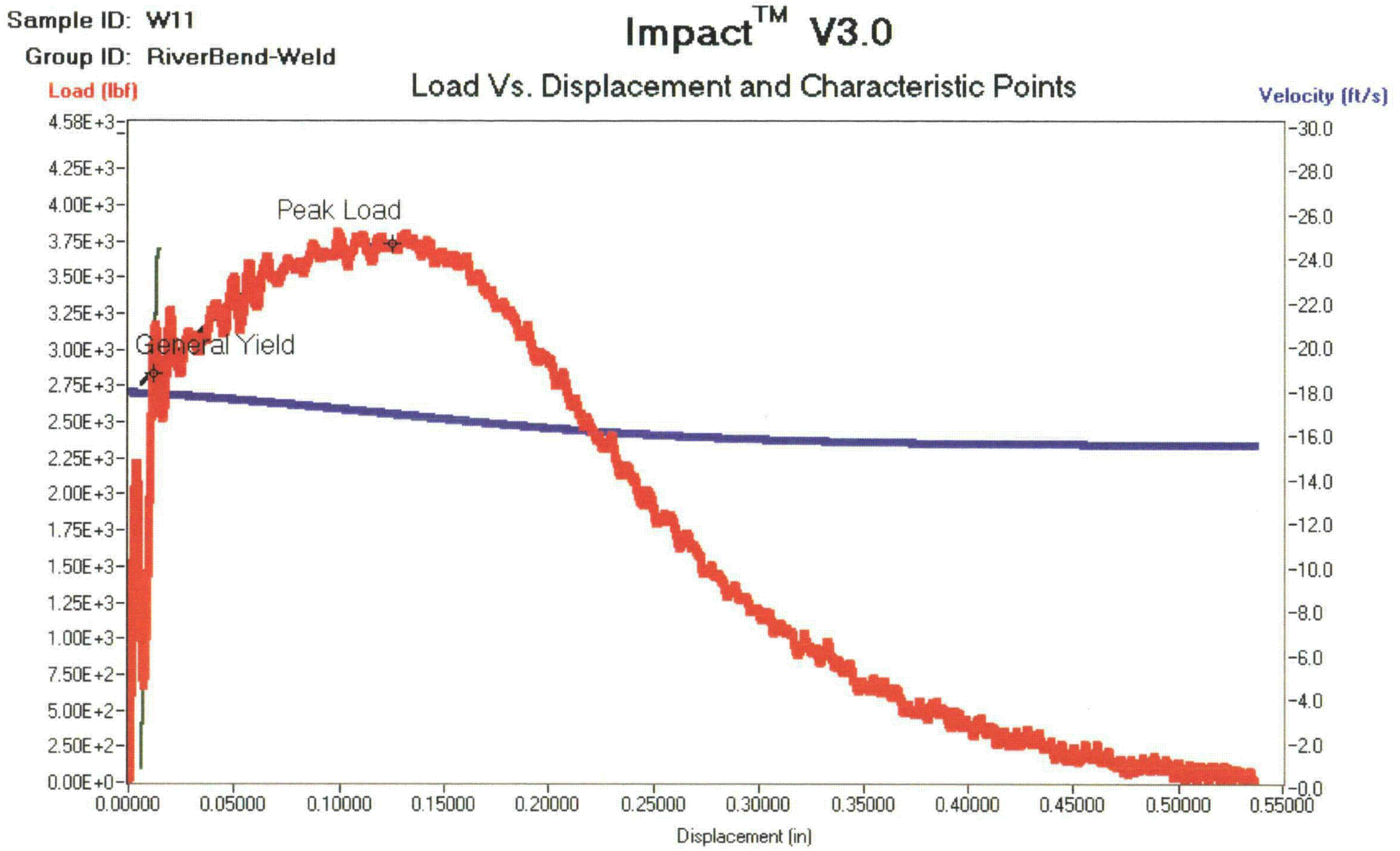

	Load (lbf)	Displacement (in)	Velocity (ft/s)	Time (s)	Energy (ft lbf)
General Yield	2.8396E+3	1.220E-2	1.791E+1	5.083E-5	1.61360E+0
Peak Load	3.7355E+3	1.246E-1	1.699E+1	5.870E-4	3.37092E+1
End of Signal	7.4351E+0	5.356E-1	1.558E+1	2.738E-3	7.97809E+1

Sample ID
W3
Comments
River Bend 183 Degree Surveillance Capsule

Impact™ V3.0
Summary Report

Test Parameters	Value
Group ID	RiverBend-Weld
Date	11/11/2002 12:09
Operator	Dr. Michael P. Manahan, Sr.
Temperature	131.2 °F
Oscilloscope	MPM Internal Oscilloscope
Striker	8mm Metals
Interpolation	Point-Point Linear
Encoder Controller	MPM Encoder System
Velocity Determination	Encoder
Material	Metal
Size	Type A
Orientation	Isotropic
Notch Type	V Notch, no Side-Groove
Units Normalization	None
Energy Adjustment	1.0558
Length	2.1654 in
Width	0.3937 in
Thickness	0.3937 in
Span	1.5748 in
Uncracked Ligament	0.3150 in
Notch Rafius	0.0098 in
Failure Type	complete fracture
Post Test Comments	good test
Impact Velocity	17.949 ft/s
Striker Energy	80.221 ft lbf
Dial Gage Energy	79.000 ft lbf
Encoder Energy	80.221 ft lbf
Latch Angle	134.15°
Final Angle	104.15°
Potential Energy	306.769 ft lbf
Windage & Friction	0.655 ft lbf
Percent Shear	93.31 %
Lateral Expansion	0.0710 in

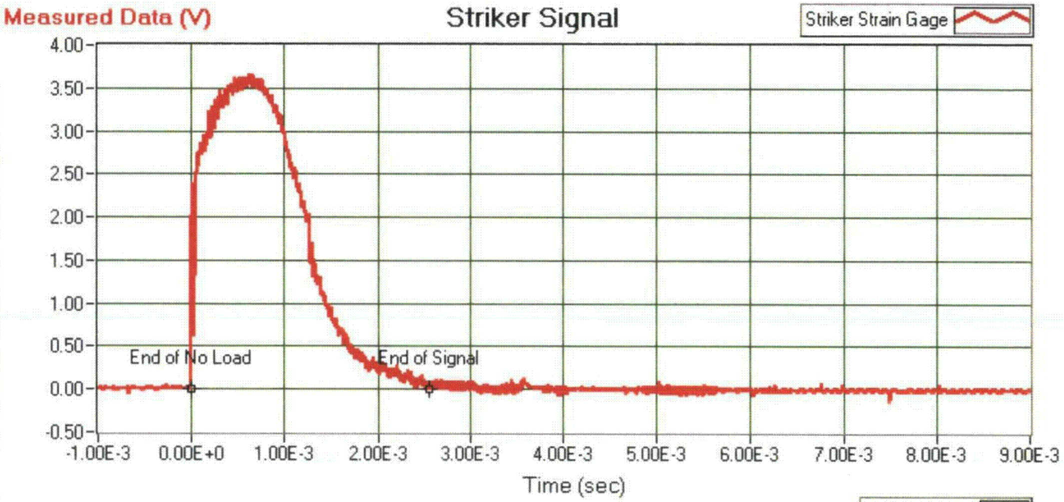

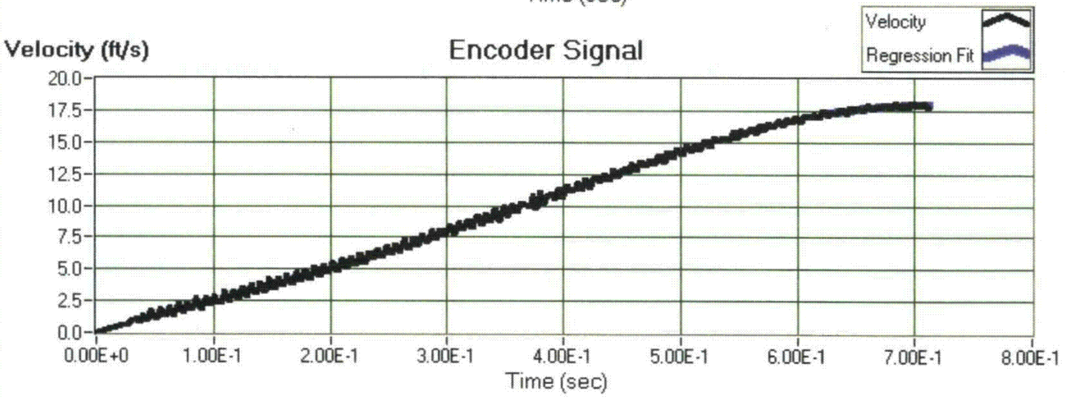

	Load (lbf)	Displacement (in)	Velocity (ft/s)	Time (s)	Energy (ft lbf)
General Yield	2.8306E+3	1.370E-2	1.790E+1	5.683E-5	1.78574E+0
Peak Load	3.7872E+3	1.305E-1	1.694E+1	6.150E-4	3.54886E+1
Brittle Fracture	2.1819E+3	2.572E-1	1.591E+1	1.260E-3	6.92854E+1
Arrest Load	1.6204E+3	2.605E-1	1.590E+1	1.277E-3	6.98113E+1
End of Signal	1.5431E+1	5.006E-1	1.557E+1	2.555E-3	8.02205E+1

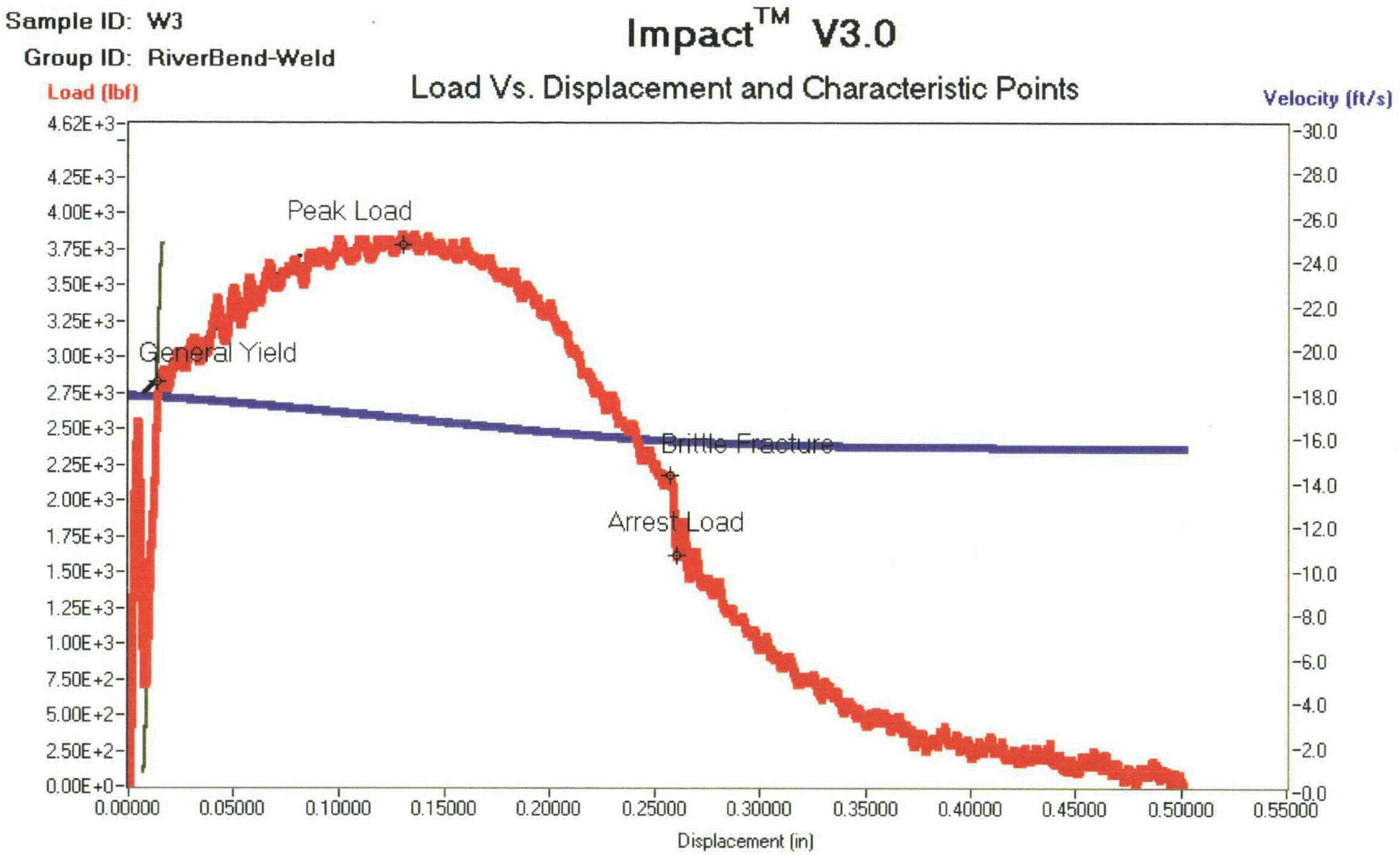

	Load (lbf)	Displacement (in)	Velocity (ft/s)	Time (s)	Energy (ft lbf)
General Yield	2.8306E+3	1.370E-2	1.790E+1	5.683E-5	1.78574E+0
Peak Load	3.7872E+3	1.305E-1	1.694E+1	6.150E-4	3.54886E+1
Brittle Fracture	2.1819E+3	2.572E-1	1.591E+1	1.260E-3	6.92854E+1
Arrest Load	1.6204E+3	2.605E-1	1.590E+1	1.277E-3	6.98113E+1
End of Signal	1.5431E+1	5.006E-1	1.557E+1	2.555E-3	8.02205E+1

Sample ID

W12

Comments

River Bend 183 Degree Surveillance Capsule

Impact™ V3.0

Summary Report

Test Parameters	Value
Group ID	RiverBend-Weld
Date	11/11/2002 12:44
Operator	Dr. Michael P. Manahan, Sr.
Temperature	159.3 °F
Oscilloscope	MPM Internal Oscilloscope
Striker	8mm Metals
Interpolation	Point-Point Linear
Encoder Controller	MPM Encoder System
Velocity Determination	Encoder
Material	Metal
Size	Type A
Orientation	Isotropic
Notch Type	V Notch, no Side-Groove
Units Normalization	None
Energy Adjustment	1.0483
Length	2.1654 in
Width	0.3937 in
Thickness	0.3937 in
Span	1.5748 in
Uncracked Ligament	0.3150 in
Notch Rafius	0.0098 in
Failure Type	complete fracture
Post Test Comments	good test
Impact Velocity	17.948 ft/s
Striker Energy	77.203 ft lbf
Dial Gage Energy	76.100 ft lbf
Encoder Energy	77.203 ft lbf
Latch Angle	134.15°
Final Angle	105.14°
Potential Energy	306.769 ft lbf
Windage & Friction	0.655 ft lbf
Percent Shear	97.12 %
Lateral Expansion	0.0655 in

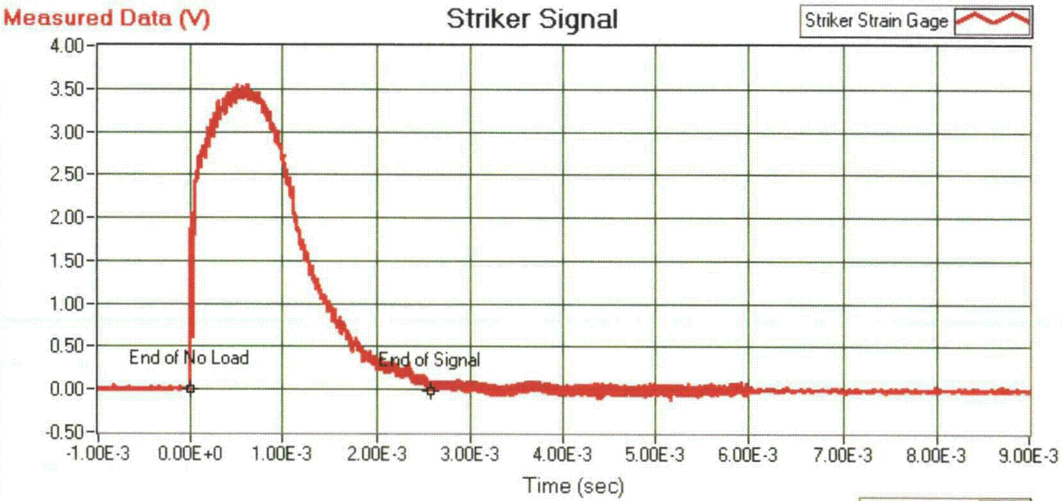

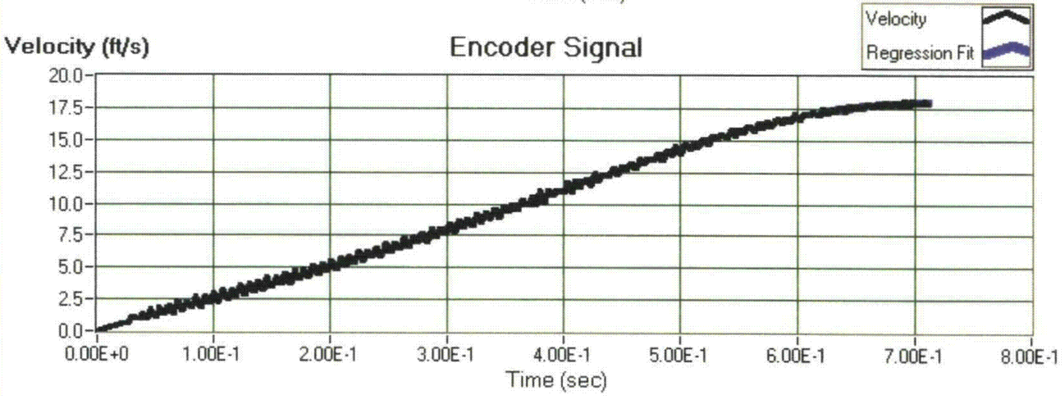

	Load (lbf)	Displacement (in)	Velocity (ft/s)	Time (s)	Energy (ft lbf)
General Yield	2.6662E+3	1.220E-2	1.790E+1	5.083E-5	1.55411E+0
Peak Load	3.6306E+3	1.232E-1	1.703E+1	5.800E-4	3.20465E+1
Brittle Fracture	2.4591E+3	2.294E-1	1.617E+1	1.114E-3	6.06504E+1
Arrest Load	2.1506E+3	2.319E-1	1.615E+1	1.127E-3	6.11251E+1
End of Signal	1.8165E+1	5.061E-1	1.564E+1	2.574E-3	7.72030E+1

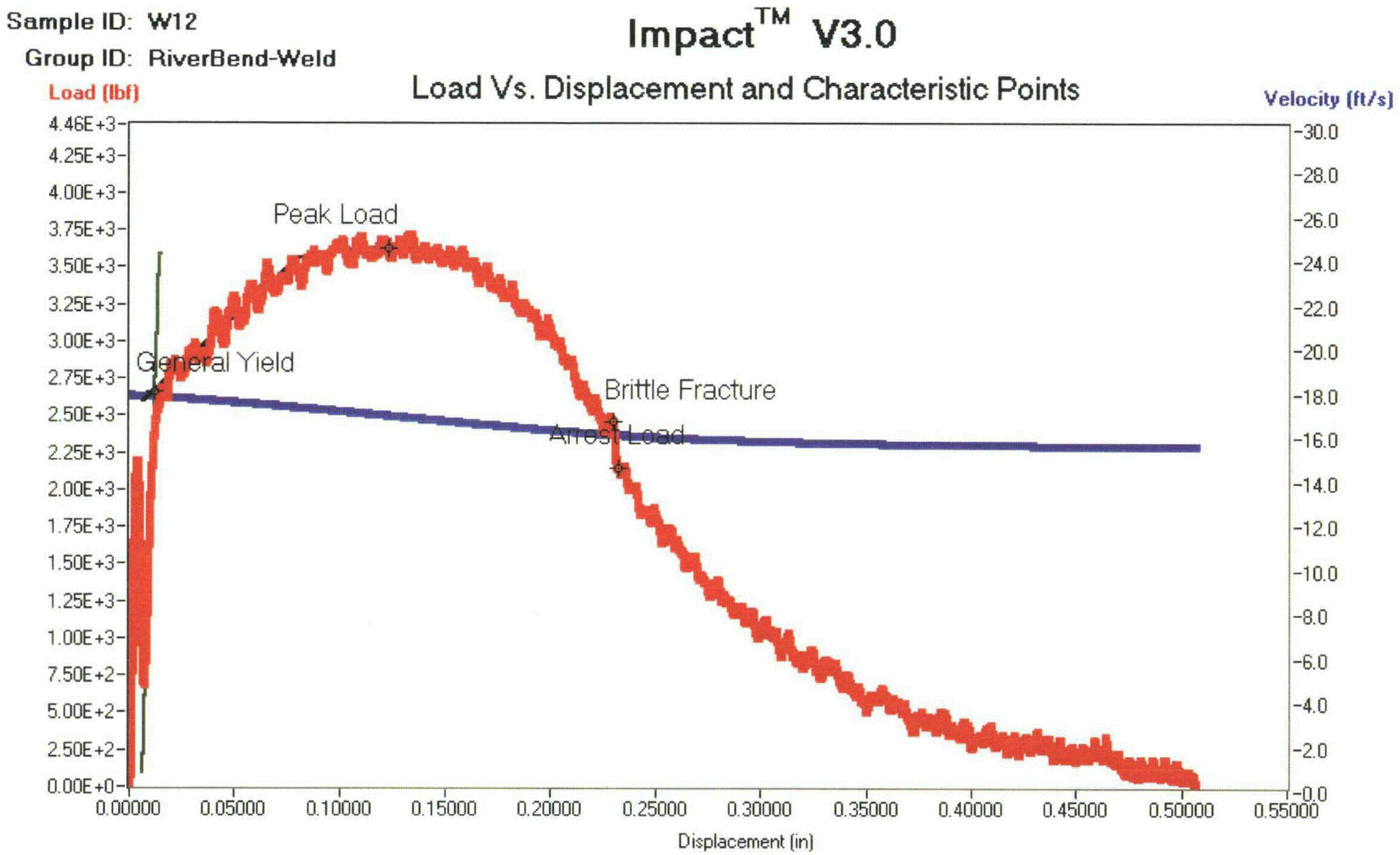

	Load (lbf)	Displacement (in)	Velocity (ft/s)	Time (s)	Energy (ft lbf)
General Yield	2.6662E+3	1.220E-2	1.790E+1	5.083E-5	1.55411E+0
Peak Load	3.6306E+3	1.232E-1	1.703E+1	5.800E-4	3.20465E+1
Brittle Fracture	2.4591E+3	2.294E-1	1.617E+1	1.114E-3	6.06504E+1
Arrest Load	2.1506E+3	2.319E-1	1.615E+1	1.127E-3	6.11251E+1
End of Signal	1.8165E+1	5.061E-1	1.564E+1	2.574E-3	7.72030E+1

Sample ID

W7

Comments

River Bend 183 Degree Surveillance Capsule

Impact™ V3.0

Summary Report

Test Parameters	Value
Group ID	RiverBend-Weld
Date	11/11/2002 12:26
Operator	Dr. Michael P. Manahan, Sr.
Temperature	199.8 °F
Oscilloscope	MPM Internal Oscilloscope
Striker	8mm Metals
Interpolation	Point-Point Linear
Encoder Controller	MPM Encoder System
Velocity Determination	Encoder
Material	Metal
Size	Type A
Orientation	Isotropic
Notch Type	V Notch, no Side-Groove
Units Normalization	None
Energy Adjustment	1.0471
Length	2.1654 in
Width	0.3937 in
Thickness	0.3937 in
Span	1.5748 in
Uncracked Ligament	0.3150 in
Notch Rafius	0.0098 in
Failure Type	complete fracture
Post Test Comments	good test
Impact Velocity	17.957 ft/s
Striker Energy	96.330 ft lbf
Dial Gage Energy	95.000 ft lbf
Encoder Energy	96.330 ft lbf
Latch Angle	134.15°
Final Angle	98.93°
Potential Energy	306.769 ft lbf
Windage & Friction	0.655 ft lbf
Percent Shear	100.00 %
Lateral Expansion	0.0780 in

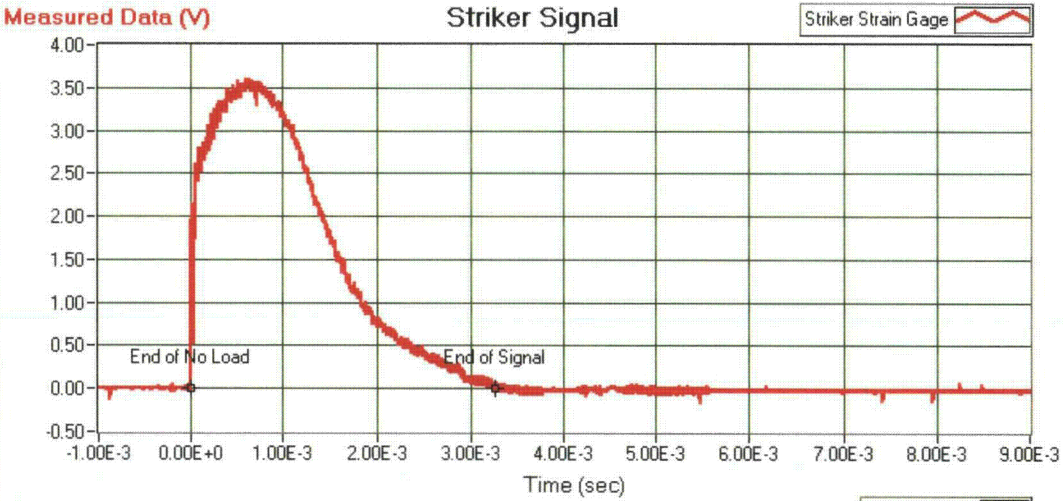

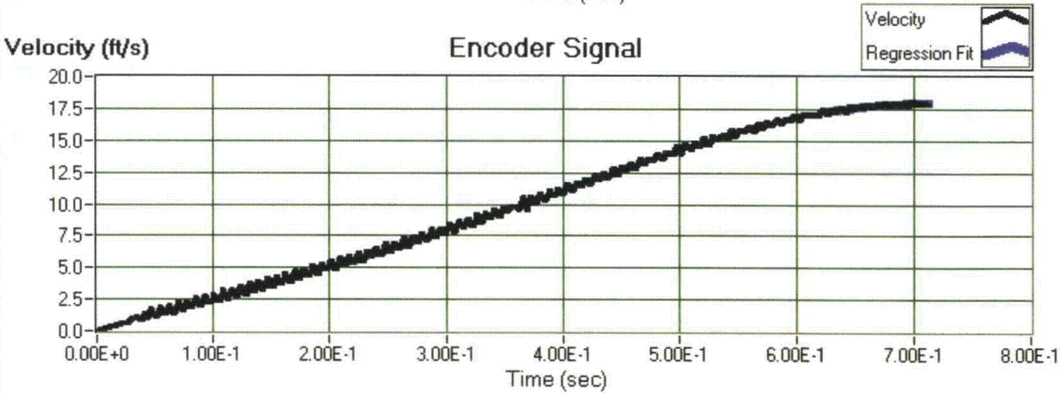

	Load (lbf)	Displacement (in)	Velocity (ft/s)	Time (s)	Energy (ft lbf)
General Yield	2.6792E+3	1.307E-2	1.791E+1	4.983E-5	1.54219E+0
Peak Load	3.6963E+3	1.386E-1	1.691E+1	6.500E-4	3.65400E+1
End of Signal	1.5420E+1	6.249E-1	1.503E+1	3.261E-3	9.63297E+1

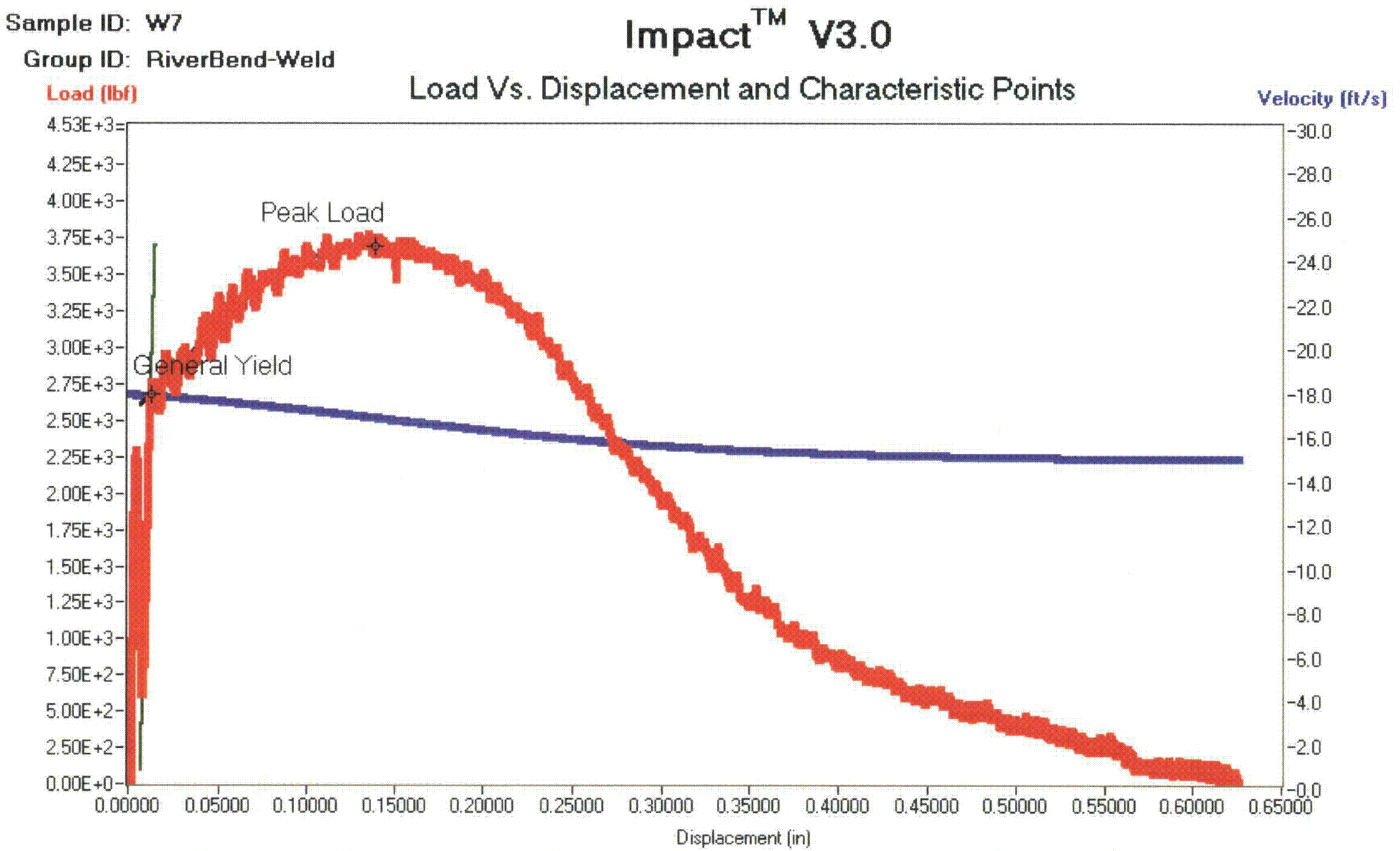

	Load (lbf)	Displacement (in)	Velocity (ft/s)	Time (s)	Energy (ft lbf)
General Yield	2.6792E+3	1.307E-2	1.791E+1	4.983E-5	1.54219E+0
Peak Load	3.6963E+3	1.386E-1	1.691E+1	6.500E-4	3.65400E+1
End of Signal	1.5420E+1	6.249E-1	1.503E+1	3.261E-3	9.63297E+1

Appendix A-3 HAZ Data

Sample ID

H12

Comments

River Bend 183 Degree Surveillance Capsule

Impact™ V3.0

Summary Report

Test Parameters	Value
Group ID	RiverBend-HAZ
Date	11/12/2002 10:42
Operator	Dr. Michael P. Manahan, Sr.
Temperature	-102.6 °F
Oscilloscope	MPM Internal Oscilloscope
Striker	8mm Metals
Interpolation	Point-Point Linear
Encoder Controller	MPM Encoder System
Velocity Determination	Encoder
Material	Metal
Size	Type A
Orientation	Other
Notch Type	V Notch, no Side-Groove
Units Normalization	None
Energy Adjustment	1.1736
Length	2.1654 in
Width	0.3937 in
Thickness	0.3937 in
Span	1.5748 in
Uncracked Ligament	0.3150 in
Notch Rafius	0.0098 in
Failure Type	complete fracture
Post Test Comments	good test
Impact Velocity	17.932 ft/s
Striker Energy	11.529 ft lbf
Dial Gage Energy	11.200 ft lbf
Encoder Energy	11.529 ft lbf
Latch Angle	134.14°
Final Angle	128.68°
Potential Energy	306.728 ft lbf
Windage & Friction	0.635 ft lbf
Percent Shear	13.01 %
Lateral Expansion	0.0070 in

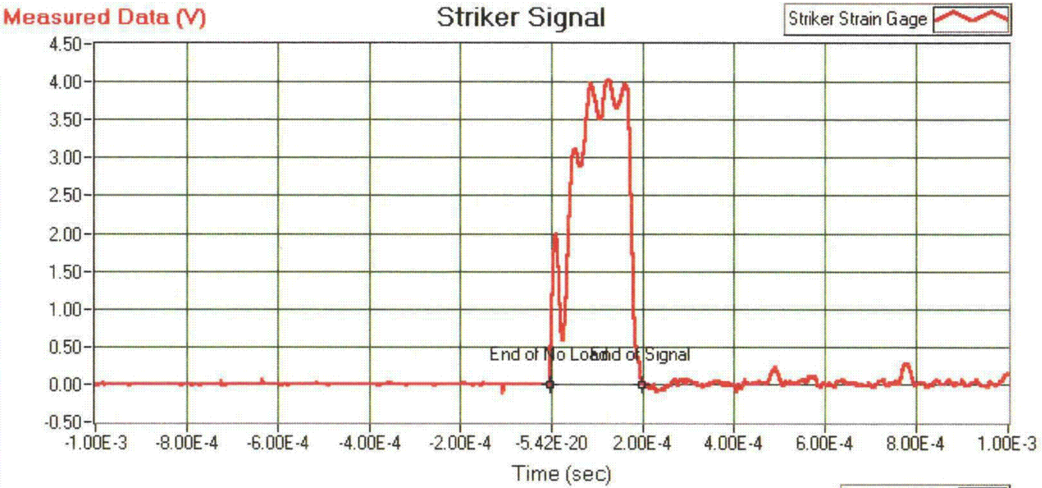

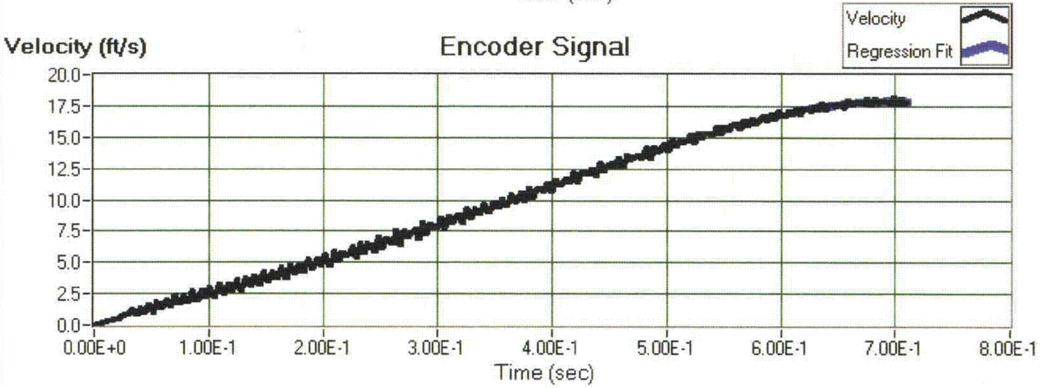

	Load (lbf)	Displacement (in)	Velocity (ft/s)	Time (s)	Energy (ft lbf)
Peak Load	4.6510E+3	3.567E-2	1.767E+1	1.610E-4	1.02568E+1
Brittle Fracture	4.5701E+3	3.697E-2	1.766E+1	1.670E-4	1.07459E+1
End of Signal	1.8259E+1	4.307E-2	1.764E+1	1.960E-4	1.15290E+1

Sample ID: H12

Group ID: RiverBend-HAZ

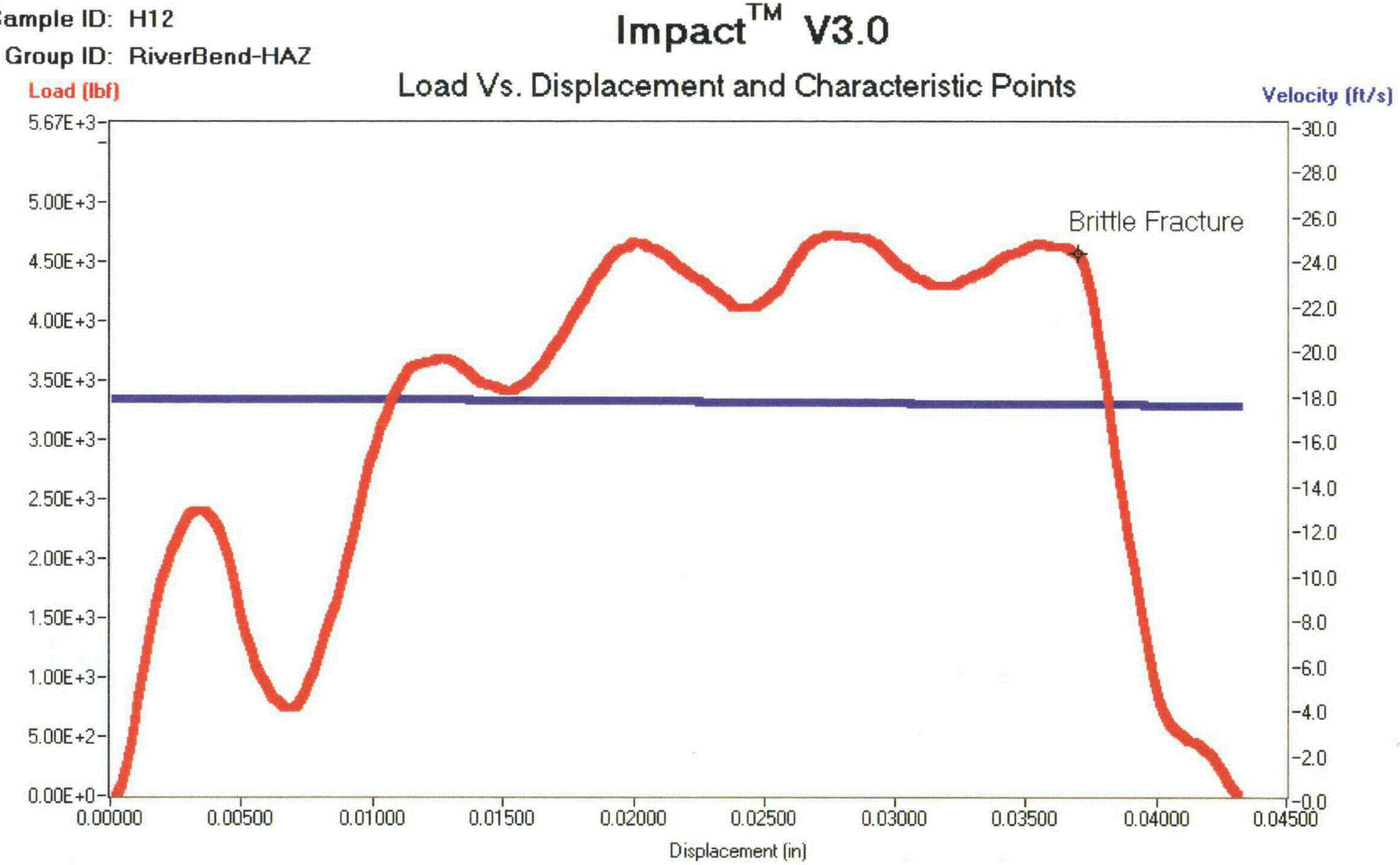

	Load (lbf)	Displacement (in)	Velocity (ft/s)	Time (s)	Energy (ft lbf)
Peak Load	4.6510E+3	3.567E-2	1.767E+1	1.610E-4	1.02568E+1
Brittle Fracture	4.5701E+3	3.697E-2	1.766E+1	1.670E-4	1.07459E+1
End of Signal	1.8259E+1	4.307E-2	1.764E+1	1.960E-4	1.15290E+1

Sample ID

H4

Comments

River Bend 183 Degree Surveillance Capsule

Impact™ V3.0

Summary Report

Test Parameters	Value
Group ID	RiverBend-HAZ
Date	11/12/2002 10:20
Operator	Dr. Michael P. Manahan, Sr.
Temperature	-102.5 °F
Oscilloscope	MPM Internal Oscilloscope
Striker	8mm Metals
Interpolation	Point-Point Linear
Encoder Controller	MPM Encoder System
Velocity Determination	Encoder
Material	Metal
Size	Type A
Orientation	Other
Notch Type	V Notch, no Side-Groove
Units Normalization	None
Energy Adjustment	1.0629
Length	2.1654 in
Width	0.3937 in
Thickness	0.3937 in
Span	1.5748 in
Uncracked Ligament	0.3150 in
Notch Rafius	0.0098 in
Failure Type	complete fracture
Post Test Comments	good test
Impact Velocity	17.931 ft/s
Striker Energy	17.375 ft lbf
Dial Gage Energy	17.000 ft lbf
Encoder Energy	17.375 ft lbf
Latch Angle	134.14°
Final Angle	126.34°
Potential Energy	306.728 ft lbf
Windage & Friction	0.635 ft lbf
Percent Shear	13.01 %
Lateral Expansion	0.0110 in

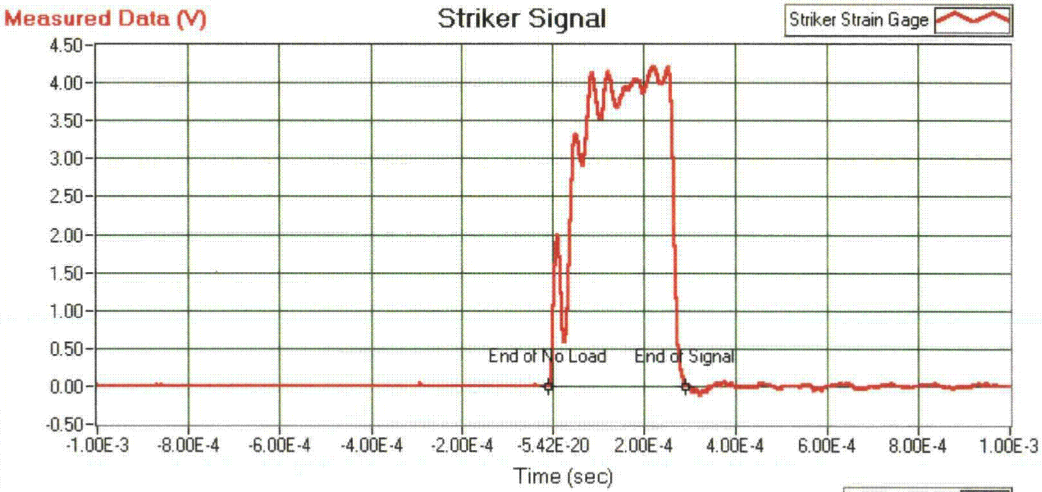

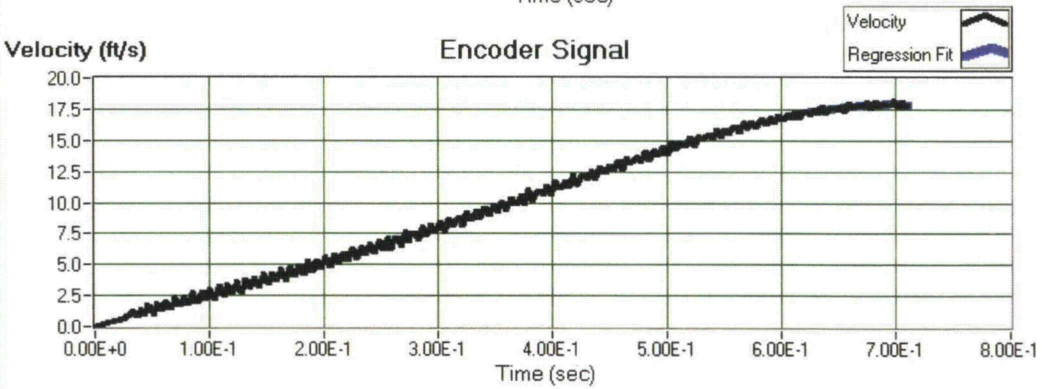

	Load (lbf)	Displacement (in)	Velocity (ft/s)	Time (s)	Energy (ft lbf)
Peak Load	4.4601E+3	5.614E-2	1.748E+1	2.530E-4	1.63340E+1
Brittle Fracture	4.3445E+3	5.701E-2	1.747E+1	2.570E-4	1.66423E+1
End of Signal	7.7733E+0	6.323E-2	1.745E+1	2.870E-4	1.73751E+1

Sample ID: H4

Group ID: RiverBend-HAZ

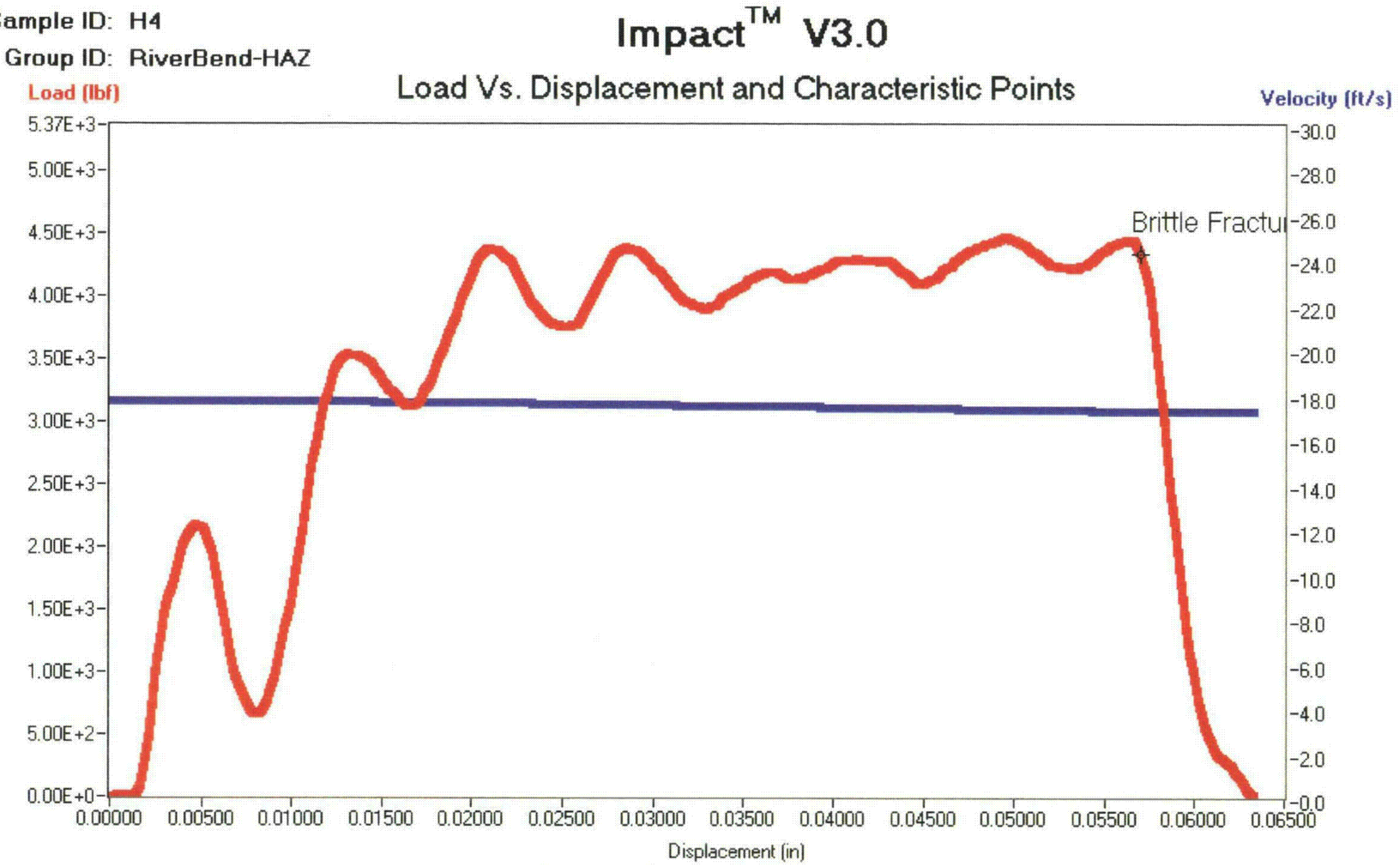

	Load (lbf)	Displacement (in)	Velocity (ft/s)	Time (s)	Energy (ft lbf)
Peak Load	4.4601E+3	5.614E-2	1.748E+1	2.530E-4	1.63340E+1
Brittle Fracture	4.3445E+3	5.701E-2	1.747E+1	2.570E-4	1.66423E+1
End of Signal	7.7733E+0	6.323E-2	1.745E+1	2.870E-4	1.73751E+1

Sample ID

h8

Comments

River Bend 183 Degree Surveillance Capsule

Impact™ V3.0

Summary Report

Test Parameters	Value
Group ID	RiverBend-HAZ
Date	11/11/2002 18:30
Operator	Dr. Michael P. Manahan, Sr.
Temperature	-63.2 °F
Oscilloscope	MPM Internal Oscilloscope
Striker	8mm Metals
Interpolation	Point-Point Linear
Encoder Controller	MPM Encoder System
Velocity Determination	Encoder
Material	Metal
Size	Type A
Orientation	Other
Notch Type	V Notch, no Side-Groove
Units Normalization	None
Energy Adjustment	1.1026
Length	2.1654 in
Width	0.3937 in
Thickness	0.3937 in
Span	1.5748 in
Uncracked Ligament	0.3150 in
Notch Rafius	0.0098 in
Failure Type	complete fracture
Post Test Comments	good test
Impact Velocity	17.944 ft/s
Striker Energy	18.657 ft lbf
Dial Gage Energy	18.400 ft lbf
Encoder Energy	18.657 ft lbf
Latch Angle	134.15°
Final Angle	125.84°
Potential Energy	306.769 ft lbf
Windage & Friction	0.655 ft lbf
Percent Shear	17.02 %
Lateral Expansion	0.0120 in

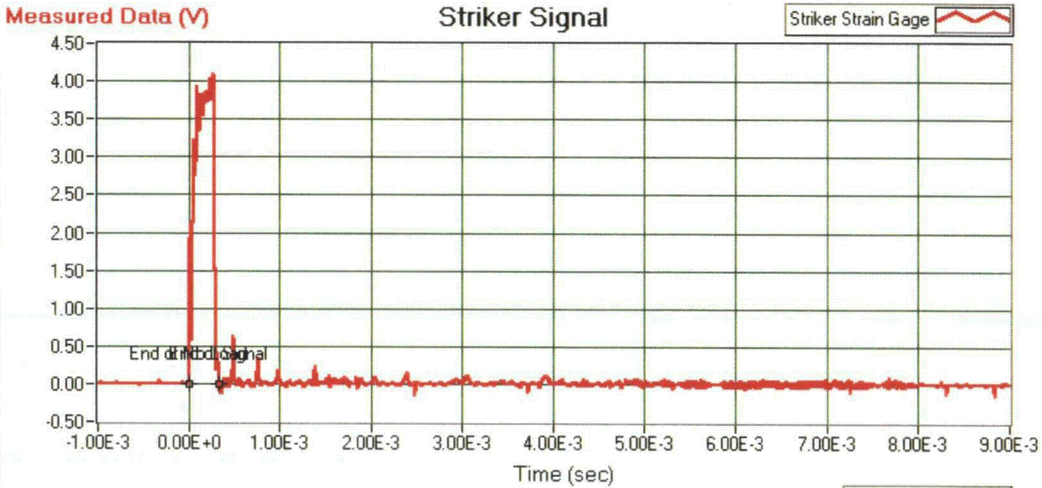

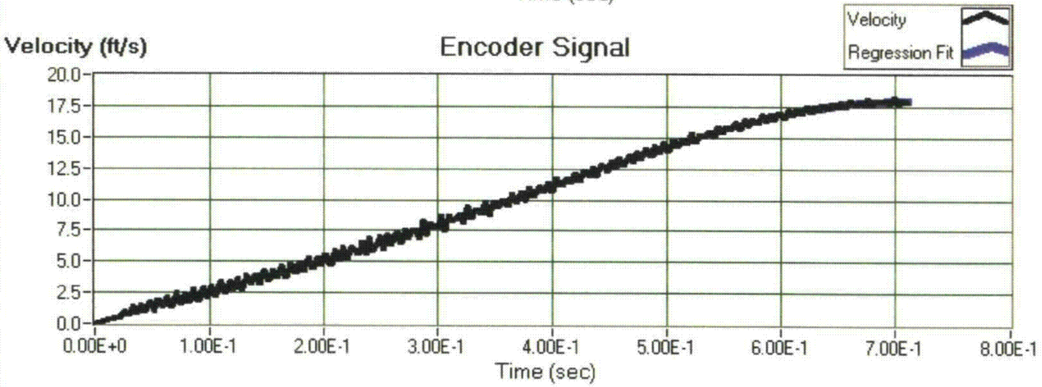

	Load (lbf)	Displacement (in)	Velocity (ft/s)	Time (s)	Energy (ft lbf)
Peak Load	4.4913E+3	5.705E-2	1.781E+1	2.590E-4	1.68865E+1
Brittle Fracture	4.1704E+3	5.961E-2	1.780E+1	2.710E-4	1.78181E+1
End of Signal	1.9687E+1	7.134E-2	1.779E+1	3.260E-4	1.86568E+1

Sample ID: h8

Group ID: RiverBend-HAZ

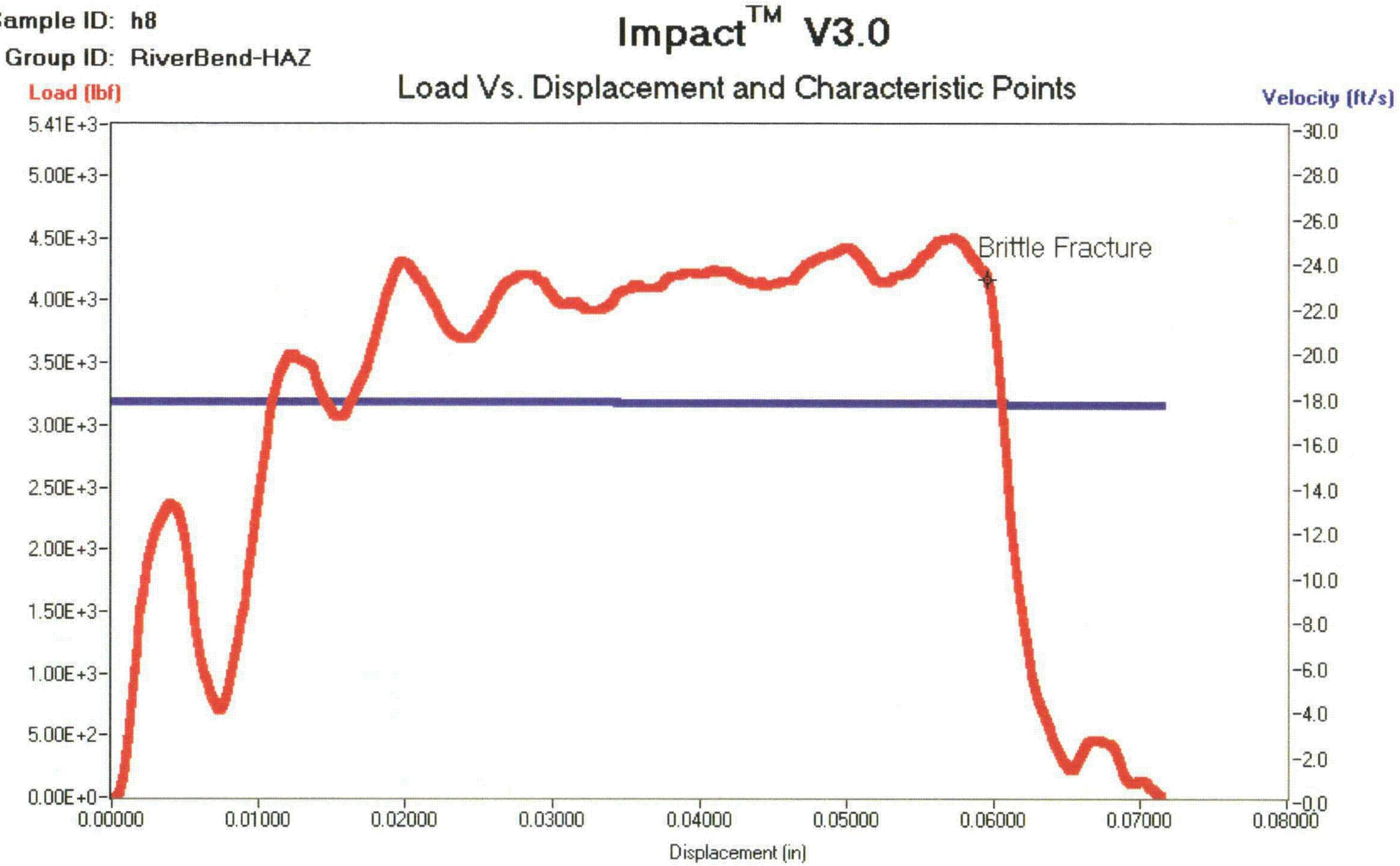

	Load (lbf)	Displacement (in)	Velocity (ft/s)	Time (s)	Energy (ft lbf)
Peak Load	4.4913E+3	5.705E-2	1.781E+1	2.590E-4	1.68865E+1
Brittle Fracture	4.1704E+3	5.961E-2	1.780E+1	2.710E-4	1.78181E+1
End of Signal	1.9687E+1	7.134E-2	1.779E+1	3.260E-4	1.86568E+1

Sample ID

H1

Comments

River Bend 183 Degree Surveillance Capsule

Impact™ V3.0

Summary Report

Test Parameters	Value
Group ID	RiverBend-HAZ
Date	11/11/2002 18:12
Operator	Dr. Michael P. Manahan, Sr.
Temperature	-61.4 °F
Oscilloscope	MPM Internal Oscilloscope
Striker	8mm Metals
Interpolation	Point-Point Linear
Encoder Controller	MPM Encoder System
Velocity Determination	Encoder
Material	Metal
Size	Type A
Orientation	Other
Notch Type	V Notch, no Side-Groove
Units Normalization	None
Energy Adjustment	1.1578
Length	2.1654 in
Width	0.3937 in
Thickness	0.3937 in
Span	1.5748 in
Uncracked Ligament	0.3150 in
Notch Rafius	0.0098 in
Failure Type	complete fracture
Post Test Comments	good test
Impact Velocity	17.957 ft/s
Striker Energy	27.669 ft lbf
Dial Gage Energy	27.500 ft lbf
Encoder Energy	27.669 ft lbf
Latch Angle	134.15°
Final Angle	122.38°
Potential Energy	306.769 ft lbf
Windage & Friction	0.655 ft lbf
Percent Shear	20.36 %
Lateral Expansion	0.0190 in

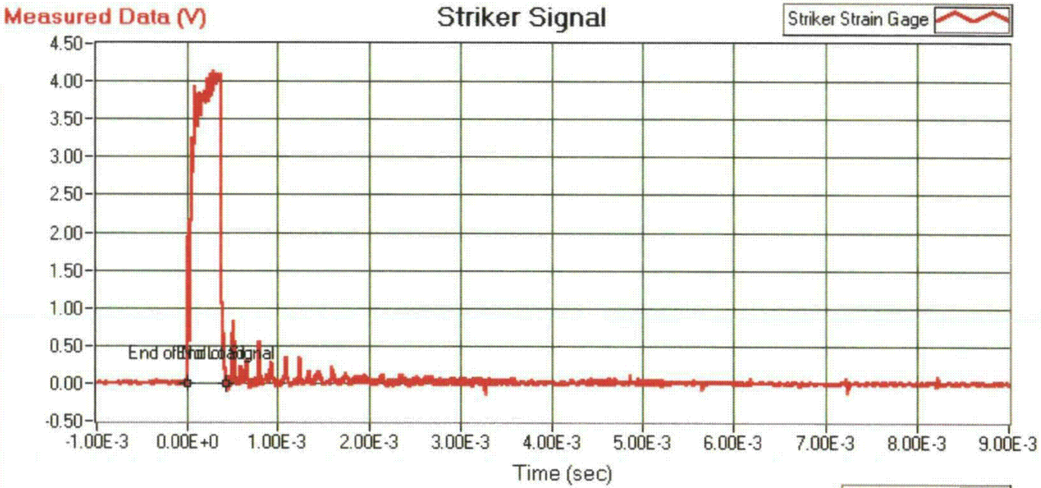

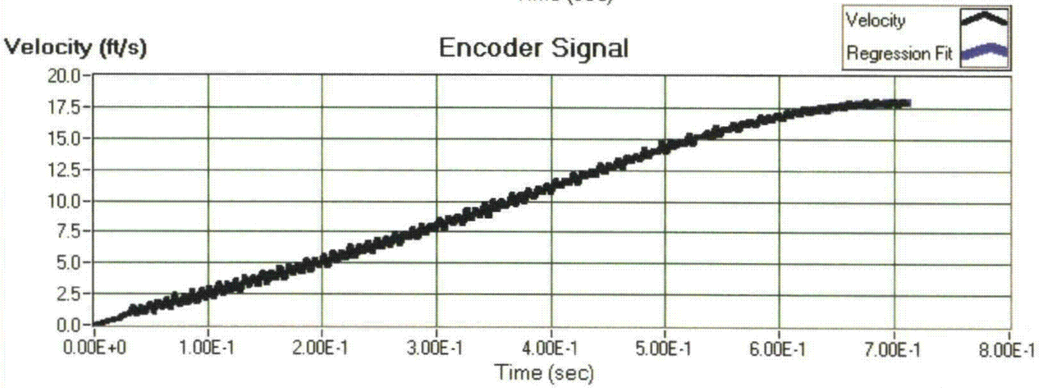

	Load (lbf)	Displacement (in)	Velocity (ft/s)	Time (s)	Energy (ft lbf)
General Yield	3.9910E+3	1.500E-2	1.789E+1	5.983E-5	2.54822E+0
Peak Load	4.6915E+3	8.024E-2	1.727E+1	3.690E-4	2.65517E+1
Brittle Fracture	4.4975E+3	8.047E-2	1.727E+1	3.700E-4	2.66294E+1
Arrest Load	8.5927E+1	9.142E-2	1.724E+1	4.230E-4	2.76674E+1
End of Signal	5.2400E+0	9.201E-2	1.724E+1	4.260E-4	2.76687E+1

Sample ID: H1
Group ID: RiverBend-HAZ

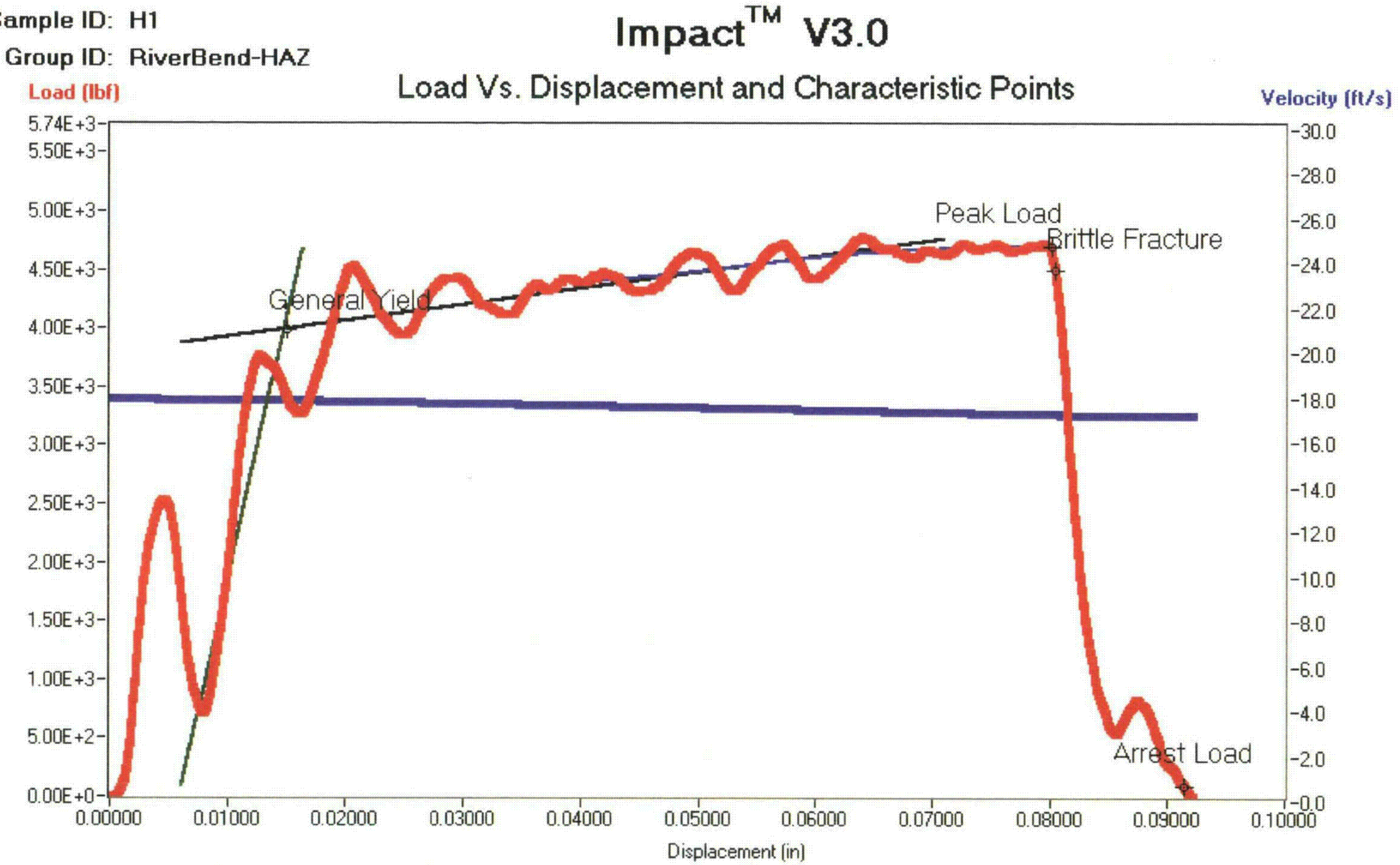

	Load (lbf)	Displacement (in)	Velocity (ft/s)	Time (s)	Energy (ft lbf)
General Yield	3.9910E+3	1.500E-2	1.789E+1	5.983E-5	2.54822E+0
Peak Load	4.6915E+3	8.024E-2	1.727E+1	3.690E-4	2.65517E+1
Brittle Fracture	4.4975E+3	8.047E-2	1.727E+1	3.700E-4	2.66294E+1
Arrest Load	8.5927E+1	9.142E-2	1.724E+1	4.230E-4	2.76674E+1
End of Signal	5.2400E+0	9.201E-2	1.724E+1	4.260E-4	2.76687E+1

Sample ID

H2

Comments

River Bend 183 Degree Surveillance Capsule

Impact™ V3.0

Summary Report

Test Parameters	Value
Group ID	RiverBend-HAZ
Date	11/12/2002 09:58
Operator	Dr. Michael P. Manahan, Sr.
Temperature	-36.6 °F
Oscilloscope	MPM Internal Oscilloscope
Striker	8mm Metals
Interpolation	Point-Point Linear
Encoder Controller	MPM Encoder System
Velocity Determination	Encoder
Material	Metal
Size	Type A
Orientation	Other
Notch Type	V Notch, no Side-Groove
Units Normalization	None
Energy Adjustment	1.0762
Length	2.1654 in
Width	0.3937 in
Thickness	0.3937 in
Span	1.5748 in
Uncracked Ligament	0.3150 in
Notch Rafius	0.0098 in
Failure Type	incomplete fracture
Post Test Comments	good test
Impact Velocity	17.932 ft/s
Striker Energy	35.155 ft lbf
Dial Gage Energy	35.000 ft lbf
Encoder Energy	35.155 ft lbf
Latch Angle	134.14°
Final Angle	119.61°
Potential Energy	306.728 ft lbf
Windage & Friction	0.635 ft lbf
Percent Shear	38.16 %
Lateral Expansion	0.0280 in

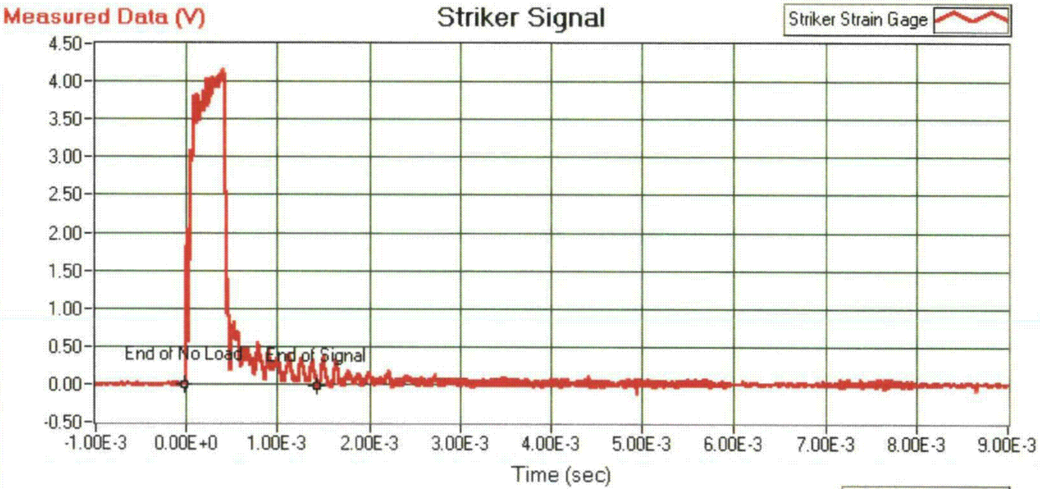

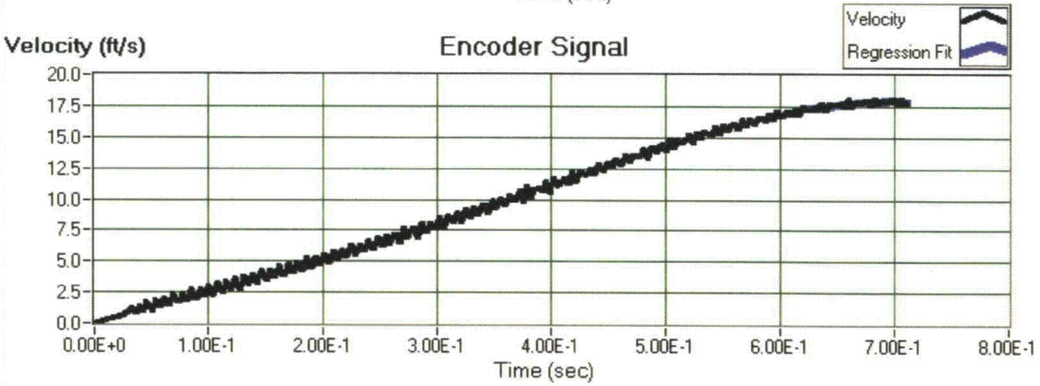

	Load (lbf)	Displacement (in)	Velocity (ft/s)	Time (s)	Energy (ft lbf)
General Yield	3.7281E+3	1.606E-2	1.787E+1	5.983E-5	2.11977E+0
Peak Load	4.4213E+3	8.972E-2	1.717E+1	4.100E-4	2.72473E+1
Brittle Fracture	4.3983E+3	9.283E-2	1.714E+1	4.250E-4	2.83783E+1
Arrest Load	5.7251E+2	1.033E-1	1.710E+1	4.760E-4	2.99221E+1
End of Signal	7.3153E+0	2.967E-1	1.695E+1	1.424E-3	3.51552E+1

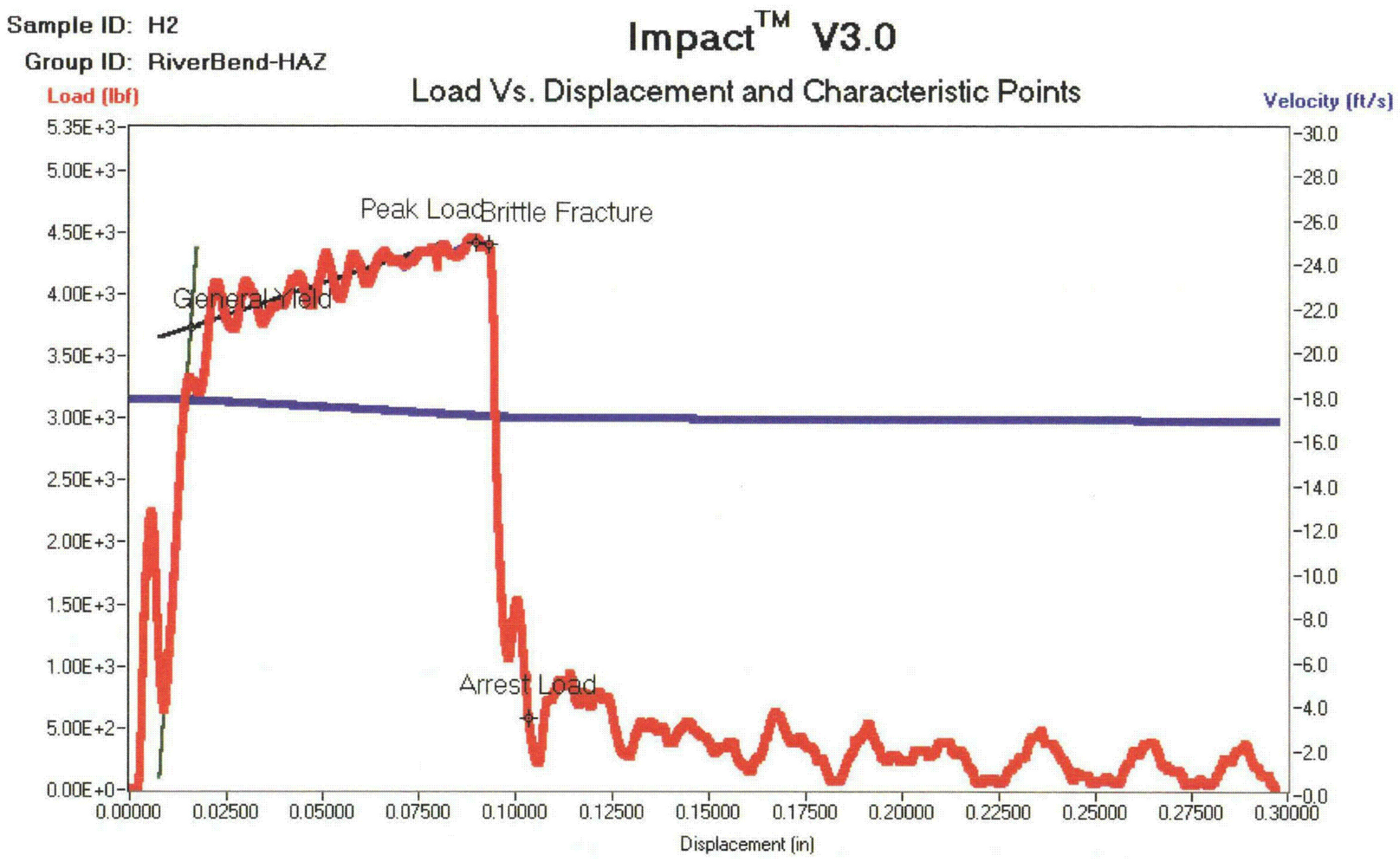

	Load (lbf)	Displacement (in)	Velocity (ft/s)	Time (s)	Energy (ft lbf)
General Yield	3.7281E+3	1.606E-2	1.787E+1	5.983E-5	2.11977E+0
Peak Load	4.4213E+3	8.972E-2	1.717E+1	4.100E-4	2.72473E+1
Brittle Fracture	4.3983E+3	9.283E-2	1.714E+1	4.250E-4	2.83783E+1
Arrest Load	5.7251E+2	1.033E-1	1.710E+1	4.760E-4	2.99221E+1
End of Signal	7.3153E+0	2.967E-1	1.695E+1	1.424E-3	3.51552E+1

Sample ID

H11

Comments

River Bend 183 Degree Surveillance Capsule

Impact™ V3.0

Summary Report

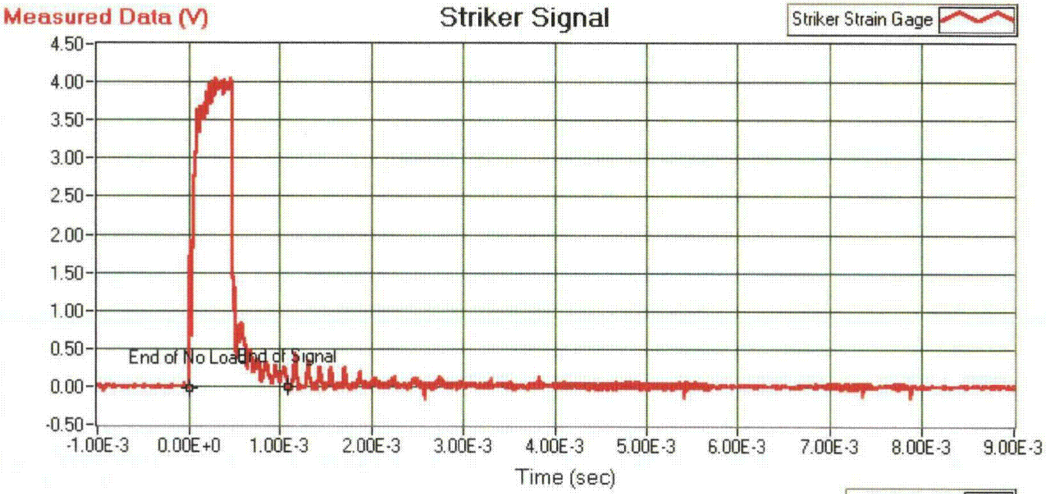

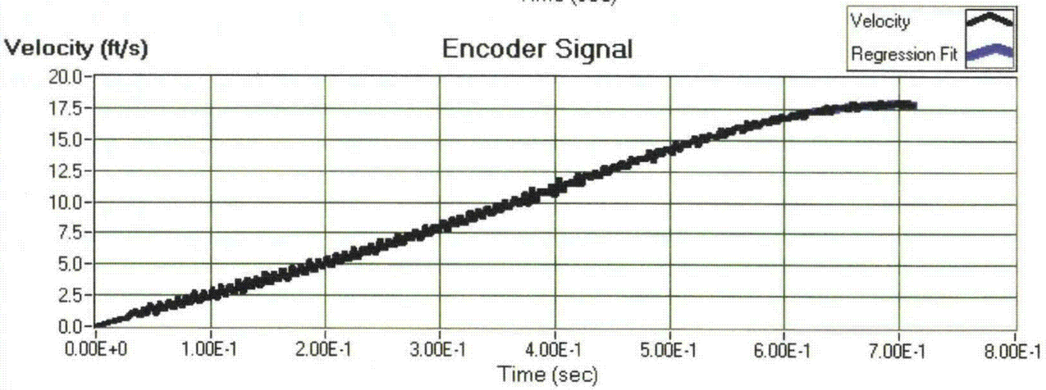

Test Parameters	Value
Group ID	RiverBend-HAZ
Date	11/12/2002 09:40
Operator	Dr. Michael P. Manahan, Sr.
Temperature	-28.5 °F
Oscilloscope	MPM Internal Oscilloscope
Striker	8mm Metals
Interpolation	Point-Point Linear
Encoder Controller	MPM Encoder System
Velocity Determination	Encoder
Material	Metal
Size	Type A
Orientation	Other
Notch Type	V Notch, no Side-Groove
Units Normalization	None
Energy Adjustment	1.0799
Length	2.1654 in
Width	0.3937 in
Thickness	0.3937 in
Span	1.5748 in
Uncracked Ligament	0.3150 in
Notch Rafius	0.0098 in
Failure Type	complete fracture
Post Test Comments	good test
Impact Velocity	17.933 ft/s
Striker Energy	36.242 ft lbf
Dial Gage Energy	36.000 ft lbf
Encoder Energy	36.242 ft lbf
Latch Angle	134.14°
Final Angle	119.21°
Potential Energy	306.728 ft lbf
Windage & Friction	0.635 ft lbf
Percent Shear	35.59 %
Lateral Expansion	0.0300 in

	Load (lbf)	Displacement (in)	Velocity (ft/s)	Time (s)	Energy (ft lbf)
General Yield	3.5934E+3	1.437E-2	1.788E+1	6.000E-5	2.06454E+0
Peak Load	4.3412E+3	9.913E-2	1.707E+1	4.640E-4	3.09157E+1
Brittle Fracture	3.9318E+3	2.016E-2	1.783E+1	8.700E-5	3.74583E+0
Arrest Load	7.0331E+2	1.104E-1	1.702E+1	5.190E-4	3.28390E+1
End of Signal	1.7318E+1	2.253E-1	1.692E+1	1.084E-3	3.62419E+1

Sample ID: H11
Group ID: RiverBend-HAZ

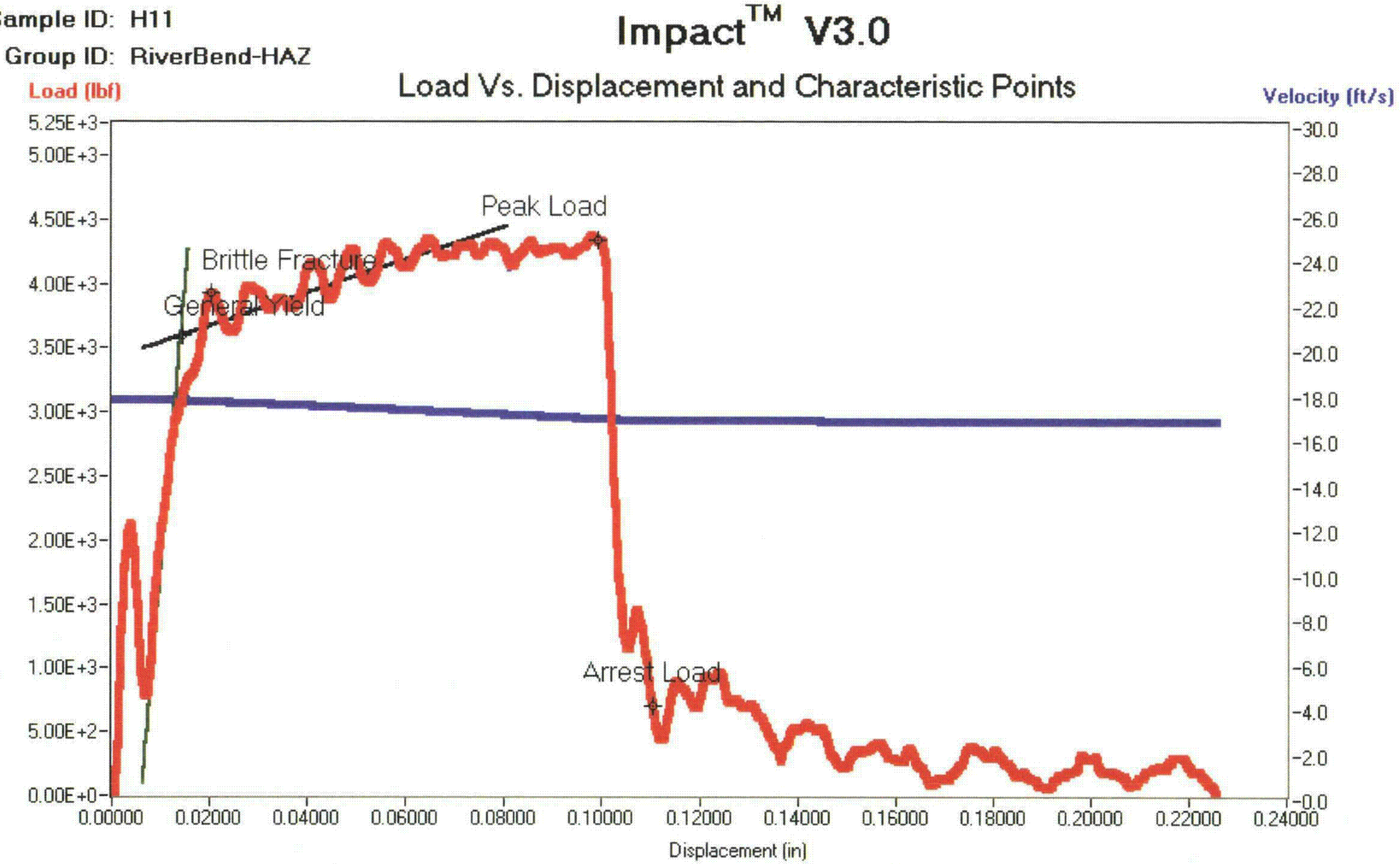

	Load (lbf)	Displacement (in)	Velocity (ft/s)	Time (s)	Energy (ft lbf)
General Yield	3.5934E+3	1.437E-2	1.788E+1	6.000E-5	2.06454E+0
Peak Load	4.3412E+3	9.913E-2	1.707E+1	4.640E-4	3.09157E+1
Brittle Fracture	3.9318E+3	2.016E-2	1.783E+1	8.700E-5	3.74583E+0
Arrest Load	7.0331E+2	1.104E-1	1.702E+1	5.190E-4	3.28390E+1
End of Signal	1.7318E+1	2.253E-1	1.692E+1	1.084E-3	3.62419E+1

Sample ID

H9

Comments

River Bend 183 Degree Surveillance Capsule

Impact™ V3.0

Summary Report

Test Parameters	Value
Group ID	RiverBend-HAZ
Date	11/11/2002 17:53
Operator	Dr. Michael P. Manahan, Sr.
Temperature	7.5 °F
Oscilloscope	MPM Internal Oscilloscope
Striker	8mm Metals
Interpolation	Point-Point Linear
Encoder Controller	MPM Encoder System
Velocity Determination	Encoder
Material	Metal
Size	Type A
Orientation	Other
Notch Type	V Notch, no Side-Groove
Units Normalization	None
Energy Adjustment	1.0543
Length	2.1654 in
Width	0.3937 in
Thickness	0.3937 in
Span	1.5748 in
Uncracked Ligament	0.3150 in
Notch Rafius	0.0098 in
Failure Type	complete fracture
Post Test Comments	good test
Impact Velocity	17.943 ft/s
Striker Energy	74.036 ft lbf
Dial Gage Energy	73.000 ft lbf
Encoder Energy	74.036 ft lbf
Latch Angle	134.15°
Final Angle	106.18°
Potential Energy	306.769 ft lbf
Windage & Friction	0.655 ft lbf
Percent Shear	64.44 %
Lateral Expansion	0.0500 in

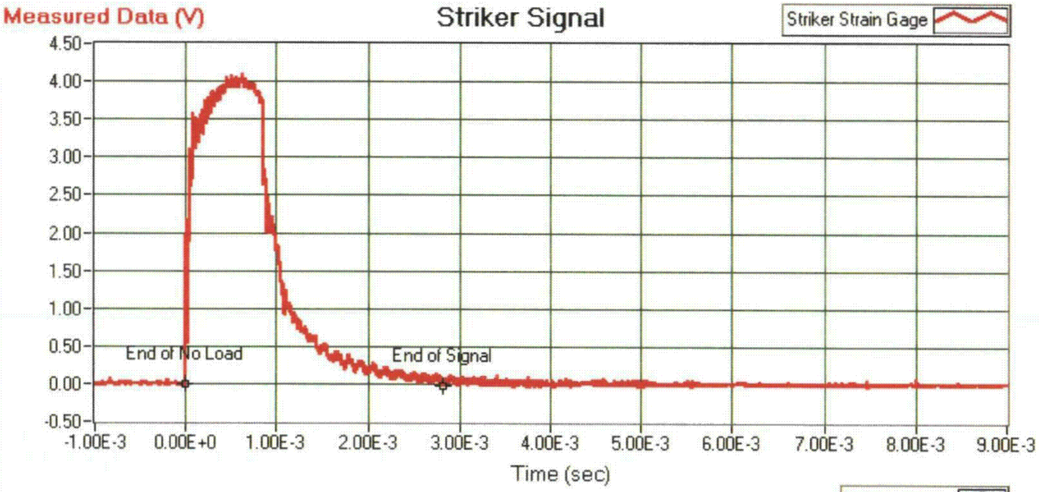

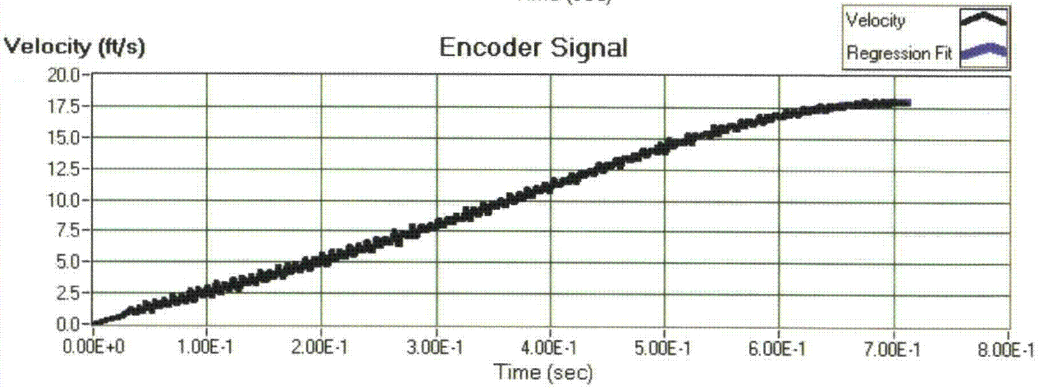

	Load (lbf)	Displacement (in)	Velocity (ft/s)	Time (s)	Energy (ft lbf)
General Yield	3.4127E+3	1.307E-2	1.789E+1	5.600E-5	1.98850E+0
Peak Load	4.2027E+3	1.196E-1	1.690E+1	5.660E-4	3.63992E+1
Brittle Fracture	3.9568E+3	1.749E-1	1.633E+1	8.430E-4	5.54339E+1
Arrest Load	2.3246E+3	1.837E-1	1.626E+1	8.880E-4	5.76989E+1
End of Signal	4.6442E+0	5.512E-1	1.575E+1	2.818E-3	7.40358E+1

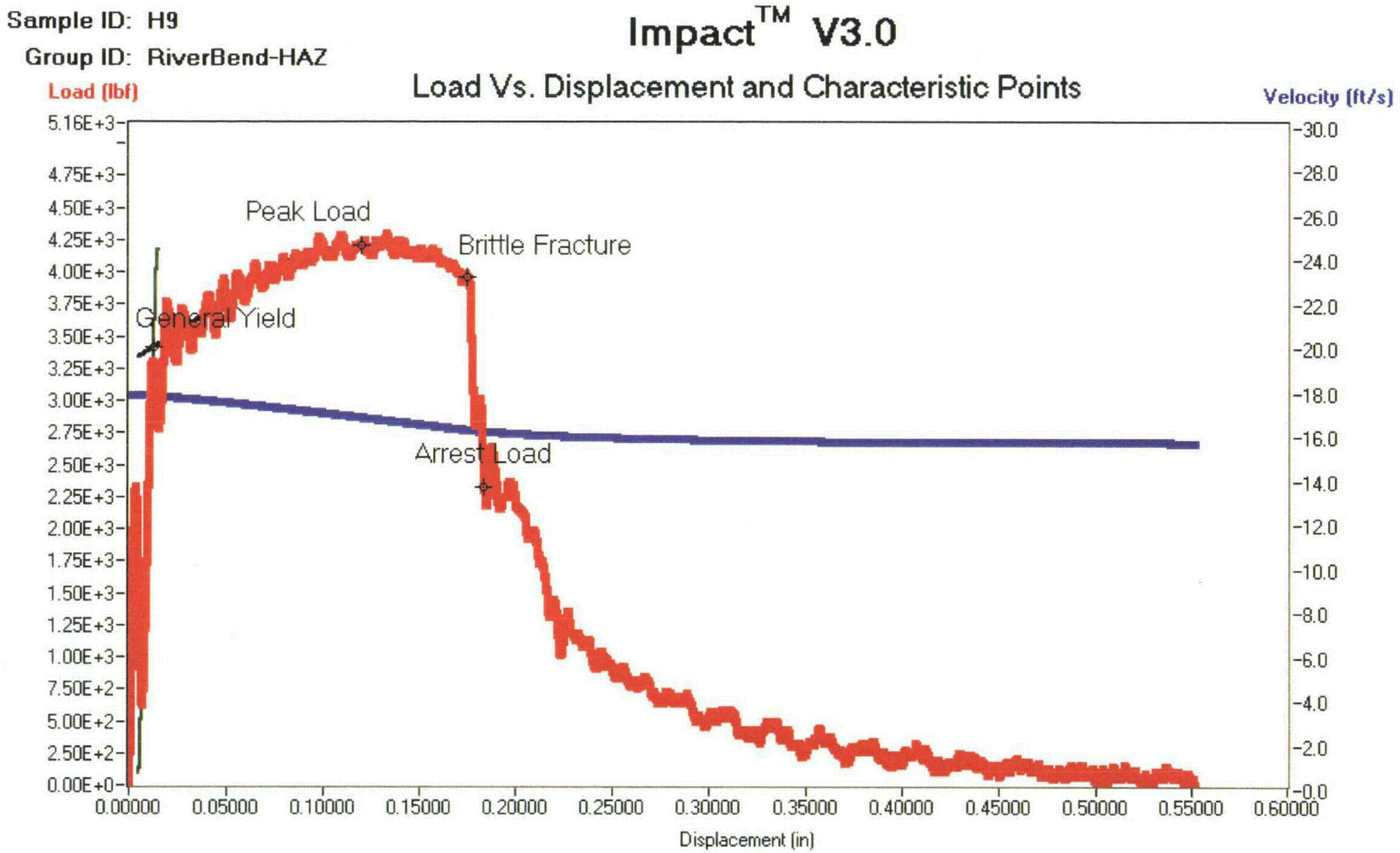

	Load (lbf)	Displacement (in)	Velocity (ft/s)	Time (s)	Energy (ft lbf)
General Yield	3.4127E+3	1.307E-2	1.789E+1	5.600E-5	1.98850E+0
Peak Load	4.2027E+3	1.196E-1	1.690E+1	5.660E-4	3.63992E+1
Brittle Fracture	3.9568E+3	1.749E-1	1.633E+1	8.430E-4	5.54339E+1
Arrest Load	2.3246E+3	1.837E-1	1.626E+1	8.880E-4	5.76989E+1
End of Signal	4.6442E+0	5.512E-1	1.575E+1	2.818E-3	7.40358E+1

Sample ID

H5

Comments

River Bend 183 Degree Surveillance Capsule

Impact™ V3.0

Summary Report

Test Parameters	Value
Group ID	RiverBend-HAZ
Date	11/11/2002 17:37
Operator	Dr. Michael P. Manahan, Sr.
Temperature	7.9 °F
Oscilloscope	MPM Internal Oscilloscope
Striker	8mm Metals
Interpolation	Point-Point Linear
Encoder Controller	MPM Encoder System
Velocity Determination	Encoder
Material	Metal
Size	Type A
Orientation	Other
Notch Type	V Notch, no Side-Groove
Units Normalization	None
Energy Adjustment	1.0271
Length	2.1654 in
Width	0.3937 in
Thickness	0.3937 in
Span	1.5748 in
Uncracked Ligament	0.3150 in
Notch Rafius	0.0098 in
Failure Type	complete fracture
Post Test Comments	good test
Impact Velocity	17.939 ft/s
Striker Energy	46.203 ft lbf
Dial Gage Energy	45.900 ft lbf
Encoder Energy	46.203 ft lbf
Latch Angle	134.15°
Final Angle	115.65°
Potential Energy	306.769 ft lbf
Windage & Friction	0.655 ft lbf
Percent Shear	53.18 %
Lateral Expansion	0.0355 in

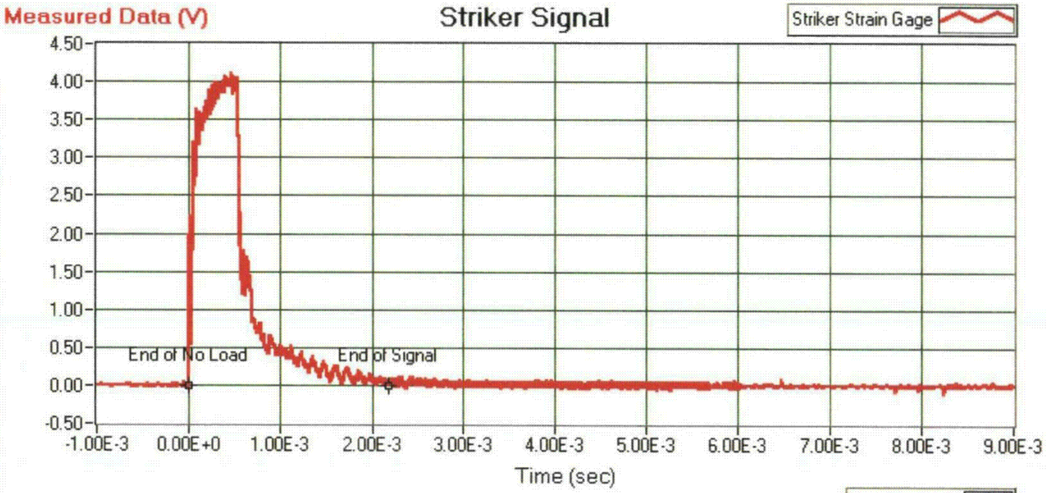

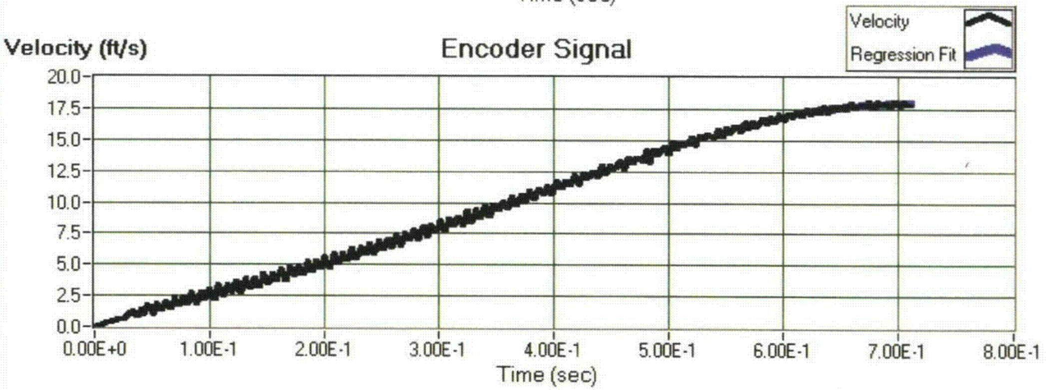

	Load (lbf)	Displacement (in)	Velocity (ft/s)	Time (s)	Energy (ft lbf)
General Yield	3.3094E+3	1.327E-2	1.788E+1	5.583E-5	1.94803E+0
Peak Load	4.1098E+3	1.020E-1	1.706E+1	4.790E-4	3.01914E+1
Brittle Fracture	3.8834E+3	5.433E-2	1.753E+1	2.490E-4	1.41553E+1
Arrest Load	9.8145E+2	1.440E-1	1.681E+1	6.860E-4	3.84384E+1
End of Signal	6.2160E+0	4.405E-1	1.657E+1	2.171E-3	4.62033E+1

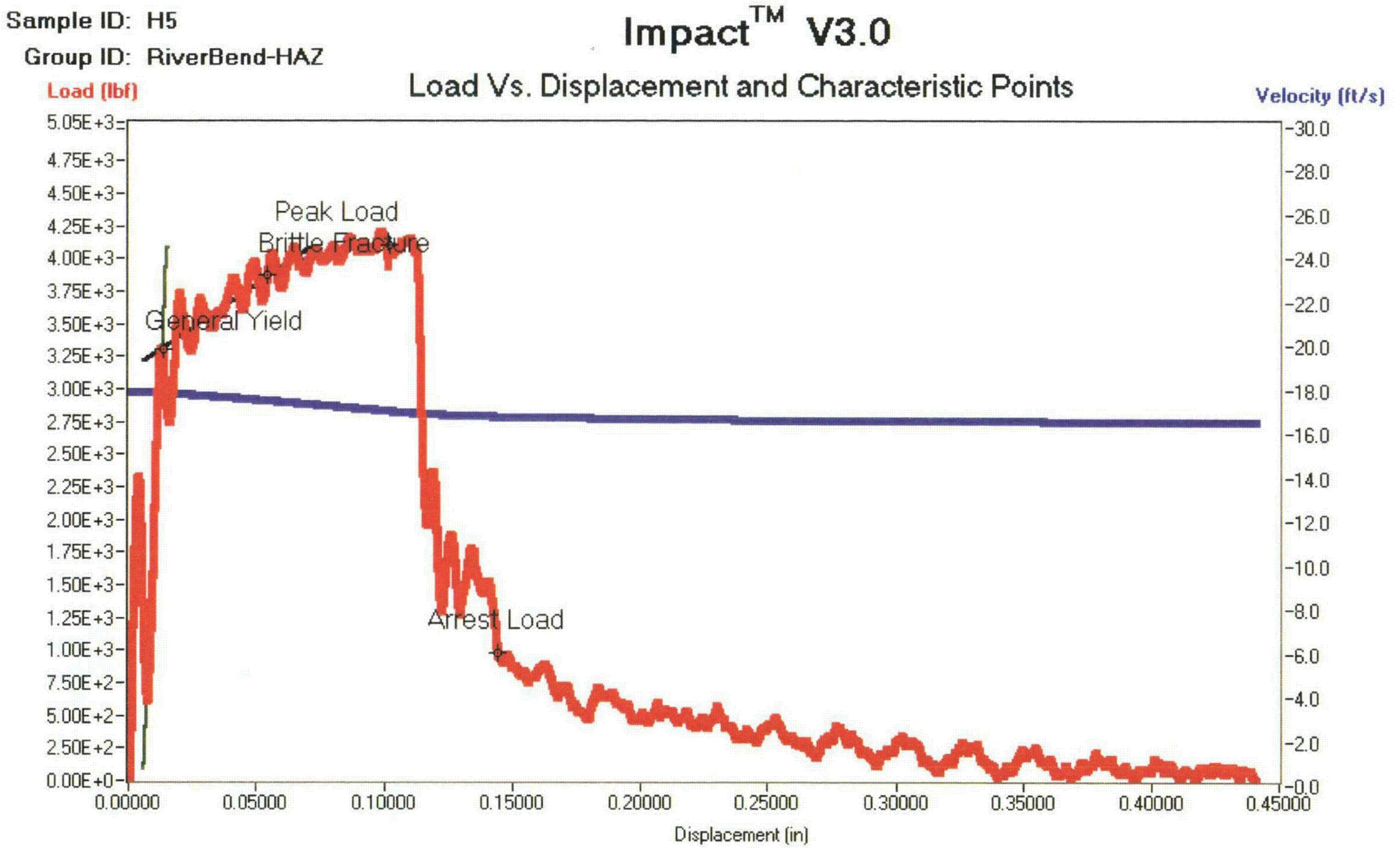

	Load (lbf)	Displacement (in)	Velocity (ft/s)	Time (s)	Energy (ft lbf)
General Yield	3.3094E+3	1.327E-2	1.788E+1	5.583E-5	1.94803E+0
Peak Load	4.1098E+3	1.020E-1	1.706E+1	4.790E-4	3.01914E+1
Brittle Fracture	3.8834E+3	5.433E-2	1.753E+1	2.490E-4	1.41553E+1
Arrest Load	9.8145E+2	1.440E-1	1.681E+1	6.860E-4	3.84384E+1
End of Signal	6.2160E+0	4.405E-1	1.657E+1	2.171E-3	4.62033E+1

Sample ID

H3

Comments

River Bend 183 Degree Surveillance Capsule

Impact™ V3.0

Summary Report

Test Parameters	Value
Group ID	RiverBend-HAZ
Date	11/11/2002 15:15
Operator	Dr. Michael P. Manahan, Sr.
Temperature	67.8 °F
Oscilloscope	MPM Internal Oscilloscope
Striker	8mm Metals
Interpolation	Point-Point Linear
Encoder Controller	MPM Encoder System
Velocity Determination	Encoder
Material	Metal
Size	Type A
Orientation	Other
Notch Type	V Notch, no Side-Groove
Units Normalization	None
Energy Adjustment	1.0371
Length	2.1654 in
Width	0.3937 in
Thickness	0.3937 in
Span	1.5748 in
Uncracked Ligament	0.3150 in
Notch Rafius	0.0098 in
Failure Type	complete fracture
Post Test Comments	good test
Impact Velocity	17.946 ft/s
Striker Energy	87.293 ft lbf
Dial Gage Energy	86.200 ft lbf
Encoder Energy	87.293 ft lbf
Latch Angle	134.15°
Final Angle	101.84°
Potential Energy	306.769 ft lbf
Windage & Friction	0.655 ft lbf
Percent Shear	100.00 %
Lateral Expansion	0.0630 in

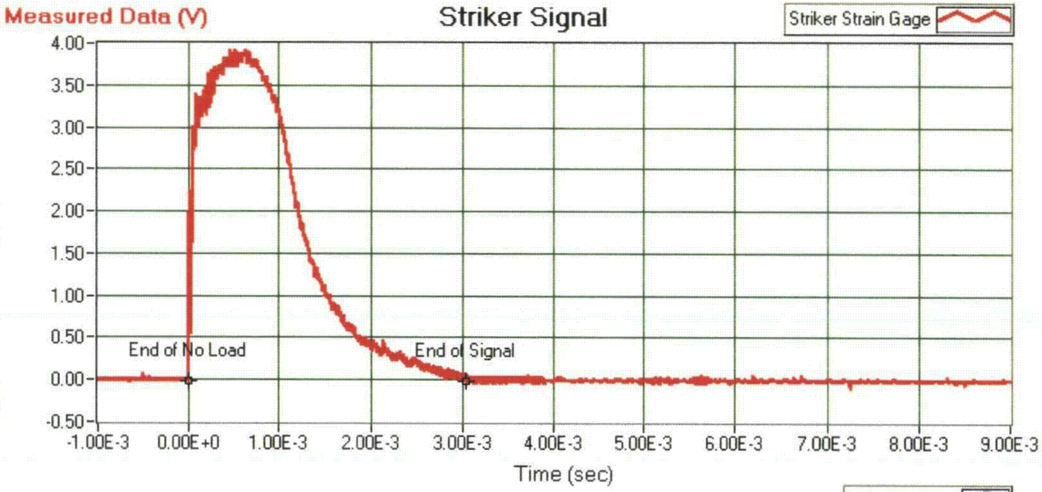

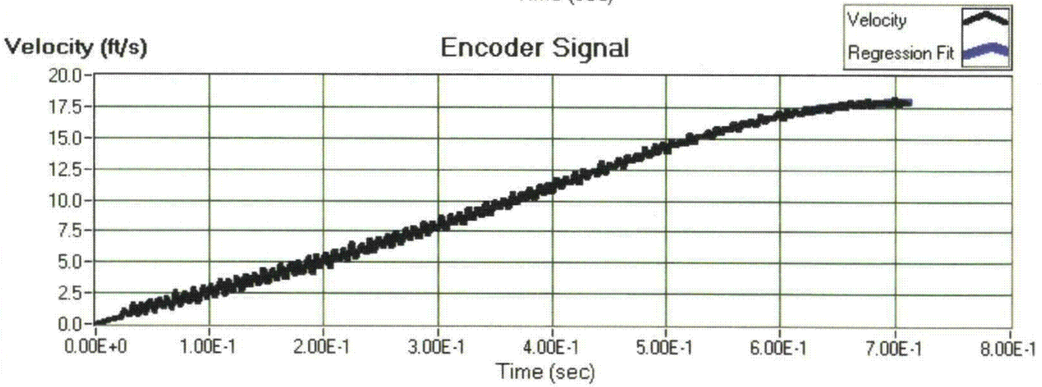

	Load (lbf)	Displacement (in)	Velocity (ft/s)	Time (s)	Energy (ft lbf)
General Yield	3.1269E+3	1.394E-2	1.789E+1	5.500E-5	1.83141E+0
Peak Load	3.9816E+3	1.263E-1	1.689E+1	5.930E-4	3.64086E+1
End of Signal	4.2538E+0	5.845E-1	1.529E+1	3.033E-3	8.72934E+1

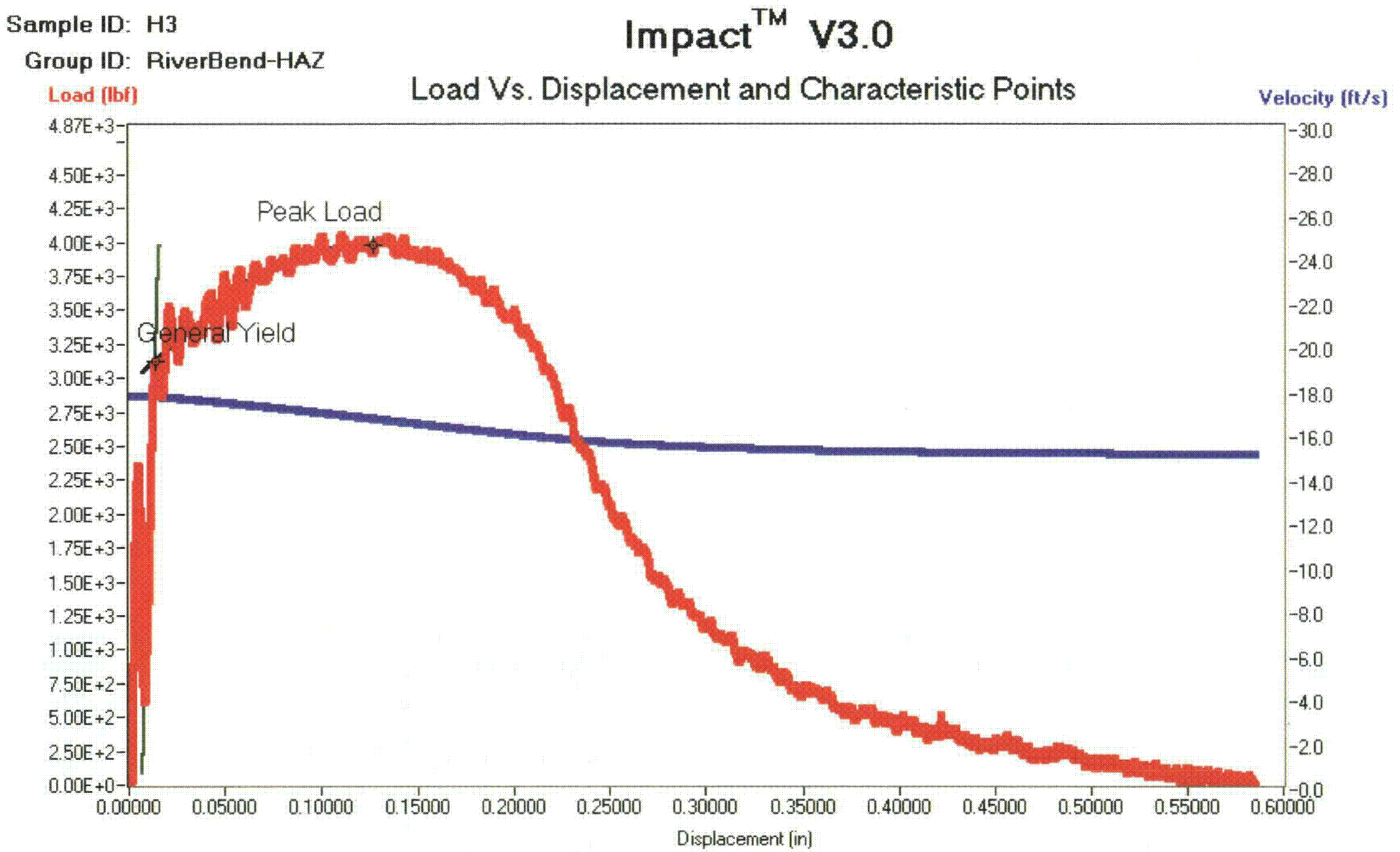

	Load (lbf)	Displacement (in)	Velocity (ft/s)	Time (s)	Energy (ft lbf)
General Yield	3.1269E+3	1.394E-2	1.789E+1	5.500E-5	1.83141E+0
Peak Load	3.9816E+3	1.263E-1	1.689E+1	5.930E-4	3.64086E+1
End of Signal	4.2538E+0	5.845E-1	1.529E+1	3.033E-3	8.72934E+1

Sample ID

H7

Comments

River Bend 183 Degree Surveillance Capsule

Impact™ V3.0

Summary Report

Test Parameters	Value
Group ID	RiverBend-HAZ
Date	11/11/2002 15:36
Operator	Dr. Michael P. Manahan, Sr.
Temperature	68.2 °F
Oscilloscope	MPM Internal Oscilloscope
Striker	8mm Metals
Interpolation	Point-Point Linear
Encoder Controller	MPM Encoder System
Velocity Determination	Encoder
Material	Metal
Size	Type A
Orientation	Other
Notch Type	V Notch, no Side-Groove
Units Normalization	None
Energy Adjustment	1.0335
Length	2.1654 in
Width	0.3937 in
Thickness	0.3937 in
Span	1.5748 in
Uncracked Ligament	0.3150 in
Notch Rafius	0.0098 in
Failure Type	incomplete fracture
Post Test Comments	good test
Impact Velocity	17.947 ft/s
Striker Energy	76.164 ft lbf
Dial Gage Energy	75.200 ft lbf
Encoder Energy	76.164 ft lbf
Latch Angle	134.15°
Final Angle	105.48°
Potential Energy	306.769 ft lbf
Windage & Friction	0.655 ft lbf
Percent Shear	73.50 %
Lateral Expansion	0.0475 in

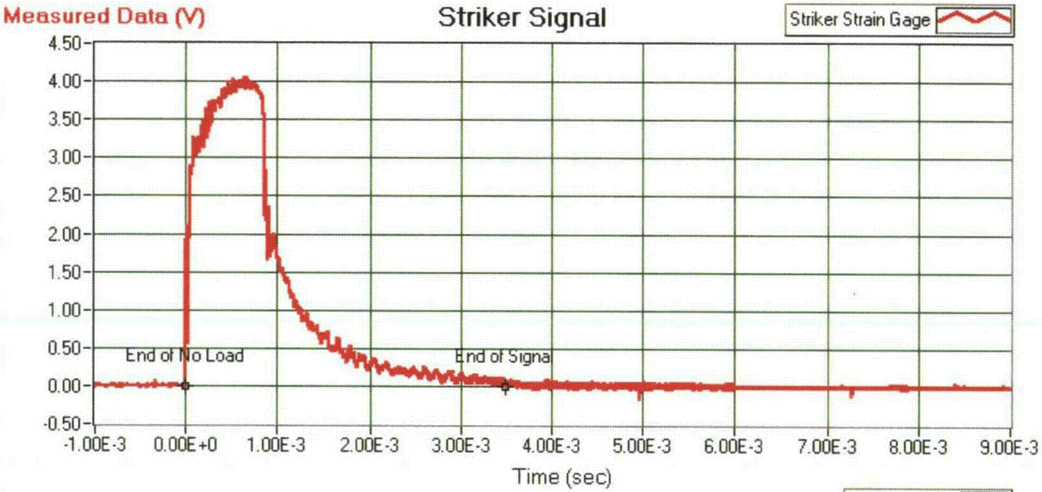

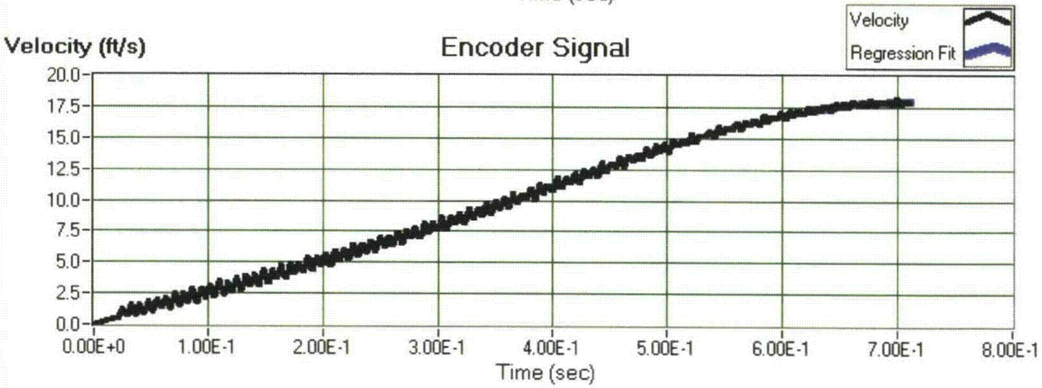

	Load (lbf)	Displacement (in)	Velocity (ft/s)	Time (s)	Energy (ft lbf)
General Yield	3.0780E+3	1.307E-2	1.790E+1	5.300E-5	1.72562E+0
Peak Load	4.0992E+3	1.360E-1	1.677E+1	6.430E-4	4.00854E+1
Brittle Fracture	3.9332E+3	1.744E-1	1.638E+1	8.360E-4	5.30133E+1
Arrest Load	1.8435E+3	1.910E-1	1.626E+1	9.210E-4	5.66262E+1
End of Signal	4.5461E+0	6.753E-1	1.564E+1	3.476E-3	7.61637E+1

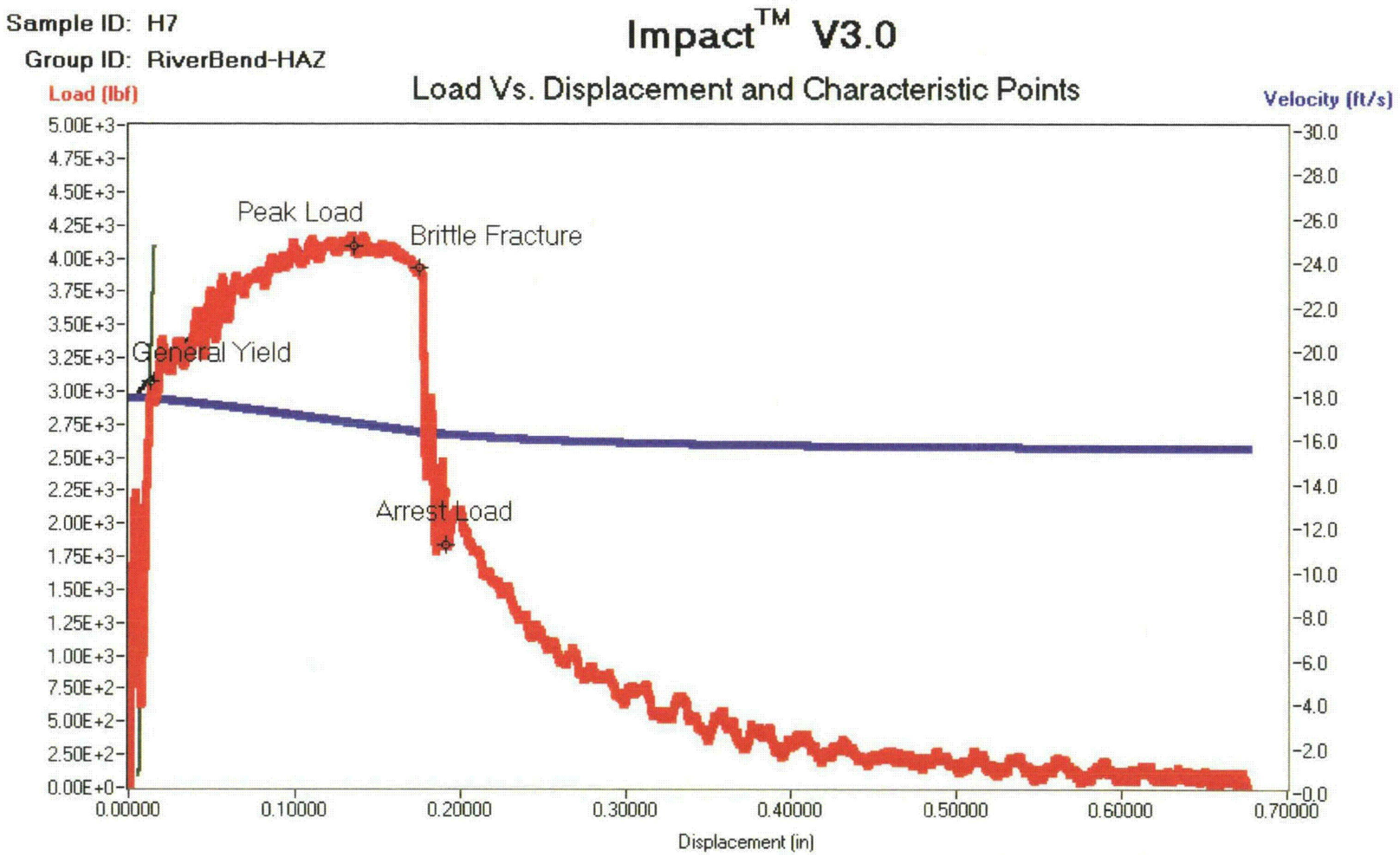

	Load (lbf)	Displacement (in)	Velocity (ft/s)	Time (s)	Energy (ft lbf)
General Yield	3.0780E+3	1.307E-2	1.790E+1	5.300E-5	1.72562E+0
Peak Load	4.0992E+3	1.360E-1	1.677E+1	6.430E-4	4.00854E+1
Brittle Fracture	3.9332E+3	1.744E-1	1.638E+1	8.360E-4	5.30133E+1
Arrest Load	1.8435E+3	1.910E-1	1.626E+1	9.210E-4	5.66262E+1
End of Signal	4.5461E+0	6.753E-1	1.564E+1	3.476E-3	7.61637E+1

Sample ID

H10

Comments

River Bend 183 Degree Surveillance Capsule

Impact™ V3.0

Summary Report

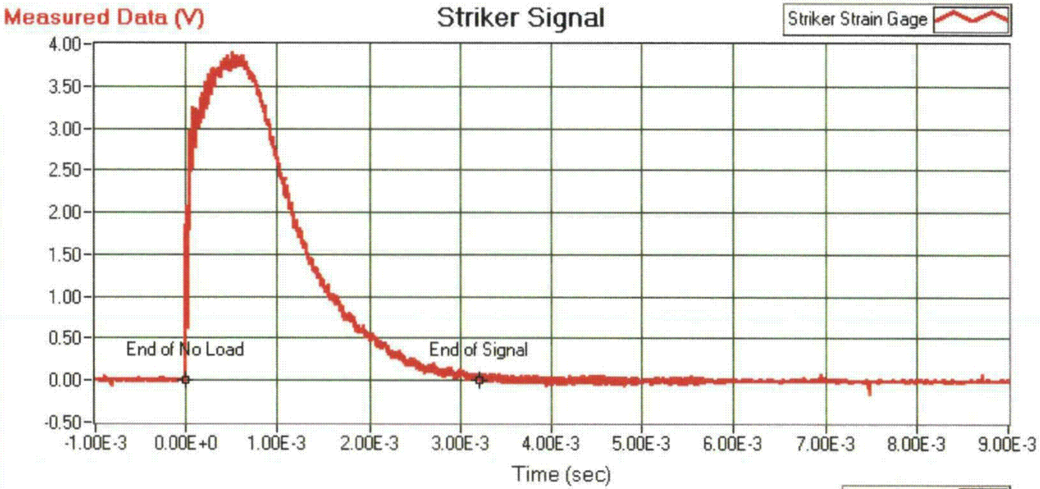

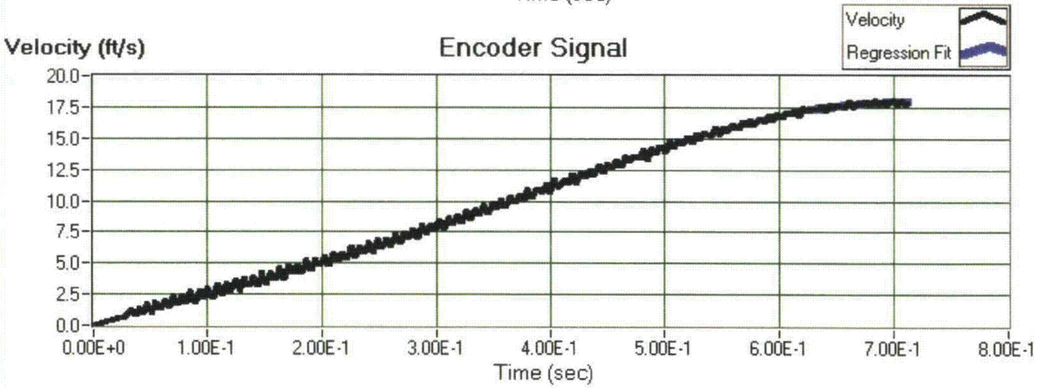

Test Parameters	Value
Group ID	RiverBend-HAZ
Date	11/12/2002 08:45
Operator	Dr. Michael P. Manahan, Sr.
Temperature	126.3 °F
Oscilloscope	MPM Internal Oscilloscope
Striker	8mm Metals
Interpolation	Point-Point Linear
Encoder Controller	MPM Encoder System
Velocity Determination	Encoder
Material	Metal
Size	Type A
Orientation	Other
Notch Type	V Notch, no Side-Groove
Units Normalization	None
Energy Adjustment	1.0516
Length	2.1654 in
Width	0.3937 in
Thickness	0.3937 in
Span	1.5748 in
Uncracked Ligament	0.3150 in
Notch Rafius	0.0098 in
Failure Type	complete fracture
Post Test Comments	good test
Impact Velocity	17.938 ft/s
Striker Energy	86.688 ft lbf
Dial Gage Energy	85.600 ft lbf
Encoder Energy	86.688 ft lbf
Latch Angle	134.14°
Final Angle	102.04°
Potential Energy	306.728 ft lbf
Windage & Friction	0.635 ft lbf
Percent Shear	100.00 %
Lateral Expansion	0.0755 in

	Load (lbf)	Displacement (in)	Velocity (ft/s)	Time (s)	Energy (ft lbf)
General Yield	2.9580E+3	1.240E-2	1.789E+1	5.183E-5	1.68029E+0
Peak Load	3.9999E+3	1.182E-1	1.697E+1	5.570E-4	3.38892E+1
End of Signal	7.7821E+0	6.174E-1	1.534E+1	3.206E-3	8.66878E+1

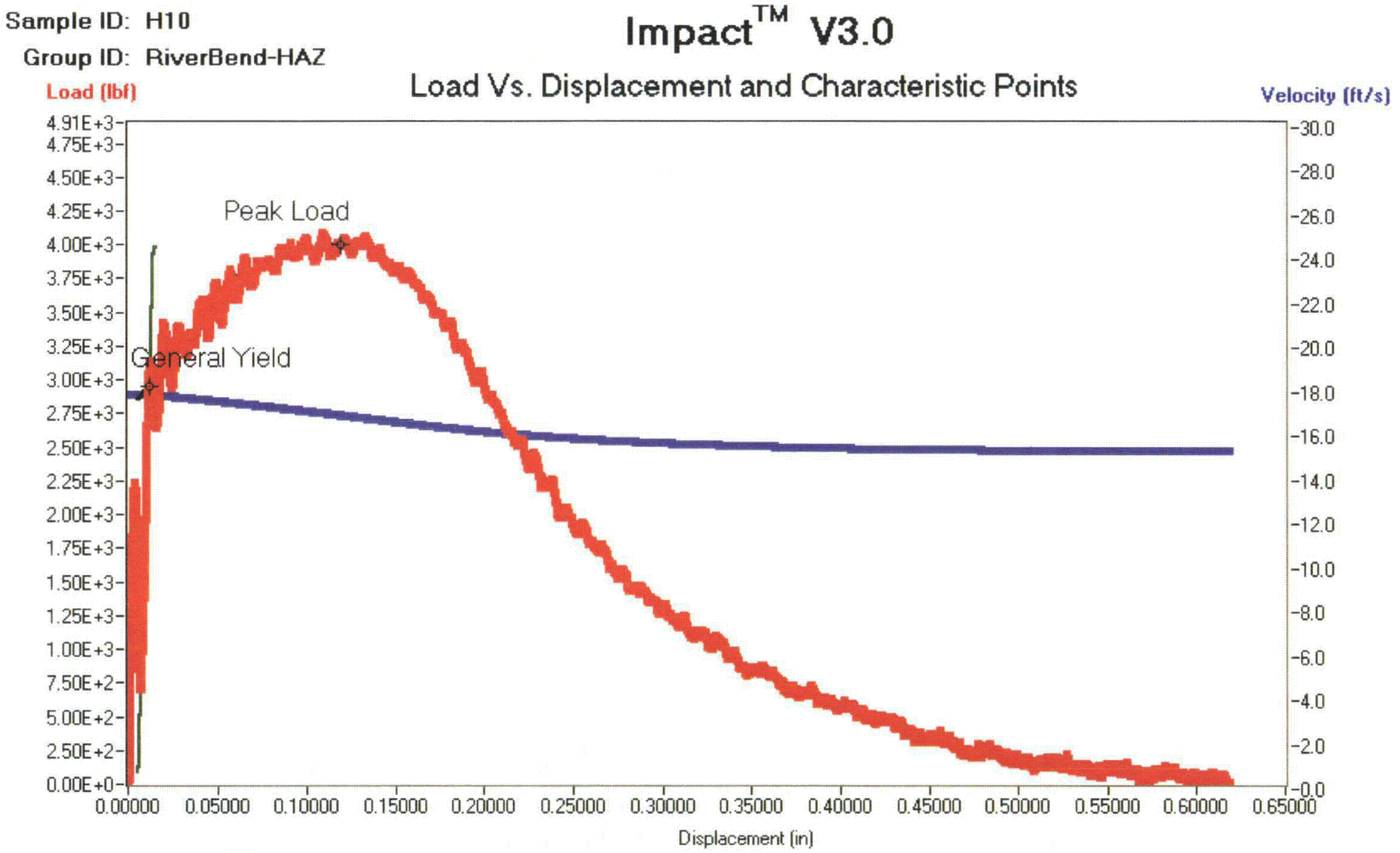

	Load (lbf)	Displacement (in)	Velocity (ft/s)	Time (s)	Energy (ft lbf)
General Yield	2.9580E+3	1.240E-2	1.789E+1	5.183E-5	1.68029E+0
Peak Load	3.9999E+3	1.182E-1	1.697E+1	5.570E-4	3.38892E+1
End of Signal	7.7821E+0	6.174E-1	1.534E+1	3.206E-3	8.66878E+1

Sample ID

H6

Comments

River Bend 183 Degree Surveillance Capsule

Impact™ V3.0

Summary Report

Test Parameters	Value
Group ID	RiverBend-HAZ
Date	11/12/2002 08:58
Operator	Dr. Michael P. Manahan, Sr.
Temperature	128.8 °F
Oscilloscope	MPM Internal Oscilloscope
Striker	8mm Metals
Interpolation	Point-Point Linear
Encoder Controller	MPM Encoder System
Velocity Determination	Encoder
Material	Metal
Size	Type A
Orientation	Other
Notch Type	V Notch, no Side-Groove
Units Normalization	None
Energy Adjustment	1.0370
Length	2.1654 in
Width	0.3937 in
Thickness	0.3937 in
Span	1.5748 in
Uncracked Ligament	0.3150 in
Notch Rafius	0.0098 in
Failure Type	complete fracture
Post Test Comments	good test
Impact Velocity	17.933 ft/s
Striker Energy	101.501 ft lbf
Dial Gage Energy	100.200 ft lbf
Encoder Energy	101.501 ft lbf
Latch Angle	134.14°
Final Angle	97.27°
Potential Energy	306.728 ft lbf
Windage & Friction	0.635 ft lbf
Percent Shear	100.00 %
Lateral Expansion	0.0630 in

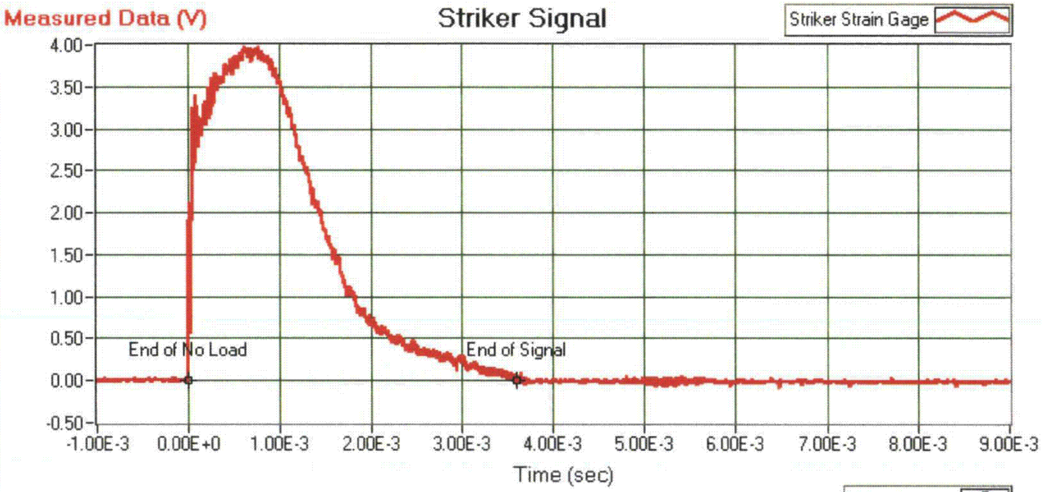

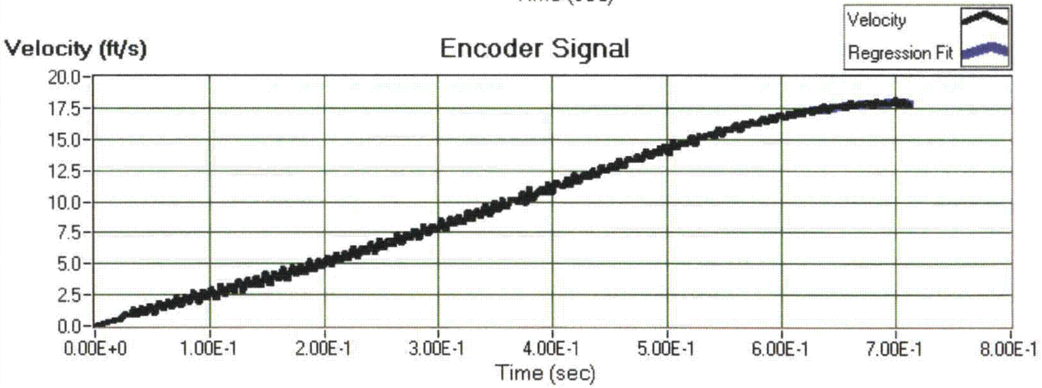

	Load (lbf)	Displacement (in)	Velocity (ft/s)	Time (s)	Energy (ft lbf)
General Yield	2.9771E+3	1.217E-2	1.789E+1	5.080E-5	1.66958E+0
Peak Load	4.0554E+3	1.466E-1	1.668E+1	6.980E-4	4.27435E+1
End of Signal	7.1075E+0	6.781E-1	1.479E+1	3.606E-3	1.01501E+2

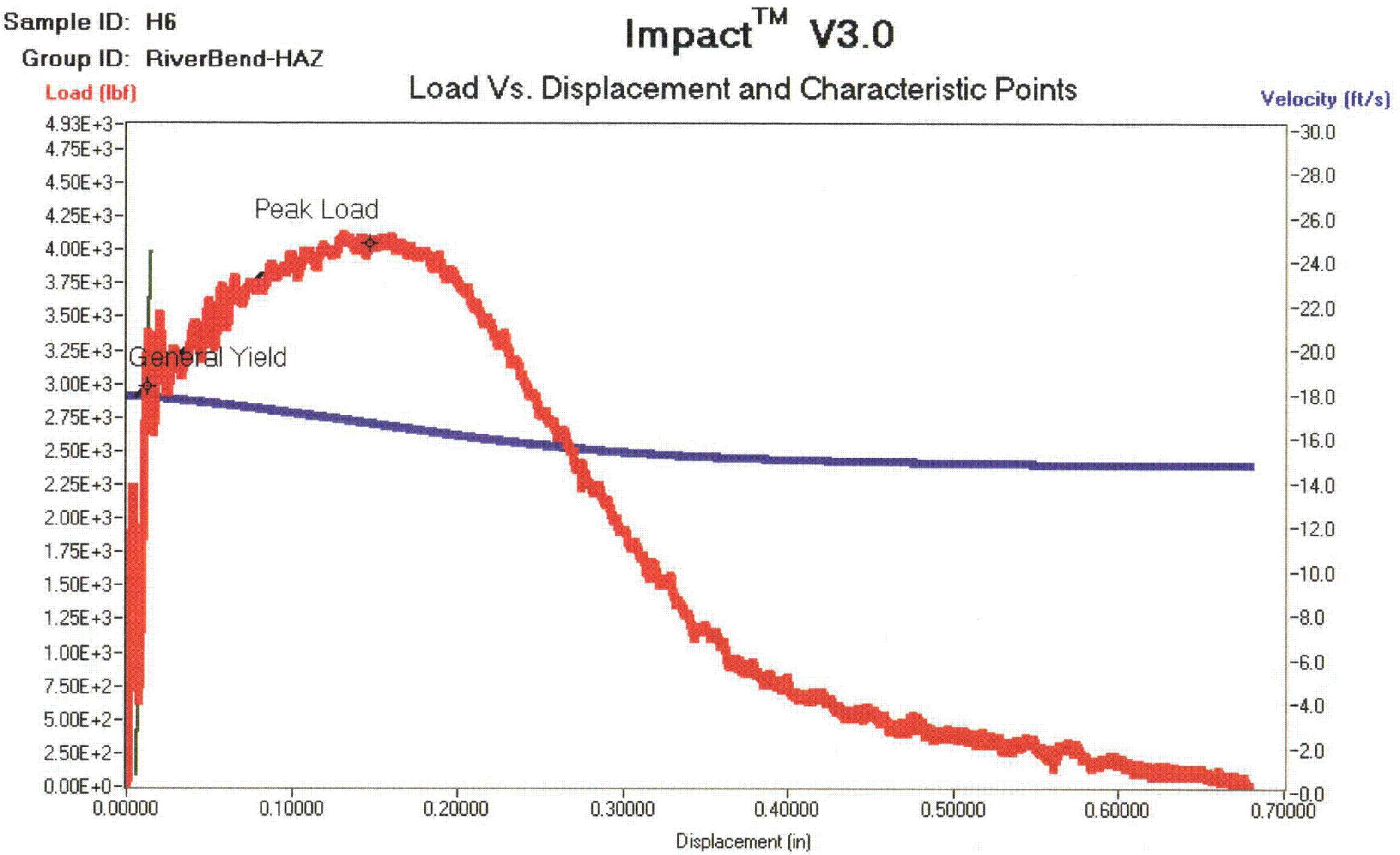

	Load (lbf)	Displacement (in)	Velocity (ft/s)	Time (s)	Energy (ft lbf)
General Yield	2.9771E+3	1.217E-2	1.789E+1	5.080E-5	1.66958E+0
Peak Load	4.0554E+3	1.466E-1	1.668E+1	6.980E-4	4.27435E+1
End of Signal	7.1075E+0	6.781E-1	1.479E+1	3.606E-3	1.01501E+2

Export Control Restrictions

Access to and use of EPRI Intellectual Property is granted with the specific understanding and requirement that responsibility for ensuring full compliance with all applicable U.S. and foreign export laws and regulations is being undertaken by you and your company. This includes an obligation to ensure that any individual receiving access hereunder who is not a U.S. citizen or permanent U.S. resident is permitted access under applicable U.S. and foreign export laws and regulations. In the event you are uncertain whether you or your company may lawfully obtain access to this EPRI Intellectual Property, you acknowledge that it is your obligation to consult with your company's legal counsel to determine whether this access is lawful. Although EPRI may make available on a case-by-case basis an informal assessment of the applicable U.S. export classification for specific EPRI Intellectual Property, you and your company acknowledge that this assessment is solely for informational purposes and not for reliance purposes. You and your company acknowledge that it is still the obligation of you and your company to make your own assessment of the applicable U.S. export classification and ensure compliance accordingly. You and your company understand and acknowledge your obligations to make a prompt report to EPRI and the appropriate authorities regarding any access to or use of EPRI Intellectual Property hereunder that may be in violation of applicable U.S. or foreign export laws or regulations.

The Electric Power Research Institute (EPRI), with major locations in Palo Alto, California; Charlotte, North Carolina; and Knoxville, Tennessee, was established in 1973 as an independent, nonprofit center for public interest energy and environmental research. EPRI brings together members, participants, the Institute's scientists and engineers, and other leading experts to work collaboratively on solutions to the challenges of electric power. These solutions span nearly every area of electricity generation, delivery, and use, including health, safety, and environment. EPRI's members represent over 90% of the electricity generated in the United States. International participation represents nearly 15% of EPRI's total research, development, and demonstration program.

Together...Shaping the Future of Electricity

Program:

Nuclear Power

1021555

Electric Power Research Institute
3420 Hillview Avenue, Palo Alto, California 94304-1338 • PO Box 10412, Palo Alto, California 94303-0813 USA
800.313.3774 • 650.855.2121 • askepri@epri.com • www.epri.com